THE SYNTHESIS AND PHARMACOLOGICAL EVALUATION OF SALVINORIN A ANALOGUES AS OPIOID RECEPTOR PROBES

By

Kimberly M. Lovell

Submitted to the graduate degree program in Medicinal Chemistry and the Graduate Faculty of the University of Kansas in partial fulfillment of the requirements for the degree of Doctor of Philosophy.

_____
Chairperson: Dr. Thomas E. Prisinzano

_____
Dr. Brian S. J. Blagg

_____
Dr. Michael F. Rafferty

_____
Dr. Paul R. Hanson

_____
Dr. Jeffery P. Krise

Date Defended: June 30th, 2011

The Dissertation Committee for Kimberly M. Lovell
certifies that this is the approved version of the following dissertation:

THE SYNTHESIS AND PHARMACOLOGICAL EVALUATION OF SALVINORIN A ANALOGUES AS OPIOID RECEPTOR PROBES

_____
Chairperson: Dr. Thomas E. Prisinzano

Date approved: June 30th, 2011

ABSTRACT

Kappa opioid (KOP) receptors have been shown to be involved in the control of several abuse related effects of central nervous system stimulants. KOP receptor agonists have been shown to modulate the activity of dopamine neurons and decrease self-administration of cocaine in a variety of species, while KOP receptor antagonists have the potential to be utilized as opioid abuse therapies and in the treatment of relapse.

With this in mind, investigations were performed on the novel KOP receptor agonist neoclerodane diterpene salvinorin A. This natural product is the active component of the hallucinogenic mint plant *Salvia divinorum* and the first non-nitrogenous natural product having high affinity and efficacy at KOP receptors. Salvinorin A contains a furan ring, which in other furan containing natural products such as teucrin A and aflatoxin B_1 has been identified to cause hepatotoxicity. In efforts to develop a more desirable pharmacological tool, structural modifications were made to salvinorin A in efforts explore the role of the furan ring in affinity and activity at KOP receptors and to reduce its potential for hepatotoxicity. Several ketone analogues were found to retain affinity at KOP receptors relative to salvinorin A and were versatile intermediates for the synthesis of other analogues. Surprisingly, benzisoxazole (**187**) was found to have increased affinity for MOP receptors. 2-Furanyl salvinorin A (**185**) was found to have similar efficacy and activity compared to salvinorin A. In addition, Captisol® was identified as a new vehicle for salvinorin A administration in pharmacological assays to eliminate some of the drawbacks of currently used vehicles. These studies assist with the identification of the pharmacophore of salvinorin A as well as the determination of structure-activity relationships, all of which will increase the potential for identification of novel opioid therapeutics.

ACKNOWLEDGEMENTS

I thank the NIH Training Grant for funding and the opportunity to perform two scientific rotations outside my field. Thank you to Dr. Laura Bohn at Scripps Florida and Drs. Daniel Flynn and Michael Rafferty at Deciphera Pharmaceuticals for the opportunities to intern. Because of you all, I am a much more well-rounded scientist able to see the big picture of medicinal research. Thank you to Christina M. Dersch and Dr. Richard B. Rothman at the National Institute on Drug Abuse for their collaboration with the binding assays and [^{35}S]GTPγS assays referenced. Additional thanks to Katherine Smith and Dr. Scott Runyan for their collaboration with the calcium mobilization (FLIPR) assay. Thank you to The University of Kansas Department of Medicinal Chemistry and special thanks to my committee.

I have been blessed by the opportunity to be surrounded by some of the most amazing people in my past five years of graduate school. I have the most amazing family who has never stopped supporting me through everything. Mom and Dad, your unconditional love, support, and encouragement mean the world to me and have allowed me to be successful. Ryan, you have always been there for me and provided me with a realistic view of the world that sometimes I just do not to see. Charles, you have been my constant support here in Lawrence and I will forever miss the chance of running into you on campus. Grandma Ginny, Granddad, Grandma Shirley, my Aunts, Uncles, and cousins, thank you for giving me wonderful memories, laughs, and support. To my phenomenal friends and lab mates who have made graduate school the shortest and longest five-years of my life. Laura and Angelica, I cannot possibly imagine getting through graduate school without both of you. Anthony, Karrie, Tammi, Mike, and Andrew, you are some of the most bizarre, most kind, and most entertaining people I have ever been around. Because of you all, I was always (most of the time) excited to go to work. You guys made work fun and always reminded me not to take myself too seriously. Finally, I must thank the Prisinzano family for opening up their home to me and teaching me that real spaghetti sauce does not come from a can. And Tom, thank you for all of your support and encouragement. Without you, I do not think I would have had what it took to be successful. Thank you for always seeing in me what I did not see in myself.

TABLE OF CONTENTS

LIST OF TABLES

LIST OF FIGURES

LIST OF SCHEMES

CHAPTER I: INTRODUCTION

Ancient History of Natural Products

The use of natural products and natural product extracts in medicine has taken place since ancient times.[1] Throughout history, natural products have played an important role in ethnopharmacology with the earliest recorded medicinal therapies based on natural product extracts.[1,2] Civilizations in Mesopotamia began around 3500 BCE with one of the earliest being the Sumerian civilization which lasted until 2600 BCE.[2] Evidence of medicinal practices from the Sumerian civilization has been preserved on cuneiform clay tablets relating to the concept of a medical practitioner and prescription regimes.[2] Artifacts of Egyptian medicine from 2900 BCE have been found along with evidence of trade between Mesopotamia, Egypt, and southern Arabia.[1,2] Much of this trade focused on aromatic woods, spices, and aromatic gums.[2] Aromatic gum myrrh, isolated from the trees *Cammiphora abyssinica* and *Commiphora momol*, was a key component of ancient trade.[3] Historically, myrrh was used in drug preparations for its analgesic properties.[3] Additional evidence of the importance of natural products from a historical perspective is seen in ancient Chinese and Indian cultures around 1000 BCE.[1] Indian Ayurvedic medicine has been around for over four thousand years and today is still utilized in medicine, especially in India.[1,4] Several labs around the world are presently identifying a number of the pharmacological active compounds of Ayurvedic therapies.[4] Plant alkaloids have predominantly been identified as the active components of ancient therapeutics.[4] Still today, over 75% of the world population relies on traditional remedies for medicinal therapeutics.[3] Even in developed nations, many people continue to use traditional medicinal approaches to bring healing and well-being including *Hypericum perforatum* (St. John's wort) and *Ginkgo biloba* L.

Natural Products in Medicine

Before the identification of single pharmaceutical compounds, natural extracts were used for treatments ranging from pain to infections.[5] With the advancement in scientific technology, the active components of natural extracts were able to be identified and characterized resulting in the modernization of pharmaceutical therapy.[6] Natural products have greatly influence modern pharmaceutical industry and to date, the majority of drugs developed in pharmaceutical industry are based on natural product leads or modification of a natural product scaffold.[7-10] Natural products are single chemical compounds produced by a living organism that occur naturally and are often unique for a particular class of organisms. Natural products themselves, along with modified derivatives, have resulted in clinical agents in almost all therapeutic areas.[7] In 2000, approximately one-third of the top-selling drugs were natural products or derivatives of natural products.[5] In addition to providing a number of drugs, natural products have also greatly influenced what is known about therapeutic targets and biological pathways.[11] Natural products provide biochemical tools to elucidate specific pathways of disease.[7] Natural product medicinal chemistry has directly shaped our knowledge of the body and illness and how we currently treat disease.[11] Structural diversity found throughout natural products make them a priceless source of original lead compounds for therapeutic use.[10]

Biological activity found with natural products is attributed to their evolutionary purpose.[8] Bacteria have been around for over three billion years and secondary metabolites have developed as a response to their local environments.[8] If the metabolites were useful for the survival of the bacterial species then the gene products were propagated and further optimized in future generations.[8] The evolution of organisms including plants, animals and microbes have

developed venoms and other protective secondary metabolites for defensive and survival purposes.[12]

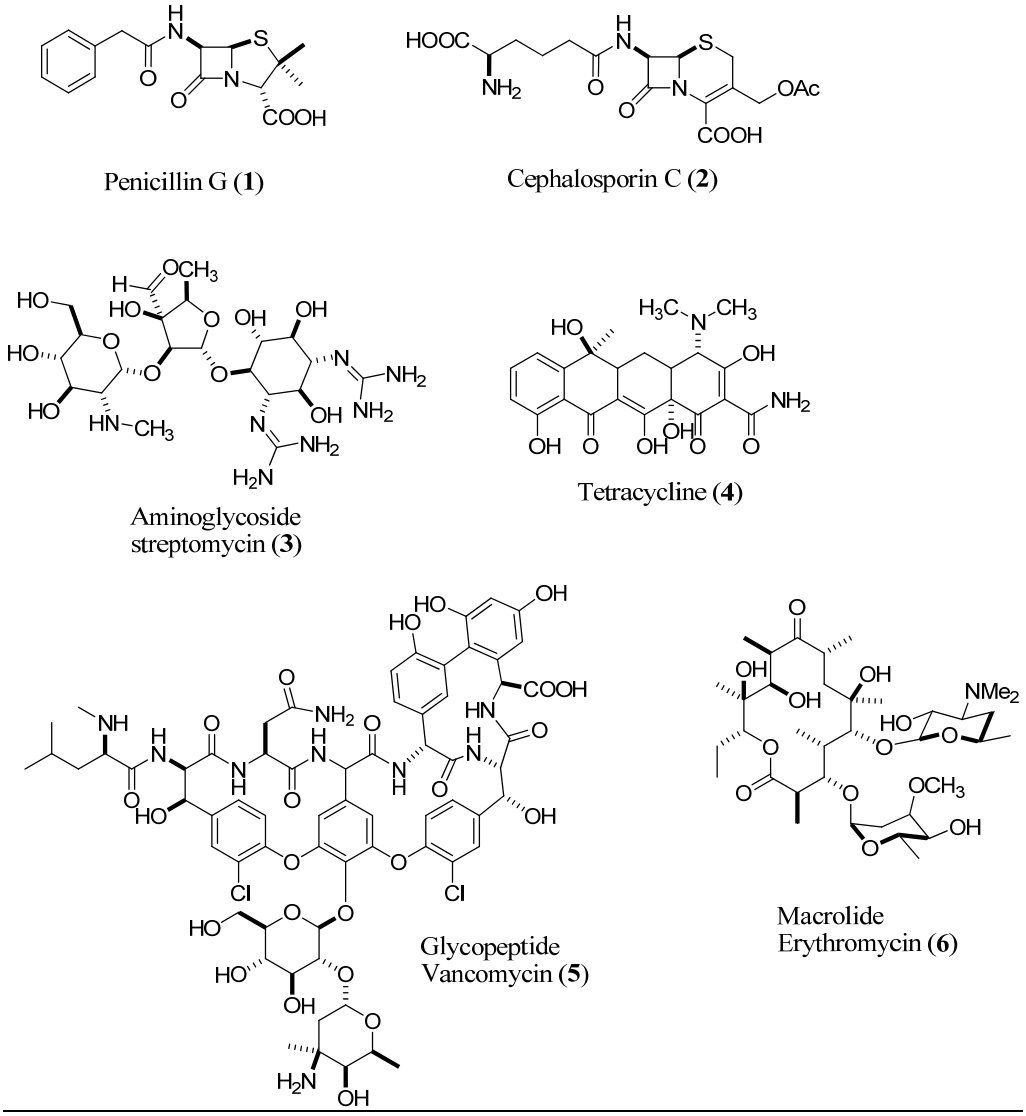

Figure 1: Structures of Selected Antibiotic Agents

Given the rationale for secondary metabolite evolution, the number of natural products with biological activity is not surprising. Specifically, natural product research has significantly influenced the areas of anti-cancer and anti-infective therapeutics, with the majority of these compounds being identified from plant or microbial sources.[8,13] Natural products in medicine

have had great success by drastically improving the average quality of life and doubling life expectancy.[8]

Approximately 80% of antibacterial agents are related to natural product scaffolds.[8,9] The beginnings of the golden age of antibacterial pharmaceuticals began in 1928 with Alexander Fleming's discovery of the first medicinally useful penicillin (**1**) (**Figure 1**) antibiotic resulting from a contamination of *Penicillium notatum* in a bacterial colony.[14] Isolation and purification of the fungi took over a decade and it was not until 1941 that the first clinical trial with crude penicillin was successful in humans. Large-scale fermentation and isolation of penicillin required the development of new technologies and was pushed forward by the needs of World War II. By 1943, large quantities of penicillin were being produced for the troops and scientific exploration into this class of natural products was expanding quickly. In 1948, cephalosporin C (**2**), a ring-expanded derivative of penicillin was isolated from *Cephalosporium sp*.[15] Through semi-synthesis and total synthesis efforts, over 100,000 penicillin and cephalosporin derived molecules have been produced.[16]

In addition to penicillins and cepalosporins, aminoglycosides (**3**), tetracyclines (**4**), glycopeptides (**5**), and macrolides (**6**) are all antibiotic classes originating from natural sources.[15] Advances in synthetic chemistry and sustained research into natural product scaffolds that have been known for decades such as the β-lactam, tetracycline, and erythromycin scaffolds have continued to result in the identification of new agents. New compounds continue to be identified from these scaffolds that overcome the drawbacks of current therapeutics and yield new clinical candidates.[17]

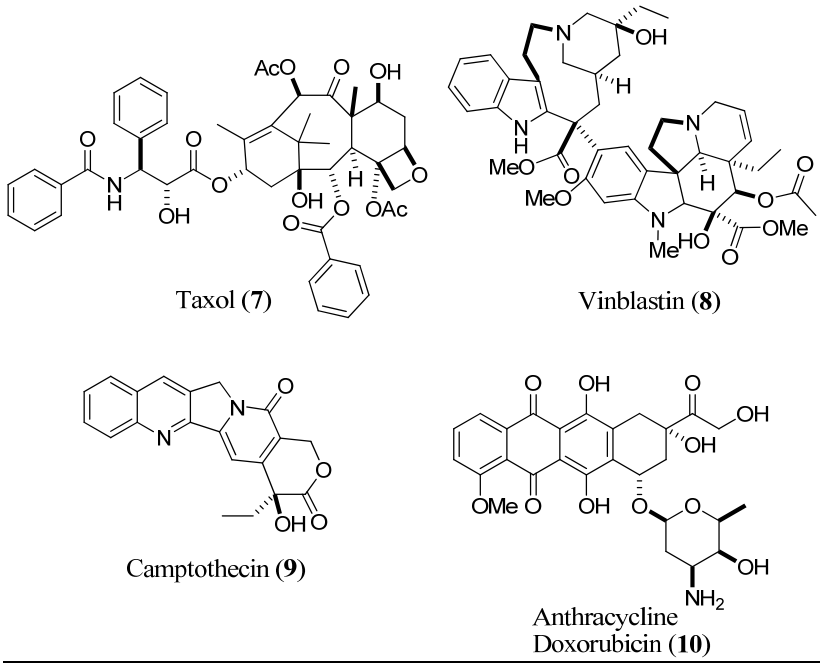

Figure 2: Structures of Selected Natural Product Derived Anticancer Agents

Natural products have had an enormous role in anti-cancer therapeutics. Approximately 80% of cancer chemotherapies on the market from 1981 – 2006 are natural products or are derived from natural sources.[9] The success of natural products in cancer therapeutics can be seen with the increased five-year survival rate of patients jumping from 50% in 1975 to 70% in 2004. Diverse natural products as cytotoxic agents have been identified including alkylating agents, tubulin polymerization agents, and topoisomerase inhibitors.[7] Examples include taxol (**7**), vinblastin (**8**), camptothecin (**9**), and anthracycline doxorubincin (**10**) (**Figure 2**).[18-27] In addition to providing novel therapeutics, natural products have lead to an increase in understanding cancer pathology and have elucidated previously unknown biological pathways and targets to explore for improved therapeutics.

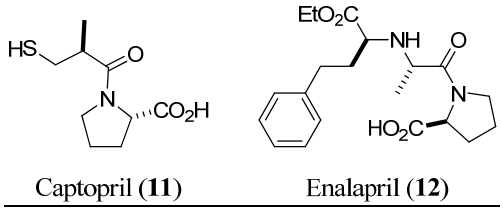

Figure 3: Structures of Selected Natural Product Derived ACE Inhibitors

Many natural product drugs or natural product derived drugs target the therapeutic areas of antibiotics and anticancer agents due to their evolutionary purposes, however almost all areas of medicine are affected by natural products.[9] Therapeutic targets for the treatment of high-blood pressure were identified based on natural products and investigations into the pharmacological effects of pit viper (*Bothrops jaraca*) venom.[28,29] The pit viper venom acts by lowering the blood pressure of the prey, ultimately leading to death. Angiotensin converting enzyme (ACE) in the renin-angiotensin system was identified as the enzyme targeted by the peptide toxin of the pit viper.[30] Small molecule therapeutics were developed based SAR studies of the toxin resulting in a new class of therapeutics ACE inhibitors for the treatment of hypertension including captopril (**11**) and enalapril (**12**) (**Figure 3**).[31-33]

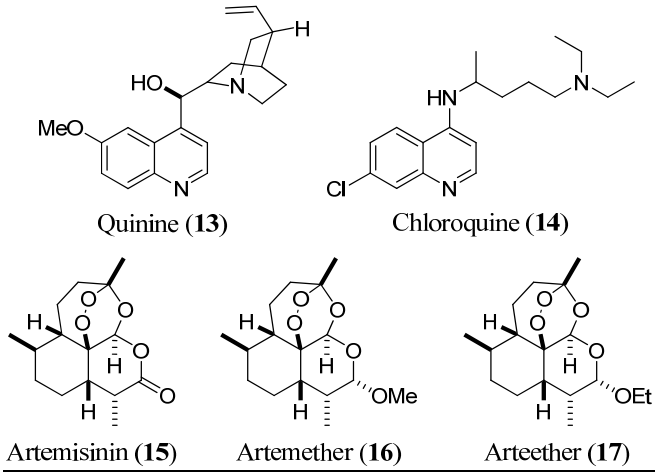

Figure 4: Natural Products and Natural Product Derived Compounds to Treat Malaria

Natural products have had a huge impact on antimalarial agents with the examples of the alkaloid quinine (**13**) and derivative chloroquine (**14**) (**Figure 4**), along with sesquiterpene lactone artemisinin (**15**).[34] The first mention of using cinchona bark, active component quinine, to treat malaria was around the start of the 1500s and with colonization of South America by the Europeans. At approximately the same time, the use of cinchona bark to treat malaria quickly spread to Europe. After use in its crude form for hundreds of years, quinine was first isolated from the *Cinchona* genus in 1820.[35] In 1854, the Dutch set up *Cinchona* plantations in Java to handle the therapeutic demand. The fascinating story of natural product quinine and its impact on world history continued in World War II when the Japanese troops cut off the Allied forces from their main supply of quinine.[35] Partially, as a result of the loss of the *Cinchona* plantations, a large amount research was performed that ultimately identified the synthetic compound chloroquine as a therapeutic for malaria.[36] Exploiting the same mechanism of action as quinine, chloroquine has been the most influential and successful drug for the treatment of malaria in the last fifty years.[35-37] However, over time chloroquine resistance spread requiring the need for new therapeutic agents.[36] Natural sources have continued to provide diverse structural scaffold with unique mechanisms of action as leads for the treatment of malaria.[34,38] Artemisinin, isolated from *Artemisia annua*, was identified as an anti-malarial agent.[39,40] Artemisinin lead to the development of analogues artemether (**16**) and arteether (**17**), which have become widely used particularly in areas with high-levels of chloroquine-resistance.[33,41-43]

Relatively recent investigations into marine natural products have opened in an entirely new environment for natural product isolation and identification.[44] A recent example of natural products success in CNS therapeutics and marine natural products includes the FDA approval of

Ziconotide (Prialt) (**18**) (**Figure 5**), which is a first-in-class drug for the management of severe chronic pain without generating tolerance that is associated with opioid pain management.[44-47] Ziconotide is a peptide neurotoxin that selectively and potently inhibits N-type voltage gated calcium channels ($Ca_v2.2$) and is isolated from *Conus magus*.[48] Cone snails are marine mollusks from the genus *Conus* and have evolved to produce an estimated 100,000 different small peptide toxins known as conotoxins.[48-51] Cone snails are predatory marine organisms that use conotoxins to immobilize and kill their prey.[50,51] Several other conotoxins are in clinical trials for pain management at $Ca_v2.2$ receptors but what makes these toxins even more exceptional is that different classes of conotoxins have different mechanisms of action. These conotoxins show the potential of therapeutic pain management through a neurotensin receptor agonist or reversible, non-competitive norepinephrine transport inhibitor.[49] Additionally, other conotoxin subclasses antagonize nicotinic acetylcholine receptors in competitive or noncompetitive manners or target NMDA receptors.[49,52] Conotoxins are being evaluated for their antinociceptive, antiepileptic, cardiotherapeutic, and neuroprotective therapeutic potential.[49]

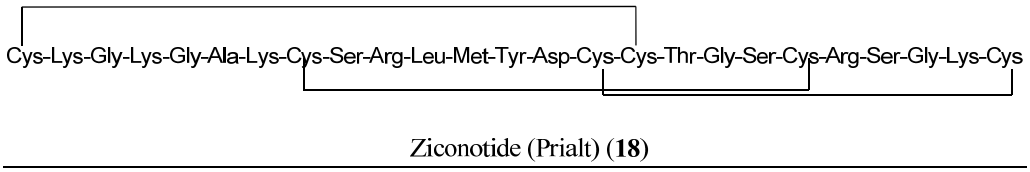

Figure 5: Structure of the Cone Snail Toxin Marketed as Prialt

Drawbacks of Natural Products

Even with the success of natural product based therapeutics, pharmaceutical industry has continued to decrease its investments in natural product research, with the majority of Big Pharma companies closing their natural products divisions.[6,10] Many of these decisions are based

on the difficulties associated with discovering a natural product drug candidate. Natural product chemistry requires reliable access and supply of the source plant or microorganism, which in itself can be challenging. Political concerns associated with the intellectual property rights of the local governments in which the source was identified and the regulations established by the 1993 Rio Convention on Biodiversity can make access to the plant difficult.[6,10,13,53] In 2010, the Nagoya Protocol was established that extended the previous treaty clarifying specifics on how to compensate nations, properly access material, and preserve biodiversity.[54] The consequences of the Nagoya Protocol are still unknown but hope to limit bureaucratic challenges in obtaining new biomass. Additionally, seasonal and environmental changes that effect species composition can result in assay inconsistency and the possibility of species extinction also contribute to difficulties with achieving the necessary supply.[6]

If a reliable supply of the medicinal species is obtained, other factors still limit the success of natural product research. Often natural products exhibit high potency and selectivity for a desired target but poor pharmacokinetic properties including solubility, bioavailability, exposure, stability, and detrimental metabolic profiles that can limit their potential for success and therapeutic utility.[55] Semi-synthetic structural modifications of these complex natural products have previously resulted in the discovery of compounds with improved pharmacological properties.[55] However, difficulties arise in working with natural products. Frequently natural products are highly complex with numerous oxygen-containing functional groups and many chiral centers.[6,10] The structural complexity of natural products can lead to obstacles and challenges in performing simple chemical transformations to make the compounds more therapeutically applicable.[55] Their complexity causes significant time requirements due to challenges in working with natural products, the necessity of indentify the active component, and

extensive structural elucidation.[5,6,10] Once the desired component is elucidated, the high risk of duplicity and identification of a known compound that is not patentable is a huge risk for pharmaceutical companies.[5,11]

Additionally, the advent of high-throughput screening further jeopardizes the success of natural product identification in pharmaceutical industry.[5] The focus of pharmaceutical industry has drastically changed and demands large numbers of compounds to fully utilize the capabilities of their high-throughput screens, which is not agreeable with natural products.[6,9,56] The quantity of compounds desired and the speed of identifying a hit successfully is only achievable though large library synthesis.[5,9]

Natural products are not very amenable to HTS for a number of reasons. Natural products are often found in low concentration that may not be effectively detected by the high-throughput screen.[6] Natural product extracts can have multiple components that result in synergistic or antagonist activity and consequently result in the interpretation of greater activity or less activity than is actually present.[6] There is also the challenge with fluorescent or colored compounds, which can lead to a misinterpretation of data. Poor solubility and stability in the assay system can cause difficulty in data analysis or the complete oversight of a potential therapeutic.[6]

Even with the challenges in natural product research, natural products still remain the greatest source of structural diversity and seemingly limitless potential.[53] With advances in scientific methodology, natural products have a chance for resurgence in pharmaceutical industry.[11] Technological advances in areas including bioassay-guided fractionation, fermentation, HPLC, solid-phase extraction, NMR, and mass spectrometry have all contributed to a decrease in time required for dereplication, isolation and structure identification.[11,57]

Additional advancements in synthetic methodology, molecular biology, genomics, combinatorial biosynthesis, and assay development all lead to a renewed interest in natural product research. Combination of these scientific areas has the potential to isolate and optimize novel natural product scaffolds in an efficient and lucrative manner. With only a small percent of the world's biodiversity previously tested for biological activity, an immeasurable number of natural sources remain available for medicinal use.[13,58,59]

Opioids

Despite some of the drawbacks associated with natural product research, natural products have continued to have great influence on modern medicine. One of the most explored uses of natural products is found with opium. Extracts of the opium poppy *Papaver somniferum* L. (Papaveraceae) have been used for centuries to treat pain and induce sleep.[60] Historical evidence links opium use as far back as 3500 BCE in the Sumerian culture and Greek writings around 200 BCE describe the importance of opium in their medicinal practices.[61] Crude opium extracts were used until the active component of the opium poppy was identified in the early 1800s. The alkaloid morphine (**19**) (**Figure 6**) was first isolated from the opium poppy in 1806 by Sir William Setürner.[62] However, due to its structural complexity, the structure was not proposed until 1923 by Robinson and the first synthesis did not occur until 1952 by Gates and Tschudi.[62] Setürner's isolation of morphine resulted in a paradigm shift in standards for pharmaceutical industry as morphine was the first pharmacological active pure compound to be isolated from its medicinal extract.[6] This changed pharmaceutical industry from extracts and elixirs to pure chemical agents of exact doses and consistency in chemical composition.

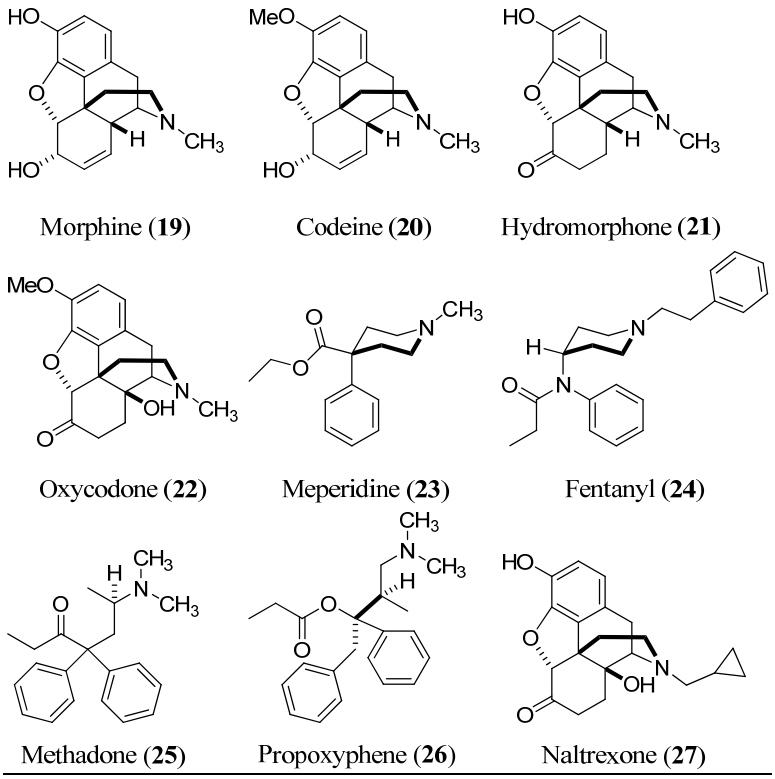

Figure 6: Structures of Some of the Most Commonly Used Opioids

For over 2,000 years, opioids have remanded some of the most therapeutically useful agents for the treatment of pain.[60] Mild to moderate pain is treated first with non-steroidal anti-inflammatory agents (NSAIDs) and is followed by the addition of narcotic analgesics if the pain persists.[60] The use of narcotic analgesics is not without severe side effects including constipation, respiratory depression, tolerance, and physical dependence.[60,63-65] These effects are related to their agonist activity at MOP receptors.[60] The most clinically relevant side effect of chronic opioid use is constipation.[66-68] Agonist activity of MOP receptors in the bowel decreases peristaltic waves resulting in retention of bowel contents. Respiratory depression is one of the most severe side effects associated with opioid use and results from the interaction of opioids with the respiratory center in the brain stem.[60,69] Death resulting from overdose is most

commonly a result of respiratory depression.[63] Long-term use of opioids often results in tolerance and physical dependence.[60] After continuous exposure, opioids decrease in effectiveness and larger doses are required to achieve the same therapeutic response. Physical dependence occurs when the body adapts to the drug and cessation causes withdrawal symptoms. Other less serious side effects include nausea, vomiting, pruritis, and drug-drug interactions.[60,70]

The negative side-effects associated with morphine and other opioids have caused limitations in their therapeutic use. However, opioid analgesics derived from the natural product morphine are still the most prescribed class of analgesics.[60] In efforts to identify new derivatives with fewer adverse effects, the structure of morphine has been extensively explored. Some of the most commonly used narcotic agents, (largely developed as a result of SAR studies of morphine) include morphine (**19**), codeine (**20**), hydromorphone (**21**), oxycodone (**22**), meperidine (**23**), fentanyl (**24**), methadone (**25**), propoxyphene (**26**), and naltrexone (**27**) (**Figure 6**). In addition to the identification of new therapeutic agents, these studies have increased understanding of opioid receptors.

Opioid Receptor Background

Opioid receptors are member of the G-protein coupled receptor (GPCR) superfamily.[60] Typically, opioid receptors couple to $G_{i/o}$ proteins but in *in vitro* models, opioid receptors additionally have been shown to couple with G_s proteins.[71,72] Coupling with $G_{i/o}$ proteins results in a decrease in cAMP production (leading to inhibition of adenylate cyclase) and a decrease of intracellular calcium.[73,74] The βγ subunit causes intracellular effects by interacting with potassium channels.[74]

Although morphine had been used as a potent analgesic since its isolation by Setürner in 1806, the concept of opioid receptors was not proposed until 1954 and it was not until the early 1970's that opioid receptors in mammalian brains tissue were identified.[75-77] Binding experiments using radiolabeled naloxone antagonized the pharmacological effects of morphine and verified the existence of opioid receptors.[60] The work of Martin in 1976 determined that opioids with structure variation, such as morphine (**19**), ketocyclazocine (**28**), and *N*-allylnormetazocine (SKF 10047) (**29**) (**Figure 7**), resulted in different pharmacological effects.[78,79] Due to these pharmacological differences, Martin classified opioid receptors into three subtypes: μ opioid (MOP) receptors, κ opioid (KOP) receptors, and δ opioid (DOP) receptors.[60,78-81]

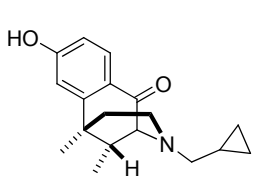

Ketocyclazocine (**28**)

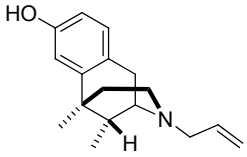

SKF 10,047 (**29**)
(*N*-allylnormetazocine)

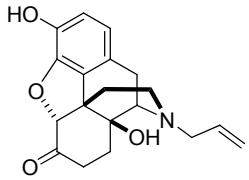

Naloxone (**32**)

Leu-Enkephalin (**30**)	Tyr-Gly-Gly-Phe-Leu
Met-Enkephalin (**31**)	Tyr-Gly-Gly-Phe-Met
β-Endorphin (**33**)	Tyr-Gly-Gly-Phe-Met-Thr-Ser-Glu-Lys-Ser-Gln-Thr-Pro-Leu-Val-Thr-Leu-Phe-Lys-Asn-Ala-Ile-Ile-Lys-Asn-Ala-Tyr-Lys-Lys-Gly-Glu
Dynorphin A (**34**)	Tyr-Gly-Gly-Phe-Leu-Arg-Arg-Ile-Arg-Pro-Lys-Leu-Lys-Trp-Asp-Asn-Gln

Figure 7: Selected Opioid Ligands and Peptides

Each opioid receptor subtype differs in receptor density, receptor distribution, and their endogenous ligands.[82] In 1975, leucine-enkephalin (**30**) and methionine-enkephalin (**31**) were the first peptides to be isolated from brain tissue showing opioid activity determined through

antagonism with naloxone (**32**). Met-enkephalin and leu-enkephalin are DOP receptor agonists and are pentapeptides that only differ in their C-terminal amino acid.[83] β-Endorphin (**33**) was isolated from pituitary glands in 1976 and determined to be the endogenous ligand for MOP receptors.[84] The endogenous peptide for KOP receptors is dynorphin A (**34**) and was isolated by Goldstein and coworkers from pituitary glands.[85,86] Dynorphin A is a tridecapeptide and has the highest degree of selectivity for KOP receptors relative to other dynorphins.[85,86]

Pharmacological differences of opioid receptor subtypes were described in the 1970's but it was not until the 1990's when each subtype was cloned and purified to further confirm the existence of the three distinct receptor populations. Receptor subtypes have been suggested and identified by ligand binding and physiological studies but have yet to be identified by gene products.[87-90] The first opioid receptor cloned was the DOP receptor and occurred in 1992 concurrently in two labs: Briggitte Kiefer in France and Chris Evans at the University of California at Los Angeles.[91] Closely following, in 1993, the MOP receptor was cloned in the Uhl laboratory at the National Institute of Health and the KOP receptor was cloned in the Akil lab at University of Michigan.[92,93]

Therapeutic Potential of KOP Receptor Modulation

Morphine and structure-activity relationship studies based on this scaffold have been thoroughly investigated over the past 200 years, with specific focus on the MOP receptor subtype.[60] The therapeutic utility of opioids is still limited due to its negative side effect profile. Identification of novel opioid ligands with diverse scaffolds show promise in having different pharmacological and side effect profiles.[94-96] These scaffolds include neoclerodane diterpenes, flavonoids, sesquiterpenes, peptides, and other alkaloids. With the past focus on MOP receptor

modulation and extensive research into opioid receptor pharmacology, currently there are not any therapeutics on the market that selectively target KOP receptors. KOP receptor modulation shows immense therapeutic potential and KOP receptors have been implicated in the treatment of drug abuse, peripheral pain management, and depression.[60,75,97-100] Several areas of research that could benefit from KOP receptor modulation are highlighted below.

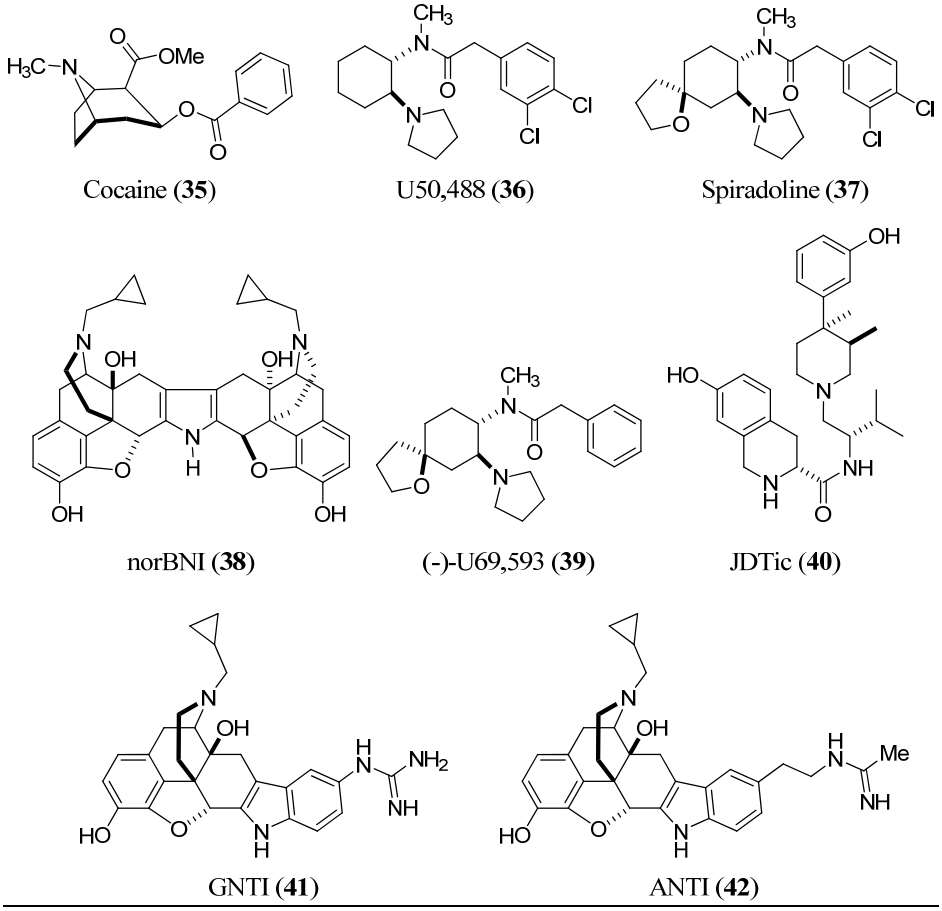

Figure 8: Compounds **35** – **42**

KOP Receptor Agonists in Drug Abuse

KOP receptor modulation of the dopamine system has shown the potential utility of KOP receptor therapeutics for the treatment of cocaine abuse.[60] Cocaine (**35**) (**Figure 8**) blocks the reuptake of norepinephrine, serotonin and dopamine, but the behavioral effects after acute

administration are generally attributed to the increase in extracellular dopamine levels in the nucleus accumbens.[60,101] Several neurochemical pathways, including KOP receptors, modulate the central dopamine system. A substantial amount of literature illustrates that KOP receptor agonists decrease dopamine levels and therefore act as functional antagonists of cocaine.[60,101,102]

KOP agonists produce effects that are opposite of those produced by dopamine agonists.[101] Additionally, KOP agonists have been shown to decrease self-administration of cocaine, decrease cocaine-induced reinstatement, and to inhibit cocaine place preference and locomotor sensitization.[96,101,103-107] Glick *et al*. were the first to determine that self-administration of morphine and cocaine were decreased by acute administration of KOP receptor agonists U50,488 (**36**) and spiradoline (**37**).[104] Lower doses were able to significantly decrease morphine and cocaine self-administration without significantly altering bar-pressing rates to access water. In some rats, decrease in self-administration could be seen for 5 – 6 days. Pretreatment of *nor*BNI (**38**) antagonized the effects of U50,488 linking KOP pathway activation to modulation of self-administration. Schenk and coworkers showed that U69,593 (**39**) attenuates cocaine self-administration and the reinstatement of drug-seeking behavior in response to an experimenter-administered dose of cocaine.[101] U69,593 had a greater effect to attenuate self-administration when cocaine doses were self-administered in descending order opposed to ascending order. When cocaine was given in descending order, U69,593 significantly reduced responding at lower doses of cocaine (0.03 – 0.125 mg/kg per infusion) but responding was maintained for higher cocaine doses (0.25 – 1.00 mg/kg per infusion). After a period of cocaine self-administration and extinction, U69,593 reduced the ability of cocaine to reinstate the extinguished lever-pressing behavior at high doses of cocaine (20.0 mg/kg). Other studies have expanded these finding to monkeys.[105,106] KOP agonists only seem to consistently decrease

cocaine self-administration when rats are trained to self-administer with a cue (conditioned reinforcement) opposed to unconditioned drug reinforcement.[108,109]

KOP agonists have been reported to block cocaine-induced conditioned place preference.[103,110,111] In 1995, Crawford and coworkers investigated the effects of U50,488 on cocaine-induced locomotor activity and cocaine-induced place preference.[103] U50,488 was given subcutaneously at 5 mg/kg and cocaine was administered i.p. at 10 mg/kg based on pilot studies. Rats pretreated with saline opposed to U50,488 had significantly greater photobeam interruptions following cocaine administration that was measured for twenty minutes. The effects of acute versus chronic administration of U50,488 were also evaluated and it was found that chronic and acute administration of U50,488 similarly affected cocaine-induced locomotor activity. In the cocaine-induced place preference paradigm, pretreatment of U50,488 was found to attenuate the preference for the cocaine-paired chamber. When U50,488 was given on its own, rats did not show significant aversion from the non-preferred chamber, which is very promising due to the known aversive potential of other KOP agonists.[112,113] Investigations into the cocaine-induced conditioned place preference paradigm continue to show that KOP agonists appear to minimize the rewarding effects of cocaine.[108,114]

Also of interest is that it appears KOP receptors modulate MOP opioid receptors by opposing their actions.[108,115] Dynorphin or U50,488 have been shown to dose-dependently antagonize morphine analgesia in rodent models of the tail-flick and hot-plate tests.[116-121] Studies also suggest that KOP receptors play a role in morphine tolerance.[115] Tolerance is a frequent side-effect of long term opioid use that results in a decrease in analgesic effect and an increase in abuse potential.[122-124] Tolerance is a result of many cellular processes including superactivation of the cAMP pathway, receptor desensitization, and receptor down

regulation.[115,124-127] Coadministration of U50,488 with morphine has been shown to prevent morphine tolerance.[118,120,128,129] KOP receptors have also been implicated in the attenuation of morphine reinforcing effects.[104,130-132] Further understanding of the interactions of MOP and KOP receptors could result in new therapeutics for the treatment of drug abuse.

KOP Receptor Antagonists in Drug Abuse

It has also been shown that KOP receptor antagonists have potential utility in the treatment of drug abuse. KOP receptor antagonism through pharmacological antagonism or gene disruption of KOP receptors have been implicated to modulate a component of stress-induced drug craving, which is one model of drug relapse.[133] Depression and stress have been linked as a potential motivating factor in cocaine relapse.[134] Therapeutic agents that attenuate depression and the effects of stress have potential to treat relapse in cocaine abuse. Beardsley and coworkers investigated the ability of KOP receptor antagonist JDTic (**40**) to block reinstatement of cocaine-seeking behavior by footshock-induced stress.[135] JDTic doses of 10 and 30 mg/kg significantly reduced the number of lever presses relative to vehicle while the dose of 3 mg/kg was nearly significant ($p = 0.0575$). JDTic did not block cocaine-primed reinstatement of responding at any tested dose demonstrating that JDTic does not suppress all behavior. Additionally, 10 and 30 mg/kg doses of JDTic blocked the diuretic effects of U50, 488H further implicating KOP receptor antagonism as the mechanism of action.

KOP Receptor Ligands in Pain Management

Opioid drugs associated with pain management work primarily at MOP receptors and remain the prototypical standard when treating severe pain.[99] Unfortunately, a number of

negative side effects are associated with agonism of MOP receptors including previously mentioned constipation, respiratory depression, tolerance, and physical dependence diminish their therapeutic utility.[99] Development of a KOP receptor ligand with antinociceptive effects would results in the identification of an analgesic without the negative side effects associated with MOP receptor agonists.[136] However, KOP receptor agonists have drawbacks of their own including sedation, dsyphoria, and in some cases, hallucinogenic effects.[137-142] These negative side effects are associated with KOP receptor activation in the CNS. KOP receptors are located in the CNS and in the periphery. Therefore, the development of a peripherally restricted KOP agonist would be lacking the CNS neuropsychiatric effects.[98,99]

A number of pain models have been established which investigate different types of pain stimuli including mechanical, thermal, electrical, or chemical.[99] KOP agonists have shown antinociceptive effects in a number of these pain models.[99] KOP agonists have been found to have antinociceptive effects in cutaneous and mechanical visceral nociceptive models and to inhibit inflammation induced hyperalgesia.[143-145] Additionally, in a colorectal distension rodent model, KOP agonists increased the threshold to colorectal distention and attenuated the magnitude of the response.[143] Several peripherally restrictive KOP receptor agonists have been developed and undergone clinical trials as peripherally restricted KOP agonists for the treatment of dyspepsia, irritable bowel syndrome, and pancreatitis. Due to lack of efficacy without causing CNS effects, these compounds failed clinical trials.[98,99] However, tetrapeptides FE 200665 and FE 200666 are under clinical development and have been reported to have a greater therapeutic window than the previous compounds.[146] KOP receptor modulation for the treatment of visceral pain is promising due to the successes of a number of behavioral assays. Further development of KOP ligands with better pharmacological profiles will hopefully identify improved therapeutics

with reduced propensity for side effects such as constipation, respiratory depression, tolerance, and physical dependence.

KOP Receptor Ligands in Depression

KOP function is involved in stress-related conditions and KOP receptor antagonists have been reported to have antidepressant activity.[99] The cAMP response element-binding protein (CREB) is a transcription factor that regulates gene expression, including the peptide precursor prodynorphin.[147-150] Further investigation into this observation has shown that dynorphin and KOP receptor agonist result in aversive and depressive-like effects in humans and rodents.[150-152] Studies determined that increased levels of CREB in the nucleus accumbens of rodent models resulted in signs of depression and that stress also activated CREB in the nucleus accumbens.[150,153,154] Inversely, decrease in CREB function lead to antidepressant-like effects comparable to those of known antidepressants.[150,155] The depressive-like behavior resulting from elevated CREB levels were reversed by KOP antagonist *nor*BNI, further implicating KOP receptors in depression.[154]

The antidepressant-like effects of *nor*BNI, GNTI (**41**), ANTI (**42**), and other KOP antagonists have been explored by a number of research groups which have confirmed each other's findings into the antidepressant-like effects of KOP antagonists.[155-158] Beardsley and coworkers expanded these findings by investigating the antidepressant-like effects of KOP antagonists *nor*BNI and JDTic in Sprague-Dawley rats.[135] Immobility, swimming, and climbing were measured in 5 second segments during the 5 minute forced swim test. Desipramine, a tricyclic antidepressant, decreased immobility and increased climbing for all doses tested and increased swimming at dose 5.6 mg/kg compared to vehicle. *Nor*BNI decreased immobility and

increased swimming at doses of 1 and 10 mg/kg but did not affect climbing relative to vehicle. JDTic decreased immobility and increased swimming at doses 0.3, 1, and 3 mg/kg without affecting climbing compared to vehicle. Retest of the forced swim test was performed one week after initial test and drug injection. Desipramine and *nor*BNI did not differ from vehicle in measurement of immobility, swimming or climbing. High doses of JDTic (3 and 10 mg/kg) still showed positive effects by reducing immobility time. KOP receptor antagonists *nor*BNI and JDTic show similar profiles to SSRI antidepressants by decreasing immobility and increasing swimming time in the forced swim test.

Correlation of KOP receptors and the modulation of the dopamine system in the brain cause concern with the potential use of KOP antagonists as antidepressants as the majority of drugs of abuse are associated with modulation of dopamine function.[159,160] Therefore, investigations into the intracranial self-stimulation (ICSS) behavior and KOP antagonist ANTI were performed.[161] It was found that ANTI doses eight-times higher than required for antidepressant-like effects in the forced swim test did not alter ICSS behavior. Additionally, KOP antagonist effects on dopamine by direct administration of KOP antagonists into the nucleus accumbens are significantly less relative to cocaine and amphetamine.[162] Currently, no evidence has been found reporting similarities in behavioral effects of KOP antagonists with those associated with drugs of abuse.[150] Drawbacks to known KOP antagonists include their long duration of action and the limited number of studies published about the therapeutic potential of KOP antagonism for depression.[150] Recently several chemical series have been identified that have lacked long-lasting inhibition in a diuresis assay, unlike previously known KOP antagonist.[163] Identification and development of novel KOP receptor antagonists with

more drug-like pharmacodynamic and pharmacokinetic properties has the potential to further explore the therapeutic area of depression by utilizing a previously unexplored therapeutic target.

KOP Receptor Ligands and Other Therapeutic Potential

Additionally, KOP receptors have been linked to immunomodulation and neuroprotective effects.[60] The therapeutic utility of opioid receptors and their potential immunomodulatory role is a relatively recent field. KOP receptors have been recognized on cells from the immune system and human microglia cells have been identified to contain KOP receptor binding sites on the cell surface.[164,165] KOP receptors also have been linked to activated T-cells due to the elucidation of KOP receptor expression on CD4+ and CD8+ cells.[164,166] Future investigation into this area has the potential for novel therapeutic development.

KOP receptors have been implicated to have a role in neuroprotection.[167] Depending on the seizure model employed, KOP agonists have exhibited anticonvulsant effects in some models.[167] Specifically, KOP agonist ethylketocyclazocine displayed naloxone-sensitive anticonvulsant activity in an electrically induced convulsion model of rats.[167,168] The modulation of the KOP system after traumatic or ischemic injury has been reported in rat and rabbit models.[167,169,170] In different animal models, KOP modulation has shown the ability decrease hippocampus neuronal damage resulting from ischemia, improve concussion-induced injury and forebrain ischemia, and improve motor recovery after spinal injury.[167] However, to date, the neuroprotective effect of KOP receptors remains contradictory and controversial.

Drawbacks of Current KOP Ligands

The lack of known ligands with KOP receptor activity, desirable biological effects, and suitable ADMET properties has limited the therapeutic utility of KOP receptors. Known KOP agonists commonly cause sedation, dysphoria, and psychomimetic effects.[96] Additionally, KOP antagonists such as *nor*BNI, GNTI, and JDTic all share the pharmacological property of long duration of activity *in vivo*.[171-177] Several hypotheses for the long duration of activity include being trapped in lipid membranes, biotransformation to long-lasting metabolites, and uncoupling of the KOP receptor signaling complexes. In 2007, Bruchas and coworkers showed that KOP antagonists disrupt KOP receptor signaling through activation of c-Jun N-terminal Kinase (JNK) in a KOP receptor dependent mechanism.[178] Investigations into new structural classes could lead to the identification of ligands that have more desirable properties for a marketed therapeutic.[163] One structural class to be investigated includes neoclerodane diterpenes, a subclass of the more broadly defined terpene class of natural products.

Terpenes

Neoclerodane diterpenes are members of the terpene class of natural products. Terpenes provide interesting chemical targets for organic chemists and pharmacologists. Their structural complexity and diversity, along with their unique pharmacological profiles results in attractive structural scaffolds for synthetic and biological investigation. Terpenes are secondary metabolites and are consequently found in negligible concentrations in living organisms.[179] Many current therapeutic agents are terpenes including taxol as an anticancer drug and artemisinin as an antimalarial agent.[8] Terpenes are derived from a common biosynthetic pathway originating with mevalonate and biosynthesized from units of isoprene, which have the

chemical formula C_5H_8.[179,180] The classification of terpenes is based on the varying number of isoprene units present in the carbon skeleton.[179] Terpene classification includes hemiterpenes, monoterpenes, sesquiterpenes, diterpenes, sesterterpenes, and triterpenes, each consisting of one through six isoprene units.[181] Additional terpene classifications include tetraterpenes, containing eight isoprene units, and polyterpenes composed of isoprene chains. The classification system is further divided into subclasses.[179]

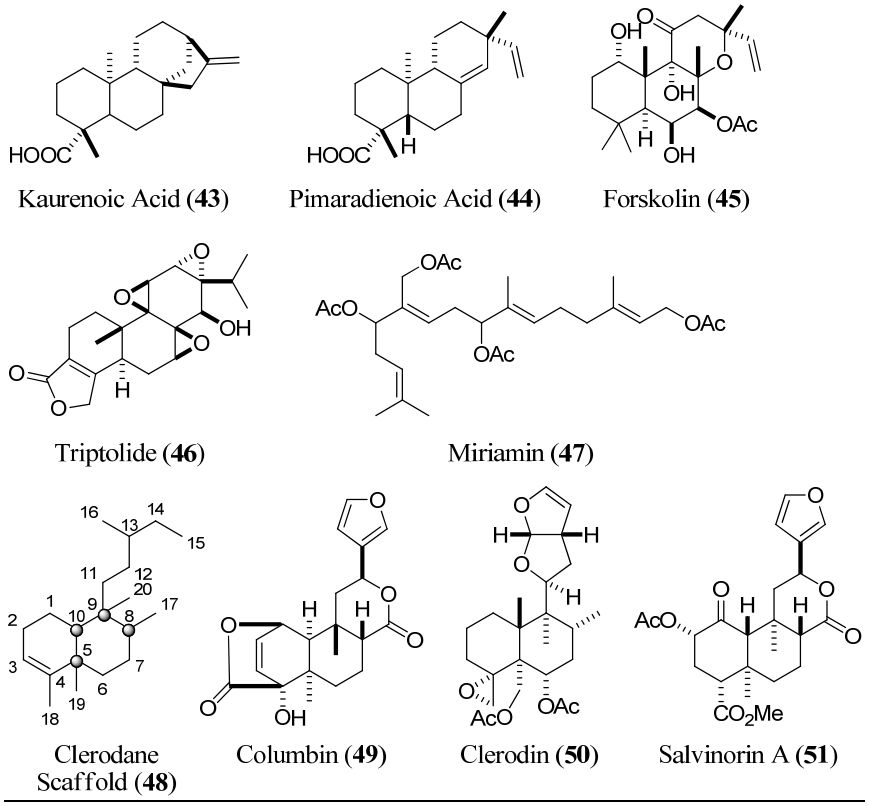

Figure 9: Structures of Selected Diterpene Natural Products

Specifically focusing on diterpenes, over 50 different subclasses have been assigned based on biosynthetic ring construction inclucing labdanes, kauranes, gibberellins, taxanes, and beyeranes. Many of these subclasses are comprised of secondary metabolites with biological activity including cardiovascular, anti-cancer, anti-inflammatory, analgesic, antimicrobial, and

antifeedant effects.[181-183] Kaurane and pimarane-type diterpenes including kaurenoic acid (**43**) (**Figure 9**) and pimaradienoic acid (**44**) have been identified to have cardiovascular effects attributed to inhibition of extracellular Ca^{+2} influx.[184] Kaurenoic acid has also been shown to have antimicrobial activity, anti-parasitic activity, and anti-inflammatory activity.[184-186] A number of terpenoids from the labdane subclass have displayed anti-cancer activity including forskolin (**45**), isolated from *Coleus forskholii*. Forskolin has been reported to decrease proliferation and induce apoptosis while also being associated with anti-hypertensive activity.[180] Taxol, isolated from *Taxus brevifollia*, is a member of the taxane subclass and is a currently available anticancer agent. *Tripterygium wilfordii* Hook F. has been used for centuries in traditional Chinese medicine to treat rheumatoid arthritis, immune complex nephritis, and systemic lupus erythematosus.[187,188] Diterpene triptolide (**46**) was identified from this extract and shown to have anti-inflammatory and immunosuppressive properties.[187] Studies have shown that triptolide blocks gene transcription of several transcription factors including NF-κB and AP-1.[188-190] A number of diterpenes are known for their antifeedant activity including miriamin (**47**) isolated from the eggs of *Arion sp.*, a species of slug.[191] The soft eggs are laid in clusters which were identified to contain diterpene miriamin that acts as a chemical deterrent.[191]

Another well known subclass of diterpenes is the clerodane class. Clerodanes are ubiquitous throughout nature and are found in a variety of plants, fungi, and microorganisms.[192] A natural product is regarded to be a clerodane if it contains four isoprene units and four contiguous stereocenters on a *cis* or *trans* decalin ring system (**48**).[192] Approximately 25% of clerodanes contain the *cis* ring fusion and an example of this is the natural product columbin (**49**).[192] Diterpenoid furanolactone **49** has been isolated from several plants including *Sphenocentrum jollyanum* Pierre (Menispermaceae) and *Jateorhiza columba* Miers

(Menispermacea).[193,194] It is sold in a crude drug preparation called Calumbae Radix or Tinosporae Radix.[193] Columbin itself has been shown to have dose dependent anti-inflammatory activity and chemopreventative activity against colorectal cancer.[193-195] The other 75% of clerodanes contain the *trans* ring fusion resembling clerodin. Clerodin (**50**) was orginially originally isolated from *Clerodendrum infortunatum* L. (Lamiaceae) and is an insect antifeedant with potential as a natural pesticide.[196-198] Along with the relative configuration of the *trans* or *cis* junctions of the fused rings, clerodanes are further classified by their relative configuration at C-8 and C-9.[192] This additional clarification results in four types of clerodane skeletons as defined with respect to configuration of ring fusion and substitution pattern at C-8 and C-9: *trans-cis* (TC), *trans-trans* (TT), *cis-cis* (CC) and *cis-trans* (CT).[192] Clerodanes are further classified by their absolute stereochemistry. Compounds that have the same absolute stereochemistry as clerodin are termed neoclerodanes and compounds that are enantiomers of clerodin are referred to as *ent*-neoclerodanes.[199,200]

Another clerodane with unique biological activity is salvinorin A (**51**). Salvinorin A is the active component of *Salvia divinorum* known for its hallucinogenic effects.[137,201] Salvinorin A (**51**) is a tricyclic *trans-cis* neoclerodane diterpene containing seven chiral centers. Additionally, salvinorin A is oxidized relative to the clerodane scaffold which manifests as four carbonyls at C-1, C-17, C-18, and C-21. Two of the carbonyls are esters off of the C-2 and C-4 positions of the decalin core, and the C-17 carbonyl is part of a δ-lactone ring system. Additionally, an oxygen bridge between C-15 and C-16 results in the formation of a furan ring extending off of C-12. Along with the functionality present on salvinorin A, C-8 has been shown to undergo epimerization readily in acidic or basic conditions. Despite the molecular complexity,

several total syntheses of salvinorin A have been accomplished and structural modifications have been completed.[202-204]

The biological activity and structural complexity of natural products and neoclerodane diterpenes have driven their study in total synthesis efforts and pharmacological investigation into their biological and structure-activity relationship (SAR) studies. However, difficulties in conducting these studies result from the structural complexity, sensitivity to conditions of many typical organic reactions, potential problems in acquiring the natural product or plant material for extraction, and the unknown sites of action of neoclerodane diterpenes.[205] The lack of precedent for chemical methodology required to transform neoclerodanes contributes to the limited number of SAR studies to date. Furthermore, developing reactions that are chemoselective for molecules that are often polyfunctionalized and contain multiple chiral centers is an extremely difficult undertaking. Determination of the molecular basis of activity through semi-synthetic means requires access to the natural product in substantial quantities, which can be difficult or impossible to obtain. Additionally, the site of action of neoclerodane diterpenes is often unknown, increasing the difficulty in SAR development. Despite these challenges, several neoclerodane diterpenes, including salvinorin A, isolated from *Salvia divinorum*, have been investigated through total synthesis, semi-synthetic, and pharmacological studies.

CHAPTER II. SALVINORIN A

Salvinorin A

Salvia divinorum L. Epling & Jativa (Lamiaceae) is a widely available psychoactive plant that has been used for hundreds of years in the traditional divination rituals of the Mazatec Indians of Oaxaca, Mexico due to its hallucinogenic effects.[206] *S. divinorum* is a member of the sage family and is indigenous to Oaxaca, Mexico.[206,207] In addition to its use in divination ceremonies, the Mazatec Indians also use *S.divinorum* for headaches, rheumatism, and *panzón de barrego*, a semimagical disease.[207] *S. divinorum* is also known in the public eye for its notorious use as a recreational drug.[208,209] Due to its hallucinogenic effects, several countries and states have schedule *S. divinorum* as a schedule I controlled substance. The main active component of *S. divinorum* is neoclerodane diterpene salvinorin A (**51**).[137,201,206,210] Salvinorin A rivals the potency of other classical hallucinogens such as lysergic acid diethylamide (LSD) (**52**) (**Figure 10**) and 4-bromo-2,5-dimethoxyamphetamine (DOB) (**53**).[137,201,206,210,211] However, unlike LSD and DOB, salvinorin A does not have activity at serotonin $5HT_{2A}$ receptors.[210,212] In 2002, salvinorin A was identified as a potent and selective KOP receptor agonist.[137] Salvinorin A is the first non-nitrogenous natural product having high affinity and efficacy at KOP receptors.[137] Its unique structure has little structural similarity to other known opioid receptor ligands in that it does not contain a basic nitrogen. Morphine (**19**), cyclazocine (**54**), fentanyl (**24**), SNC 80 (**55**), U50,488 (**36**), 3FLB (**56**), and dynorphin A (**34**) are all known opioid ligands and all have a basic amino group, which was a stipulation for affinity at opioid receptors in traditional opioid pharmacology.[213-217] It was accepted that the positively charged nitrogen of the ligand interacts with a highly conserved aspartate residue in TM III of the opioid receptor.[215,218,219] Salvinorin A

lacks a basic amino group, which consequently led to reevaluation of the necessity of a basic nitrogen for opioid receptor affinity and efficacy.[220]

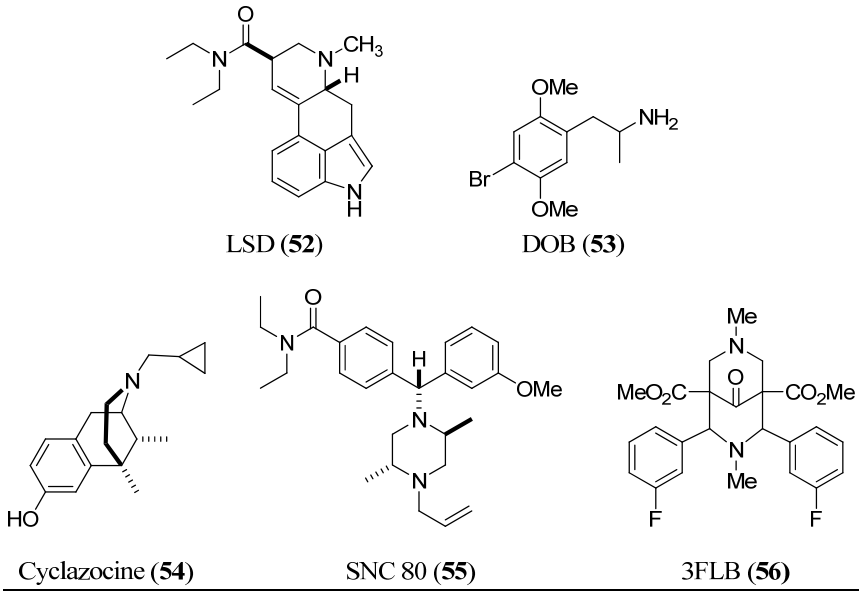

Figure 10: Selected Classical Hallucinogens and KOP Receptor Ligands

Salvinorin A KOP receptor Pharmacology

In vitro Pharmacology

In 2002, Roth and coworkers identified salvinorin A as the first non-nitrogenous, naturally occurring opioid receptor agonist.[137] More specifically, salvinorin A was determined to be potent and selective for KOP receptors. The molecular pharmacological profile of salvinorin A was examined through a large scale screening of at 51 molecular targets including human cloned GPCRs, ligand-gated ion channels, and transporters with the support of the NIMH Psychoactive Drug Screening Program. Salvinorin A was found to only inhibit [^{3}H]-bremazocine-labeled KOP receptors and did not bind to cloned MOP or DOP receptors, identifying an opioid subtype specific ligand. The functional properties of salvinorin A were then evaluated in a two model system. Salvinorin A was evaluated for its ability to inhibit

forskolin-stimulated cAMP production in KOP receptor stably expressed HEK-293 cells and *in situ* in guinea pig caudate membranes. In both systems, salvinorin A was identified as a potent KOP receptor agonist. A more detailed report of the functional properties of salvinorin A was reported in 2004 by Chavkin *et al*.[221] The ability of salvinorin A to inhibit forskolin-stimulated cAMP activity, intracellular calcium mobilization and potassium conductance were all evaluated. In all assays tested, salvinorin A was shown to be a potent and full agonist compared to known KOP receptor agonist U69,593. KOP receptor subtypes have been suggested through ligand binding and physiological studies but have not been identified through gene coding.[222-224] Asnonoff and coworkers evaluated salvinorin A's ability to selectively bind to KOP_1 or KOP_2 receptors utilizing ligand-binding evidence. Salvinorin A showed selective affinity at KOP_1 receptors and not at KOP_2 receptors (K_i = 18.7 nM vs. K_i > 10,000).[87]

Wang and coworkers evaluated the pharmacological activity of salvinorin A in CHO cells and determined that salvinorin A had affinity and potency similar to U50,488 (Salvinorin A: K_i = 7.9 nM, EC_{50} = 4.6 nM vs. U50,488: K_i = 11.0, EC_{50} = 2.2 nM).[225] Additionally, they evaluated salvinorin A's ability to promote receptor internalization and down-regulation of KOP receptors. Previous studies have shown that activation of KOP receptors by U50,488, U69,593, and other KOP agonists down-regulate and internalize KOP receptors to variable extents.[226-228] The resulting down-regulation and internalization of receptors is largely believed to play a role in tolerance.[123,124,229] Using fluorescence flow cytometry, incubation of salvinorin A with cells expressing FLAG-hKOP receptors resulted in a dose-dependent reduction of cell surface fluorescence demonstrating internalization of the FLAG-hKOP receptors. Salvinorin A is less potent than U50,488 for inducing internalization of KOP receptors (30 – 40% vs. 15%).[87]

In vivo Pharmacology

Salvinorin A and Psychoactive Effects

Traditionally, two methods of ingestion are reported: chewing whole leaves or crushing the leaves to extract juices which are then swallowed.[210] Initial pharmacological investigations by Seibert determined that the active component of *S. divinorum* is deactivated in the gastrointestinal system and in tradition methods of ingestion the psychoactive effects have resulted from oral absorption. Salvinorin A absorption through oral mucosa produced effects within 5 to 10 minutes that plateau at approximately an hour and decreased in the following hour. Vaporization and inhalation of leaves caused effects within 30 seconds with peak effects occurring from 5 to 10 minutes and subsiding around 30 minutes. Doses of 200 – 500 μg of pure salvinorin A produced effects that are behaviorally comparable to those of traditional ingestion methods making salvinorin A one of the potent naturally occurring hallucinogens to date.

In 2011, Johnson and coworkers investigated the effects of salvinorin A in human subjects.[230] Using a double-bind, placebo controlled study, 16 doses of salvinorin A were evaluated in ascending order with four placebo doses inserted into the sequence. Salvinorin A was administered via vaporization and inhalation at doses ranging from 0.375 – 21 μg/kg. Subjective effects along with physiological effects were measure for one hour. Time and dose-dependent effects were observed with the maximal effects seen at 2 minutes, the first time point evaluated. Using the Hallucinogen Rating Scale and the Mysticism Scale, salvinorin A administration resulted in dose-related increases on most subscales starting at the dose of 4.5 μg/kg. Over the range of doses tested, no significant effects on heart rate and blood pressure were detected along without any observation of resting or kinetic tremors. These finding suggest

that salvinorin A has subjective hallucinogenic effects similar to other classical hallucinogens and is physiologically safe at the doses tested.

Mendelson and coworkers investigated the sublingual administration of ascending doses of salvinorin A ranging from 0 – 4 mg in a placebo-controlled study.[231] Subjective effects were measured by two Visual Analog Scales and the Subjective Drug Effects Questionnaire (SDEQ), Altered States of Consciousness Questionnaire (APZ-OAV), and Positive and Negative Affect Schedule (PANAS) two and four hours after drug administration. Physiological effects including heart rate, blood pressure, O_2 saturation, and body temperature were also measured. Blood and urine samples were collected for the highest dose (4 mg) and in two subjects at 1 mg dose that reported slight VAS intoxication effects. For all doses tested, no significant difference in subjective effects and physiological effects were observed and blood and urine analysis found that most concentrations were below the limit of quantitation.

Hooker and coworkers investigated the pharmacokinetic properties of salvinorin A in living brain concentrations by using positron emission spectroscopy (PET) in female baboons (*Papio anubis*).[232] Through synthesis of a ^{11}C-labeled salvinorin A derivative, use of PET, and intravenous administration, they found that salvinorin A rapidly entered the brain and reached maximum concentrations at approximately 40 seconds and had a half-life of 8 minutes. The highest concentrations of salvinorin A were found in the cerebellum and the cortex and it is hypothesized that the high concentrations in these brain regions account for the hallucinogenic effects. Kinetic analysis suggests two modes of metabolism and excretion occur through the biliary and renal systems. These findings are consistent with the observed effects when smoking *S. divinorum*. Based on the maximum brain concentration, they deduce that less than 10 μg of salvinorin A in the human brain is required to cause hallucinations.

Salvinorin A and Metabolism

Schmidt *et al*. identified salvinorin B as a major metabolite of salvinorin A in *ex vivo* non-human primate studies.[233] Salvinorin B concentrations *in vivo* were below the limit of detection suggesting salvinorin B is rapid cleared or accumulates in tissue or organs.[233,234] A study in human volunteers by Pichini and coworkers found that based on a theoretically administered dose, only 0.8% of salvinorin A is excreted unchanged in urine when 0.58 mg of *S. divinorum* leaves are smoked.[235]

Tsujikawa et al. further evaluated the metabolism of salvinorin A in rat plasma, specifically focusing on esterase metabolism.[236] Four esterases are found in rat plasma including butyrylcholinesterase (BChE), acetylcholinesterase (AChE), arylesterase (ArE), and carboxylesterase (CES), and each could be responsible for salvinorin A metabolism. To determine the role of each esterase, salvinorin A was incubated in rat plasma, with and without the addition of NaF, a known esterase inhibitor, and known selective esterase inhibitors. Analyses were complete using LC-MS/MS and several metabolites formed were thought to result from C-2 deacetylation. To substantiate these findings, salvinorin A was incubated in the presence of NaF, which inhibited the formation of these metabolic products. Additionally, BNPP, a CES inhibitor, and PMSF, a serine esterase inhibitor (CES is a serine esterase), were found to inhibit salvinorin A metabolism in a concentration-dependent manner. Inhibitors of BChE, AChE, and ArE caused minimal degradation products of salvinorin A implicating CES as the esterase responsible for salvinorin A metabolism in rat plasma. Tsujikwaka and coworkers also identified lactone hydrolysis by a calcium-dependent lactonase.

Teskin and coworkers investigated salvinorin A's *in vitro* metabolism with ten CYP450 isoforms and UGT2B7, the major enzyme involved in drug metabolism via glucuronidation.[237-240] Salvinorin A was separately incubated with each CYP450 for one hour at 50 μM concentration.[237] A significant decrease in concentration was seen when salvinorin A was incubated with CYP2D6, CYP1A1, CYP2E1, and CYP2C18. Further analysis of salvinorin A metabolism was performed by incubating salvinorin A with 5 μM concentrations of the CYP450 isoforms active at higher concentrations. The CYP450 isoforms also showed a statistically significant reduction of salvinorin A at 5 μM. Salvinorin A was also incubated with UGT2B7 at concentrations of 5, 10, and 50 μM. A statistically significant difference in metabolism was seen between the three doses relative to the control (51%, 18.1%, and 7%, respectively). Comparing the percentages of metabolism at the different concentrations for CYP450 and UGT2B7 metabolism, higher rates of metabolism were seen at lower doses suggesting saturable metabolism and Michaelis-Menten kinetics. These studies suggest that salvinorin A may be a substrate for CYP2D6, CYP1A1, CYP2E1, CYP2C18, and UGT2B7.

Salvinorin A and Toxicity

The first study to investigate the potential toxicity associated with salvinorin A as a pure isolated compound was performed by Mowry and coworkers.[241] Animal studies that explored the acute effects of salvinorin A in rats showed no statistically significant effect of rat heart rate and cardiac conduction. However, pulse pressure did non-significantly increase after exposure. Additionally, salvinorin A did not cause changes in body temperature or galvanic skin response. The chronic effects of salvinorin A were measured in mice and concluded that after fourteen days of i.p. salvinorin A injections, no significant histologic changes were seen in the spleen,

blood, brain, liver, kidneys, and bone marrow at the doses tested. Mowry concluded that salvinorin A had little physiologic effect and has relatively low toxicity.

Salvinorin A and CNS Effects

In 2007, Butelman and coworkers investigated the effects of salvinorin A in a prolactin neuroendocrine biomarker assay.[242] Intravenous administration of salvinorin A and U69,593 (0.0032, 0.01, 0.032, 0.056 mg/kg) resulted in dose-dependent and time-dependent increases in prolactin levels. In male subjects, increases in prolactin levels were seen 5 minutes after salvinorin A injection. At 90 minutes no dose was significantly different than vehicle prolactin levels. U69,593 had a longer duration of action with increased prolactin levels still noticeable at the end of the 120 minute testing period. Gonadally intact female monkeys have quantitatively greater salvinorin A effects. Therefore, prolactin levels in gonadally intact female monkeys were also evaluated. A dose of 0.0032 mg/kg causes only slight effect in males where as in females this dose caused larger prolactin elevations. Subcutaneous administration of salvinorin A was investigated at 0.032 mg/kg. Subcutaneous injection produced much lower prolactin levels and a slower onset with peak effects not occurring until the 60 minute time point. Subcutaneous injection of salvinorin A (0.032 mg/kg) in females produced effects by 15 minutes and lasted until the 120 minute time point. To test the role of KOP receptors in the effects of salvinorin A, nalmefene was utilized. A low dose (0.01 mg/kg) of nalmefene antagonizes MOP receptors where a higher dose (0.1 mg/kg) antagonizes both MOP and KOP receptors. Pretreatment of 0.01 mg/kg nalmefene did not cause statistically significant changes in prolactin levels but a higher dose of 0.1 mg/kg antagonized the neuroendocrine effects of salvinorin A. Pretreatment with ketanserin, a 5-HT_2 antagonist showed no antagonism of salvinorin A. Additionally,

Butelman *et al*. showed 98.4% homology between the rhesus monkey OPRK1 gene and human OPRK1 gene, which codes the KOP receptor.

Butelman and coworkers were the first to investigate the fast onset and entry into the central nervous system and the unconditioned behavioral effects of salvinorin A in primates.[243] Behavioral scales were utilized that are known to measure the effects of centrally penetrating KOP receptor agonists. Sedation, postural relaxation, facial relaxation, and ptosis were all measured. Intravenous doses of 0.032 and 0.1 mg/kg salvinorin A in chaired subjects resulted in dose-dependent increases in sedation scores with statistical significance found at the 5, 15, and 30 minute time points. Using identical salvinorin A doses with subject in their home cage, salvinorin A caused dose-dependent effects on sedation and postural effects at the 5 and 15 minute time points or at the 5, 15, and 30 minute time points, respectively. Dose-dependent and time-dependent facial relaxation and ptosis were also seen following intravenous administration of salvinorin A. The behavioral effects of salvinorin A were compared to known KOP agonist U69,593. U69,593 also resulted in dose-dependent behavioral effects with a less defined time course and longer lasting effects. Pretreatment of opioid antagonist nalmefene was given prior to salvinorin A injection and almost fully prevented the behavioral effects of salvinorin A. Additionally, nalmefene was given 11 minutes after salvinorin A injection to test the ability to reverse the behavioral effects of salvinorin A. Nalmefene did cause rapid reversal of ongoing salvinorin A-induced facial relaxation and ptosis. Pretreatment of CB_1 antagonist rimonabant and serotonergic antagonist ketanserin were both ineffective at preventing salvinorin A-induced behavioral effects, further implicating KOP receptors in the modulation of salvinorin A's behavioral effects in nonhuman primates.

Further investigations by Butelman and coworkers compared the behavioral effects of salvinorin A resulting from intravenous and subcutaneous administration.[244] Unconditioned behavioral effects of facial relaxation and ptosis were measured and found that intravenous administration resulted in a more robust response and a faster onset than subcutaneous administration. In fact, subcutaneous administration did not cause significant differences compared to vehicle in the measurement of facial relaxation. Intravenous administration of salvinorin A and U69,593 resulted in dose-dependent ptosis in all subjects and the unconditioned behavioral effect was reversed by opioid antagonists quadazocine and naltrexone. Peripherally restricted KOP agonist ICI204448 did not cause facial relaxation but did result in ptosis with much less potency that salvinorin A or U69,593. This suggests that at high doses, ICI204448 can result in centrally mediated effects. Additionally, the serotonergic agonist psilocybin did not result in facial relaxation or ptosis at any dose tested.

Salvinorin A and Drug Discrimination

The first study to investigate salvinorin A's discriminative effects in non-human primates was performed by Butelman and coworkers.[245] Rhesus monkeys were previously trained to discriminate KOP agonist U69,593 from vehicle. Administration of U69,593 in trained monkeys produced dose-dependent generalizations in all subjects. Systemic subcutaneous administration of salvinorin A fully substituted for U69,593 in a dose-dependent manner. Pretreatment with opioid antagonist quadazocine at an appropriate does of 0.32 mg/kg fully blocked the discriminative effects of salvinorin A and U69,593 in all test subjects. In two of the three subjects, long acting KOP selective antagonist GNTI blocked the effects of salvinorin A. A control experiment was performed using NMDA antagonist ketamine, which has been known to

produce psychomimetic effects or hallucinations in humans. Ketamine was not generalized by the rhesus monkeys trained to discriminate U69,593, therefore further implicating salvinorin A's mechanism of action as a selective KOP receptor agonist in non-human primates.

Drug discrimination studies were extended to rat by Willmore-Fordham and coworkers.[246] They found that salvinorin A fully substituted for U69,593 at doses of 1, 1.9, and 3 mg/kg in behavioral response of appropriate drug lever selection without systematically decrease in the number of times the lever was pressed as does increased. Pretreatment with KOP antagonist *nor*BNI (10 mg/mL, 3 μL, i.c.v.) one hour before salvinorin A administration blocked salvinorin A discriminative effects. Co-administration of *nor*BNI and salvinorin A resulted in the majority of vehicle lever responses.

Further investigation by Baker and coworkers extended these findings in rats.[247] Rats were trained to discriminate 0.13 mg/kg U69,593, 3.0 mg/kg U50,488, or 2.0 mg/kg salvinorin A; lower doses than previously evaluated. In rats trained to discriminate U69,593, salvinorin A was found to result in a dose-dependent increase in drug-appropriate responding and full substitution for U69,593 at 1.0 mg/kg. In U50,488 trained rats, salvinorin A once again resulted in U50,488-appropriate responding and fully substituted for U50,488 at 3.0 mg/kg. In salvinorin A trained rats, U69,593 and U50,488 resulted in complete stimulus generalization.

Discriminative hallucinogenic activity has been evaluated in rodents to a much greater extent than in nonhuman primates. Li *et al*. extended these findings by evaluating hallucinogenic activity in nonhuman primates.[248] Rhesus monkeys were trained to discriminate between 0.32 mg/kg of 5-HT_{2A} receptor agonist DOM and vehicle. A number of known hallucinogens and drugs from other classes, including amphetamines, NMDA receptor antagonists, and D_2/D_3 receptor agonists, were given to determine the discriminative stimulus effects of DOM. Of

interest was that salvinorin A and U69,593 failed to substitute for DOM in monkeys. This further illustrates that salvinorin A does not exert its hallucinogenic effects through 5-HT_{2A} receptors.

Butelman *et al*. showed that rhesus monkeys trained to discriminate salvinorin A generalized arylacetamide KOP receptor agonists U69,593 and U50,488, which had been previously shown in rats.[244,247] Butelman also investigated structurally diverse KOP receptor agonist bremazocine, which was also generalized in these nonhuman primates. Peripherally selective KOP receptor agonist ICI204,448 was only generalized in one of three subjects, further linking salvinorin A discriminative effects to central KOP agonist effects. MOP agonist fentanyl, DOP agonist SNC80, 5-HT_2 agonist psilocybin, and NMDA antagonist ketamine were also investigated and found not to be generalized at any dose in subjects trained to discriminate salvinorin A. Opioid antagonist quadazocine (0.32 mg/kg) reversed the discriminative effects of salvinorin A for all salvinorin A doses and 5-HT_2 antagonist ketanserin did not block the discriminative effects of salvinorin A.

Killinger *et al*. expanded the evaluation of salvinorin A discriminative effects to another species; the Sprague-Dawley rat.[249] Rats were trained to discriminate either serotonergic hallucinogen LSD or noncompetitive NMDA antagonist ketamine. Salvinorin A did not substitute for LSD in LSD-trained rats or ketamine in ketamine-trained rats up to doses that significantly reduced responding.

Salvinorin A and Antinociceptive Effects

In 2005, Wang *et al*. investigated the antipruritic and antinociceptive activities of three non-arylacetamide KOP receptor agonists: TRK-820, 3FLB, and salvinorin A.[225] Antiscratching

effects were measured in the compound 48/80-induced scratch assay and antinociceptive effects were measured using the acetic acid abdominal constriction test. In the compound 48/80-induced scratch assay TRK-820 was found to potently inhibit scratching while 3FLB showed no inhibition and salvinorin A produced very low activity. Additionally, in the abdominal constriction assay, TRK-820 had potent antinociceptive effects, 3FLB showed no effect, and salvinorin A produced inconsistent and no dose-related effects.

Conflicting results were published by McCurdy and coworkers in 2006 when they evaluated the effects of intraperitoneal injection of salvinorin A in the tail-flick test, hot-plate test, and the acetic acid abdominal constriction assay.[250] They found that salvinorin A produced short-acting (peak effects at the 10 minute time-point) antinociceptive effects in mice in the tail-flick test, hot-plate test, and the acetic acid abdominal constriction assay. Furthermore, results in the tail-flick test showed pretreatment with *nor*BNI inhibited the increased latencies. They also hypothesize that the differences in antinociceptive effects compared to Wang and coworkers was a result of the time frame evaluated. Wang and coworkers administered salvinorin A 20 minutes prior to measuring abdominal constrictions while McCurdy found salvinorin A's peak effects are at 10 minutes and at 20 minutes the analgesic effect of salvinorin A were no longer present.

Investigation by John and coworkers provided more evidence for the antinociceptive effects of salvinorin A.[251] They found that intrathecal injection of salvinorin A caused a dose-dependent antinociceptive effect in mice measured in the tail-flick test. Tail-flick latencies were not altered by pretreatment of MOP receptor antagonist β-FNA or DOP receptor agonist NTI, but the increase of tail-flick latencies were abolished by pretreatment of KOP antagonist *nor*BNI.[251]

Ansonoff and coworkers investigated the antinociceptive and hypothermic effects of salvinorin A in wild-type and KOR-1 knock-out mice.[87] Salvinorin A intracerebroventricular injection of 7.5 μg showed significant antinociceptive effects at the 15 minute time-point of the tail-flick test in wild-type mice. By 30 minutes, tail-flick latencies were not significantly different from vehicle. A 50 μg intracerebroventricular injection of salvinorin A was evaluated and antinociceptive effects were seen at the 15 minute time-point but significant drug effect was sustained until the 45 minute time-point in wild-type mice. Significant hypothermia, measured by rectal body temperature, was not seen at salvinorin A dose of 7.5 μg but was reported at a dose of 50 μg, lasting at least 120 minutes in wild-type mice. Neither dose-dependent antinociceptive nor hypothermic effects were seen in KOR-1 KO mice. The analgesic and hypothermic efficacy of salvinorin A is consistent with other KOP agonists.

Salvinorin A and Gastrointestinal Effects

Limited research has been performed evaluating salvinorin A's effects on gastrointestinal function. Capasso *et al*. evaluated salvinorin A's ability to inhibit enteric cholinergic transmission in the guinea-pig ileum.[252] Ileum strips were subjected to electrical field stimulation (EFS) and the contractile responses were measured. Exposing the ileum to salvinorin A or U50,488 resulted in partial dose-dependent decreases in amplitude of EFS-evoked contractions. Inhibition of enteric cholinergic transmission by salvinorin A did not occur in the presence of opioid antagonist naloxone or KOP receptor antagonist *nor*BNI. EFS contraction inhibition was not affected by exogenous acetylcholine, further implicating salvinorin A's effects through activation of prejunctional KOP receptors. Additional work by Capasso *et al*. evaluated salvinorin A's ability to reduce inflammation-induced hypermotility in mice.[253] Small intestine

hypermotility and inflammation were induced with two administrations of croton oil. Doses of salvinorin A tested ranged from 0.01 – 10 mg/kg. Salvinorin A produced a dose-dependent decrease in intestinal motility starting at 3 and 0.3 mg/kg in control animals and croton-oil treated mice, respectively. Interesting to note is the increase in sensitivity of salvinorin A in croton-oil treated mice. U50,488 was also evaluated and showed a dose-dependent decrease in intestinal motility comparable in control and croton-oil treated mice. The decreases in motility cause by salvinorin A and U50,488 were both antagonized by *nor*BNI.

Salvinorin A and Drug Abuse

Morani *et al*. investigated salvinorin A's ability to act like other KOP agonists and attenuate cocaine-induced drug-seeking in rats.[254] Doses of 0.3 or 1.0 mg/kg salvinorin A via intraperitoneal administration were found to dose-dependently decrease cocaine-produced reinstatement after a 20 mg/kg intraperitoneal priming dose of cocaine. At a dose of 0.3 mg/kg, salvinorin A did not reduce cocaine hyperactivity. Additionally, salvinorin A doses of 0.3 and 1.0 mg/kg did not significantly decrease sucrose self-administration.

In 2008, Chartoff and coworkers investigated salvinorin A's ability to modulate cocaine induced locomotor-stimulant effects and c-Fos expression in the dorsal striatum when salvinorin A was given chronically or acutely.[255] Acute salvinorin A administration 5 minutes prior to cocaine injection significantly attenuated cocaine-stimulated locomotor activity in a 2 hour time frame to that of rats treated with vehicle or salvinorin A and saline. Acute salvinorin A administration also blocked the locomotor effects of the dopamine receptor agonist SKF 82958. Chronic salvinorin A exposure showed an initial decrease in locomotor activity in the first 15 minutes after drug administration but then significantly increased cocaine-stimulated locomotor

activity for the remainder of the 3 hour period measured relative to vehicle. Also, previous salvinorin A administration showed the ability to potentiate the locomotor effects of cocaine compared to the rats administered vehicle and potentiated the effects of SKF 82958. Previous repeat exposure to salvinorin A and the activity chamber increased the locomotor response to cocaine, while rats only exposed to salvinorin A, without exposure to the activity chamber did not potentiate the locomotor responses to cocaine relative to controls. Cocaine has been shown to induce c-Fos in several brain regions including the dorsal striatum. Stimulus-induced expression of c-Fos occurs from the activation of cAMP and/or Ca^{+2} second messengers. Acute salvinorin A administration resulted in a decreased amount of c-Fos expression in the dorsal striatum but expression was increased when salvinorin A was given repeatedly in the activity chamber. When salvinorin A was administered repeatedly in the home cage, c-Fos expression in the dorsal striatum was unaffected. This study shows the ability of salvinorin A to modulate the locomotor effects of cocaine through mediation of dopamine neurotransmission in the dorsal striatum.

Salvinorin A and Depression

Selective KOP receptor ligands have shown the ability to cause changes in mood in humans and motivation behavior in animals.[97,152,256] Therefore, Carlezon *et al*. investigated the ability of salvinorin A to cause depressive-like effects in rats using the behavioral models of the forced swim test and the intracranial self-stimulation (ICSS) test.[97] Salvinorin A was found to dose-dependently increase immobility and decrease swimming behavior at doses between 0.25 and 2.0 mg/kg. No significant changes in climbing behavior were observed at any dose, and diving was not seen throughout the tests. These behavioral effects are opposite to those seen

with SSRIs.[97,257] To confirm the changes in immobility and swimming were due to salvinorin A's depressive-like effects and not changes in locomotor activity, locomotor activity was measured in an open field following the same doses of salvinorin A given in the forced swim test. No difference in locomotor activity was seen at any dose tested. The ICSS behavioral assay delivers electricity-induced brain stimulation to an area of the brain associated with mediating reward. In this experiment, electrodes were located in the medial forebrain bundle at the level of the lateral hypothalamus. For doses of 0.5, 1.0, and 2.0 mg/kg, salvinorin A was found to dose-dependently increase ICSS thresholds. This suggests that salvinorin A reduces the reward impact of the medial forebrain bundle, which reflects anhedonia and further indicates salvinorin A's prodepressant-like effects. Additionally, microdialysis studies showed that at a dose of 1.0 mg/kg, salvinorin A decreased extracellular dopamine concentrations in the nucleus accumbens without affecting 5-HT levels.

Zhang and coworkers investigated the effects of salvinorin A on basal dopamine levels in the caudate putamen and the nucleus accumbens along with salvinorin A's ability to cause locomotor changes and induce conditioned place preference or aversion in mice.[258] Salvinorin A levels were explored at doses of 0.32, 1.0, and 3.2 mg/kg intraperitoneal. Microdialysis studies showed a dose-dependent decrease of dopamine levels in the caudate putamen with significant decreases observed at doses of 1.0 and 3.2 mg/kg. Pretreatment with *nor*BNI blocked the effect on dopamine levels at salvinorin A's highest given dose. However, significant decreases in dopamine levels were not seen in the nucleus accumbens. Conditioned place aversion and decreased locomotor activity were also seen at the same salvinorin A doses of 1.0 and 3.2 mg/kg. Pretreatment with *nor*BNI attenuated the conditioned place aversion and decreased locomotor activity resulting from salvinorin A administration.

Further investigation of salvinorin A's depressive-like effects was carried out by Ebner and coworkers.[259] They evaluated the ability of salvinorin A to decrease dopamine levels in the core or shell of the nucleus accumbens and salvinorin A's effect on intracranial self-stimulation and sucrose-reinforced responding. The salvinorin A dose of 2.0 mg/kg via intraperitoneal administration was tested as it previously showed ability to increase ICSS threshold and immobility in the forced swim test.[97] Salvinorin A was found to significantly decrease phasic dopamine release in the core and shell of the nucleus accumbens without influencing dopamine reuptake.[259] ICSS behavioral testing showed that 2.0 mg/kg salvinorin A dose-dependently and time-dependently increased ICSS thresholds compared to vehicle. This increase is attributed to a decrease in the rewarding impact of the medial forebrain bundle stimulation. Changes in motivation following salvinorin A injection were additionally measured by progressive ratio responding for sucrose reward. At 2.0 mg/kg, salvinorin A was found to lower breakpoints in progressive ratio responding. Decreased responding for sucrose pellets is recognized as decrease in motivation.

Salvinorin A and Sedation

Fantegrossi *et al*. examined the sedative and/or ataxic properties of salvinorin A in the inverted screen test.[260] All doses of salvinorin A significantly increased climbing time at the 5 minute time point but did not produce dose-dependent effects on climbing behavior. Behaviorally equivalent doses of MOP agonist remifentanil (0.01 mg/kg) and KOP agonist U69,593 (1.0 mg/kg) compared to 2.0 mg/kg salvinorin A were evaluated and found to have similar effects in sedation and motor impairment relative to salvinorin A. Motor incoordination of salvinorin A and U69,593 were significantly attenuated by pretreatment of *nor*BNI but were

not altered by pretreatment of DOP antagonist naltrindole or low dose of opioid antagonist naloxone (0.1 mg/kg). Motor effects of remifentanil were not modified by pretreatment of naltrindole or *nor*BNI but were significantly reduced by naloxone.

Salvinorin A and Cannabinoid Receptors

Braida *et al*. evaluated the hallucinogenic and rewarding effects of salvinorin A in zebrafish by measuring swimming behavior and conditioned place preference.[261] Additionally, they investigated the potential involvement of CB_1 receptors with salvinorin A. Low doses of salvinorin A (0.1 – 10 μg/kg) were evaluated and zebrafish were injected intramuscularly into the caudal musculature. Salvinorin A was found to modify normal swimming behavior in a biphasic manner. Low doses of salvinorin A (0.1 and 0.2 μg/kg) statistically accelerated swimming behavior while higher doses of 5 and 10 μg /kg statistically decreased swimming behavior relative to vehicle. Pretreatment of *nor*BNI or CB_1 antagonist rimonabant reversed swimming behavioral effects comparable to vehicle. Low doses of salvinorin A (0.2 and 0.5 μg/kg) resulted in a statistical increase in time spent in the drug-associated compartment with 0.5 μg/kg dose having the greatest reinforcing effects. Salvinorin A dose of 1.0 μg/kg resulted in no effect relative to vehicle and a higher dose of 80 μg/kg resulted in aversion. Validation of the CCP test was completed by evaluating cocaine and KOP agonist spiradoline. Cocaine increased the time spent in the drug-paired compartment while spiradoline decreased the time spent in the drug-paired compartment. Pretreatment with *nor*BNI or rimonabant reduced the time spent in the drug-paired compartment relative to salvinorin A.

A follow-up study by Braida *et al*. investigated the involvement of the KOP receptor and endocannabinoid systems in Wistar rats by testing low doses of salvinorin A in the conditioned

place preference and intracerebroventricular self-administration paradigms.[262] Subcutaneous administration of salvinorin A resulted in dose-dependent positive CPP response at dose 0.1 μg/kg – 40 μg/kg, a neutral response at 80 μg/kg and a negative CPP response at 160 μg/kg relative to vehicle. The CPP effect of salvinorin A was significantly blocked by pretreatment with *nor*BNI or CB_1 antagonist rimonabant. Additionally, microdialysis showed that 40 μg/kg of salvinorin A, the dose resulting maximum CPP response, significantly increased extracellular dopamine levels in the shell of the nucleus accumbens. Results from intracerebroventricular self-administration studies found the same biphasic trend with lower and higher doses of salvinorin A. Low doses of 0.1 and 0.5 μg/infusion resulted in a significant increase in the number of drug-associated lever pressings and a dose of 1 μg/infusion resulted in a significant decrease in the number of drug-associated lever pressings relative to vehicle. Pretreatment with *nor*BNI or rimonabant both statistically reduced the number of drug-associated lever pressing relative to salvinorin A alone.

An additional study by Braida and coworkers investigated salvinorin A's anxiolytic-like and antidepressant-like behavior in rodent models using the elevated plus maze, the forced swim test, and the tail suspension test.[263] In the elevated plus maze test, salvinorin A was shown to cause significant differences relative to vehicle at doses ranging from 0.1 and 160 μg/kg with no progressive dose-related increase in effect. Salvinorin A's anxiolytic-like effects were reversed by both KOP receptor antagonist *nor*BNI and CB_1 receptor antagonist AM251. Results of the forced swim test contradicted those of Carlezon and coworkers who determine that intraperitoneal administration of salvinorin A caused pro-depressant-like effects in rats.[97] Braida *et al*. tested subcutaneous lower doses of salvinorin A and found that at doses ranging from 0.001 – 10 μg/kg dose-dependently decreased immobility and increased swimming. Additionally,

pretreatment with *nor*BNI and AM251 reversed these effects. The tail suspension test was performed on mice and doses between 0.001 – 1 μg/kg resulted in a decrease in immobility and effects were reversed by pretreatment of *nor*BNI and AM251. These studies suggest both KOP receptors and CB_1 receptors mediate the behavioral and rewarding effects of salvinorin A.

Direct agonist activity of salvinorin A at CB_1 receptors is improbable due to previous studies investigating salvinorin A's binding affinity at these receptors.[137,221] Therefore, Walentiny and coworkers evaluated salvinorin A in several *in vitro* and *in vivo* assays to screen for cannabinoid activity to more fully understand the endocannabinoid system's role in the pharmacological effects of salvinorin A.[264] Salvinorin A did not have affinity in cells transfected with human CB_1 receptor when radiolabeled agonist or antagonist was used for displacement. Additionally, salvinorin A did not activate CB_1 receptors in G protein and calcium flux functional assays or block the effects of CP55,940 in the [^{35}S]GTPγS assay, a characteristic of cannabinoid antagonists. However, rimonabant antagonized U69,593 in a dose-dependent manner in the [^{35}S]GTPγS assay. This *in vitro* data suggests that salvinorin A does not act directly at CB_1 receptors or modulate its signaling cascade. Four *in vivo* assays were performed measuring locomotor activity, tail flick, rectal temperature, and ring immobility. THC was found to dose-dependently decrease spontaneous activity and body temperature, while causing dose-dependent antinociception and catalepsy. Salvinorin A also resulted in a dose-dependent decrease in spontaneous activity and body temperature and dose-dependent antinociception and catalepsy. Of note, salvinorin A altered body temperature and catalepsy to a lesser extent than THC. Coadministration of KOP antagonist JDTic reversed the *in vivo* effects of salvinorin A but coadministration of rimonabant had no effect. THC *in vivo* effects were attenuated by rimonabant; JDTic had no effect on locomotor suppression, antinociception, or catalepsy.

However, JDTic did antagonize THC's hypothermic effects. Additionally, salvinorin A failed to substitute at any dose in THC-trained mice. These studies conclude that the effects of salvinorin A are not mediated by direct or indirect modulation of the endocannabinoid system. It appears that the relationship between salvinorin A and the endocannabinoid system is a consequence of rimonabant's ability to antagonize KOP receptors.

Molecular Modeling Studies

Opioid receptors are members of the membrane-bound GPCR superfamily and consequently their three-dimensional structures have not been elucidated by crystallography. The binding site of salvinorin A will not be certain until the co-crystal structure of salvinorin A and KOP is solved.[95] However, several investigators have undertaken the task to understand its binding through molecular modeling, site-directed mutagenesis, and chimeric receptor studies.[137,265-269] After identifying salvinorin A as a potent and selective KOP receptor agonist, Roth and coworkers performed molecular modeling studies in efforts to elucidate salvinorin A's interactions with the KOP receptor. They utilized a previous model of the KOP receptor with known agonist U69,593 as a starting point.[137] Their modeling parameters proposed the furan ring of salvinorin A is directed towards TM1 with the furan oxygen interacting with Q115, the 4-methoxycarbonyl is orientated towards TM5 and TM6 with the carbonyl oxygen hydrogen bonding with Y312, and the carbonyls of the C-2 acetate and lactone are interacting with Y313 and Y139, respectively. They also identified seven variable residues in the KOP receptor that are not conserved in the MOP or DOP receptors. These variable amino acids result in different steric and electronic effects for KOP receptors comparable to MOP and DOP receptors in the region proposed for the salvinorin A binding site.

In 2005, Yan *et al*. examined salvinorin A binding to KOP receptors through molecular modeling, site-directed mutagenesis, radioligand binding and functional assay analysis of the mutated constructs, and cysteine-substitution mutagenesis.[269] Through their molecular modeling predictions and mutant construct synthesis they found Y312A and Y312F mutants do not alter the affinity of salvinorin A for KOP receptors. Therefore their model proposes little to no interaction with Y312. The retained affinity of salvinorin A with the Y313F mutant but loss of affinity with the Y313A mutant suggests a hydrophobic interaction between the aromatic ring of tyrosine and the C-2 acetate. Mutations of Y320A, Y320F, Y119A, and Y119F results in loss of affinity for salvinorin A suggesting hydrogen bond participation. This model orientates the hydrogen bond interactions of Y320 and Y119 with the furanyl oxygen. The proposed model also positions the C-4 methyl ester in close proximity to Ile294 and Glu297. Cysteine-substitution mutagenesis studies were performed with the hypothesis that if the cysteine mutation is in close proximity to the thiol of synthesized 2-thiosalvinorin B or the C-2 acetoxy of salvinorin A, then the affinity of the mutant with 2-thiosalvinorin B would be increased or maintained and the affinity with salvinorin A would likely decrease. A C315S mutation was combined with cysteine substitutions of several key residues in the binding pocket. Of specific interest was the C315S-Y313C double mutant. The C315S-Y313C preserved the affinity of 2-thiosavlinorin B but decreased affinity of salvinorin A further supporting the interaction of Y313 with the C-2 acetoxy. Additionally, Yan and coworkers synthesized salvinorin A affinity labels to covalently bind to the C315 anchoring residue.[268] This study confirmed that a free cysteine is involved with or near the binding site of KOP with salvinorin A.

In efforts to explain the binding interactions of KOP receptors with semi-synthetic salvinorin A derivatives that had meanwhile been synthesized, Kane and coworkers suggested a

new model utilizing chimeric and single-point mutant opioid receptors.[266] While confirming the affinity of the chimeric receptors for their ability to bind diprenorphine, this study emphasized the importance of TM II, TMVII, and extracellular loop-2; with specific implications of Q115, Y119, Y313, and Y320. This model predicts a vertical orientation of salvinorin A in the receptor binding site. A follow up study also implicated I316 as an amino acid when mutated to alanine results in loss of salvinorin A affinity by interrupting a lipophilic α-helical bundle in TM VII.[265]

An additional publication by Vortherms *et al*. focuses on opioid receptor subtype selectively of salvinorin A and how the orientation of the transmembrane helices of MOP and DOP receptors prevent salvinorin A binding.[267] KOP chimeric mutants with modifications in the TM2 and E2L retained affinity for naloxone but lost affinity for salvinorin A demonstrating the ligand binding pocket was still intact. Site-mutations of nonconserved amino acids in helix 2 implicated interest in V108 and V118, which resulted in a decrease of affinity for salvinorin A. Taking into consideration the loss in affinity of salvinorin A with V108 and V118 mutations, a modified receptor orientation was proposed. The new model predicted that V108 and V118 indirectly effect salvinorin A binding through the helical rotation of TM II and are major determinants of salvinorin A selectivity for KOP receptors.

Molecular modeling studies hypothesize that the furan ring is involved in stabilization of salvinorin A in the KOP receptor active site. Previous studies have shown that substitution of the furan ring is tolerated to retain affinity and efficacy at KOP receptors. Additionally, past furan modifications have resulted in compounds with diverse pharmacology profiles. Further structural modification of the 3-furan moiety will result in further understanding of structure activity relationships and the ideal interactions in the KOP receptor binding pocket.

Furthermore, these studies utilize an original scaffold in opioid pharmacology with the potential to develop new therapeutics with fewer side effects than traditional opioids.

Through the identification of key amino acids involved in binding salvinorin A to the KOP receptor, models have predicted that the furan ring is involved in stabilization of salvinorin A in the KOP receptor active site. Based on the information that if the furan ring is involved in stabilization of salvinorin A in the KOP receptor active site then modification of the furan ring will result in modulation of pharmacological activity along with a further understanding of structure activity relationships and the ideal interactions of salvinorin A in the KOP receptor binding pocket is proposed.

Salvinorin A Structure Activity Relationship Studies

Due to the activity of salvinorin A at KOP receptors, medicinal chemistry efforts have been performed to explore the SAR of salvinorin A. Several reviews have been written summarizing past synthetic modifications and structure-activity relationships of salvinorin A.[95,96,212,270] The SAR known at this time, not including furan modifications, is summarized in **Figure 8**. Reduction or removal of the carbonyl at the C-1 position is tolerated and yet the introduction of an alkene at C-1 – C-10 showed antagonist activity.[271-273] At the C-2 position, bioisosteric replacements of the ester functionality with amides, carbonates, and carbamates are tolerated.[271,274-283] In general, small alkyl groups favor affinity at KOP receptors. Methoxymethyl and ethoxymethyl ethers at the C-2 position are among the most potent salvinorin A analogues reported to date.[271] Aromatic groups at C-2 tend to favor affinity at MOP receptors with the example of the C-2 benzoyl ester named herkinorin.[282] Herkinorin has interesting pharmacological properties in that activity changed from KOP to MOP opioid

receptors. Modification of the C-4 position by reduction or hydrolysis reduces affinity at KOP receptors and replacement of the methyl ester with small alkyl groups is tolerated.[271,284,285] Alterations of the C-17 position by reduction or removal of the lactone is tolerated but subsequent methylation of the lactol resulted in decrease in affinity.[281] Introduction of a C-8 – C-17 alkene was also tolerated. Modifications to the furan ring will be discussed in depth.

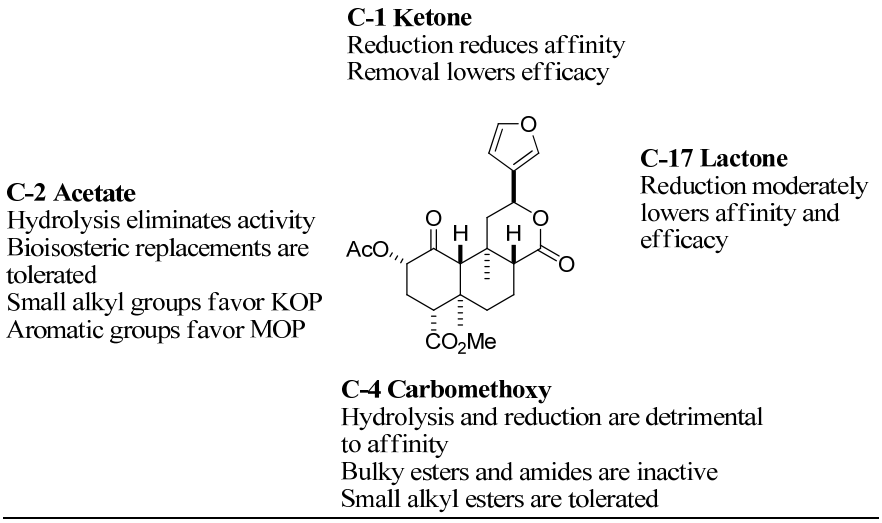

Figure 11: Structure Activity Relationship Summary

Furan Modifications

Specific interest in derivation of salvinorin A continues to be focused around the furan ring due to the poor ADMET properties of furan. The concern for hepatoxicity has resulted in the synthesis of a number of semi-synthetic derivatives and isolation of novel neoclerodanes from *S. divinorum* containing the core structure of salvinorin A with modified furan rings.[286-289] These derivatives focus on elucidating replacements for the furan ring and exploration of structure-activity relationships.

Previous studies have shown that substitution of the furan ring is tolerated to retain affinity and efficacy at KOP receptors.[286-289] Additionally, past furan modifications have

resulted in compounds with diverse pharmacological profiles. Synthesis of semi-synthetic analogues of salvinorin A with modified furan substituents would be beneficial for the identification of compounds with therapeutic potential for the treatment of drug abuse and other disease states associated with KOP receptor modulation. Modification of the furan ring utilizes an original scaffold in opioid pharmacology with the potential to develop new therapeutics with fewer side effects than traditional opioids.

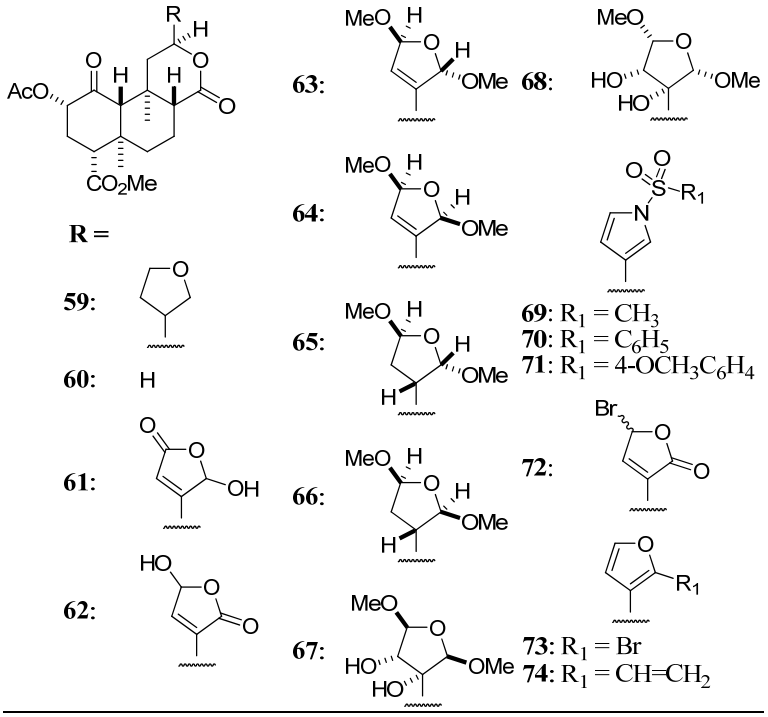

Figure 12: Compounds **59** – **74**

Past modification to the furan ring includes reduction of the furan ring to tetrahydrosalvinorin A (**59**) (**Figure 12**).[281,289] Compound **59** was found to have reduced affinity for KOP receptors compared to salvinorin A. Depending on the assay used, compound **59** had either 39-fold or 7-fold lower affinity than salvinorin A at KOP receptors.[281,289] The C-13*R* epimer of **59** was separated by HPLC and retained high affinity for KOP receptors relative to

salvinorin A (K_i = 3.7 nM vs. K_i = 1.9 nM) but was 17-fold less efficacious than salvinorin A.[281,289] This demonstrates that an aromatic may not be necessary for affinity at KOP receptors.[289] However, complete removal of the furan ring resulted in a compound greater than 1700-fold less active than salvinorin A at KOP receptors (**60**).[287,289] Photoxidation of salvinorin A yielded natural products salvidivin A (**61**) and salvidivin B (**62**).[289] γ-Hydroxybutenolide **61** had antagonist activity at MOP and KOP receptors (K_e = 760 nM and K_e = 440 nM, respectively).[289]

Treating salvinorin A with bromine in a mixture of DCM and MeOH at room temperature resulted in a mixture of *trans* (**63**) and *cis* (**64**) 2,5-dimethoxydihydrofuran isomers, which were separable by HPLC.[289,290] *Trans* isomer **63** had an approximate 3-fold higher binding affinity at MOP receptors than the epimeric mixture (K_i = 3,190 nM vs. K_i >10,000 nM). The *cis* (**64**) isomer had a 2-fold increase in affinity at KOP receptors compared to **63** or the epimeric mixture and had comparable affinity at MOP receptors to **63**. In the [^{35}S]GTPγS functional assay, **63** and **64** were both weak nonselective antagonists at MOP, KOP, and DOP receptors. Hydrogenation of **63** and **64** with 5% Rh/C in MeOH yielded the *trans* (**65**) and *cis* (**66**) dimethoxytetrahydrofuran derivatives, which were separated by HPLC.[289] Compound **65** had a K_i = 25 nM and **66** had a K_i = 125 nM, 13-fold and 66-fold lower affinity for KOP receptors comparable to salvinorin A, respectively. Additionally, reduction of the alkene in **63** changed the functional activity from an antagonist to an agonist (EC_{50} = 2,350 nM, E_{max} = 95% relative to U69,593). As a mixture, the *cis* isomer **64** was selectively oxidized over the *trans* isomer (**63**) with $KMnO_4$ in THF and H_2O at -10°C to afford a mixture of the natural products salvinicin A (**67**) and salvinicin B (**68**).[290,291] Diterpene **67** is a partial KOP agonist (K_i = 390 nM, EC_{50} = 4.1 μM, 80% relative to U50,488) and **68** is a MOP antagonist (KOP K_i = 700 μM, MOP K_e = 1.9

μM).[291] Treatment of mixture of **65** and **66** with methanesulfonamide at 95°C in acetic acid afforded a mixture of the methanesulfonylpyrrole (**69**) and its C-8 epimer.[287] Using this methodology, benzenesulfonamides **70** and **71** were synthesized. *N*-sulfonylpyrroles **69**, **70**, and **71** had reduced affinities and efficacies compared to salvinorin A but were found to be partial agonists compared to U50,488 and salvinorin A (E_{max} = 70%, 60%, 60%, respectively).

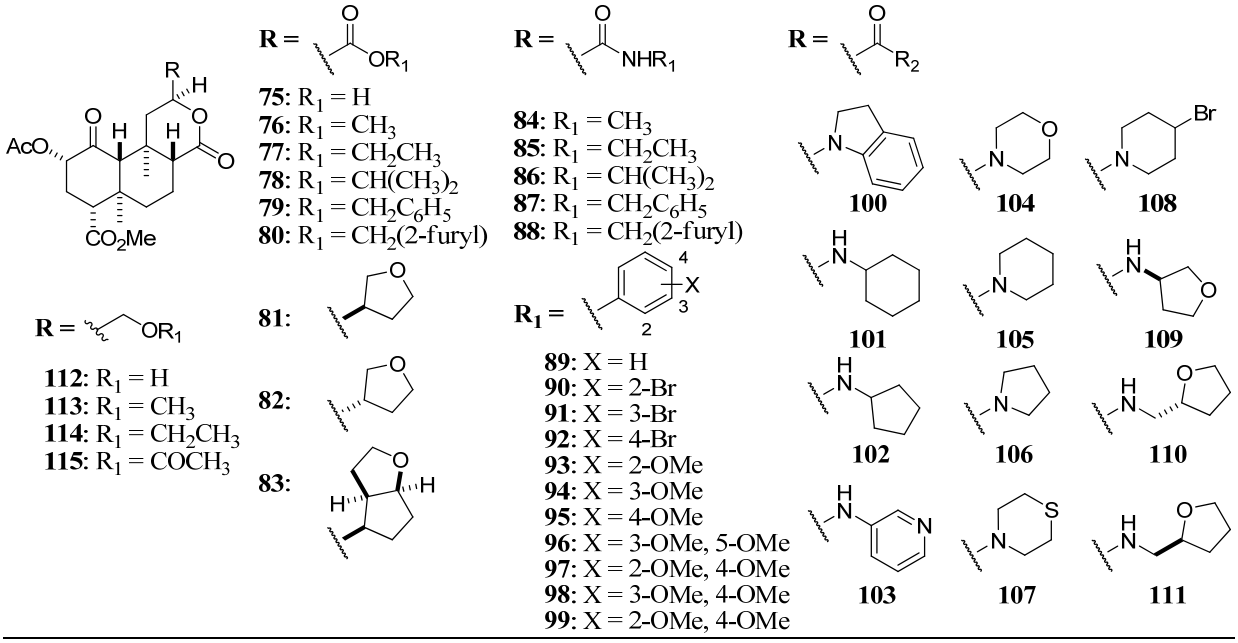

Figure 13: Compounds **75** – **115**

Exposure of salvinorin A to bromine in DMF at 0°C gave way to dihydrofuran **72** as a mixture of C-15 α and β isomers and the C-15 β isomer was found to be stable.[290] Treatment of salvinorin A with *N*-bromosuccinimide in acetonitrile or chloroform gave the 2-bromofuran product (**73**).[286,289,290] Bromo analogue **73** was well-tolerated at KOP receptors and retained affinity relative to salvinorin A (K_i = 3.0 nM vs. K_i = 1.9 nM).[289] Additionally, compound **73** was found to be a full agonist with an EC_{50} = 50 nM and E_{max} = 104% relative to U69,593. The retained affinity and efficacy at KOP receptors observed with the introduction of a C-16 bromide

suggests that steric bulk is tolerated in the binding site of the furan ring. Stille coupling of **73** to tributylvinyltin afforded the 2-vinylfuran product (**74**).[286] Introduction of the vinyl group was also well-tolerated (K_i = 7.1 nM, EC_{50} = 4.6 nM, E_{max} = 120% relative to U50,488).

A valuable intermediate that has been utilized to synthesize a number a furan modified analogues is the C-13 carboxylic acid (**75**) (**Figure 13**). Carboxylic acid **75** is achieved by oxidative degradation of salvinorin A by $NaIO_4$ and catalytic $RuCl_3 \cdot 3H_2O$ in a mixture of CCl_4, CH_3CN, and H_2O. Standard coupling conditions have been used to synthesize a number of esters and amides off the salvinorin A core (**76** – **111**).[286,292] The C-13 methyl ester was prepared by treatment of **75** with (trimethylsilyl)diazomethane ($TMSCHN_2$) (**76**).[286] Other alkyl esters were synthesized in the presence of EDCI, HOBt, and Et_3N.[286,292] A large variety of amides were produced from **75** using appropriate amine, EDCI, HOBt, and in some cases with the addition of Et_3N.[286,292] Additionally, carboxylic acid **75** was also reduced to the primary alcohol (**112**) with $BH_3 \cdot THF$ in THF at 55°C. Alcohol **112** was alkylated with alkyl iodides in the presence of Ag_2O to afford alkyl ethers (**113**, **114**).[286] The primary alcohol was also acetylated (**115**) using acetic anhydride and Et_3N. Alkyl esters **76** – **78**, and **83** had roughly 40- to 80-fold less affinity at KOP receptors while retaining functional activity as full agonists.[286] Aryl esters **79** and **80** showed no affinity at KOP, DOP, or MOP receptors. In the amide derivative series, aromatic amide substitutions (**87** – **99**) were not tolerated at KOP receptors.[286,292] Nonaromatic substitution with the cyclohexane (**101**) and cyclopentane (**102**) derivatives had affinity for KOP receptors but a decrease relative to salvinorin A with a greater than 10-fold and 5-fold loss, respectively. Constricting cyclohexylamine **101** in to a piperidine (**105**) resulted in a 14-fold increase in affinity relative to **101** (K_i = 140 nM vs. K_i = 1,930 nM). Further constriction of **105** to pyrrolidine (**106**) produced a decrease in affinity (K_i = 1,210 nM), while bioisosteric

replacement to the morpholine (**104**) and thiomorpholine (**107**) did not further enhance affinity at KOP receptors but showed partial agonist activity (K_i = 230 nM, ED_{50} = 5110 nM, E_{max} = 85% relative to U50,488 and K_i = 160 nM, ED_{50} = 3780 nM, E_{max} = 57% relative to U50,488). Addition of a bromine in analogue **108** resulted in a decrease in affinity (K_i = 1,250 nM). Tetrahydrofuran amides (**109**, **110**, **111**) had weak to no affinity at KOP receptors, however, compound **109** showed selective low affinity at DOP receptors (DOP K_i = 3,090 nM). Alcohol analogues (**113** – **115**) showed roughly a 200-fold loss in affinity relative to salvinorin A.[286]

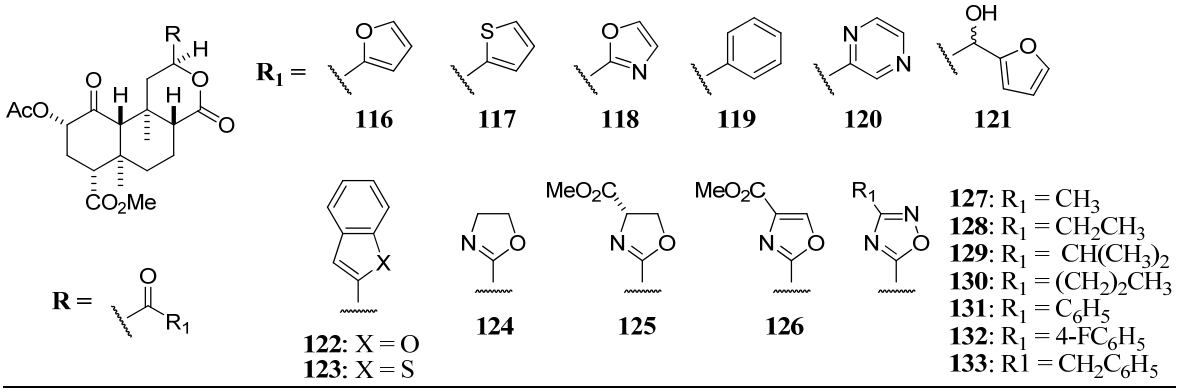

Figure 14: Compounds **116** – **133**

Carboxylic acid **75** also has been utilized to form the acid chloride and exposed to appropriate aryltributyl tin reagents under Stille conditions affording a variety of arylketones (**116** – **120**) (**Figure 14**).[286] Arylketone **116** was reduced using sodium borohydride to yield the corresponding alcohol (**121**) as a mixture of C-13 epimers. The majority of arylketone derivatives were reported to have no affinity at KOP receptors with only the 2-thiophene **117** and 2-pyrazine **120** analogues retaining low nanomolar affinity and full agonist activity (K_i = 38 nM and 83 nM).[286] Alcohol **121** was evaluated as full agonist with a K_i = 20 nM, EC_{50} = 35 nM, E_{max} = 111% relative to U50,488). Carboxylic acid **75** was treated with either (2-hydroxybenzyl)triphenyl- or (2-thiobenzyl)triphenyl phosphonium bromide in the presence of

CDMT and Et_3N to afford the benzofuran (**122**) and benzothiophene (**123**).[292] Derivatives **122** and **123** had little to no affinity at KOP receptors (K_i = 2,340 nM and K_i > 10,000 nM).

The C-13 carboxylic acid **75** was also reacted with ethanolamine or L-serine methyl ester hydrochloride using standard amide coupling conditions followed by cyclization with bis(2-methoxyethyl)aminosulfur trifluoride (Deoxo-Fluor) to yield oxazolines **124** and **125**.[287,289] Oxazoline **124** showed loss in affinity relative to salvinorin A (K_i = 300 nM).[289] Oxazoline **125** was converted to oxazole **126** by treatment with bromotrichloromethane and DBU.[287] A variety of oxadiazoles (**127** – **133**) have been synthesized by treating carboxylic acid **75** with appropriate amidoximes in the presence of EDCI and HOBt followed by heating in toluene and HPLC purification.[286,287,289,292,293] Additionally, Simpson and coworkers reported that oxadiazole **127** results in a 29-fold loss in affinity relative to salvinorin A (K_i = 56 nM) and is a functional antagonist at both KOP and MOP receptors (KOP: K_e = 360 nM MOP: K_e = 430 nM).[289] However oxadiazoles **127** – **133** were synthesized by Béguin and coworkers and all were found to have no appreciable binding at KOP receptors.[286]

Additionally, carboxylic acid **75** has been transformed to the C-13 aldehyde through the thioester intermediate (**134**) (**Figure 15**). Carboxylic acid **75** was treated with 2-chloro-4,6-methoxy-1,3,5-triazine (CDMT) and *N*-methyl morpholine (NMM) followed by the addition of ethanethiol. Thioester **134** was then reduced with triethylsilane and Pd/C to afford the aldehyde (**135**).[286,292] *B*-allyl-(10*S*)-(trimethylsilyl)-9-borabicyclo[3.3.2]decane (prepared in situ from commercially available 9-[(1*R*,2*R*)-pseudoephedrinyl]-(10*S*)-(trimethylsilyl)-9-borabicyclo [3.3.2]decane and allylmagnesium bromide) achieved the asymmetric allylation (**136**) of the C-13 aldehyde (**135**).[292] To determine the stereochemistry of the allylic alcohol product, the Mosher ester (**137**) was prepared with oxalyl chloride and (*R*)-(+)-α-methoxy-α-

trifluoromethylphenylacetic acid. Allylic alcohol **136** was acylated with acryloyl chloride in the presence of Et_3N and DMAP, and the subsequent ester was subjected to ring closing metathesis using 2nd generation Grubb's catalyst to afford the 5,6-dihydro-2*H*-pyran-2-one product (**138**). Unfortunately, these modifications lead to a drastic decrease in affinity at KOP receptors (K_i = 8,060 nM).[292]

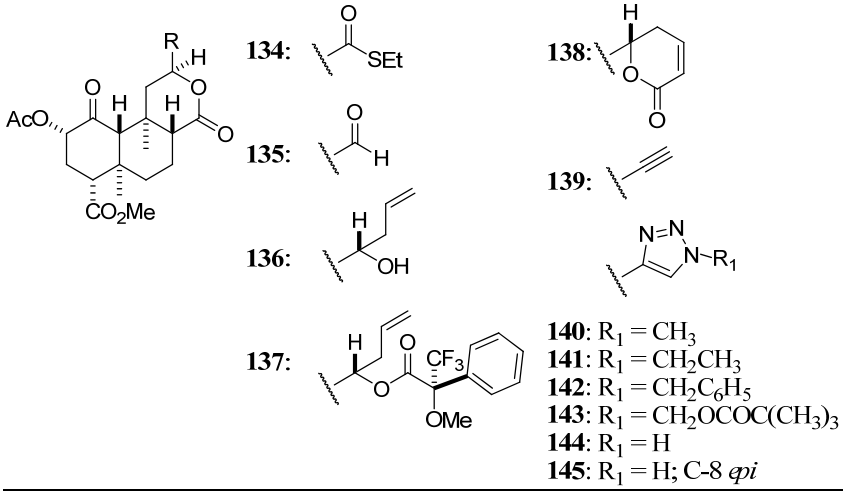

Figure 15: Compounds **134** – **145**

Using Seyferth-Gillbert homologation conditions aldehyde **135** was converted to the terminal alkyne (**139**).[293] Alkyne product **139** was coupled with various azides under copper(I)-catalyzed click reaction conditions to afford 1,4-disubstituted-1,2,3-triazoles (**140** – **143**).[293] The pivalyl triazole **143** was treated with 1N NaOH and reacetylated to give a mixture of C-8 epimers and the *N*-unsubstituted triazoles (**144**, **145**). All triazoles synthesized resulted in loss of affinity at KOP receptors (K_i > 1,000 nM).

The Diels-Alder reaction has been performed on salvinorin A using the furan ring as the 4π diene.[294] Very reactive/electron-poor dienophiles such as diethyl acetylenedicarboxylate, dimethyl acetylene dicarboxylate, and 4,4,4-trifluoro-2-butynoate were cyclized using traditional

heating methods or microwave radiation yielding derivatives **146** – **149** (**Figure 16**), respectively. Additionally, **150** was synthesized from generating benzyne from 2-(trimethylsilyl)phenyl trifluoromethanesulfonate and cesium fluoride in CH_3CN but the relative configuration is unable to be determined. Salvinorin A was also heated with 3,6-epoxy-3,6-dihydrotribenzocycloheptatrienone or 3,6-epoxy-3-methyl-3,6-dihydrotribenzocycloheptatrien-one in toluene to afford **151** and **152**, respectively.[294] Cycloadduct **151** was identified as a mixture of *exo* and *endo* while **152** was a single compound. Bicycles **146** – **150** were exposed to $Fe_2(CO)_9$ in toluene and heat to undergo reductive elimination of water to yield aromatic compounds **153** – **157**. Cyclic analogues **146** and **147** had reduced but still appreciable affinity but reduced efficacy at KOP receptors relative to salvinorin A (K_i = 120 nM, ED_{50} = 2150 nM, E_{max} = 90% and K_i = 60 nM, ED_{50} = 980 nM, E_{max} = 100% relative to U50,488 in efficacy assay). Introduction of the methyl group to trienone analogue **151** altered KOP receptor affinity 45-fold with further investigations pending to rationalize this observation (K_i > 13,000 nM vs. K_i = 290 nM). Non-heterocyclic aromatic rings of **153** – **157** had reduced affinity at KOP receptors relative to salvinorin A.

In addition to the large variety of replacements for the furan ring, the stereochemistry of C-12 has been inverted (**158**).[286] Heating salvinorin A in 5% aqueous KOH afforded the diacid and then the free hydroxyl at C-2 was reacetylated with Ac_2O and pyridine. Refluxing in acetic acid promoted cleavage at C-1 and lactonization to afford the inverted center at C-12, and subsequent methylation of the acid at C-4 using $TMSCHN_2$ provided 12-*epi* salvinorin A (**158**). The binding of affinity of *epi*-salvinorin A was 16-fold less than the natural epimer but interestingly showed partial agonist effects at KOP receptors (EC_{50} = 84 nM, E_{max} = 67% relative to U50,488).[286]

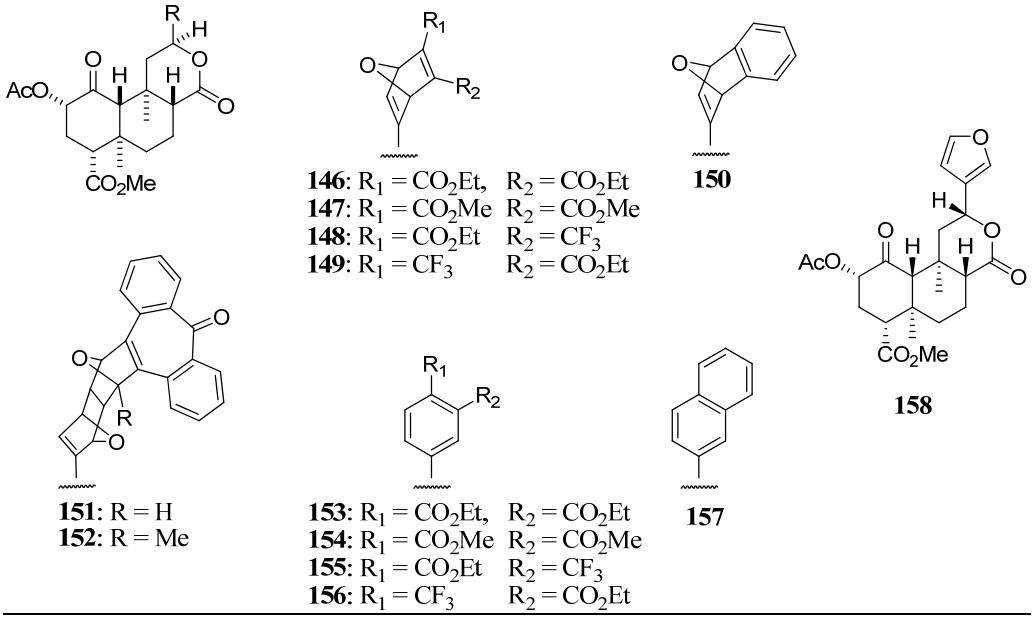

Figure 16: Compound **146** – **158**

A number of salvinorin A derivatives have been made, largely focusing at the C-2 and the C-13 position.[96,212,270] Further investigations into salvinorin A derivatives with modified furan substituents will results in the identification of novel compounds with unique pharmacological profiles, shown with previous furan modifications.[286,287,289,290,292] Continued exploration of salvinorin A derivatives with modified furan moieties with strategic introduction of steric bulk and hydrogen bonding interactions will lead to further understanding of the structure activity relationships of salvinorin A.

CHAPTER III. RATIONALE AND SPECIFIC AIMS

Salvinorin A has shown great therapeutic potential, but optimization is required for human use as a KOP receptor agonist due to several drawbacks. These drawbacks include hallucinogenic and dysphoric effects along with its poor pharmacokinetic properties including ADMET (absorption, disposition, metabolism, excretion, and toxicity) properties. Desirable ADMET properties are essential for the development of therapeutic agents. Natural products, such as salvinorin A, often have excellent potency and selectivity for a specific biological target but have unsatisfactory ADMET properties. Assessment of ADMET properties has recently been incorporated early into the drug discovery process and assists to direct the project to derivatives with a greater chance of clinical success. Elimination of poor ADMET characteristics in a natural product or any drug candidate is essential for a drug development campaign. ADMET properties are often modified through semi- or total synthesis.

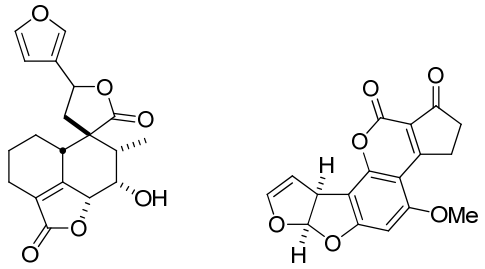

Teurcin A (**57**) Aflatoxin B_1 (**58**)

Figure 17: Diterpenes with Associated Toxicity

Salvinorin A has several ADMET properties that need to be addressed to fully utilize salvinorin A's therapeutic potential. Salvinorin A has been shown to have hallucinogenic and dysphoric effects in human and animal models that need to be modulated to develop a therapeutic agent. Additionally, furan containing natural products have been linked to

hepatotoxicity.[295-297] Inspection of the structure of salvinorin A suggests that the furan ring of salvinorin A is a potential metabolic problem.[292] Furan-containing natural products have historically shown limited therapeutic utility due to their potential for bioactivation and consequent hepatoxicity.[295-297] Previous metabolic studies on teucrin A (**57**) (**Figure 17**), a structurally similar neoclerodane diterpene from *Teucrium chamaedrys* L., has been shown to be metabolized by CYP450s to afford a highly reactive enedial intermediate which forms stable peptide conjugates leading to hepatoxicity.[298-300] Aflatoxin B_1 (**58**), a difurano-containing natural product produced by an *Aspergillus* species, is also known to have associated toxicity.[301] Aflatoxin B_1 is thought to undergo bioactivation by CYP450s to a comparable enedial intermediate resulting in hepatic carcinogenic effects.[301] Salvinorin A shares a common toxic feature with these other furan-containing natural products not ideal for medicinal use.[96] One way to circumvent the potential toxicity associated with salvinorin A would be to identify analogues with modified furan substituents. Preferably, semi-synthetic modifications to the furan ring would introduce structural replacements with little to no potential for toxicity while still retaining activity and affinity at KOP receptors. These modifications would be beneficial for the identification of compounds with therapeutic potential for the treatment of drug abuse and other disease states associated with KOP receptor modulation.

Salvinorin A is a highly lipophilic molecule that has poor solubility in aqueous solution. Aqueous solubility is a requirement for pharmacological testing therefore a vehicle is used. The vehicle chosen has the ability to alter bioavailability and increase or decrease the toxicity associated with the drug.[302] Detergents, solvents, or vegetables oils are commonly used vehicles with Tween-20 and Tween-80 as the most common detergents, DMSO and ethanol as the most common solvents, and emulphor-620 as the most common vegetable vehicle utilized.[302] Vehicle

formulations for salvinorin A are various and range from Tween-80:ethanol:saline (1:1:8) to DMSO:H_2O (3:1).[244,259] Current available vehicles for salvinorin A administration have drawbacks associated with them largely associated to the use of ethanol or DMSO.[270] Ethanol potentiates the effects of opioid receptors potentially obscuring biological results and DMSO has been shown to modulate the potency of other opioids, such as morphine, following acute or chronic administration.[303] Identification of a different vehicle for salvinorin A would be useful for simplifying pharmacological data analysis.

Salvinorin A has also been shown by Teskin and coworkers to be a P-glycoprotein (P-gp) substrate but not a P-gp inhibitor.[237] Using the P-gp ATPase assay, 5 μM and 10 μM concentrations of salvinorin A significantly increased P-gp-mediated ATPase activity in a concentration-dependent manner suggesting that salvinorin A is a P-gp substrate. Salvinorin A is a highly lipophilic molecule that has been shown to rapidly cross the blood brain barrier in PET imaging studies.[232] Teskin and coworkers use MDCK-MDR1 cells to determine salvinorin A's permeability across cell membranes expressing P-gp.[237] MDCK-MDR1 cells form a highly confluent monolayer which is used as model of transepithelial transport and is able to predict brain uptake. Secretory transport of salvinorin A was higher than absorptive transport further associating salvinorin A with P-gp. P-gp activity could also contribute to salvinorin A's short duration of action. Better understanding the role P-gp plays in mediating the effects of salvinorin A would lead to analogues with greater therapeutic potential.[99]

Salvinorin A is a biologically active neoclerodane diterpene that produces potent hallucinogenic effects. Unlike classical hallucinogens, salvinorin A does not act at 5-HT_2 receptors but was identified as the first naturally occurring potent and selective KOP receptor agonist not containing a basic nitrogen.[137] The unprecedented neoclerodane diterpene activity at

a subclass of opioid receptors has lead to investigations aimed to further the understanding of structure-activity relationships and pharmacology of salvinorin A. Initial studies have shown that modification to salvinorin A's scaffold resulted in the identification of compounds that are tolerated at opioid receptors and had altered pharmacological profiles. Continued structural modification of salvinorin A will identify new analogues with diverse biological activity and more desirable pharmacological properties. The following specific aims are proposed to increase our knowledge of the chemistry and pharmacology of salvinorin A.

Specific Aim #1: Prepare and evaluate C-13 salvinorin A analogues with reduced potential for hepatoxicity.

The furan ring of salvinorin A is a concern due to its potential for hepatoxicity. The metabolism of the furan ring in structurally similar neoclerodane diterpenes has been linked to hepatoxicity. Modifications of the furan ring present in salvinorin A will further elucidate the importance the furan ring plays in binding and activity at opioid receptors while identifying compounds with a more desirable pharmacological profile. A series of amide, amine, ketone, and oxime derivatives will be synthesized as structural replacements to the furan ring in attempts to limit potential toxicity and improve pharmacokinetic properties. Additionally, the strategic addition of steric bulk and investigation into key hydrogen bonding interactions at the binding site of salvinorin A at KOP receptors will result in further elucidation of its KOP receptor binding site. These modifications are intended to show that alteration of the furan ring of salvinorin A is tolerated for KOP receptor binding and modifications at this position have the potential to modulate opioid subtype selectivity.

Specific Aim #2: Investigate Captisol® as a method to improve the solubility of salvinorin A in aqueous solution.

Neoclerodanes such as salvinorin A have poor solubility in aqueous media due to their lipophilic nature, which causes difficulty in *in vitro* and *in vivo* pharmacological investigations. Current vehicles used to improve the solubility of salvinorin A and related analogues in water or saline include either DMSO or ethanol. Both DMSO and ethanol have been associated with opioid mediated effects making their use in opioid receptor pharmacology less than ideal.[270,304,305] Investigation into the potential use of Captisol® as a vehicle for salvinorin A delivery will be investigated. β-Cyclodextrins, such as Captisol®, have been successfully utilized as a vehicle for the delivery of diterpene taxol and have the potential to assist in solubilizing neoclerodane diterpenes such as salvinorin A.[306,307]

Completion of these specific aims is intended to improve the pharmacological profile of salvinorin A through structural modifications and formulation. Synthetic modifications are intended to exploit salvinorin A as a lead molecule. These modifications are intended to improve the pharmacokinetic properties of salvinorin A with the focus to increase metabolic stability. Rational design of salvinorin A derivatives will identify novel and biologically relevant salvinorin A analogues with the potential to be used as opioid receptor probes. Investigation into a novel vehicle for neoclerodane administration also will be completed. These studies will focus on enhancing the solubility of salvinorin A while taking into consideration the drawbacks of current vehicles. The results of these studies will be discussed herein.

CHAPTER IV. RESULTS AND DISCUSSION

Introduction

In efforts to further elucidate the pharmacophore and structure-activity relationships of salvinorin A at opioid receptors, furan modified salvinorin A analogues were synthesized. Compounds were intended to limit the potential hepatoxicity associated with the furan ring and to investigate the structural requirements for activity at this position. Several series were synthesized replacing the furan ring including amide, amine, ketone, and oxime derivatives (**Figure 18**). Initially, a series of amide derivatives were synthesized replacing the furan ring. Incorporation of the amide was an attempt to retain a potential hydrogen bond interaction of the furan ring by replacement with the carbonyl, to identify a new interaction in the binding pocket with the various amide substituents, and to increase water solubility of the analogues. Reduction of the amide was investigated to determine the importance of the carbonyl in hydrogen bonding, the effect of introducing a basic amine, and as a potential solution to improve water solubility. A series of ketone derivatives were also synthesized based on similar rationale to the amide series. The intention was to identify a more desirable hydrogen bond interaction with the carbonyl and its KOP receptor binding site while accessing another interaction reliant on the ketone substituent. Initially, phenyl ketone derivatives were synthesized that included substitutions at the *ortho*, *meta*, and *para* positions with the electron donating and hydrogen bond accepting methoxy group and the electron donating and hydrogen bond donating hydroxyl group. These derivatives were proposed to investigate the hydrogen bonding, electronic, and steric effects of phenyl substitutions.

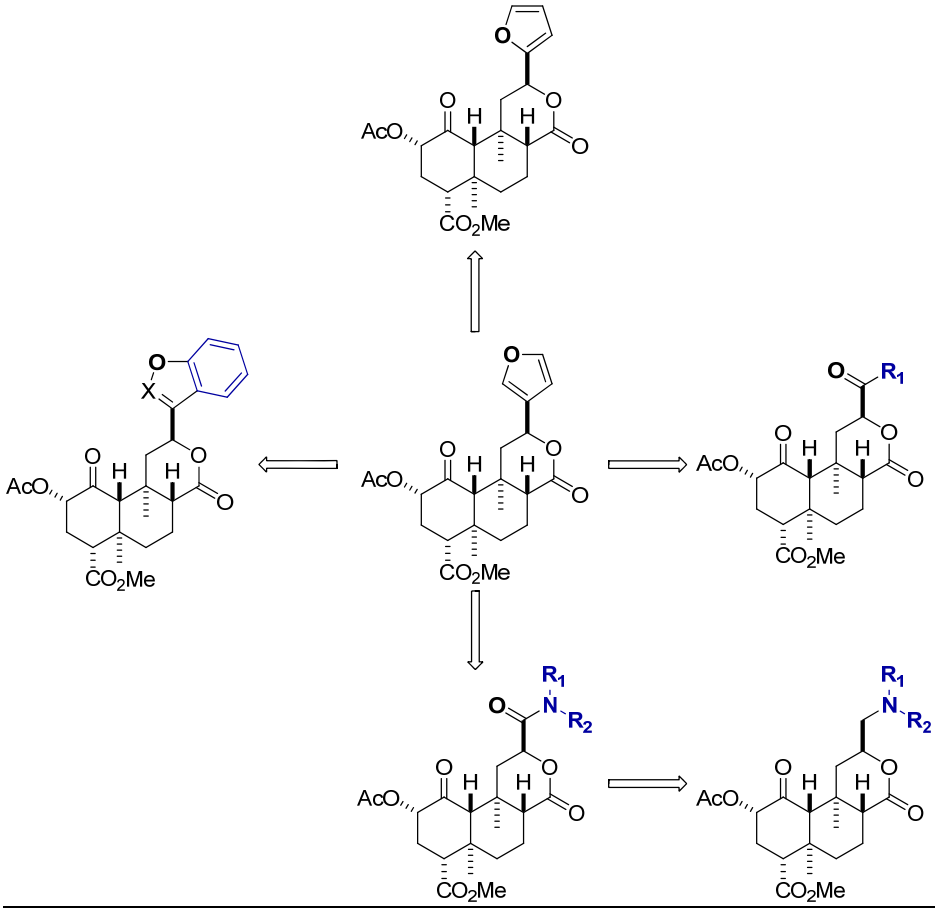

Figure 18: Design Rationale

Additionally, several of the ketone derivatives showed promise as intermediates for other desired analogues of significant importance. For example, a ketone alkene derivative showed potential to achieve the 2-furanyl analogue of salvinorin A, which is of great interest to elucidate the ideal positioning of the oxygen of the furan ring and its requirement for activity at KOP receptors. The 2-hydroxyphenyl ketone analogue had the promise to be an intermediate for a benzisoxazole derivative, which is highly sought after to further understand the steric restraints and hydrophobic nature of the furan binding pocket by the introduction of a benzene ring while retaining the oxygen position as the furan ring. Synthesis of the benzisoxazole analogue then

lead to the use of ketone derivatives to synthesize several oxime derivatives to further investigate the structural requirements to modulate subtype selectively at opioid receptor.

Analogues were then evaluated for affinity at the different opioid receptor subtypes using radioligand displacement assays. Compounds that displayed high affinity, a K_i value of approximately 150 nM or lower, were then further evaluated for efficacy at the specified opioid receptor subtype. Included herein is the synthesis of analogues along with the *in vitro* pharmacological results of select compounds.

Furan Modifications

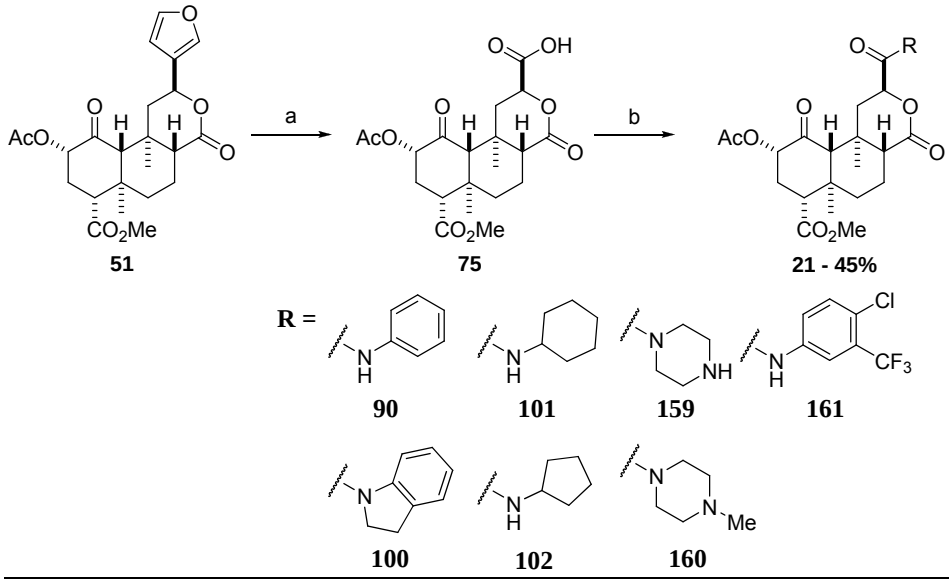

Scheme 1: Synthesis of Amide Derivatives. *Reagents and Conditions*: a) $NaIO_4$, $RuCl_3 \cdot 3H_2O$, $CH_3CN/CCl_4/H_2O$; b) NR_2, EDCI, HOBt, Et_3N, CH_2Cl_2

Amide derivatives were synthesized through carboxylic acid **75**. As previously reported, salvinorin A was reacted with $NaIO_4$ and a catalytic amount of $RuCl_3 \cdot 3H_2O$ in $CH_3CN/H_2O/CCl_4$ (2:2:3) to afford carboxylic acid **75** in 74% yield.[290] Carboxylic acid **75** was

then used to synthesize a series of amide derivatives by addition of the appropriate aniline or alkylamine, EDCI, HOBt, and Et_3N in anhydrous CH_2Cl_2 at room temperature for 24 hours (**89**, **100** – **102**, **159** – **161**).[292] Yields of all amide derivatives synthesized ranged from 21 – 45%.

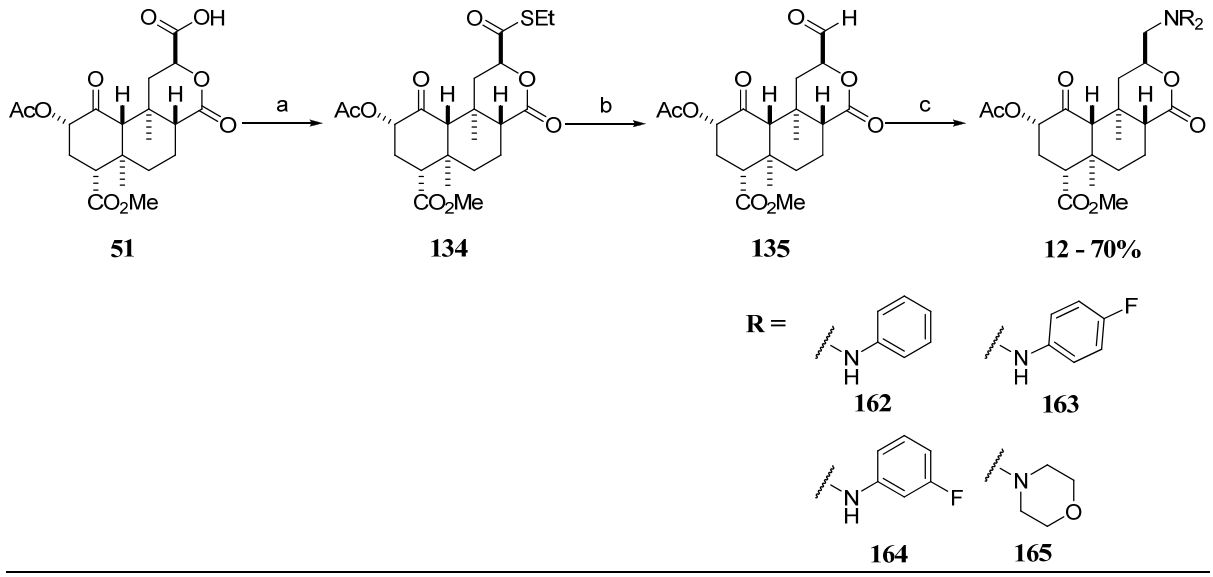

Scheme 2: Synthesis of Amine Derivatives. *Reagents and Conditions*: a) CDMT, NMM, EtSH, CH_2Cl_2; b) Pd/C, Et_3SiH, CH_2Cl_2; c) HNR_2, $NaBH(OAc)_3$, DCE

Amines were synthesized utilizing reductive amination conditions once the C-13 aldehyde was in hand. Reductive amination was used to circumvent difficulties and degradation products resulting from the functionality of the salvinorin A core. To synthesize the desired aldehyde, carboxylic acid **75** was exposed to CDMT and *N*-methylmorpholine in anhydrous THF followed by the addition of ethanethiol at room temperature for 48 hours to afford thioester **134** in 88% yield.[286,292] Thioester **134** was then reacted with 10% palladium on carbon and Et_3SiH in anhydrous CH_2Cl_2 and stirred at room temperature over night to yield aldehyde **135** in 82% yield.[292] Aldehyde **135** was then exposed to the appropriate amine, sodium

triacetoxyborohydride, in 1,2-dichloroethane and stirred at room temperature overnight. Desired amines **162** – **165** were achieved ranging from 12 – 70% yield.

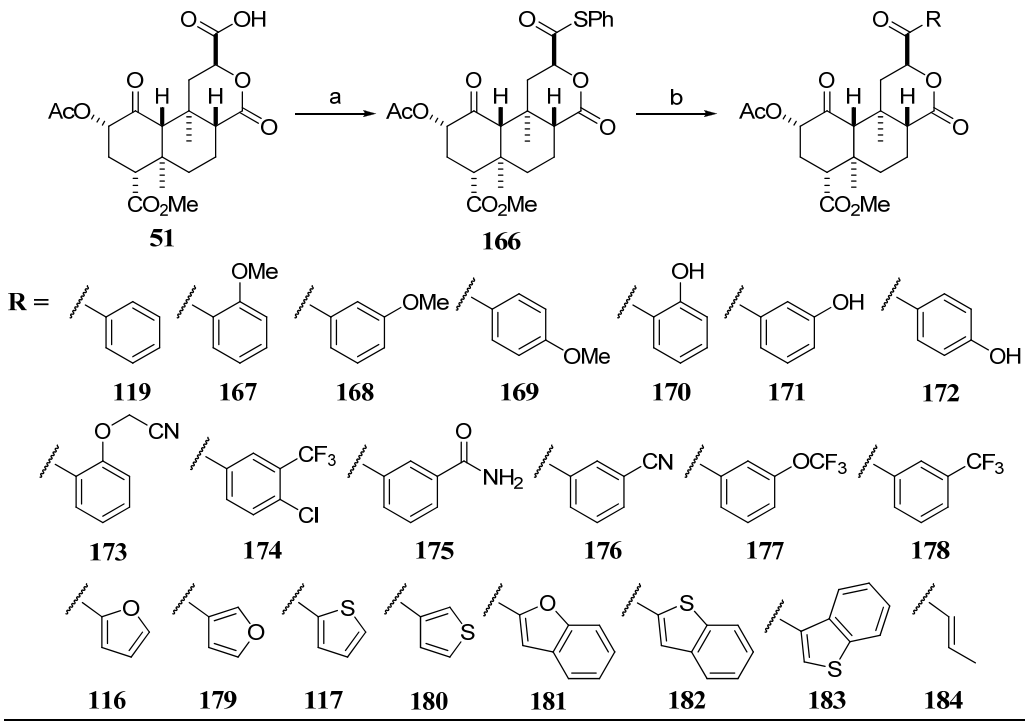

Scheme 3: Synthesis of Ketone Derivatives. *Reagents and Conditions*: a) CDMT, NMM, HSPh, CH_2Cl_2; b) $RB(OH)_2$,CuTC, $Pd(dba)_2$, PEt_3, THF

A series of ketone derivatives were also synthesized. Many different methodologies of carbon-carbon bond forming reactions are known in scientific literature. However, many of these methods are not amenable to substrates with high functionality along with acid and base sensitivity of salvinorin A. Asymmetric allylation of aldehyde **135** was achieved in 50% yield with *B*-allyl-(10*S*)-(trimethylsilyl)-9-borabicyclo[3.3.2]decane (prepared in situ from 9-[(1*R*,2*R*)-pseudoephedrinyl]-(10*S*)-(trimethylsilyl)-9-borabicyclo[3.3.2]-decane and allylmagnesium bromide).[292] Attempts to perform Grignard reactions using aldehyde **135** were met with limited

success due to poor solubility of **135** in THF and ether at low temperatures resulting in low yields (0 – 20%).[308] Béguin and coworkers were able to synthesize several ketone derivatives through *in situ* formation of the acid chloride followed by coupling stannanes via Stille coupling in low to moderate yields (7 – 57%).[286] This procedure is also limited by the commercial availability and toxicity of stannane reagents.

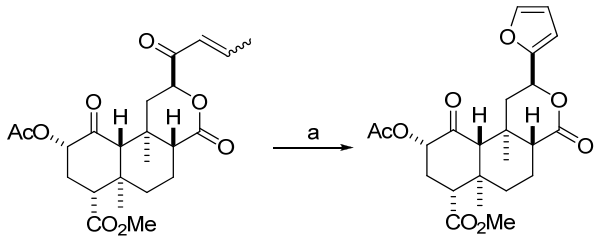

184 **185**

Scheme 4: Synthesis of 2-Furanyl Salvinorin A. *Reagents and Conditions*: a) SeO_2, bromobenzene, reflux

The structural complexity of salvinorin A limits traditional approaches to chemical transformations to be performed on salvinorin A.[294] To overcome these challenges, investigation into the Liebeskind-Srogl reaction was investigated. The Liebeskind-Srogl reaction is a palladium catalyzed cross-coupling reaction between a thiophenol ester and boronic acid requiring a stoichometric amount of copper (I) additive.[309,310] The Liebeskind-Srogl reaction occurs at neutral pH and room temperature and had previously been utilized on base sensitive substrates.[311,312] Additionally, an increasing number of boronic acid are commercially available, which further contributes to the convenience of analogue development. With promising credentials, the thiophenol ester at the C-13 position was synthesized using the same CDMT and *N*-methylmorpholine previously developed with substitution of ethanethiol for thiophenol.

Thioester **166** was synthesized in 47% yield. Using bis(dibenzylideneacetone)palladium (0), copper (I) thiophene carboxylate, and triethyl phosphate in anhydrous THF, coupling of thioester **166** and desired boronic acids synthesized ketone derivatives **116**, **117**, **119**, **167** – **187** in 23 – 87% yields.[311]

The 2-furanyl analogue of salvinorin A was of great interest to elucidate the ideal positioning of the oxygen of the furan ring and its requirement for activity at KOP receptors. To access this compound, ketone analogue **184** was refluxed with Se_2O in bromobenzene.[313] The initial thought was to isolate the dicarbonyl and use previously developed conditions to cyclize to the 2-furan in a two-step procedure.[314] Fortuitously, cyclization also occurred under oxidative conditions to afford analogue **185** in 18% yield from **184**.

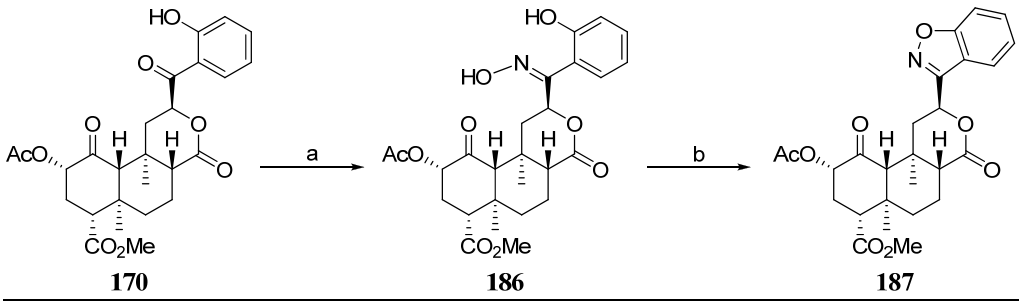

170 **186** **187**

Scheme 5: Synthesis of Benzisoxazole Derivative. *Reagents and Conditions*: a) hydroxylamine hydrochloride, pyridine, MeOH; b) DIPEA, MsCl, isopropyl acetate, 55°C

A benzisoxazole analogue of salvinorin A was also desired to further understand the steric restraints and hydrophobic nature of the furan binding pocket by the introduction of a benzene ring while retaining the oxygen position as the furan ring. This was achieved by dissolving ketone derivative **170** in MeOH followed by the addition of hydroxylamine hydrochloride and pyridine under gentle reflux. Both the *E* and *Z* hydroxylamines were formed

and the *Z* hydroxylamine was isolated in 41% yield and utilized. Hydroxylamine **186** was mesylated using methanesulfonyl chloride and diisopropylethylamine in isopropyl acetate at 55°C, which cyclized *in situ* to yield the benzisoxazole **187** in 35% yield.

After knowing how the benzisoxazole altered affinity at KOP receptors, several oxime derivatives were synthesized to further investigate the potential to modulate subtype selectively at opioid receptors. Ketone derivatives **119**, **177**, and **117** were chosen due to their affinity at KOP and MOP receptors in effort to identify structure requirements of opioid subtype selectivity. Oxime derivatives were synthesized using the previously mentioned conditions of hydroxylamine hydrochloride and pyridine under gentle reflux in MeOH. Both the *E* and *Z* hydroxylamines **188** – **190** were formed in yields ranging from 53 – 69%. Receptor binding studies were performed as a mixture of *E* and *Z* isomers.

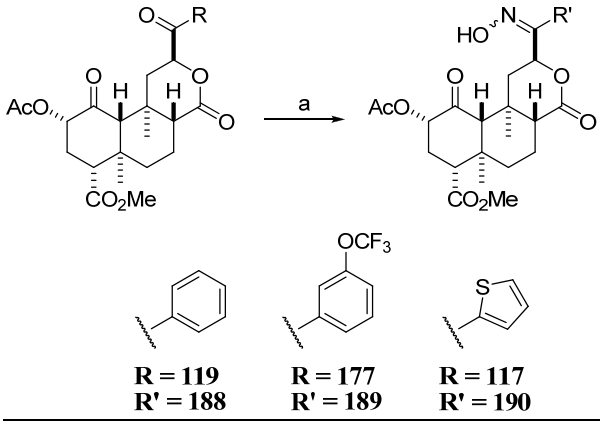

Scheme 6: Synthesis of Oxime Derivatives. *Reagents and Conditions*: a) $H_2NOH \cdot HCl$, pyridine, MeOH, 65°C

Affinity and Activity Studies

Amide Affinity

Based on the hypothesis that retention of the hydrogen bonding interaction could be maintained by the carbonyl and that the phenyl substituent would be able to participate in hydrophobic interactions comparable to the aromatic furan ring of salvinorin A, aniline derivative **90** was synthesized. This modification was not tolerated and affinity at KOP opioid receptors was lost (K_i > 10,000 nM) (**Table 1**). In efforts to limit the free rotation of the phenyl ring, the conformationally constrained indoline derivative **100** was synthesized but did not enhance affinity at opioid receptors (K_i > 10,000 nM). Several other aromatic amides were synthesized, including those with hydrogen bond accepting groups, which were not tolerated for affinity in the amide series.[292] Explorations of non-aromatic amides were then pursued based on the hypothesis that the aromatic ring was responsible in the loss of affinity. Initially, the cyclohexylamide (**101**) and cyclopentylamide (**102**) were synthesized to find that these saturated systems resulted in a greater than a 10-fold and 5-fold increase in affinity at KOP receptors relative to amide **90** (K_i = 1,930 ± 220 nM and K_i = 4,060 ± 280 nM vs. K_i > 10,000 nM). With the resulting increase in affinity for cyclohexylamide **101** and cyclopentylamide **102** derivatives, additional analogues were synthesized to evaluate non-aromatic substitutions. Piperidine and pyrrolidine amides were synthesized as contracted analogues and were found to have increased affinity of 14-fold and 1.6-fold compared to the cyclohexylamide **101**, respectively (K_i = 140 ± 10 nM and K_i = 1,210 ± 80 nM vs. K_i = 1,930 ± 220 nM). Due to the increase in affinity seen with the piperidine derivative, bioisosteric replacements of the piperidine ring were explored. Substitution of piperazine (**159**) and *N*-methylpiperazine (**160**) resulted in loss of affinity at KOP receptors while introduction of either a morpholine or a thiomorpholine ring were well tolerated

but did not increase affinity at KOP receptors (K_i = 230 ± 20 nM and K_i = 160 ± 10 nM, respectively). Anilide **161** was synthesized based on the success of Frankowski and coworkers with the identification of *N*-alkyl-octahydroisoquinolin-1-one-8-carboxamides as a nonbasic KOP opioid receptor ligand.[315] Several of their most promising analogues contained a 4-chloro-3-trifluoromethylphenyl moiety, which was incorporated into salvinorin A analogue **161**. This modification did not significantly increase affinity relative to other aromatic amide derivatives (K_i = 3,600 ± 300 nM). The affinity of this agent was not similar to the *N*-alkyl-octahydroisoquinolin-1-one-8-carboxamides synthesized by Frankowski and coworkers suggesting that their analogues are not binding in an identical manner to the neoclerodanes.

Table 1 Opioid receptor binding affinity for amide and amine derivatives

	K_i ± SD, nM		
Cmpd	**[^{3}H]DAMGO (MOP)**	**[^{3}H]DADLE (DOP)**	**[^{3}H]U69,593 (KOP)**
51[a]	1370 ± 130	>10,000	7.4 ± 0.7
90[a]	>2,800	>4,700	>10,000
100[a]	>2,800	>4,700	>10,000
101[a]	>2,800	>4,700	1,930 ± 220
102[a]	>2,800	>4,700	4,060 ± 280
159[a]	>10,000	>10,000	>10,000
160[a]	>10,000	>10,000	>10,000
161[b]	>10,000	>10,000	3600 ± 300
162[a]	>2,800	>4,700	410 ± 50
163[a]	>3,400	>5,200	510 ± 40
164[a]	>3,000	>5,000	300 ± 20
165[a]	>3,000	>5,000	560 ± 30

51 = Salvinorin A

[a] Receptor binding was performed in CHO cells which express the human MOP, DOP or KOP receptors. All results are n = 3.

[b] Results are n = 1, with sextuplet determinations and are based on inhibition of the 3H-ligand by 1 μM of the test compound

Amine Affinity

The effects of removing the carbonyl of the amide were investigated by reductive amination of aldehyde **135**. Selected amine derivatives were synthesized based on the affinities of their amide equivalent. First to be synthesized was aniline derivative **162**. Unexpectedly, **162** had a 25-fold increase in affinity evaluated against anilinoamide deriviate **90** (**162**: K_i = 410 ± 50 nM vs. **90**: K_i >10,000 nM) (**Table 1**). Efforts to increase the affinity of the amine were explored by modulating the basicity of the amine by introducing a fluorine in the *para* and *meta* position of the aromatic ring (**163**, **164**). Introduction of the fluorine substituent did not lead to significant changes in affinity (K_i = 510 ± 40 nM and K_i = 300 ± 20 nM, respectively). Additionally, the reduced morpholine amide (**165**) was synthesized to find a 2-fold loss of affinity (K_i = 560 ± 30 nM vs. K_i = 230 ± 20 nM). No further amine derivatives were synthesized due to the lack of high affinity for KOP receptors.

Ketone Affinity

With a similar hypothesis as the amide series ketone derivatives were synthesized with the expectations to retain a hydrogen bond interaction with the KOP receptor through the carbonyl of the ketone as well as maintain an aromatic interaction comparable to the furan ring of salvinorin A. Investigations started by synthesis of the phenyl ketone derivative in efforts to retain hydrogen bond accepting interaction through the carbonyl and hydrophobic interaction through the phenyl ring. Analogue **119** had roughly a 10-fold decrease in binding affinity at KOP receptors relative to salvinorin A (K_i = 68 ± 3 nM vs. K_i = 7.4 ± 0.7 nM) (**Table 2**). The difference in affinity between phenyl ketone analogue **119** and phenyl amide **90** is not readily apparent (K_i = 68 ± 3 nM vs. K_i > 10,000 nM) but could be due to the different electronic

characteristics of the carbonyl, different positioning of the phenyl ring in each derivative as a result as the sp^2 character of the amide bond, or size constraints of the KOP receptor binding

Table 2 Opioid receptor binding affinity for ketone derivatives

	K_i ± SD, nM		
Cmpd	**[^{3}H]DAMGO (MOP)**	**[^{3}H]DADLE (DOP)**	**[^{3}H]U69,593 (KOP)**
51 [a]	1370 ± 130	> 10,000	7.4 ± 0.7
119 [a]	1,490 ± 160	> 5,200	68 ± 3
167 [a]	> 14,000	> 5,200	1,070 ± 80
168 [a]	3,090 ± 260	> 5,200	290 ± 10
169 [a]	> 3,400	> 5,200	> 10,000
170 [a]	3,600 ± 40	> 5,000	500 ± 20
171 [a]	> 2,700	> 5,200	110 ± 5
172 [a]	> 3,000	> 5,000	8,470 ± 900
173	6000 ± 700 [a]	> 10,000 [b]	1010 ± 50 [a]
174 [b]	4100 ± 150	> 10,000	2800 ± 150
175	12300 ± 1300 [b]	> 5,000 [b]	40 ± 1 [a]
176 [b]	3650 ± 360	> 5,000	220 ± 10 [a]
177	4800 ± 400 [a]	2800 ± 200 [b]	9700 ± 800 [b]
178	3400 ± 150 [a]	4000 ± 350 [b]	2500 ± 300 [b]
116 [a]	> 3,200	> 5,000	81 ± 4
179 [a]	> 2,700	> 5,200	150 ± 10
117 [a]	> 8,600	> 5,000	36 ± 2
180 [a]	2,530 ± 250	> 5,000	31 ± 3
181 [c]	> 2,500	ND [d]	> 8,700
182 [a]	> 7,700	> 5,000	9,210 ± 680
183 [b]	3500 ± 300	> 5,000	1500 ± 1800
184 [a]	> 1,700	> 5,000	320 ± 20

[a] Receptor binding was performed in CHO cells which express the human MOP, DOP or KOP receptors. All results are n = 3.
[b] Results are n = 1, with sextuplet determinations and are based on inhibition of the 3H-ligand by 1 μM of the test compound
[c] Receptor binding was performed in CHO cells which express the human MOP or KOP receptors. Results are n = 1.
[d] ND = Not Determined

pocket exploited through the additional presence of the nitrogen. Phenylketone **119** was previously synthesized by Béguin and coworkers, however in their hands **119** had a K_i > 1,000 nM.[286]

Focusing on our affinity results and the ability of **119** to retain less than 100 nM affinity at KOP receptors and the potential of this scaffold to have greater metabolic stability than furan containing salvinorin A, investigations into substitutions at the *ortho*, *meta*, and *para* positions were completed with the electron donating and hydrogen bond accepting methoxy group (**167** – **169**) and the electron donating and hydrogen bond donating hydroxyl group (**170** – **172**). These substitutions were not tolerated at the *ortho* or *para* positions. *Meta* substitution of the methoxy group (**168**) and the hydroxyl group (**171**) resulted in affinity of 290 ± 10 nM and 110 ± 5 nM, respectively. Therefore, further exploration of *meta* substituted phenyl ketones were continued. Specific interest was to synthesize a carboxamide derivative due to the past successes of Wentland and coworkers who unexpectedly identified high affinity at opioid receptors when the 8-position hydroxyl of cyclazocine (**54**) (**Figure 10**) was substituted with a carboxamido group.[316,317] Hoping an observation in past opioid pharmacology held true in the ketone series of compounds as well, carboxamido analogue **175** was synthesized. Carboxamide (**175**) had a K_i value of 40 ± 1 nM. The addition of a cyano moiety in the *meta* position of the phenyl ring (**176**) decreased affinity relative to **119** (**176**: K_i = 220 ± 10 nM vs. **119**: K_i = 68 ± 3 nM). Further exploration of substation at the *meta* position with the addition of electron donating groups such as trifluoromethoxy (**177**) and trifluoromethyl (**178**) resulted in a substantial loss in affinity at KOP receptors indicating that the decrease in electron density of the phenyl ring is not tolerated (**177**: K_i = 9700 ± 800 nM and **178**: K_i = 2500 ± 300 nM).

Additionally, the effects of introducing heteroaromatic groups as replacements for the phenyl ring were investigated. Introduction of the 2-furan (**116**) and 3-furan (**179**) ketone probed the optimal interaction with the furan ring and the binding pocket. Bioisosteric substitution of the phenyl ketone with the 2-thiophene (**117**) and 3-thiophene (**180)** was well tolerated and increased affinity at KOP receptors comparable to the phenyl ketone derivative (**117**: K_i = 36 ± 2 nM, **180**: K_i = 31 ± 3 nM vs. **119**: K_i = 68 ± 3 nM). Béguin *et al*. had also previously synthesized **116** and **117** and reported a K_i > 1,000 nM for **116** and similar affinity with our results for **117** (K_i = 38 ± 10 nM).[286] With our successful introduction of heteroaromatic substituents, the size tolerated at the C-13 position was examined through synthesis of the 2-benzofuran (**181**), 2-benzothiophene (**182**), and 3-benzothiophene (**183**) analogues. The introduction of steric bulk associated with the additional aromatic ring was not tolerated at KOP receptors (**182**: K_i = 9,210 ± 680 nM and **183**: K_i = 1500 ± 1800 nM). Alkene **184** was also synthesized to investigate the scope of the Liebeskind-Srogl reaction and to probe the requirement of an aromatic ketone substituent for affinity at KOP receptors. Alkene **184** showed 44-fold loss in affinity relative to salvinorin A (K_i = 320 ± 20 nM).

Table 3 Opioid receptor binding for furan derivatives

	K_i ± SD, nM		
Cmpd	**[^{3}H]DAMGO (MOP)**	**[^{3}H]DADLE (DOP)**	**[^{3}H]U69,593 (KOP)**
51[a]	1370 ± 130	> 10,000	7.4 ± 0.7
185[b]	1400 ± 3 [b]	> 10,000 [b]	8.7 ± 0.4 [a]
187[b]	470 ± 20 [a]	> 10,000	450 ± 220 [b]
188[b]	> 10,000	> 10,000	1740 ± 5
189[b]	1300 ± 10	1700 ± 4	> 10,000
190[b]	230 ± 5	670 ± 10	44 ± 0.3

[a] Receptor binding was performed in CHO cells which express the human MOP, DOP or KOP receptors. All results are n = 3.
[b] Results are n = 1, with sextuplet determinations and are based on inhibition of the 3H-ligand by 1 μM of the test compound

Additional Affinity Studies

The ideal positioning of a possible hydrogen bond with the oxygen in the furan ring of salvinorin A and the KOP receptor was investigated by changing the position of the oxygen in the furan ring (**185**) (**Table 3**). Radioligand binding studies indicate that **185** has a $K_i = 8.7 \pm 0.4$ nM affinity at KOP receptors (**Table 3**), which is comparable to the affinity of salvinorin A at KOP receptors. Further investigations into this compound are currently underway.

Benzisoxazole **187** was synthesized in efforts to probe the steric limitations of the KOP opioid receptor binding site and it was found that **187** lost affinity at KOP receptors while increasing affinity at MOP receptors relative to salvinorin A ($K_i = 470 \pm 20$ nM). These finding suggest that **187** is either binding to a different binding site or that the introduction of steric bulk at this position is not well tolerated at KOP receptors. However, the MOP receptor binding site is able to accommodate the introduction the hydrophobic aromatic ring present in derivative **187**. The hypothesis that KOP receptors cannot tolerate steric bulk when introduced at this manner is also seen with some of the ketone analogues (**181** – **183**).

With the increase in affinity observed for analogue **187** at MOP receptors, studies were completed to determine the effects of introducing an oxime at the ketone position (**188** – **190**). Thus, to determine if the introduction of an oxime could modulate opioid receptor subtype selectivity, several oxime derivatives were synthesized. Preliminary affinity studies of **188** identified that the introduction of an oxime in this compound resulted in loss of affinity for both KOP and MOP receptors compared to its ketone derivative while **189** increased affinity 4-fold relative to its ketone equivalent. Oxime **190** retained affinity at KOP receptors and increased affinity at MOP receptors relative to its corresponding ketone analogue **117** (**190**: KOP: $K_i = 44$

± 0.30 nM and MOP: K_i = 230 ± 4 nM vs. **117**: KOP K_i = 36 ± 2 nM and MOP: K_i > 8,600 nM). Pharmacological evaluation of the separated *E* and *Z* isomers is currently ongoing.

Selected Efficacy Results

Efficacy studies were completed using the [^{35}S]GTPγS assay and the fluorometric imaging plate reader (FLIPR) assay. The [^{35}S]GTPγS assay measures efficacy by measuring G protein activation followed by ligand binding to the GPCR.[318] Efficacy is measured by analyzing of the binding of non-hydrolyzable [^{35}S]GTPγS to Gα subunits.[318] The FLIPR assay utilizes chimeric G proteins to measure changes in intracellular calcium with fluorescent calcium sensitive dyes.[319] Human $G\alpha_{16}$ is one of the most promiscuous G proteins in relation to its number of GPCRs interactions. Upon agonist binding, $G\alpha_{16}$ stimulates phospholipase Cβ activation through the G_q pathway resulting in calcium mobilization, which is then measured with fluorescent calcium sensitive dyes using the flourometric imaging plate reader.[319,320] Opioid receptors are intrinsically G_i-coupled therefore each opioid receptor is cotransfected with $G\alpha_{16}$ in CHO cells to stimulate the G_q pathway.[320]

In the GTPγS assay, phenyl ketone **119** shows a promising pharmacological profile as a partial agonist but results in a significant decrease in activity relative to salvinorin A (ED_{50} = 2,280 ± 550 nM, E_{max} = 74 ± 6% relative to U50,488) (**Table 4**). Analogue **176** also was shown to be a partial agonist with significant loss in activity relative to salvinorin A at KOP receptors in the FLIPR assay (ED_{50} = 1100 ± 380 nM, E_{max} = 78 ± 5% relative to U69,593) (**Table 5**). Derivatives **116**, **117**, **175** and **180** are full agonists in the GTPγS assay with significant loss in activity relative to salvinorin A with the most potent analogue being **175** which has an 18-fold loss in efficacy relative to salvinorin A. In the FLIPR assay, cyanoketone analogue **175** showed

a 12-fold loss in activity relative to salvinorin A in the FLIPR assay (**175**: ED_{50} = 75.4 ± 21 nM, E_{max} = 97 ± 2% vs. **51**: ED_{50} = 6.11 ± 0.04 nM, E_{max} = 97 ± 5%, relative to U69,593). Of all derivatives tested for activity, the most promising analogue was 2-furanyl salvinorin A (**185**) which had an EC_{50} of 138 ± 11 nM and an E_{max} of 104 ± 2% relative to U50,488 in the GTPγS assay and an EC_{50} = 12.2 ± 4.4 nM and an E_{max} = 97 ± 8% relative to U69,593 in the FLIPR assay. Analogue **185** identifies the potential to synthesize compounds with varying connectivity relative to salvinorin A while still retaining high affinity and efficacy.

Table 4 Opioid receptor activity measured in the [^{35}S]GTPγS assay

Cmpd	KOP ED_{50} ± SD[a]	KOP E_{max} ± SD[b]
51	40 ± 6	124 ± 6
119	2,280 ± 550	74 ± 6
116	2,860 ± 700	94 ± 8
117	1,630 ± 230	95 ± 4
175	730 ± 90	92 ± 4
180	620 ± 50	88 ± 2
185	140 ± 10	104 ± 2

[a] ED_{50} = Effective dose for 50% maximal response.
[b] Emax is % which compound stimulates binding compared to (-)-U50,488 (500 nM) at KOP receptors.
n = 3

The initial binding model proposed by Roth and coworkers of the KOP receptor binding site and salvinorin A has continued to be revised.[137] The exact interactions of salvinorin A and the KOP receptor still is not known due to the lack of KOP receptor-salvinorin A co-crystal structure. Elucidation of the interactions of salvinorin A and the KOP receptor have been attempted through molecular modeling, site-directed mutagenesis, chimeric receptor synthesis,

and SAR studies.[267-269] Furan analogues synthesized through these studies have assisted in explaining how the furan substituent of salvinorin A influences affinity and activity at the KOP receptor binding site. Focusing on the furan interactions with the KOP receptor binding site,

Table 5 Opioid receptor activity measured in the FLIPR assay

Cmpd	KOP ED_{50} ± SD[a]	KOP E_{max} ± SD[b] %
U69,593[c]	12.5 ± 5.4	100
51[d]	6.11 ± 0.04	97 ± 5
175[c]	75.4 ± 21	97 ± 2
176[c]	1100 ± 380	78 ± 5
185[c]	12.2 ± 4.4	97 ± 8

[a] ED_{50} = Effective dose for 50% maximal response.
[b] Emax is % which compound stimulates binding compared to (-)-U69,593 at KOP receptors.
[c] N = 3
[d] N = 2

Yan and *et al*. identified the importance of Y320 and Y119 by site-directed mutagenesis of Y320A, Y320F, Y119A, and Y119F that resulted in loss of affinity.[269] Due to the loss of affinity of these substitutions it was hypothesized that Y320 and Y119 were stabilizing the furan ring of salvinorin A through hydrogen bonding interactions with the furanyl oxygen. However, a computational model proposed by Singh and coworkers implicated that a direct hydrogen bond was not formed with the furanyl oxygen.[321] 2-Furanyl salvinorin A (**175**) was able to retain affinity at KOP receptors relative to salvinorin A, which supports Singh and coworkers findings that the furan ring of salvinorin A interacts with KOP receptors through hydrophobic interactions and not a hydrogen bond (**175**: K_i = 8.7± nM vs. **51**: K_i = 7.4 ± 0.7 nM). Moving the furanyl oxygen did not alter affinity and activity at KOP receptors implicating that the oxygen does not

directly interact with the KOP receptor binding site. This identifies a new scaffold for modification in the efforts to further elucidate the KOP receptor binding site and more efficacious salvinorin A analogues. Additionally, the loss in affinity seen with the majority of ketone analogues shows the importance in the positioning of the aromatic group. Homologation through introduction of the carbonyl functionality generally decreases affinity relative to salvinorin A, which could result from the change in connectivity from the salvinorin A core and the aromatic substituent. These observations further corroborate that the furan ring is acting through aromatic interactions and not directly through hydrogen bonding. Additional ligand based models are required to further understand salvinorin A binding at KOP receptors.

Salvinorin A and Solubility

As a neoclerodane diterpene, salvinorin A is highly lipophilic and consequently has poor solubility in aqueous solvents. To assist in solubility, vehicles are utilized, which have the potential to modulate bioavailability and toxicity.[302] Therefore, choice of vehicle can alter the biological data of an assay, especially if the vehicle causes measurable effects. Currently, a number of vehicle formulations ranging from Tween-80:ethanol:saline (1:1:8) to DMSO:H_2O (3:1) are used to solubilize salvinorin A.[244,259] Use of these vehicles is less than ideal due to the known effects of DMSO and ethanol in analgesia.[270,304,305] DMSO, being an amphipathic molecule, is efficient for use as a solvent for compounds with poor water solubility.[322] However, DMSO causes a number of effects on its own and can lead to incorrect data interpretation. Specifically of interest in opioid receptor pharmacology is the ability of DMSO at high doses of i.v. or i.p. administration to cause in significant analgesia in both the hot-plate and tail flick tests in both local and systemic manners.[304] Additionally, ethanol has been showed to potentiate the inhibitory effects of endogenous opioids at concentrations as low as 0.1%.[305] Ethanol also appears to enhance the action of endogenous opioids by inhibiting substance P release.[305] Identification of a new vehicle to assist in salvinorin A solubility is needed without potential pharmacological interactions at opioid receptors. A new vehicle could also lead to the deconvolution pharmacological findings. Therefore, investigation in to the potential use of Captisol® as a vehicle for salvinorin A was completed.

Captisol® is a modified β-cyclodextrin (β-CD) known also as $(SBE)_{7m}$-β-CD. SBE refers to sulfobutyl ether substitutions variably substituted at the 2-, 3-, and 6- position of β-CD while 7 refers to the average degree of subsitution.[323] β-Cyclodextrins are cyclic oligosaccharides linked through 1,4 glycosidic bonds into a macrocycle resulting in a cone-like structure.[324] They have a

hydrophobic interior that encapsulates lipophilic drugs and a hydrophilic exterior that increases aqueous solubility through the formation of inclusion complexes through non-covalent interactions.[324-326] Complexation of the cyclodextrin and the drug molecule is a dynamic process that results in rapid and quantitative release, which is not a limiting factor.[326] Cylcodextrins have shown considerable potential as a drug carrying agents and the ability to assist with dosage formulation.[325] However, the use of β-CD itself is limited due to its solubility problems along with associated renal toxicity.[327] As a result, many β-CD derivatives have been synthesized with improved aqueous solubility and toxicity profiles. Two of the most pharmacologically relevant derivatives meeting the standards for high quality and safety are $(SBE)_{7m}$-β-CD (Captisol®) and hydroxypropyl-β-CD (HP).[327-332]

β-CD derivatives have been investigated as a solubilizing agent for paclitaxel due to side-effects cause by its formulation with Cremophor EL®.[307,324] Successful formulation was found to include paclitaxel with RAME-β-CD (randomly methylated).[324] Paclitaxel is a diterpene which has poor aqueous solubility, P-gp efflux, and cytochrome P450 metabolism, like salvinorin A.[306] Testosterone has also been evaluated with $(SBE)_{7m}$-β-CD and HP-β-CD to act as a solubilizing and an osmotic pump agent.[323] Testosterone was chosen as a model drug due to its poor water solubility and $(SBE)_{7m}$-β-CD was found to increase the solubility approximately 70% greater than HP-β-CD. Prednisolone, another poorly water-soluble drug, has also been formulated with $(SBE)_{7m}$-β-CD and showed controlled and complete drug release.[333] Melphalan, carmustine, and etomidate have all been effectively formulated with Captisol®.[327,334] With the successes of Captisol® as a solubilizing agent for a number of known therapeutics along with poorly water-soluble compounds, we investigated its ability to assist in salvinorin A solubility.

In preliminary studies, an excess of salvinorin A was added to solutions of Captisol® at concentration of 0.5, 1.0, 1.5, 2.0 and 2.5 M in sterile water. Excess salvinorin A was added into duplicate 2 mL screw cap vials which contained approximately 1 mL of the Captisol® solution. The vials were sonicated for 72 hours and then set at room temperature for 24 hours. Vials were then centrifuged at 7700 rpm for 10 minutes and the supernatant was passed through 0.45 µm nylon non-sterile Fisherbrand® syringe filters and immediately analyzed by HPLC without diluting (column: Phenomenex Luna C18 (250 × 4.5 mm, 5 µm); mobile phase: 60% CH_3CN:40% H_2O; flow rate: 5.00 mL/min; injection volume: 100 µL). Wavelengths 209.4 nm and 214.06 nm were both evaluated.

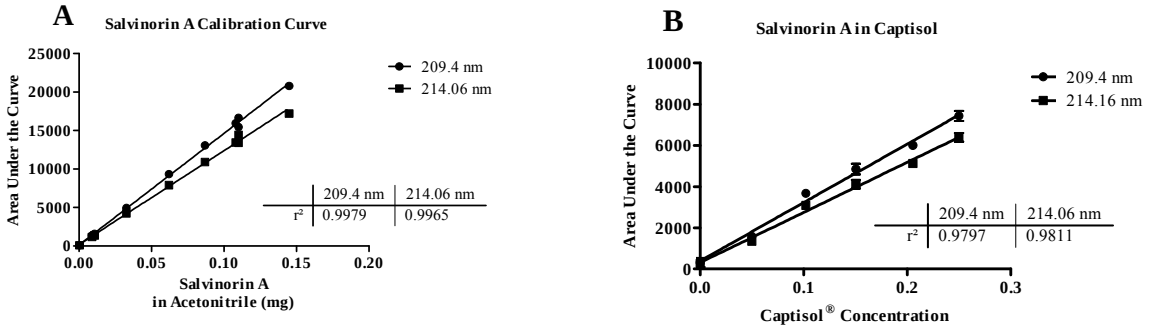

Figure 19: (A) Calibration Curve of Salvinorin A; **(B)** Effect of Concentration of Captisol® on Solubility of Salvinorin A

The amount of salvinorin A was calculated from the peak area of the salvinorin A standard curve under the same HPLC conditions as described (**Figure 19**). The solubility of salvinorin significantly increased with increasing concentrations of Captisol®. The effects of different concentrations of Captisol® on the solubility of salvinorin A are summarized in **Table 6** as fold increased relative to salvinorin A in sterile water. The solubility of salvinorin A was

highest with the greatest concentration of Captisol®. Use of 2.5 M Captisol® was found to increase the aqueous solubility of salvinorin A approximately 50-fold.

Table 6 Increase in Solubility of Salvinorin A with varying amounts of Captisol®

Captisol® (M)	Salvinorin A (mg/mL ± SD)		Fold Increase	
	209.4 nm	214.06 nm	209.4 nm	214.06 nm
0.25	0.504 ± 0.0287	0.510 ± 0.0291	39	59
0.206	0.406 ± 0.0135	0.406 ± 0.0186	32	47
0.151	0.326 ± 0.0312	0.324 ± 0.0291	25	37
0.102	0.245 ± 0.0108	0.239 ± 0.0130	19	28
0.0500	0.101 ± 0.0212	0.0973 ± 0.0223	8.0	11

Increasing concentrations of Captisol® in sterile water increased the solubility of salvinorin A, which identifies a new vehicle for salvinorin A delivery. One of the most used formulations to assist with salvinorin A solubility in *in vivo* studies is the mixture of Tween-80:ethanol:saline (1:1:8). This vehicle cocktail still uses ethanol, which is unsatisfactory given its known opioid effects.[305] Even with the use of ethanol, only 0.2 mg/mL of salvinorin A is able to be solubilized in solution.[308] By using Captisol® we were able to successfully solubilized 0.5 mg/mL of salvinorin A in sterile water with the potential to limit the negative effects of currently known vehicles. Thus, we have identified Captisol® as a solubilizing agent to assist in the pharmacological evaluation of salvinorin A and salvinorin A derivatives.

CHAPTER V. CONCLUSIONS

Furan derivatives of salvinorin A were synthesized to further elucidate the pharmacophore of salvinorin A while identifying analogues with more desirable pharmacological properties. The focus of compounds synthesized was specifically to minimize the potential for hepatoxicity while establishing structural requirements for affinity and activity. Several series of analogues were synthesized through rational design that replaced the furan ring with amide, amine, ketone, and oxime substituents. The intentions in the amide and ketone series were to retain hydrogen bond potential with the carbonyl, possible introduction of additional interactions in the binding pocket of KOP receptors due to the new substituent, and to improve the pharmacological characteristics of the analogues by enhancing toxicity profiles and water solubility. Amines synthesized were to reveal the importance of the carbonyl, investigate the effects of introducing a basic amine, and to improve water solubility. Lastly, several oxime analogues were synthesized to further investigate the structural requirements to modulate subtype selectivity at opioid receptors. A summary of the affinity and efficacy trends identified is summarized in **Figure 20**.

Investigations into amide and amine derivatives concluded that aliphatic amide analogues had greater affinity at opioid receptors compared to the aromatic amide derivatives. Additionally, aromatic amines had improved affinity relative to the parent amide but aliphatic amines appeared to have comparable affinity to the corresponding amide. Ketone analogues were synthesized utilizing a high yielding method to prepare arylketones via palladium mediated coupling of the appropriate boronic acid and a thioester. Exploration of the ketone series identified phenylketone **119** as having < 100 nM affinity at KOP receptors. Based on this finding, studies were carried out to determine the effects of hydrogen bonding, electronic effects,

and steric effects of phenyl substitution at the *ortho*, *meta*, and *para* positions. Several substitutions at the *meta* position were found to retain affinity relative to phenylketone **119**. Introduction of a carboxamido or cyano substituent resulted in analogues with KOP receptor affinity of 40 ± 1 nM and 220 ± 10 nM, respectively. The introduction of the electron withdrawing groups trifluoromethoxy and trifluoromethyl were not tolerated. Substituent modifications on the phenyl ring resulted in compounds with altered affinity and selectivity at opioid receptors. Ketone and amide replacements generally decreased affinity and efficacy relative to salvinorin A.

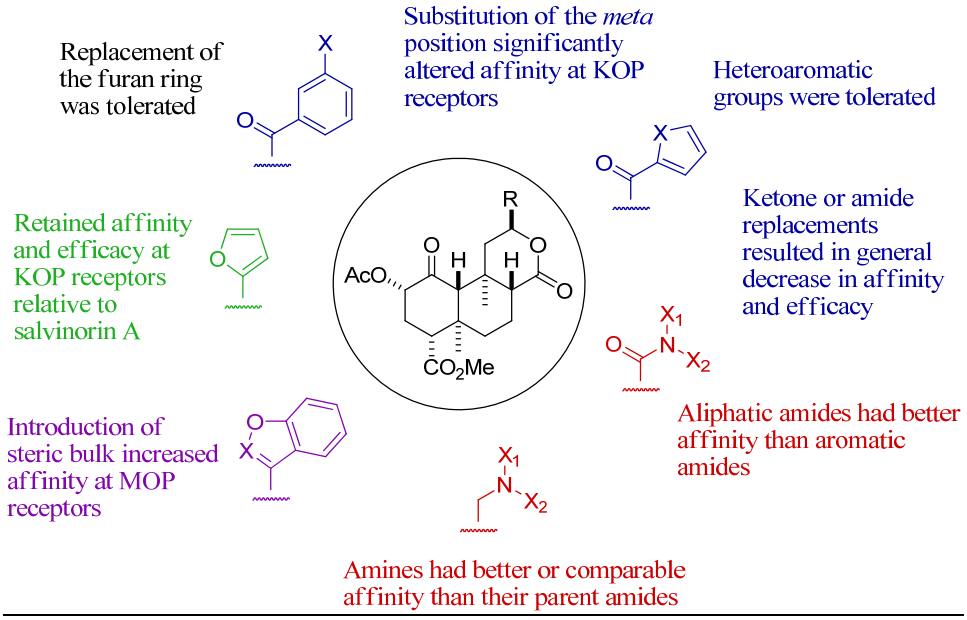

Figure 20: Affinity and Efficacy Relationships Established Through These Studies

Heteroaromatic groups were substituted for the phenyl ring and were found to be tolerated. The introduction in size of the ketone substituent generally decreased affinity at KOP receptors. A trend relating to the introduction of steric bulk and increased affinity of MOP

receptors was observed. Depending on the substituent introduced, it appears that increased size resulted in improved affinity at MOP receptors. The trend of introducing steric bulk and increasing MOP receptor affinity was observed with the introduction of a benzisoxazole moiety, which increased affinity at MOP receptors relative to salvinorin A. The benzisoxazole derivative leads one to believe that steric bulk at this position is not tolerated at KOP receptors but MOP receptors are better able to accommodate the bulk with a potential explanation being additional hydrophobic interactions. Additionally, the 2-furanyl salvinorin A (**185**) analogue was able to maintain affinity and activity at KOP receptors relative to salvinorin A. Proposed molecular modeling studies implicate the importance of the furan ring of salvinorin A through interaction with specific tyrosine residues through either hydrogen bonding or aromatic interactions.[267-269,321] The retention of affinity and activity observed with 2-furanyl salvinorin A (**185**) supports that the furan ring is interacting at the KOP receptor through aromatic interactions and not directly through hydrogen bonding. The development of additional ligand based models will further elucidate the interaction of the furan ring of salvinorin A at KOP receptors. Throughout this work, several furan derivatives have been identified that retain affinity at KOP receptors and others in which affinity has been observed at MOP receptors. Analogues without a furan ring have a decreased potential for hepatoxicity compared to salvinorin A, which increases potential for the development of a therapeutic agent.

Studies were also completed to evaluate Captisol® as a vehicle for salvinorin A administration. Results are summarized in **Figure 21**. Increasing concentrations of Captisol® increased the solubilized amount of salvinorin A in solution. The concentration of salvinorin A in 2.5 M Captisol® was able to reach the concentration of 0.5 mg/mL, the highest concentration of salvinorin A in aqueous solution to date. The use of Captisol® as a delivery agent for

salvinorin A and derivatives has the potential to deconvolute data analysis by eliminating the use of DMSO or ethanol.

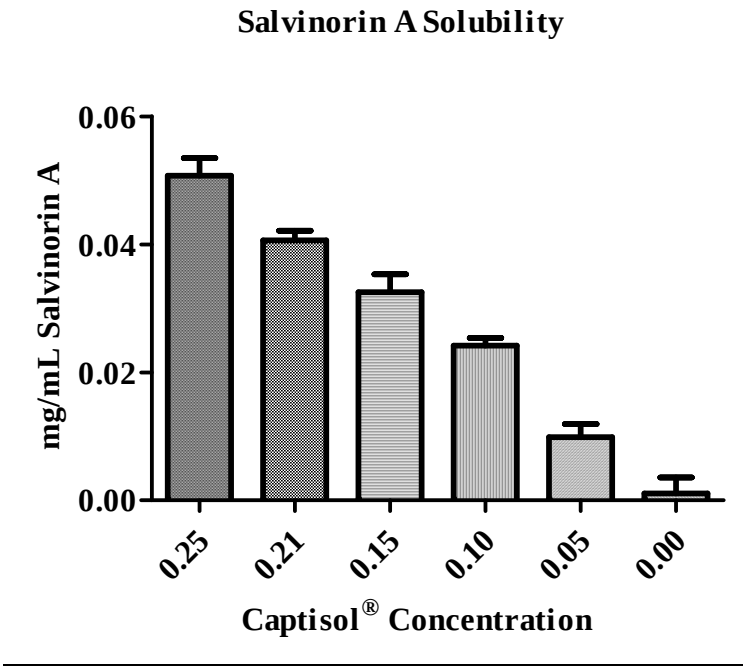

Figure 21: Summary of Salvinorin A Solubility Results

These studies have helped to further elucidate the structure-activity relationships and pharmacophore of salvinorin A. Information from these studies will help to direct future exploration of the salvinorin A scaffold and determine how it interacts at opioid receptors. Specific emphasis was made to improve the pharmacological profile of salvinorin A analogues to increase the potential to lead to identification of novel opioid therapeutics. Moving forward, interest includes the elucidation of structure-activity relationships for 2-furanyl substituents and analogue development of compounds with both C-2 and C-12 substitutions to increase potency.

CHAPTER VI. EXPERIMENTALS

Unless otherwise indicated, all reagents were purchased from commercial suppliers and were used without further purification. Melting points were determined on a Thomas-Hoover capillary melting apparatus. NMR spectra were recorded on a Bruker DRX-400 with qnp probe or a Bruker AV-500 with cryoprobe using δ values in ppm (TMS as internal standard) and *J* (Hz) assignments of ^{1}H resonance coupling. High resolution mass spectrometry data were collected on either a LCT Premier (Waters Corp., Milford, MA) time of flight mass spectrometer or an Agilent 6890 N gas chromatograph in conjunction with a quarto Micro GC mass spectrometer (Micromass Ltd, Manchester UK). Thin-layer chromatography (TLC) was performed on 0.25 mm plates Analtech GHLF silica gel plates using ethyl acetate/*n*-hexanes, in 1:1 ratio as the solvent system unless otherwise noted. Spots on TLC were visualized by uv (254 or 365 nm), if applicable, and phosphomolybdic acid in ethanol. Column chromatography was performed with Silica Gel (32 – 63 μ particle size) from Bodman Industries (Atlanta, GA). Analytical HPLC was carried out on an Agilent 1100 Series Capillary HPLC system with diode array detection at 209.4 nm on an Agilent Eclipse XDB-C18 column (250 × 10 mm, 5 μm) with isocratic elution in 60% CH_3CN/40% H_2O at a flow rate of 5.0 mL/min unless otherwise noted, or on a Phenomenex Luna column (250 × 4.5 mm, 5 μm) with isocratic elution in 60% CH_3CN/40% H_2O unless otherwise noted. The systematic name for salvinorin A (**1**) is (2*S*,4a*R*,6a*R*,7*R*,9*S*,10a*S*,10b*R*)-methyl 9-acetoxy-2-(furan-3-yl)-6a,10b-dimethyl-4,10-dioxo-dodecahydro-1*H*-benzo[*f*]iso-chromene-7-carboxylate. Salvinorin A was isolated from *S. divinorum* as previously described.[276]

General Procedure A

A solution of **51**(1 equiv), appropriate amine (1.5 equiv), EDCI (2.5 equiv), HOBt (2.5 equiv) and Et_3N (10 equiv) in 20 mL DCM was stirred at room temperature overnight. An additional 15 mL of DCM was added and then reaction mixture was then washed with saturated aqueous $NaHCO_3$ (3 × 15 mL), H_2O (3 × 15 mL), brine (15 mL), and dried over anhydrous Na_2SO_4. The solvent was evaporated *in vacuo* and the resulting residue purified by flash column chromatography on silica gel using mixtures of EtOAc/*n*-hexanes and triturated in EtOAc/*n*-hexanes to afford desired product.

General Procedure B

To an oven dried round bottom flask under argon was added **51** (1 equiv), CDMT (3 equiv), *N*-methylmorpholine (6 equiv) was stirred in anhydrous THF. After 1 hour, appropriate thiol (3 equiv) was added and reaction stirred at room temperature for 48 hours. The reaction was quenched with H_2O (25 mL) and extracted with Et_2O (3 × 30 mL). The combined Et_2O portion was washed with saturated aqueous $NaHCO_3$ (3 × 20 mL), 2N HCl (3 × 20 mL), brine (3 × 20 mL), and dried over anhydrous Na_2SO_4. The solvent was evaporated *in vacuo* and the resulting residue purified by flash column chromatography on silica gel using mixtures of EtOAc/*n*-hexanes and triturated in EtOAc/*n*-hexanes to afford desired product.

General Procedure C

A solution of **135** (1 equiv), appropriate amine (1.05 equiv), and sodium triacetoxyborohydride (2.2 equiv) in 1,2-dichloroethane was stirred at room temperature overnight. The reaction mixture was then quenched with $NaHCO_3$ (10 mL) and extracted with DCM (3 × 15 mL). The

combined DCM extracts were washed with saturated aqueous $NaHCO_3$ (3 × 15 mL), brine (3 × 15 mL) and dried over anhydrous Na_2SO_4. The solvent was evaporated *in vacuo* and the resulting residue purified by flash column chromatography on silica gel using mixtures of EtOAc/*n*-hexanes and triturated in EtOAc/*n*-hexanes to afford desired product.

General Procedure D

A solution of **119** (1 equiv), appropriate boronic acid (3 equiv), copper(I) thiophene-2-carboxylate (1.5 equiv), and bis(dibenzylideneacetone)palladium(0) (5 mol%) in anhydrous THF under argon was stirred at room temperature. To the stirring solution, triethyl phosphite (20 mol %) was added. The reaction mixture was stirred at room temperature and monitored by TLC until complete. Reactions were typically complete in 2 – 5 hours. The mixture was then washed with saturated aqueous $NaHCO_3$ (3 × 15 mL), brine (15 mL) and dried over anhydrous Na_2SO_4. The solvent was evaporated *in vacuo* and the resulting residue purified by flash column chromatography on silica gel using mixtures of EtOAc/*n*-hexanes and triturated in EtOAc/*n*-hexanes to afford desired product.

General Procedure E

Appropriate ketone derivative (1 equiv) was dissolved in MeOH followed by the addition of hydroxylamine hydrochloride (2 equiv) and pyridine (10 equiv). Reaction mixture was heated to a gentle reflux and monitored by TLC. Upon completion, reaction was cooled to room temperature and solvent evaporated. The crude product was dissolved in 20 mL EtOAc and washed with aqueous 2 N HCl (3 × 10 mL), brine (15 mL), and dried over anhydrous Na_2SO_4. The solvent was evaporated *in vacuo* and the resulting residue purified by flash column

chromatography on silica gel using mixtures of EtOAc/*n*-hexanes and triturated in EtOAc/*n*-hexanes to afford desired product.

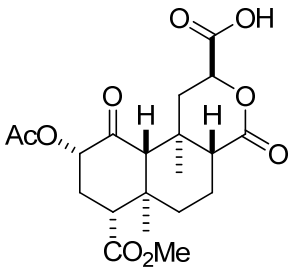

(2*S*,4a*R*,6a*R*,7*R*,9*S*,10a*S*,10b*R*)-9-acetoxy-7-(methoxycarbonyl)-6a,10b-dimethyl-4,10-dioxododecahydro-1*H*-benzo[*f*]isochromene-2-carboxylic acid (75).

A solution of **51** (Salvinorin A; 2.00 g, 4.62 mmol, 1 equiv) in CCl_4:CH_3CN:H_2O (2:2:3, 70 mL) was stirred at room temperature. To the stirring solution, $NaIO_4$ (11.88 g, 55.4 mmol, 12 equiv) was added followed by a catalytic amount of $RuCl_3 \cdot 3H_2O$. The mixture was stirred for 3 hours and then filtered through a pad of Celite. The Celite was washed thoroughly with EtOAc and the organic layer was collected. The organic layer was washed with saturated aqueous $NaHCO_3$ (3 × 50 mL) and the aqueous layer collected. And then the aqueous layer was acidified to pH 2 with 2N HCl and extracted with EtOAc (3 × 100 mL). The organic layer was then washed with H_2O (3 × 30 mL), brine (3 × 30 mL), and dried over anhydrous Na_2SO_4. The solvent was evaporated *in vacuo* to yield a a white solid, mp 245 – 248 °C; which was used without further purification. ^{1}H NMR (500 MHz, $CDCl_3$) δ 6.31 (s, 1H), 5.34 – 5.27 (m, 1H), 5.01 (dd, *J* = 6.7, 10.5 Hz, 1H), 3.72 (d, *J* = 6.7 Hz, 3H), 2.84 (dd, *J* = 5.6, 11.2 Hz, 1H), 2.57 (dd, *J* = 6.7, 13.5 Hz, 1H), 2.36 (s, 1H), 2.30 (td, *J* = 7.0, 12.4 Hz, 2H), 2.20 (s, 3H), 2.18 – 2.08 (m, 2H), 1.80 – 1.73 (m, 1H), 1.70 – 1.58 (m, 2H), 1.50 (dd, *J* = 10.7, 13.4 Hz, 1H), 1.37 (s, 3H), 1.08 (s, 3H). ^{13}C NMR (126 MHz, $CDCl_3$) δ 202.21, 172.91, 171.92, 171.25, 170.54, 75.84, 73.63, 63.68, 53.24, 52.20, 50.31,

42.22, 38.76, 37.83, 35.46, 30.76, 20.92, 18.30, 16.48, 15.78. HRMS(*m/z*): [M-H] calcd for $C_{20}H_{25}O_9$, 409.1499; found, 409.1455. HPLC t_R = 2.024 min; purity = 96.20%.

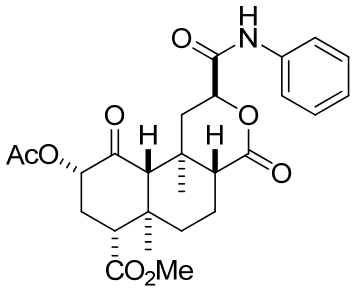

(2*S*,4a*R*,6a*R*,7*R*,9*S*,10a*S*,10b*R*)-methyl 9-acetoxy-6a,10b-dimethyl-4,10-dioxo-2-(phenyl-carbamoyl)dodecahydro-1*H*-benzo[*f*]isochromene-7-carboxylate (90).

Compound **90** was synthesized from **75** using **Procedure A** and aniline to afford 0.189 g (47.4%) as a white solid, mp 136 – 140 ºC; ^{1}H NMR (500 MHz, $CDCl_3$) δ 8.14 (s, 1H), 7.54 (dd, *J* = 1.0, 8.6 Hz, 2H), 7.38 – 7.31 (m, 2H), 7.18 – 7.13 (m, 1H), 5.18 (dd, *J* = 8.2, 11.9 Hz, 1H), 5.03 (dd, *J* = 6.1, 11.0 Hz, 1H), 3.72 (s, 3H), 2.77 (ddd, *J* = 5.3, 13.1, 16.8 Hz, 2H), 2.36 – 2.25 (m, 2H), 2.19 (d, *J* = 9.4 Hz, 4H), 2.15 – 2.03 (m, 2H), 1.82 – 1.74 (m, 1H), 1.72 – 1.60 (m, 2H), 1.60 – 1.51 (m, 1H), 1.42 (s, 3H), 1.11 (s, 3H). ^{13}C NMR (126 MHz, $CDCl_3$) δ 201.62, 171.68, 170.29, 169.85, 167.32, 136.77, 129.27, 125.16, 120.18, 76.01, 74.84, 63.96, 53.49, 52.15, 51.21, 42.00, 39.18, 37.92, 35.52, 30.87, 20.73, 18.19, 16.44, 15.59. HRMS (*m/z*): [M+Na] calcd for $C_{26}H_{31}NO_8Na$, 508.1948; found, 508.1970. HPLC t_R = 5.568 min; purity = 98.23%.

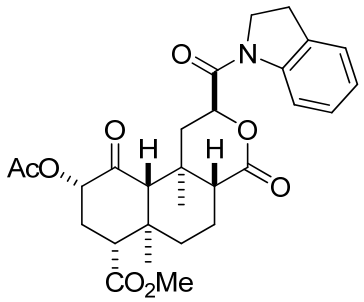

(2*S*,4a*R*,6a*R*,7*R*,9*S*,10a*S*,10b*R*)-methyl 9-acetoxy-2-(indoline-1-carbonyl)-6a,10b-dimethyl-4,10-dioxododecahydro-1*H*-benzo[*f*]isochromene-7-carboxylate (100).

Compound **100** was synthesized from **75** using **Procedure A** and indoline to afford 0.086 g (34.1%) as a white solid, mp 146 – 149 ºC; ^{1}H NMR (500 MHz, $CDCl_3$) δ 8.21 – 8.16 (m, 1H), 7.22 (t, *J* = 7.0 Hz, 2H), 7.11 – 7.04 (m, 1H), 5.22 (t, *J* = 7.8 Hz, 1H), 5.19 – 5.11 (m, 1H), 4.34 – 4.26 (m, 1H), 4.08 – 4.00 (m, *J* = 7.3, 9.5 Hz, 1H), 3.73 (s, 3H), 3.23 (t, *J* = 8.5 Hz, 2H), 2.77 (dd, *J* = 6.1, 10.7 Hz, 1H), 2.54 (dd, *J* = 8.3, 13.5 Hz, 1H), 2.43 (dd, *J* = 3.2, 11.6 Hz, 1H), 2.33 – 2.26 (m, 2H), 2.16 (s, 3H), 2.11 (dd, *J* = 3.2, 13.9 Hz, 1H), 1.92 (dd, *J* = 7.3, 13.5 Hz, 1H), 1.75 (dd, *J* = 3.1, 12.9 Hz, 1H), 1.72 – 1.54 (m, 3H), 1.42 (d, *J* = 8.4 Hz, 3H), 1.07 (s, 3H). ^{13}C NMR (126 MHz, $CDCl_3$) δ 202.44, 171.81, 171.30, 169.98, 166.93, 142.42, 131.61, 127.76, 124.92, 124.88, 117.53, 75.12, 73.58, 64.74, 53.33, 52.12, 49.15, 47.75, 42.15, 37.83, 37.50, 35.28, 30.80, 28.21, 20.74, 18.31, 17.17, 16.12. HRMS (*m/z*): [M+H] calcd for $C_{28}H_{34}NO_8$, 512.2285; found, 512.2294. HPLC t_R = 6.680 min; purity = 98.00%.

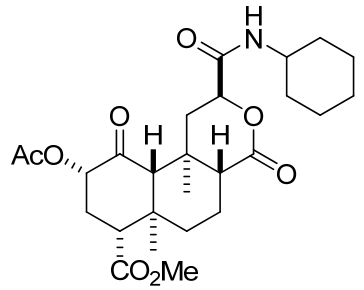

(2*S*,4a*R*,6a*R*,7*R*,9*S*,10a*S*,10b*R*)-methyl 9-acetoxy-2-(cyclohexylcarbamoyl)-6a,10b-dimethyl -4,10-dioxododecahydro-1*H*-benzo[*f*]isochromene-7-carboxylate (101).

Compound **101** was synthesized from **75** using **Procedure A** and cyclohexylamine to afford 0.053 g (21.0%) as a white solid, mp 141 – 145 ºC; ^{1}H NMR (500 MHz, $CDCl_3$) δ 6.26 (d, *J* = 8.3, 1H), 5.16 (dd, *J* = 8.0, 12.1, 1H), 4.86 (dd, *J* = 6.1, 10.8, 1H), 3.81 – 3.69 (m, 4H), 2.77 – 2.66 (m, 2H), 2.35 – 2.20 (m, 2H), 2.17 (d, *J* = 3.8, 4H), 2.13 – 2.06 (m, 1H), 2.06 – 2.00 (m, 1H), 1.88 (t, *J* = 15.0, 2H), 1.81 – 1.69 (m, 4H), 1.66 – 1.47 (m, 4H), 1.44 – 1.22 (m, 7H), 1.10 (d, *J* = 8.9, 3H). ^{13}C NMR (126 MHz, $CDCl_3$) δ 201.56, 171.68, 170.65, 169.80, 168.32, 76.01, 74.83, 64.07, 53.54, 52.09, 51.11, 48.38, 42.01, 39.35, 37.98, 35.46, 33.17, 32.99, 30.92, 25.50, 24.99, 24.97, 20.69, 18.20, 16.41, 15.65. HRMS (*m/z*): [M+H] calcd for $C_{26}H_{38}NO_8$, 492.2598; found, 492.2597. HPLC t_R = 5.793 min; purity = 98.29%.

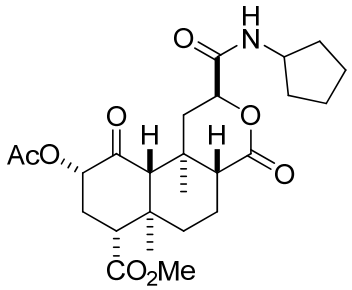

(2*S*,4a*R*,6a*R*,7*R*,9*S*,10a*S*,10b*R*)-methyl 9-acetoxy-2-(cyclopentylcarbamoyl)-6a,10b-dimeth-yl-4,10-dioxododecahydro-1*H*-benzo[*f*]isochromene-7-carboxylate (102).

Compound **102** was synthesized from **75** using **Procedure A** and cyclopentylamine to afford 0.058 g (24.4%) as a white solid, mp 188 – 190 ºC; ^{1}H NMR (500 MHz, $CDCl_3$) δ 6.30 (d, *J* = 7.6 Hz, 1H), 5.16 (dd, *J* = 7.9, 12.1 Hz, 1H), 4.86 (dd, *J* = 6.1, 10.8 Hz, 1H), 4.19 (dd, *J* = 7.2, 14.4 Hz, 1H), 3.72 (s, 3H), 2.77 – 2.66 (m, 2H), 2.35 – 2.20 (m, 2H), 2.17 (s, 4H), 2.10 (dd, *J* = 3.2, 14.0 Hz, 1H), 2.00 (m, 3H), 1.78 (d, *J* = 13.1 Hz, 1H), 1.73 – 1.49 (m, 7H), 1.44 – 1.30 (m,

5H), 1.09 (s, 3H). ^{13}C NMR (126 MHz, $CDCl_3$) δ 201.55, 171.69, 170.63, 169.82, 168.82, 76.03, 74.84, 64.12, 53.59, 52.12, 51.17, 51.14, 42.03, 39.34, 38.01, 35.48, 33.15, 33.05, 30.94, 23.88, 23.87, 20.71, 18.22, 16.43, 15.64. HRMS (*m/z*): [M+H] calcd for $C_{25}H_{36}NO_8$, 478.2441; found, 478.2422. HPLC t_R = 5.098 min; purity = 95.33%.

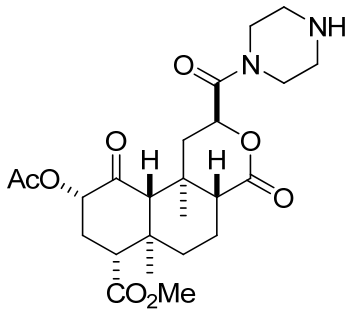

(2*S*,4a*R*,6a*R*,7*R*,9*S*,10a*S*,10b*R*)-methyl 9-acetoxy-6a,10b-dimethyl-4,10-dioxo-2-(piperazine -1-carbonyl)dodecahydro-1*H*-benzo[*f*]isochromene-7-carboxylate (159).

Compound **159** was synthesized from **75** using **Procedure A** and piperazine to afford 0.105 g (44.9%) as a white solid, mp 180 – 183 ºC; ^{1}H NMR (500 MHz, $CDCl_3$) δ 5.23 (t, *J* = 7.7 Hz, 1H), 5.20 – 5.11 (m, 1H), 3.72 (s, 4H), 3.55 (s, 1H), 3.46 (d, *J* = 35.7 Hz, 2H), 2.87 (s, 2H), 2.81 – 2.72 (m, 1H), 2.44 – 2.25 (m, 5H), 2.17 (s, 3H), 2.11 – 2.03 (m, 1H), 1.88 (dd, *J* = 7.2, 13.7 Hz, 1H), 1.78 – 1.53 (m, 6H), 1.38 (d, *J* = 3.9 Hz, 3H), 1.06 (s, 3H). ^{13}C NMR (126 MHz, $CDCl_3$) δ 202.49, 171.89, 171.45, 170.06, 167.45, 75.18, 71.45, 64.80, 53.44, 52.19, 49.14, 47.16, 46.53, 45.95, 43.82, 42.20, 37.89, 35.27, 30.89, 20.82, 18.36, 17.30, 16.21. HRMS (*m/z*): [M+H] calcd for $C_{24}H_{35}N_2O_8$, 479.2393; found 479.2405.

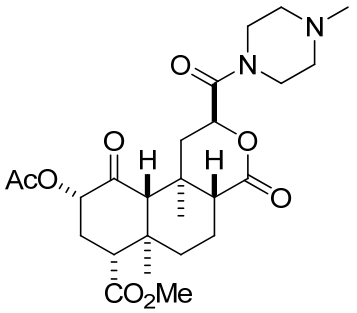

(2*S*,4a*R*,6a*R*,7*R*,9*S*,10a*S*,10b*R*)-methyl 9-acetoxy-6a,10b-dimethyl-2-(4-methylpiperazine-1-carbonyl)-4,10-dioxododecahydro-1*H*-benzo[*f*]isochromene-7-carboxylate (160).

Compound **160** was synthesized from **75** using **Procedure A** and *N*-methyl piperazine to afford 0.083 g (34.9%) as a white solid, mp 124 – 127 ºC; ^{1}H NMR (500 MHz, $CDCl_3$) δ 5.22 (t, *J* = 7.7 Hz, 1H), 5.19 – 5.12 (m, 1H), 3.72 (s, 4H), 3.59 (s, 1H), 3.49 (d, *J* = 29.0 Hz, 2H), 2.76 (dd, *J* = 5.4, 11.4 Hz, 1H), 2.50 – 2.26 (m, 11H), 2.16 (d, *J* = 5.4 Hz, 3H), 2.10 – 2.03 (m, 1H), 1.89 (dd, *J* = 7.3, 13.6 Hz, 1H), 1.74 (d, *J* = 12.8 Hz, 1H), 1.70 – 1.52 (m, 3H), 1.37 (s, 3H), 1.06 (s, 3H). ^{13}C NMR (126 MHz, $CDCl_3$) δ 202.40, 171.82, 171.34, 169.96, 167.28, 75.10, 71.44, 64.75, 55.15, 54.62, 53.39, 52.11, 49.10, 46.07, 45.79, 42.63, 42.13, 37.84, 37.80, 35.22, 30.84, 20.75, 18.29, 17.26, 16.15. HRMS (*m/z*): [M+H] calcd for $C_{25}H_{37}N_2O_8$, 493.2550; found 493.2570.

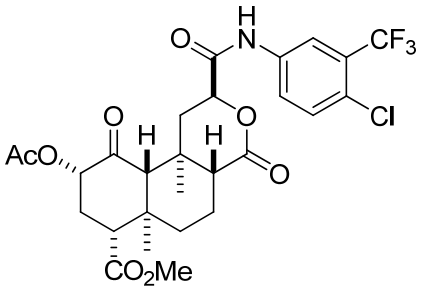

(2*S*,4a*R*,6a*R*,7*R*,9*S*,10a*S*,10b*R*)-methyl 9-acetoxy-2-(4-chloro-3-(trifluoromethyl)phenyl-carbamoyl)-6a,10b-dimethyl-4,10-dioxododecahydro-1*H*-benzo[*f*]isochromene-7-carboxylate (161).

Compound **161** was synthesized from **75** using **Procedure A** and 4-chloro-3-(trifluoromethyl)aniline to afford 0.074 g (41.5%) isolated as a white solid, mp = 141 – 144 °C; ^{1}H NMR (500 MHz, $CDCl_3$) δ 8.40 (s, 1H), 7.89 (d, *J* = 2.5 Hz, 1H), 7.78 (dd, *J* = 2.6, 8.7 Hz, 1H), 7.47 (d, *J* = 8.7 Hz, 1H), 5.17 (dd, *J* = 8.1, 11.9 Hz, 1H), 5.04 (dd, *J* = 6.0, 11.3 Hz, 1H), 3.72 (s, 3H), 2.80 (dd, *J* = 6.0, 13.9 Hz, 1H), 2.74 (dd, *J* = 4.4, 12.4 Hz, 1H), 2.36 – 2.28 (m, 2H), 2.17 (s, 4H), 2.15 – 2.04 (m, 2H), 1.84 – 1.78 (m, 1H), 1.71 – 1.51 (m, 3H), 1.42 (s, 3H), 1.11 (s, 3H). ^{13}C NMR (126 MHz, $CDCl_3$) δ 201.42, 171.45, 169.97, 169.75, 167.58, 135.63, 132.14, 128.92 (q, $^2J_{CF}$ = 31.6 Hz), 127.70 (d, $^3J_{CF}$ = 1.7 Hz), 124.02, 122.43 (q, J_{CF} = 273.5 Hz), 119.04 (q, $^3J_{CF}$ = 5.5 Hz), 75.87, 74.74, 63.82, 53.47, 52.03, 51.28, 41.90, 39.07, 37.84, 35.41, 30.76, 20.57, 18.08, 16.33, 15.32. HRMS (*m/z*): [M+NH_4] calcd for $C_{27}H_{33}ClF_3N_2O_8$, 605.1878; found 605.1899. HPLC t_R = 14.957 min; purity = 99.08%.

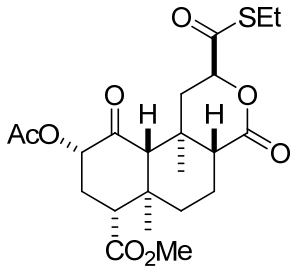

(2*S*,4a*R*,6a*R*,7*R*,9*S*,10a*S*,10b*R*)-methyl 9-acetoxy-2-(ethylthiocarbonyl)-6a,10b-dimethyl-4,10-dioxododecahydro-1*H*-benzo[*f*]isochromene-7-carboxylate (134).

Compound **134** was synthesized from **51** using **Procedure B** and ethanethiol to afford 1.130 g (88.0% yield) as a white solid, mp 187 – 191 °C; ^{1}H NMR (500 MHz, $CDCl_3$) δ 5.18 – 5.11 (m,

1H), 4.97 (dd, *J* = 7.2, 9.7 Hz, 1H), 3.72 (s, 3H), 2.90 (q, *J* = 7.4 Hz, 2H), 2.73 (dd, *J* = 5.4, 11.4 Hz, 1H), 2.62 (dd, *J* = 7.2, 13.7 Hz, 1H), 2.35 – 2.26 (m, 2H), 2.18 (s, 3H), 2.17 – 2.10 (m, 2H), 2.10 – 2.02 (m, 1H), 1.81 – 1.73 (m, 1H), 1.70 – 1.62 (m, 1H), 1.62 – 1.51 (m, 2H), 1.37 (s, 3H), 1.27 (td, *J* = 2.3, 7.3 Hz, 3H), 1.08 (s, 3H). ^{13}C NMR (126 MHz, $CDCl_3$) δ 201.81, 199.44, 171.72, 170.08, 170.04, 80.41, 75.01, 64.42, 53.54, 52.24, 50.57, 42.13, 39.54, 37.96, 35.59, 30.85, 23.23, 20.81, 18.33, 16.36, 16.09, 14.54. HRMS(*m/z*): [M +Na] calcd for $C_{22}H_{30}O_8SNa$, 477.1559; found, 477.1536. HPLC t_R = 26.93 min; purity = 98.31%.

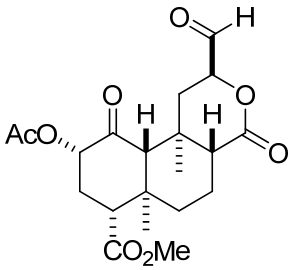

(2*S*,4a*R*,6a*R*,7*R*,9*S*,10a*S*,10b*R*)-methyl 9-acetoxy-2-formyl-6a,10b-dimethyl-4,10-dioxo-dodecahydro-1*H*-benzo[*f*]isochromene-7-carboxylate (135).

A solution of **134** (0.700 g, 1.54 mmol), triethylsilane (0.737 mL, 4.62 mmol), and 10% palladium on carbon (32.7 mg, 0.31 mmol) were added to 20 mL DCM under argon and stirred at room temperature overnight. Upon completion, the reaction mixture was filtered through Celite and the solvent was removed under reduced pressure. The crude solid was triturated using EtOAc/*n*-hexanes (1:25) (40 mL) and collected by filtration and dried to afford 0.498 mg (81.9% yield) of **135** as a white solid, mp 194 – 197 °C; ^{1}H NMR (500 MHz, $CDCl_3$) δ 9.68 (s, 1H), 5.16 (dd, *J* = 8.6, 11.6 Hz, 1H), 4.89 (dd, *J* = 7.2, 9.8 Hz, 1H), 3.73 (s, 3H), 2.75 (dd, *J* = 5.2, 11.6 Hz, 1H), 2.52 (dd, *J* = 7.1, 13.7 Hz, 1H), 2.36 – 2.24 (m, 2H), 2.18 (s, 3H), 2.16 – 2.07 (m, 1H), 1.96 (dd, J = 3.1, 11.8 Hz, 1H), 1.78 (dt, *J* = 3.1, 13.4 Hz, 1H), 1.72 – 1.50 (m, 4H), 1.39 (s, 3H), 1.09

(s, 3H). ^{13}C NMR (126 MHz, $CDCl_3$) δ 201.91, 197.98, 171.69, 170.36, 170.11, 79.71, 75.05, 64.50, 53.52, 52.24, 50.98, 42.16, 37.93, 36.64, 35.39, 30.82, 20.80, 18.35, 16.41, 16.37; HRMS (*m/z*): [M+H] calcd for $C_{20}H_{27}O_8$, 395.1706; found, 395.1712. HPLC t_R = 7.561 min; purity = 95.63%.

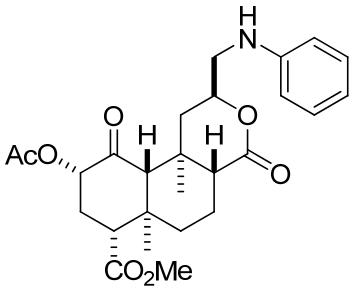

(2*S*,4a*R*,6a*R*,7*R*,9*S*,10a*S*,10b*R*)-methyl 9-acetoxy-6a,10b-dimethyl-4,10-dioxo-2-((phenyl-amino)methyl)dodecahydro-1*H*-benzo[*f*]isochromene-7-carboxylate (162).

Compound **162** was synthesized from **135** using **Procedure B** and aniline to afford 0.199 g (69.9%) as a white solid, mp 113 – 116 ˚C; ^{1}H NMR (500 MHz, $CDCl_3$) δ 7.23 – 7.16 (m, 2H), 6.75 (t, *J* = 7.3 Hz, 1H), 6.61 (dt, *J* = 4.1, 8.2 Hz, 2H), 5.21 – 5.08 (m, 1H), 4.73 (d, *J* = 3.0 Hz, 1H), 4.07 (s, 1H), 3.73 (s, 3H), 3.44 (d, *J* = 13.5 Hz, 1H), 3.18 (dd, *J* = 6.4, 13.7 Hz, 1H), 2.80 – 2.68 (m, 1H), 2.35 – 2.25 (m, 3H), 2.19 (d, *J* = 2.3 Hz, 3H), 2.17 – 2.11 (m, 2H), 2.02 – 1.94 (m, 1H), 1.82 – 1.73 (m, 1H), 1.68 – 1.49 (m, 2H), 1.43 (d, *J* = 12.4 Hz, 1H), 1.38 (d, *J* = 6.2 Hz, 3H), 1.09 (s, 3H). ^{13}C NMR (126 MHz, $CDCl_3$) δ 202.35, 171.76, 171.50, 170.26, 147.63, 129.62, 118.38, 113.41, 76.52, 75.29, 64.20, 53.70, 52.23, 51.40, 48.97, 42.28, 39.92, 38.30, 35.22, 30.89, 20.82, 18.32, 16.54, 15.47. HRMS (*m/z*): [M+H] calcd for $C_{26}H_{34}NO_7$, 472.2335; found, 472.2346. HPLC t_R = 6.676 min; purity = 99.24%.

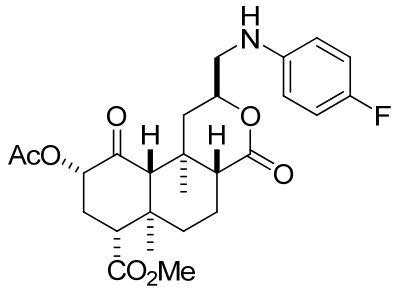

(2*S*,4a*R*,6a*R*,7*R*,9*S*,10a*S*,10b*R*)-methyl 9-acetoxy-2-((4-fluorophenylamino)methyl)-6a,10b-dimethyl-4,10-dioxododecahydro-1*H*-benzo[*f*]isochromene-7-carboxylate (163).

Compound **163** was synthesized from **135** using **Procedure B** and 4-fluoroaniline aniline to afford 0.105 g (46.4%) as a white solid, mp 120 – 123 ˚C; ^{1}H NMR (500 MHz, $CDCl_3$) δ 6.93 – 6.87 (m, 2H), 6.57 – 6.52 (m, 2H), 5.16 – 5.09 (m, 1H), 4.71 (d, *J* = 3.0 Hz, 1H), 3.96 (s, 1H), 3.72 (s, 3H), 3.37 (d, *J* = 11.9 Hz, 1H), 3.13 (dd, *J* = 6.8, 13.6 Hz, 1H), 2.78 – 2.69 (m, 1H), 2.35 – 2.25 (m, 3H), 2.20 – 2.11 (m, 5H), 2.01 – 1.95 (m, 1H), 1.79 (d, *J* = 13.1 Hz, 1H), 1.67 – 1.50 (m, 3H), 1.38 (s, 3H), 1.10 (s, 3H). ^{13}C NMR (126 MHz, $CDCl_3$) δ 202.30, 171.73, 171.37, 170.26, 156.43 (d, J_{CF} = 263.05 Hz), 143.96 (d, $^{4}J_{CF}$ = 1.76 Hz), 116.05 (2C, d, $^{2}J_{CF}$ = 22.37 Hz) 114.44 (2C, d, $^{3}J_{CF}$ = 7.46 Hz), 76.38, 75.31, 64.29, 53.77, 52.22, 51.48, 49.87, 42.31, 40.03, 38.34, 35.26, 30.93, 20.80, 18.35, 16.54, 15.47. HRMS (*m/z*): [M+H] calcd for $C_{26}H_{33}NO_7F$, 490.2241; found, 490.2236. HPLC t_R = 7.333 min; purity = > 99.99%.

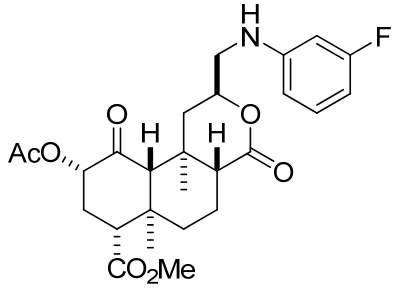

(2*S*,4a*R*,6a*R*,7*R*,9*S*,10a*S*,10b*R*)-methyl 9-acetoxy-2-((3-fluorophenylamino)methyl)-6a,10b-dimethyl-4,10-dioxododecahydro-1*H*-benzo[*f*]isochromene-7-carboxylate (164).

Compound **164** was synthesized from **135** using **Procedure B** and 3-fluoroaniline aniline to afford 0.034 g (15.2%) as a white solid, mp 118 – 121˚C; ^{1}H NMR (500 MHz, $CDCl_3$) δ 7.11 (dd, *J* = 8.2, 14.9, 1H), 6.42 (dd, *J* = 7.3, 9.4 Hz, 1H), 6.37 (dd, *J* = 1.6, 8.1 Hz, 1H), 6.29 (dt, *J* = 2.3, 11.4 Hz, 1H), 5.16 – 5.08 (m, 1H), 4.71 (d, *J* = 3.0 Hz, 1H), 4.20 (s, 1H), 3.73 (s, 3H), 3.37 (s, 1H), 3.17 (s, 1H), 2.78 – 2.67 (m, 1H), 2.34 – 2.25 (m, 3H), 2.21 – 2.09 (m, 5H), 2.01 – 1.94 (m, 1H), 1.79 (d, *J* = 13.1 Hz, 1H), 1.69 – 1.48 (m, 3H), 1.38 (s, 3H), 1.10 (s, 3H). ^{13}C NMR (126 MHz, $CDCl_3$) δ 202.28, 171.73, 171.28, 170.24, 164.26 (d, J_{CF} = 243.49 Hz), 149.45 (d, $^{3}J_{CF}$ = 10.52 Hz), 130.71 (d, $^{3}J_{CF}$ = 10.18 Hz), 109.15 (d, $^{4}J_{CF}$ = 2.24 Hz), 104.84 (d, $^{2}J_{CF}$ = 21.54 Hz), 100.19 (d, $^{2}J_{CF}$ = 25.32 Hz), 76.29, 75.29, 64.26, 53.76, 52.22, 51.49, 48.98, 42.30, 40.01, 38.32, 35.27, 30.93, 20.80, 18.34, 16.55, 15.47. HRMS (*m/z*): [M+H] calcd for $C_{26}H_{33}NO_7F$, 490.2241; found, 490.2234. HPLC t_R = 7.642 min; purity = > 99.99%.

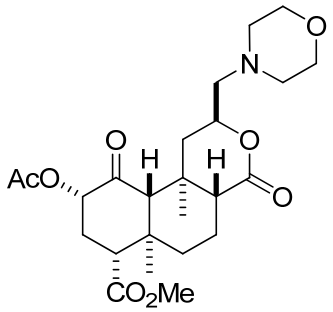

(2*S*,4a*R*,6a*R*,7*R*,9*S*,10a*S*,10b*R*)-methyl 9-acetoxy-6a,10b-dimethyl-2-(morpholinomethyl)-4,10-dioxododecahydro-1*H*-benzo[*f*]isochromene-7-carboxylate (165).

Compound **165** was synthesized from **135** using **Procedure B** and morpholine to afford 0.047 g (11.9 %) as a white solid, mp 193 – 195; ^{1}H NMR (500 MHz, $CDCl_3$) δ 5.17 – 5.09 (m, 1H),

4.68 – 4.59 (m, 1H), 3.70 (d, *J* = 2.4 Hz, 3H), 3.67 (t, *J* = 4.7 Hz, 4H), 2.77 – 2.65 (m, 1H), 2.57 – 2.40 (m, 6H), 2.34 – 2.23 (m, 2H), 2.22 – 2.14 (m, 4H), 2.14 – 2.07 (m, 2H), 1.95 – 1.88 (m, 1H), 1.74 (dd, *J* = 3.0, 10.1 Hz, 1H), 1.65 – 1.49 (m, 3H), 1.34 (d, *J* = 6.4 Hz, 3H), 1.06 (s, 3H). ^{13}C NMR (126 MHz, $CDCl_3$) δ 202.29, 171.79, 171.49, 170.28, 76.46, 75.21, 67.15, 64.35, 63.60, 54.75, 53.71, 52.22, 51.44, 42.23, 40.80, 38.32, 35.14, 30.93, 20.85, 18.34, 16.55, 15.36. HRMS (*m/z*): [M+H] calcd for $C_{24}H_{36}NO_8$, 466.2441; found, 466.2449. HPLC t_R = 3.838 min; purity = 95.61%.

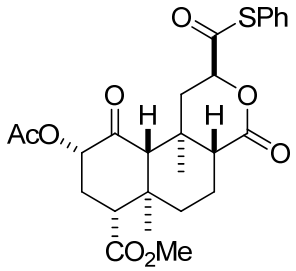

(2*S*,4a*R*,6a*R*,7*R*,9*S*,10a*S*,10b*R*)-methyl 9-acetoxy-6a,10b-dimethyl-4,10-dioxo-2-(phenylthiocarbonyl)dodecahydro-1*H*-benzo[*f*]isochromene-7-carboxylate (166).

Compound **166** was synthesized from **51** using **Procedure B** and thiophenol to afford 0.335 g (47.6%) as a white solid, mp 136 – 140 ºC; ^{1}H NMR (500 MHz, $CDCl_3$) δ 7.47 – 7.38 (m, 5H), 5.14 (dd, *J* = 8.6, 11.6 Hz, 1H), 5.09 (dd, *J* = 7.2, 9.6 Hz, 1H), 3.72 (s, 3H), 2.74 (dd, *J* = 5.2, 11.6 Hz, 1H), 2.65 (dd, *J* = 7.2, 13.7 Hz, 1H), 2.37 – 2.22 (m, 2H), 2.22 – 2.10 (m, 6H), 1.84 – 1.74 (m, 1H), 1.74 – 1.50 (m, 3H), 1.39 (s, 3H), 1.09 (s, 3H). ^{13}C NMR (126 MHz, $CDCl_3$) δ 201.80, 197.76, 171.71, 170.01, 169.87, 134.91, 130.09, 129.62, 126.07, 80.51, 75.03, 64.39, 53.56, 52.21, 50.64, 42.17, 39.52, 37.96, 35.68, 30.89, 20.77, 18.38, 16.38, 16.20. HRMS (*m/z*): [M+H] calcd for $C_{26}H_{31}O_8S$, 503.1740; found 503.1720. HPLC t_R = 8.507 min; purity = >99.99%.

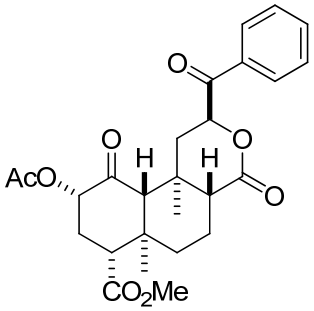

(2*S*,4a*R*,6a*R*,7*R*,9*S*,10a*S*,10b*R*)-methyl 9-acetoxy-2-benzoyl-6a,10b-dimethyl-4,10-dioxo-dodecahydro-1*H*-benzo[*f*]isochromene-7-carboxylate (119).

Compound **119** was synthesized from compound **166** using **Procedure D** and phenyl boronic acid to afford 0.221 g (82.4%) isolated as an off-white solid, mp = 164 – 167 °C. ^{1}H NMR (500 MHz, $CDCl_3$) δ 7.93 – 7.86 (m, 2H), 7.60 (t, *J* = 7.4 Hz, 1H), 7.48 (t, *J* = 7.8 Hz, 2H), 5.85 (t, *J* = 8.3 Hz, 1H), 5.13 – 5.03 (m, 1H), 3.69 (s, 3H), 2.74 – 2.58 (m, 2H), 2.25 (dd, *J* = 6.8, 13.5 Hz, 2H), 2.18 – 2.06 (m, 6H), 1.78 – 1.48 (m, 4H), 1.44 (s, 3H), 1.06 (s, 3H). ^{13}C NMR (126 MHz, $CDCl_3$) δ 202.20, 195.39, 171.79, 171.15, 170.06, 134.58, 133.66, 129.32, 129.15, 75.46, 75.06, 65.03, 53.46, 52.19, 49.53, 42.20, 38.44, 37.93, 35.78, 30.90, 20.80, 18.47, 16.97, 16.22. HRMS (*m/z*): [M+Na] calcd for $C_{26}H_{30}O_8Na$, 493.1838; found 493.1819. HPLC t_R = 6.003 min; purity = 95.36%.

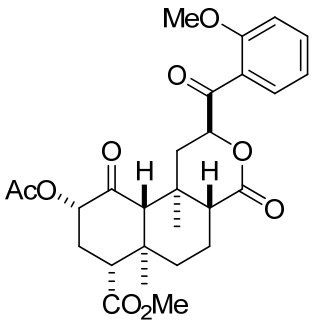

(2*S*,4a*R*,6a*R*,7*R*,9*S*,10a*S*,10b*R*)-methyl 9-acetoxy-2-(2-methoxybenzoyl)-6a,10b-dimethyl-4,10-dioxododecahydro-1*H*-benzo[*f*]isochromene-7-carboxylate (167).

Compound **167** was synthesized from compound **166** using **Procedure D** and 2-methoxyphenyl boronic acid to afford 0.082 g (66.2%) isolated as a white solid, mp = 186 – 188 °C. ^{1}H NMR (500 MHz, $CDCl_3$) δ 7.79 (dd, *J* = 1.8, 7.8 Hz, 1H), 7.56 – 7.47 (m, 1H), 7.07 – 6.99 (m, 1H), 6.96 (d, *J* = 8.2 Hz, 1H), 5.89 (t, *J* = 8.1 Hz, 1H), 5.10 – 5.02 (m, 1H), 3.92 (s, 3H), 3.69 (s, 3H), 2.75 – 2.63 (m, 2H), 2.30 – 2.19 (m, 2H), 2.16 – 2.06 (m, 6H), 1.72 (dt, *J* = 3.2, 13.3 Hz, 1H), 1.68 – 1.46 (m, 3H), 1.40 (s, 3H), 1.05 (s, 3H). ^{13}C NMR (126 MHz, $CDCl_3$) δ 202.11, 197.37, 171.83, 171.72, 169.99, 159.03, 135.43, 131.80, 124.34, 121.47, 112.15, 79.32, 75.08, 65.20, 55.96, 53.51, 52.16, 49.69, 42.24, 38.20, 38.08, 35.76, 30.96, 20.84, 18.51, 16.90, 16.26. HRMS (*m/z*): [M+NH_4] calcd for $C_{27}H_{36}O_9N$, 518.2390; found 518.2369. HPLC t_R = 6.040 min; purity = >99.99%

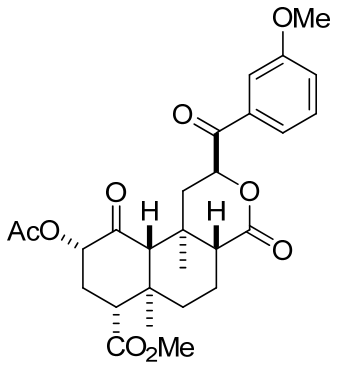

(2*S*,4a*R*,6a*R*,7*R*,9*S*,10a*S*,10b*R*)-methyl 9-acetoxy-2-(3-methoxybenzoyl)-6a,10b-dimethyl-4,10-dioxododecahydro-1*H*-benzo[*f*]isochromene-7-carboxylate (168).

Compound **168** was synthesized from compound **166** using **Procedure D** and 3-methoxyphenyl boronic acid to afford 0.093 g (60.9%) isolated as a white solid, mp = 162 – 164 °C. ^{1}H NMR (500 MHz, CDCl3) δ 7.48 – 7.43 (m, 2H), 7.40 (dd, *J* = 5.8, 10.3 Hz, 1H), 7.16 (ddd, *J* = 1.1,

2.6, 8.1 Hz, 1H), 5.86 (t, *J* = 8.3 Hz, 1H), 5.16 – 5.06 (m, 1H), 3.86 (s, 3H), 3.72 (s, 3H), 2.77 – 2.61 (m, 2H), 2.28 (dd, *J* = 7.1, 13.5 Hz, 2H), 2.20 – 2.09 (m, 6H), 1.80 – 1.73 (m, 1H), 1.67 (dt, *J* = 8.0, 14.9 Hz, 1H), 1.62 – 1.52 (m, 2H), 1.46 (s, 3H), 1.08 (s, 3H). ^{13}C NMR (126 MHz, CDCl3) δ 202.16, 195.34, 171.78, 171.14, 170.04, 160.31, 134.96, 130.32, 121.55, 121.08, 113.35, 75.51, 75.04, 65.02, 55.72, 53.45, 52.18, 49.49, 42.19, 38.59, 37.92, 35.79, 30.89, 20.80, 18.46, 16.93, 16.21. HRMS (*m/*z): [M+H] calcd for $C_{27}H_{33}O_9$, 501.2125; found 501.2112. HPLC t_R = 6.217 min; purity = 99.03%.

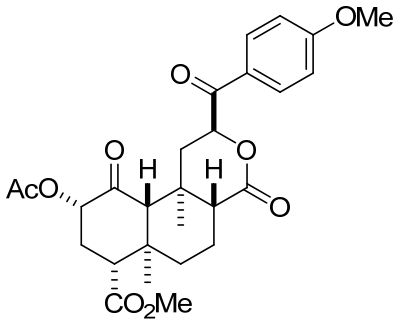

(2*S*,4a*R*,6a*R*,7*R*,9*S*,10a*S*,10b*R*)-methyl 9-acetoxy-2-(4-methoxybenzoyl)-6a,10b-dimethyl-4,10-dioxododecahydro-1*H*-benzo[*f*]isochromene-7-carboxylate (169).

Compound **169** was synthesized from compound **166** using **Procedure D** and 4-methoxyphenyl boronic acid to afford 0.069 g (50.7%) isolated as a white solid, mp = 117 – 120 °C. ^{1}H NMR (500 MHz, $CDCl_3$) δ 7.90 – 7.85 (m, 2H), 6.97 – 6.91 (m, 2H), 5.81 (t, *J* = 8.2 Hz, 1H), 5.14 – 5.01 (m, 1H), 3.87 (d, *J* = 7.1 Hz, 3H), 3.69 (s, 3H), 2.74 – 2.65 (m, 1H), 2.62 (dd, *J* = 8.7, 13.6 Hz, 1H), 2.25 (dd, *J* = 6.7, 13.8 Hz, 2H), 2.20 – 2.05 (m, 6H), 1.75 – 1.47 (m, 4H), 1.43 (s, 3H), 1.05 (s, 3H). ^{13}C NMR (126 MHz, $CDCl_3$) δ 202.25, 193.81, 171.82, 171.36, 170.07, 164.65, 131.56, 126.54, 114.55, 75.19, 75.08, 65.08, 55.81, 53.45, 52.18, 49.37, 42.21, 38.59, 37.93,

35.73, 30.90, 20.81, 18.47, 17.08, 16.20. HRMS (*m/z*): [M+NH_4] calcd for $C_{27}H_{36}O_9N$, 518.2390; found 518.2379. HPLC t_R = 6.247 min; purity = 96.68%.

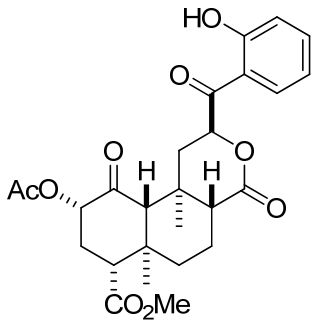

(2*S*,4a*R*,6a*R*,7*R*,9*S*,10a*S*,10*bR*)-methyl 9-acetoxy-2-(2-hydroxybenzoyl)-6a,10b-dimethyl-4,10-dioxododecahydro-1*H*-benzo[*f*]isochromene-7-carboxylate (170).

Compound **170** was synthesized from compound **166** using **Procedure D** and 2-hydroxybenzene boronic acid to afford 0.090 g (44.0%) isolated as a white solid, mp = 200 – 203 °C. ^{1}H NMR (500 MHz, $CDCl_3$) δ 11.73 (s, 1H), 7.58 (d, *J* = 8.1 Hz, 1H), 7.53 (t, *J* = 7.8 Hz, 1H), 7.03 (d, *J* = 8.5 Hz, 1H), 6.95 (t, *J* = 7.6 Hz, 1H), 5.92 (t, *J* = 8.4 Hz, 1H), 5.10 (t, *J* = 10.0 Hz, 1H), 3.72 (s, 3H), 2.72 (dd, *J* = 8.7, 13.8 Hz, 2H), 2.28 (dd, *J* = 6.8, 13.4 Hz, 2H), 2.23 – 2.09 (m, 6H), 1.84 – 1.56 (m, 4H), 1.47 (s, 3H), 1.09 (s, 3H). ^{13}C NMR (126 MHz, $CDCl_3$) δ 202.20, 200.58, 171.74, 170.98, 170.06, 163.70, 137.98, 129.64, 119.97, 119.25, 116.55, 75.08, 74.43, 64.96, 53.46, 52.22, 49.49, 42.23, 38.94, 37.93, 35.83, 30.88, 20.79, 18.49, 16.82, 16.22. HRMS (*m/z*): [M - H] calcd for $C_{26}H_{29}O_9$, 485.1812; found 485.1808. HPLC t_R = 6.986 min; purity = 96.16%.

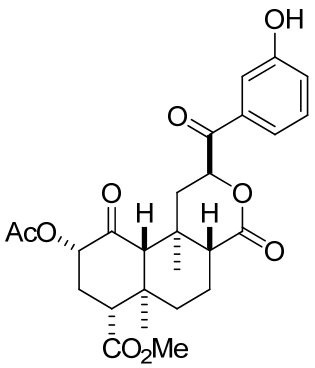

(2*S*,4a*R*,6a*R*,7*R*,9*S*,10a*S*,10b*R*)-methyl 9-acetoxy-2-(3-hydroxybenzoyl)-6a,10b-dimethyl-4,10-dioxododecahydro-1*H*-benzo[*f*]isochromene-7-carboxylate (171).

Compound **171** was synthesized from compound **166** using **Procedure D** and 3-hydroxyphenyl boronic acid to afford 0.033 g (28.9%) isolated as a white solid, mp = 131 – 135 °C. ^{1}H NMR (500 MHz, $CDCl_3$) δ 7.23 (t, *J* = 7.9 Hz, 1H), 7.16 – 7.12 (m, 1H), 7.10 (d, *J* = 7.8 Hz, 1H), 6.96 (s, 1H), 6.92 (dd, *J* = 1.9, 8.1 Hz, 1H), 5.78 (dd, *J* = 6.9, 10.2 Hz, 1H), 5.17 (dd, *J* = 8.0, 12.1 Hz, 1H), 3.73 (d, *J* = 2.0, 3H), 3.00 – 2.89 (m, 2H), 2.82 (dd, *J* = 10.3, 13.4 Hz, 1H), 2.37 – 2.25 (m, 2H), 2.21 (s, 3H), 2.19 – 2.09 (m, 2H), 1.84 (d, *J* = 9.8 Hz, 1H), 1.78 – 1.62 (m, 3H), 1.48 (s, 3H), 1.07 (s, 3H). ^{13}C NMR (126 MHz, $CDCl_3$) δ 202.84, 196.51, 172.04, 171.73, 171.59, 157.11, 133.45, 130.47, 122.70, 120.61, 114.06, 76.42, 75.37, 63.95, 52.94, 52.19, 48.83, 42.71, 38.75, 37.79, 35.85, 30.81, 21.00, 18.82, 17.22, 16.13. HRMS (*m/z*): [M-H] calcd for $C_{26}H_{29}O_9$, 485.1812; found 485.1801. HPLC t_R = 4.286 min; purity = 99.66%.

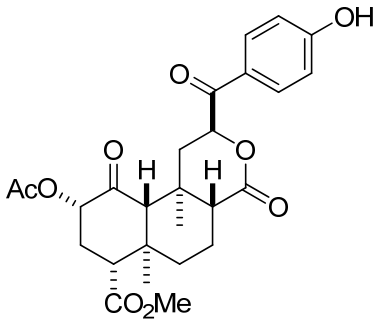

(2*S*,4a*R*,6a*R*,7*R*,9*S*,10a*S*,10b*R*)-methyl 9-acetoxy-2-(4-hydroxybenzoyl)-6a,10b-dimethyl-4,10-dioxododecahydro-1*H*-benzo[*f*]isochromene-7-carboxylate (172).

Compound **172** was synthesized from compound **166** using **Procedure D** and 4-hydroxyphenyl boronic acid to afford 0.092 g (68.0%) isolated as a white solid, mp = 232 – 236 °C. ^{1}H NMR (500 MHz, $CDCl_3$) δ 7.82 (d, *J* = 8.8 Hz, 2H), 6.85 (d, *J* = 8.8 Hz, 2H), 6.16 (s, 1H), 5.80 (t, *J* = 8.3 Hz, 1H), 5.13 – 5.08 (m, 1H), 3.72 (s, 3H), 2.72 (d, *J* = 7.7 Hz, 1H), 2.62 (dd, *J* = 8.7, 13.6 Hz, 1H), 2.30 (d, *J* = 10.7 Hz, 2H), 2.20 (s, 1H), 2.17 (s, 5H), 1.79 – 1.52 (m, 4H), 1.45 (s, 3H), 1.08 (s, 3H). ^{13}C NMR (126 MHz, $CDCl_3$) δ 202.27, 193.59, 171.80, 171.60, 170.41, 161.34, 131.84, 126.60, 116.09, 77.44, 75.25, 65.01, 53.45, 52.21, 49.43, 42.25, 38.48, 37.94, 35.71, 30.88, 20.85, 18.46, 17.06, 16.23. HRMS (*m/z*): M-H] calcd for $C_{26}H_{29}O_9$, 485.1812; found 485.1783. HPLC t_R = 4.624 min; purity = 95.63%.

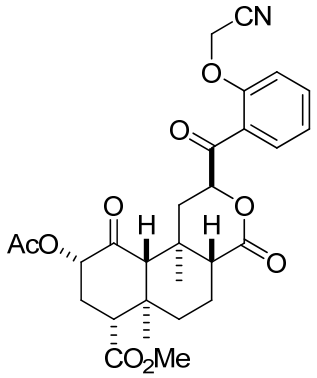

(2*S*,4a*R*,6a*R*,7*R*,9*S*,10a*S*,10b*R*)-methyl 9-acetoxy-2-(2-(cyanomethoxy)benzoyl)-6a,10b-dimethyl-4,10-dioxododecahydro-1*H*-benzo[*f*]isochromene-7-carboxylate (173).

Compound **173** was synthesized from compound **166** using **Procedure D** and 2-cyanomethoxyphenyl boronic acid to afford 0.149 g (47.1%) isolated as a light yellow solid, mp = 110 – 113 °C. ^{1}H NMR (500 MHz, $CDCl_3$) δ 7.71 (dd, *J* = 1.7, 7.7 Hz, 1H), 7.61 – 7.55 (m,

1H), 7.21 (t, *J* = 7.2 Hz, 1H), 7.06 (d, *J* = 8.2 Hz, 1H), 5.68 (dd, *J* = 7.7, 8.8 Hz, 1H), 5.16 – 5.09 (m, 1H), 4.90 (q, *J* = 15.8 Hz, 2H), 3.72 (s, 3H), 2.74 (dd, *J* = 5.5, 11.4 Hz, 1H), 2.64 (dd, *J* = 7.7, 13.6 Hz, 1H), 2.34 – 2.25 (m, 2H), 2.19 (s, 1H), 2.16 (s, 3H), 2.12 (dt, *J* = 4.6, 14.4 Hz, 2H), 1.76 (d, *J* = 13.0 Hz, 1H), 1.72 – 1.53 (m, 3H), 1.43 (s, 3H), 1.08 (s, 3H). ^{13}C NMR (126 MHz, $CDCl_3$) δ 202.21, 197.63, 171.80, 171.05, 170.09, 155.31, 134.90, 131.67, 126.48, 124.00, 114.69, 113.40, 79.36, 75.13, 64.81, 54.59, 53.49, 52.18, 50.06, 42.25, 38.04, 38.03, 35.69, 30.93, 20.83, 18.44, 16.65, 16.35. HRMS (*m/z*): [M+Na] calcd for $C_{28}H_{31}NO_9Na$, 548.1897; found 548.165. HPLC t_R = 11.818 min; purity = 98.62% using 50 CH_3CN:50 H_2O as the mobile phase.

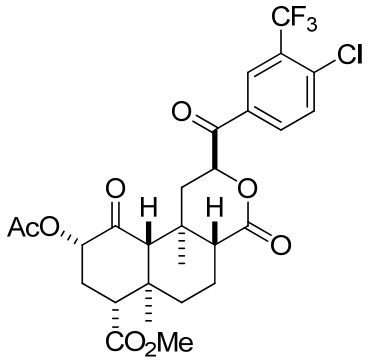

(2*S*,4a*R*,6a*R*,7*R*,9*S*,10a*S*,10b*R*)-methyl 9-acetoxy-2-(4-chloro-3-(trifluoromethyl)benzoyl)-6a,10b-dimethyl-4,10-dioxododecahydro-1*H*-benzo[*f*]isochromene-7-carboxylate (174).

Compound **174** was synthesized from compound **166** using **Procedure D** and 4-chloro-3-(trifluoromethyl)benzene boronic acid to afford 0.059 g (33.3%) isolated as a gray solid, mp = 109 – 112 °C. ^{1}H NMR (500 MHz, $CDCl_3$) δ 8.29 (d, *J* = 2.0 Hz, 1H), 8.03 (dd, *J* = 2.1, 8.4 Hz, 1H), 7.66 (d, *J* = 8.4 Hz, 1H), 5.77 (t, *J* = 8.2 Hz, 1H), 5.18 – 5.11 (m, 1H), 3.72 (s, 3H), 2.79 – 2.70 (m, 1H), 2.58 (dd, *J* = 8.0, 13.7 Hz, 1H), 2.35 – 2.26 (m, 2H), 2.21 (s, 1H), 2.16 (s, 3H), 2.14 – 2.08 (m, 2H), 1.81 – 1.52 (m, 4H), 1.47 (s, 3H), 1.09 (s, 3H). ^{13}C NMR (126 MHz,

$CDCl_3$) δ 201.92, 192.99, 171.52, 170.27, 169.90, 138.69 (d, $^3J_{CF}$ = 1.3 Hz), 133.01, 132.34, 132.23, 129.62 (q, $^2J_{CF}$ = 32.3 Hz), 128.39 (q, $^3J_{CF}$ = 5.2 Hz), 122.20 (q, J_{CF} = 273.7 Hz), 75.42, 74.85, 64.62, 53.28, 52.02, 49.73, 41.97, 37.69, 37.45, 35.50, 30.68, 20.59, 18.20, 16.65, 16.09. HRMS (*m/z*): [M+NH_4] calcd for $C_{27}H_{32}O_8F_3ClN$, 590.1769; found 590.1783. HPLC t_R = 17.187 min; purity = 95.64%.

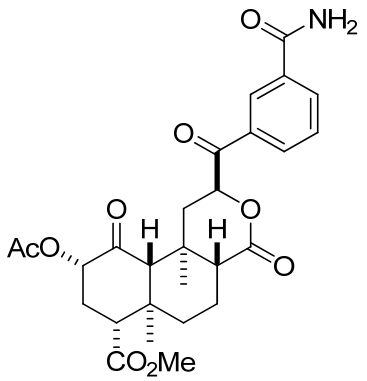

(2*S*,4a*R*,6a*R*,7*R*,9*S*,10a*S*,10b*R*)-methyl 9-acetoxy-2-(3-carbamoylbenzoyl)-6a,10b-dimethyl-4,10-dioxododecahydro-1*H*-benzo[*f*]isochromene-7-carboxylate (175).

Compound **175** was synthesized from compound **166** using **Procedure D** and 3-aminocarbonylphenyl boronic acid to afford 0.062 g (37.8%) isolated as a white solid, mp = 148 – 152 °C. ^{1}H NMR (500 MHz, $CDCl_3$) δ 8.30 (s, 1H), 8.07 (d, *J* = 7.8 Hz, 1H), 8.02 (d, *J* = 7.9 Hz, 1H), 7.58 (t, *J* = 7.8 Hz, 1H), 6.52 – 6.31 (m, 1H), 5.88 (t, *J* = 8.4 Hz, 1H), 5.84 – 5.65 (m, 1H), 5.18 – 5.11 (m, 1H), 3.72 (s, 3H), 2.82 – 2.73 (m, 1H), 2.65 (dd, *J* = 8.4, 13.6 Hz, 1H), 2.28 (dd, *J* = 7.3, 13.3 Hz, 3H), 2.20 – 2.09 (m, 5H), 1.78 (d, *J* = 13.0 Hz, 1H), 1.75 – 1.54 (m, 3H), 1.47 (s, 3H), 1.09 (s, 3H). ^{13}C NMR (126 MHz, $CDCl_3$) δ 202.32, 194.95, 171.81, 170.95, 170.22, 168.05, 134.59, 133.96, 133.38, 132.26, 129.75, 127.79, 75.66, 75.18, 64.74, 53.40, 52.20, 49.71, 42.24, 38.11, 37.91, 35.78, 30.90, 20.82, 18.49, 16.87, 16.27. HRMS (*m/z*):

[M+Na] calcd for $C_{27}H_{31}NO_9Na$, 536.1897; found 536.1901. HPLC t_R = 3.465 min; purity = 96.22% using 40 CH_3CN:60 H_2O as the mobile phase.

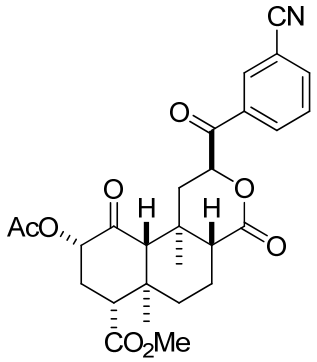

(2*S*,4a*R*,6a*R*,7*R*,9*S*,10a*S*,10b*R*)-methyl 9-acetoxy-2-(3-cyanobenzoyl)-6a,10b-dimethyl-4,10-dioxododecahydro-1*H*-benzo[*f*]isochromene-7-carboxylate (176).

Compound **176** was synthesized from compound **166** using **Procedure D** and 3-cyanophenylboronic acid to afford 0.055 g (43.9%) isolated as a white solid, mp = 124 – 127 °C. ^{1}H NMR (500 MHz, $CDCl_3$) δ 8.25 (t, *J* = 1.4 Hz, 1H), 8.18 – 8.14 (m, 1H), 7.92 – 7.88 (m, 1H), 7.66 (t, *J* = 7.8 Hz, 1H), 5.79 (t, *J* = 8.3 Hz, 1H), 5.18 – 5.10 (m, 1H), 3.72 (s, 3H), 2.80 – 2.71 (m, 1H), 2.58 (dd, *J* = 7.9, 13.7 Hz, 1H), 2.35 – 2.26 (m, 2H), 2.21 (s, 1H), 2.20 – 2.08 (m, 5H), 1.82 – 1.52 (m, 4H), 1.48 (s, 3H), 1.10 (s, 3H). ^{13}C NMR (126 MHz, $CDCl_3$) δ 202.11, 193.43, 171.71, 170.42, 170.09, 137.18, 134.85, 133.13, 132.96, 130.28, 117.76, 113.99, 75.65, 75.05, 64.78, 53.49, 52.22, 50.01, 42.18, 37.90, 37.64, 35.72, 30.88, 20.80, 18.41, 16.77, 16.30. HRMS (*m/z*): [M-H] calcd for $C_{27}H_{28}NO_8$, 494.1815; found 494.1806. HPLC t_R = 6.510 min; purity = 95.94%.

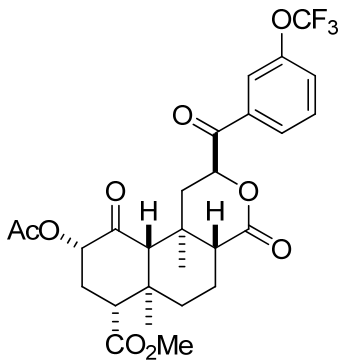

(2*S*,4a*R*,6a*R*,7*R*,9*S*,10a*S*,10b*R*)-methyl 9-acetoxy-6a,10b-dimethyl-4,10-dioxo-2-(3-(trifluoromethoxy)benzoyl)dodecahydro-1*H*-benzo[*f*]isochromene-7-carboxylate (177).

Compound **177** was synthesized from compound **166** using **Procedure D** and 3-(trifluoromethoxy)-phenylboronic acid to afford 0.038 g (24.3%) isolated as a white solid, mp = 92 – 94 °C. ^{1}H NMR (500 MHz, $CDCl_3$) δ 7.86 – 7.80 (m, 2H), 7.56 (t, *J* = 8.0 Hz, 1H), 7.48 (d, *J* = 7.2 Hz, 1H), 5.81 (t, *J* = 8.3 Hz, 1H), 5.16 – 5.09 (m, 1H), 3.72 (s, 3H), 2.78 – 2.69 (m, 1H), 2.62 (dd, *J* = 8.3, 13.6 Hz, 1H), 2.29 (dd, *J* = 7.2, 13.5 Hz, 2H), 2.19 (s, 1H), 2.18 – 2.09 (m, 5H), 1.77 (d, *J* = 13.2 Hz, 1H), 1.71 – 1.53 (m, 3H), 1.47 (s, 3H), 1.09 (s, 3H). ^{13}C NMR (126 MHz, $CDCl_3$) δ 202.15, 193.97, 171.75, 170.72, 170.07, 150.00 (q $^{3}J_{CF}$ = 1.97), 135.62, 130.91, 127.43, 126.77, 121.56, 120.56 (q J_{CF} = 258.18), 75.62, 75.06, 64.91, 53.48, 52.21, 49.77, 42.19, 38.03, 37.91, 35.76, 30.89, 20.79, 18.44, 16.88, 16.27. HRMS (*m/z*): [M+Na] calcd for $C_{27}H_{29}F_3O_9Na$, 577.1661; found 577.1621. HPLC t_R = 15.925 min; purity = 97.74%.

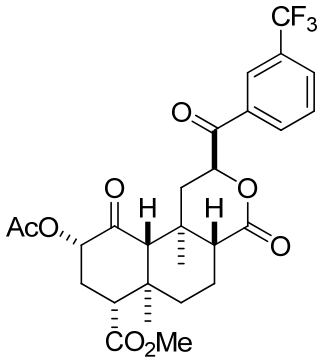

(2*S*,4a*R*,6a*R*,7*R*,9*S*,10a*S*,10b*R*)-methyl 9-acetoxy-6a,10b-dimethyl-4,10-dioxo-2-(3-(trifluoromethyl)benzoyl)dodecahydro-1*H*-benzo[*f*]isochromene-7-carboxylate (178).

Compound **178** was synthesized from compound **166** using **Procedure D** and 3-(trifluoromethyl)phenyl boronic acid to afford 0.044 g (38.8%) isolated as an off-white solid, mp = 94 – 97 °C. ^{1}H NMR (500 MHz, $CDCl_3$) δ 8.23 (s, 1H), 8.10 (d, J = 7.9 Hz, 1H), 7.88 (d, J = 7.8 Hz, 1H), 7.66 (t, J = 7.8 Hz, 1H), 5.84 (t, J = 8.3 Hz, 1H), 5.16 – 5.10 (m, 1H), 3.72 (s, 3H), 2.79 – 2.70 (m, 1H), 2.61 (dd, J = 8.2, 13.6 Hz, 1H), 2.29 (dd, J = 7.5, 13.5 Hz, 2H), 2.20 (s, 1H), 2.19 – 2.08 (m, 5H), 1.77 (d, J = 13.2 Hz, 1H), 1.75 – 1.53 (m, 3H), 1.48 (s, 3H), 1.09 (s, 3H). ^{13}C NMR (126 MHz, $CDCl_3$) δ 202.15, 194.16, 171.74, 170.66, 170.08, 134.49, 132.33, 132.05 (q, $^{2}J_{CF}$ =33.11 Hz), 130.87 (q, $^{3}J_{CF}$ = 3.41 Hz), 129.97, 126.18 (q, $^{3}J_{CF}$ = 3.84 Hz), 123.63 (q, J_{CF} = 272.85 Hz), 75.56, 75.06, 64.91, 53.49, 52.22, 49.84, 42.20, 37.92, 37.86, 35.75, 30.90, 20.80, 18.44, 16.90, 16.28. HRMS (*m/z*): [M+Na] calcd for $C_{27}H_{29}F_3O_8Na$, 561.1712; found 561.1670. HPLC t_R = 5.799 min; purity = 95.0% as determined using a Phenomenex Luna column (250 × 4.5 mm, 5 μm).

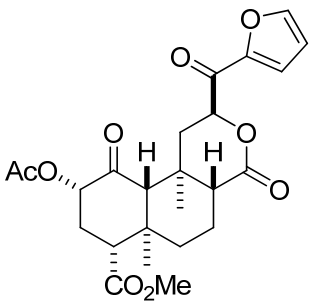

(2*S*,4a*R*,6a*R*,7*R*,9*S*,10a*S*,10b*R*)-methyl 9-acetoxy-2-(furan-2-carbonyl)-6a,10b-dimethyl-4,10-dioxododecahydro-1*H*-benzo[*f*]isochromene-7-carboxylate (116).

Compound **116** was synthesized from compound **166** using **Procedure D** and 2-furanylboronic acid to afford 0.109 g (84.6%) isolated as a white solid, mp = 207 – 209 °C. ^{1}H NMR (500 MHz, $CDCl_3$) δ 7.64 (dd, *J* = 0.7, 1.7 Hz, 1H), 7.35 (dd, *J* = 0.7, 3.7 Hz, 1H), 6.57 (dd, *J* = 1.7, 3.7 Hz, 1H), 5.60 (t, *J* = 8.4 Hz, 1H), 5.14 – 5.06 (m, 1H), 3.70 (s, 3H), 2.76 – 2.66 (m, 1H), 2.62 (dd, *J* = 8.0, 13.6 Hz, 1H), 2.26 (dd, *J* = 7.1, 13.5 Hz, 2H), 2.19 – 2.06 (m, 6H), 1.74 (d, *J* = 13.2 Hz, 1H), 1.70 – 1.49 (m, 3H), 1.42 (s, 3H), 1.06 (s, 3H). ^{13}C NMR (126 MHz, $CDCl_3$) δ 202.11, 184.26, 171.78, 170.92, 170.09, 150.12, 148.06, 120.56, 113.14, 76.23, 75.10, 64.85, 53.52, 52.20, 49.89, 42.22, 38.27, 37.97, 35.69, 30.91, 20.81, 18.43, 16.67, 16.28. HRMS (*m/z*): [M+H] calcd for $C_{24}H_{29}O_9$, 461.1812; found 461.1796. HPLC t_R = 13.29 min; purity = 97.83% using 40 CH_3CN:60 H_2O as the mobile phase.

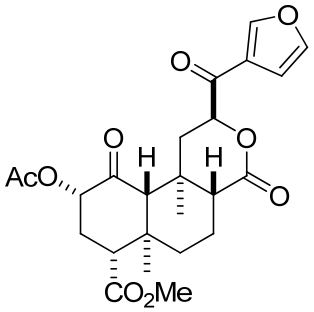

(2*S*,4a*R*,6a*R*,7*R*,9*S*,10a*S*,10b*R*)-methyl 9-acetoxy-2-(furan-3-carbonyl)-6a,10b-dimethyl-4,10-dioxododecahydro-1*H*-benzo[*f*]isochromene-7-carboxylate (179).

Compound **179** was synthesized from compound **166** using **Procedure D** and furan-3-boronic acid to afford 0.106 g (67.5%) isolated as a white solid, mp = 159 – 161 °C. ^{1}H NMR (500 MHz, $CDCl_3$) δ 8.20 (dd, *J* = 0.8, 1.3 Hz, 1H), 7.44 (dd, *J* = 1.4, 1.9 Hz, 1H), 6.79 (dd, *J* = 0.8, 1.9 Hz, 1H), 5.28 (t, *J* = 8.0 Hz, 1H), 5.17 – 5.07 (m, 1H), 3.69 (s, 3H), 2.71 (dd, *J* = 5.4, 11.4 Hz, 1H), 2.54 (dd, *J* = 7.8, 13.8 Hz, 1H), 2.33 – 2.23 (m, 2H), 2.18 (s, 1H), 2.14 (s, 3H), 2.10 – 2.01 (m, 2H), 1.79 – 1.70 (m, 2H), 1.69 – 1.58 (m, 1H), 1.55 – 1.47 (m, 1H), 1.40 (s, 3H), 1.06 (s, 3H). ^{13}C NMR (126 MHz, $CDCl_3$) δ 202.05, 191.00, 171.77, 170.83, 170.06, 149.28, 144.44, 124.23, 109.43, 78.51, 75.08, 64.82, 53.52, 52.19, 50.08, 42.18, 38.25, 37.92, 35.57, 30.90, 20.80, 18.40, 16.97, 16.32. HRMS (*m/z*): [M+H] calcd for $C_{24}H_{29}O_9$, 461.1812; found 461.1796. HPLC t_R = 5.105 min; purity = 99.67%.

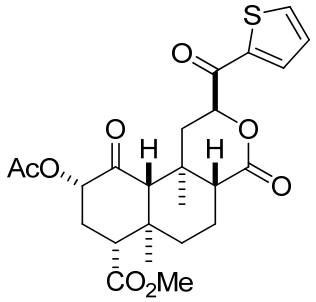

(2*S*,4a*R*,6a*R*,7*R*,9*S*,10a*S*,10b*R*)-methyl 9-acetoxy-6a,10b-dimethyl-4,10-dioxo-2-(thiophene-2-carbonyl)dodecahydro-1*H*-benzo[*f*]isochromene-7-carboxylate (117).

Compound **117** was synthesized from compound **166** using **Procedure D** and 2-thiophene boronic acid to afford 0.036 g (36.4%) isolated as an off-white solid, mp = 188 – 190 °C. ^{1}H NMR (500 MHz, $CDCl_3$) δ 7.83 (dd, *J* = 1.1, 3.9 Hz, 1H), 7.75 (dd, *J* = 1.1, 4.9 Hz, 1H), 7.18

(dd, *J* = 3.9, 4.9 Hz, 1H), 5.61 (t, *J* = 8.2 Hz, 1H), 5.17 – 5.08 (m, 1H), 3.72 (s, 3H), 2.77 – 2.68 (m, 1H), 2.63 (dd, *J* = 8.1, 13.7 Hz, 1H), 2.29 (dd, *J* = 7.6, 13.5 Hz, 2H), 2.23 – 2.07 (m, 6H), 1.72 (ddd, *J* = 9.4, 20.0, 39.3 Hz, 3H), 1.57 (d, *J* = 11.7 Hz, 1H), 1.45 (s, 3H), 1.08 (s, 3H). ^{13}C NMR (126 MHz, $CDCl_3$) δ 202.13, 188.51, 171.78, 170.85, 170.06, 140.23, 136.00, 134.26, 128.92, 77.03, 75.10, 64.86, 53.50, 52.20, 49.82, 42.21, 38.68, 37.93, 35.72, 30.90, 20.80, 18.43, 16.92, 16.28. HRMS (*m/z*): [M+Na] calcd for $C_{24}H_{28}O_8SNa$, 499.1403; found 499.1380. HPLC t_R = 5.733 min; purity = 96.12%.

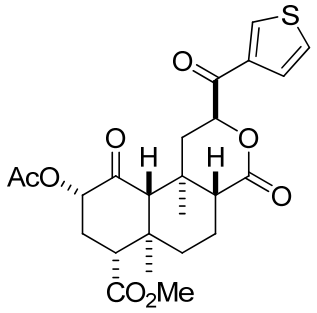

(2*S*,4a*R*,6a*R*,7*R*,9*S*,10a*S*,10b*R*)-methyl 9-acetoxy-6a,10b-dimethyl-4,10-dioxo-2-(thiophene-3-carbonyl)dodecahydro-1*H*-benzo[*f*]isochromene-7-carboxylate (180).

Compound **180** was synthesized from compound **166** using **Procedure D** and 3-thiophene boronic acid to afford 0.081 g (74.3%) isolated as an off-white solid, mp = 170 – 173 °C. ^{1}H NMR (500 MHz, $CDCl_3$) δ 8.20 (dd, *J* = 1.2, 2.8 Hz, 1H), 7.56 (dd, *J* = 1.2, 5.1 Hz, 1H), 7.37 (dd, *J* = 2.9, 5.1 Hz, 1H), 5.60 (t, *J* = 8.1 Hz, 1H), 5.17 – 5.08 (m, 1H), 3.72 (s, 3H), 2.78 – 2.67 (m, 1H), 2.61 (dd, *J* = 8.3, 13.7 Hz, 1H), 2.29 (dd, *J* = 7.5, 13.5 Hz, 2H), 2.20 (s, 1H), 2.19 – 2.06 (m, 5H), 1.71 (ddd, *J* = 12.5, 22.2, 34.2 Hz, 3H), 1.59 – 1.49 (m, 1H), 1.45 (s, 3H), 1.08 (s, 3H). ^{13}C NMR (126 MHz, $CDCl_3$) δ 202.17, 189.63, 171.78, 171.01, 170.06, 138.44, 134.68, 127.63, 127.21, 77.09, 75.08, 64.96, 53.49, 52.19, 49.71, 42.20, 38.30, 37.92, 35.69, 30.90,

20.81, 18.44, 17.05, 16.27. HRMS (*m/z*): [M+Na] calcd for $C_{24}H_{28}O_8SNa$, 499.1403; found 499.1393. HPLC t_R = 5.657 min; purity = 99.78%.

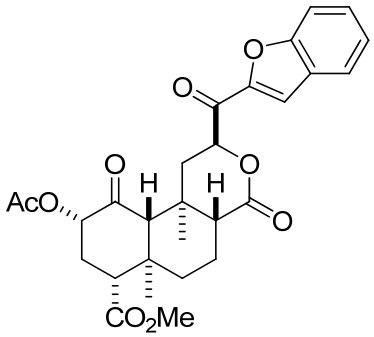

(2*S*,4a*R*,6a*R*,7*R*,9*S*,10a*S*,10b*R*)-methyl 9-acetoxy-2-(benzofuran-2-carbonyl)-6a,10b-dimethyl-4,10-dioxododecahydro-1*H*-benzo[*f*]isochromene-7-carboxylate (181).

Compound **181** was synthesized from compound **166** using **Procedure D** and 2-benzofuranyl boronic acid to afford 0.090 g (77.2%) isolated as a white solid, mp = 228 – 232 °C. ^{1}H NMR (500 MHz, $CDCl_3$) δ 7.74 (d, *J* = 7.8 Hz, 1H), 7.71 (d, *J* = 0.9 Hz, 1H), 7.60 (dd, *J* = 0.8, 8.5 Hz, 1H), 7.55 – 7.50 (m, 1H), 7.38 – 7.31 (m, 1H), 5.75 (t, *J* = 8.3 Hz, 1H), 5.16 – 5.08 (m, 1H), 3.72 (s, 3H), 2.77 – 2.67 (m, 2H), 2.29 (dd, *J* = 7.5, 13.5 Hz, 2H), 2.25 – 2.18 (m, 2H), 2.18 – 2.11 (m, 4H), 1.81 – 1.60 (m, 4H), 1.48 (s, 3H), 1.10 (s, 3H). ^{13}C NMR (126 MHz, $CDCl_3$) δ 202.15, 186.33, 171.78, 170.86, 170.04, 156.20, 149.86, 129.49, 126.98, 124.56, 123.93, 116.49, 112.90, 76.49, 75.07, 64.86, 53.49, 52.20, 49.92, 42.22, 38.22, 37.95, 35.77, 30.92, 20.80, 18.45, 16.78, 16.29. HRMS (*m/z*): [M+Na] calcd for $C_{28}H_{30}O_9Na$, 533.1788; found 533.1797. HPLC t_R = 7.558 min; purity = 99.33%.

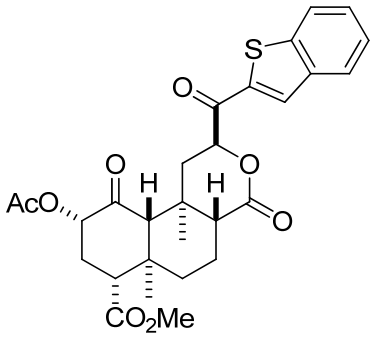

(2*S*,4a*R*,6a*R*,7*R*,9*S*,10a*S*,10b*R*)-methyl 9-acetoxy-2-(benzo[b]thiophene-2-carbonyl)-6a,10b-dimethyl-4,10-dioxododecahydro-1*H*-benzo[*f*]isochromene-7-carboxylate (182).

Compound **182** was synthesized from compound **166** using **Procedure D** and thianaphthene-2-boronic acid to afford 0.095 g (78.8%) isolated as a white solid, mp = 127 – 130 °C. ^{1}H NMR (500 MHz, $CDCl_3$) δ 8.10 (s, 1H), 7.93 (d, *J* = 8.0 Hz, 1H), 7.88 (d, *J* = 8.1 Hz, 1H), 7.54 – 7.46 (m, 1H), 7.46 – 7.40 (m, 1H), 5.74 (t, *J* = 8.2 Hz, 1H), 5.19 – 5.09 (m, 1H), 3.72 (s, 3H), 2.79 – 2.71 (m, 1H), 2.67 (dd, *J* = 8.1, 13.7 Hz, 1H), 2.34 – 2.25 (m, 2H), 2.25 – 2.18 (m, 2H), 2.17 – 2.08 (m, 4H), 1.85 – 1.73 (m, 2H), 1.73 – 1.63 (m, 1H), 1.63 – 1.53 (m, 1H), 1.48 (s, 3H), 1.09 (s, 3H). ^{13}C NMR (126 MHz, $CDCl_3$) δ 202.22, 190.04, 171.79, 170.84, 170.01, 143.20, 139.72, 139.13, 131.67, 128.45, 126.81, 125.56, 123.11, 76.90, 75.08, 64.83, 53.46, 52.19, 49.81, 42.21, 38.59, 37.90, 35.75, 30.91, 20.79, 18.44, 16.98, 16.29. HRMS (*m/z*): [M+Na] calcd for $C_{28}H_{30}O_8SNa$, 549.1559; found 549.1573. HPLC t_R = 9.577 min; purity = 98.44%.

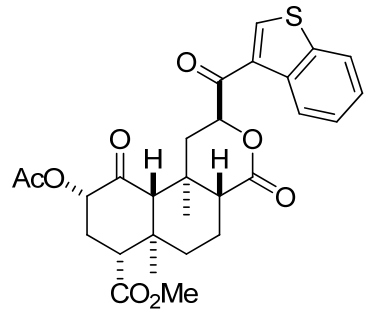

(2*S*,4a*R*,6a*R*,7*R*,9*S*,10a*S*,10b*R*)-methyl 9-acetoxy-2-(benzo[b]thiophene-3-carbonyl)-6a,10b-dimethyl-4,10-dioxododecahydro-1*H*-benzo[*f*]isochromene-7-carboxylate (183).

Compound **183** was synthesized from compound **166** using **Procedure D** and 1-benzothiphen-3-yl boronic acid to afford 0.065g (23.3%) isolated as an off-white solid, mp = 133 – 136 °C. ^{1}H NMR (500 MHz, $CDCl_3$) δ 8.72 (d, *J* = 7.9 Hz, 1H), 8.43 (s, 1H), 7.89 (d, *J* = 7.9 Hz, 1H), 7.56 – 7.50 (m, 1H), 7.46 (dd, *J* = 4.1, 11.1 Hz, 1H), 5.77 (t, *J* = 8.2 Hz, 1H), 5.18 – 5.08 (m, 1H), 3.72 (s, 3H), 2.77 – 2.70 (m, 1H), 2.65 (dd, *J* = 8.3, 13.7 Hz, 1H), 2.29 (dd, *J* = 7.2, 13.5 Hz, 2H), 2.26 – 2.18 (m, 2H), 2.13 (d, *J* = 16.9 Hz, 4H), 1.84 – 1.53 (m, 4H), 1.47 (s, 3H), 1.09 (s, 3H). ^{13}C NMR (126 MHz, $CDCl_3$) δ 202.27, 190.09, 171.80, 171.13, 170.04, 139.79, 139.45, 136.99, 131.61, 126.46, 126.16, 125.67, 122.57, 76.76, 75.12, 64.94, 53.50, 52.19, 49.68, 42.23, 38.51, 37.97, 35.68, 30.91, 20.79, 18.46, 17.06, 16.26. HRMS (*m/z*): [M+H] calcd for $C_{28}H_{31}O_8S$, 527.1740; found 527.1742. HPLC t_R = 6.64 min; purity = 96.84%.

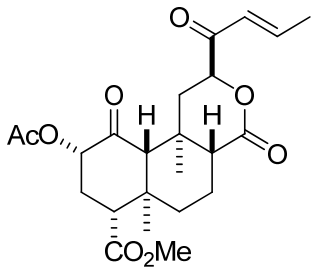

(2*S*,4a*R*,6a*R*,7*R*,9*S*,10a*S*,10b*R*)-methyl 9-acetoxy-2-((*E*)-but-2-enoyl)-6a,10b-dimethyl-4,10-dioxododecahydro-1*H*-benzo[*f*]isochromene-7-carboxylate (184).

Compound **184** was synthesized from compound **166** using **Procedure D** and *cis*-1-propen-1-ylboronic acid to afford 0.195 g (72.7%) isolated as a white solid, mp = 153 – 155 °C. ^{1}H NMR (500 MHz, $CDCl_3$) δ 6.48 (dq, *J* = 7.3, 11.4 Hz, 1H), 6.33 (dd, *J* = 1.7, 11.4 Hz, 1H), 5.19 – 5.11 (m, 1H), 4.92 (dd, *J* = 7.4, 9.3 Hz, 1H), 3.72 (s, 3H), 2.73 (dd, *J* = 5.8, 11.1 Hz, 1H), 2.52 (dd, *J*

= 7.4, 13.7 Hz, 1H), 2.33 – 2.25 (m, 2H), 2.17 (dd, *J* = 2.0, 7.0 Hz, 7H), 2.10 (dd, *J* = 3.4, 14.3 Hz, 1H), 2.00 (dd, *J* = 3.2, 11.8 Hz, 1H), 1.76 (dd, *J* = 3.3, 13.3 Hz, 1H), 1.65 (dd, *J* = 12.6, 27.3 Hz, 1H), 1.59 – 1.48 (m, 2H), 1.38 (s, 3H), 1.08 (s, 3H). ^{13}C NMR (126 MHz, $CDCl_3$) δ 201.98, 196.49, 171.76, 170.83, 170.10, 149.06, 122.82, 79.95, 75.10, 64.78, 53.60, 52.20, 50.37, 42.21, 38.05, 37.94, 35.56, 30.91, 20.81, 18.40, 16.76, 16.43, 16.35. HRMS (m/z): [M+Na] calcd for $C_{23}H_{30}O_8Na$, 457.1838; found 457.1859. HPLC t_R = 15.253 min; purity = 95.43% using 40 CH_3CN:60 H_2O as the mobile phase.

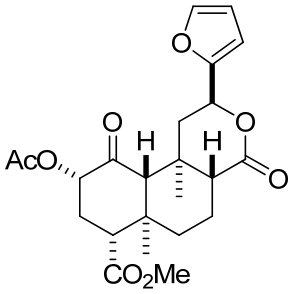

(2*S*,4a*R*,6a*R*,7*R*,9*S*,10a*S*,10b*R*)-methyl 9-acetoxy-2-(furan-2-yl)-6a,10b-dimethyl-4,10-di-oxododecahydro-1*H*-benzo[*f*]isochromene-7-carboxylate (185).

Alkene **184** (0.108 g, 0.249 mmol) was dissolved in bromobenzene (15 mL) followed by the addition of selenium (IV) oxide (0.083 g, 0.746 mmol). Reaction mixture was heated at 160°C and monitored by TLC. The solvent was evaporated *in vacuo* and the resulting residue purified by flash column chromatography on silica gel using mixtures of EtOAc/*n*-hexanes and triturated in EtOAc/*n*-hexanes to yield 0.195 g (18.1%) of **185** as a white solid, mp 198 – 200 ºC; ^{1}H NMR (500 MHz, $CDCl_3$) δ 7.39 (dd, *J* = 0.8, 1.7 Hz, 1H), 6.36 – 6.31 (m, 2H), 5.52 (dd, *J* = 5.6, 11.6 Hz, 1H), 5.18 – 5.11 (m, 1H), 3.73 (s, 3H), 2.81 – 2.72 (m, 1H), 2.45 (dd, *J* = 5.6, 13.6 Hz, 1H), 2.36 – 2.27 (m, 2H), 2.23 (s, 1H), 2.20 – 2.12 (m, 5H), 1.93 – 1.85 (m, 1H), 1.83 – 1.76 (m, 1H),

1.71 – 1.59 (m, 2H), 1.44 (s, 3H), 1.11 (s, 3H). ^{13}C NMR (126 MHz, $CDCl_3$) δ 202.17, 171.79, 171.07, 170.20, 151.41, 143.38, 110.66, 109.27, 75.27, 72.01, 64.30, 53.78, 52.21, 51.25, 42.33, 40.52, 38.36, 35.51, 30.95, 20.79, 18.36, 16.53, 15.28. HRMS (*m/z*): [M+Na] calcd for $C_{23}H_{28}O_8Na$, 455.1682; found, 455.1695. HPLC t_R = 24.103 min; purity = 97.44% using 40 CH_3CN:60 H_2O as the mobile phase.

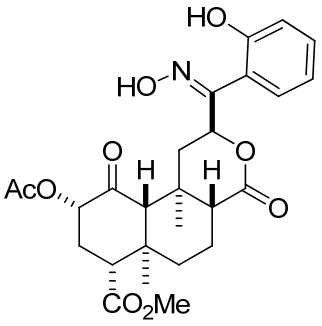

(2*S*,4a*R*,6a*R*,7*R*,9*S*,10a*S*,10b*R*)-methyl 9-acetoxy-2-((*Z*)-(hydroxyimino)(2-hydroxyphenyl) methyl)-6a,10b-dimethyl-4,10-dioxododecahydro-1*H*-benzo[*f*]isochromene-7-carboxylate (186).

Compound **186** was synthesized from **170** using **Procedure E** to afford 0.095 g (41.0%) as a white solid, mp 156 – 160 ºC; ^{1}H NMR (500 MHz, $CDCl_3$) δ 10.38 (s, 1H), 9.22 (s, 1H), 7.31 – 7.23 (m, 1H), 7.15 – 7.09 (m, 1H), 6.94 (d, *J* = 7.3 Hz, 1H), 6.84 (t, *J* = 7.6 Hz, 1H), 6.02 (dd, *J* = 5.8, 12.2 Hz, 1H), 5.23 (t, *J* = 10.0 Hz, 1H), 3.75 (s, 3H), 2.97 – 2.86 (m, 1H), 2.49 (dd, *J* = 5.9, 13.2 Hz, 1H), 2.40 – 2.24 (m, 2H), 2.24 – 2.08 (m, 5H), 1.95 (d, *J* = 9.0 Hz, 1H), 1.75 (d, *J* = 13.0 Hz, 1H), 1.56 (tt, *J* = 12.8, 25.2 Hz, 3H), 1.43 (s, 3H), 1.10 (s, 3H). ^{13}C NMR (126 MHz, $CDCl_3$) δ 201.98, 172.01, 171.35, 170.96, 157.69, 157.02, 131.42, 127.76, 119.76, 117.77, 116.12, 75.44, 71.90, 63.32, 53.06, 52.23, 51.58, 42.08, 38.08, 37.65, 35.80, 30.80, 20.97, 18.36, 16.67, 15.02. HRMS (*m/z*): [M+Na] calcd for $C_{26}H_{31}NO_9Na$, 524.1897; found, 524.1919. HPLC

t_R = 11.12 min; purity = 99.43% as determined on a Phenomenex Luna column (250 × 4.5 mm, 5 µm) using 40 CH_3CN:60 H_2O as the mobile phase.

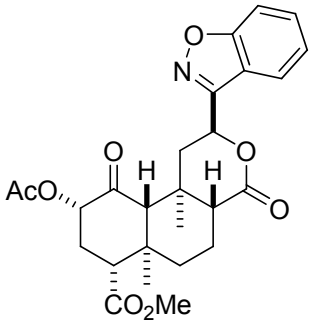

(2*S*,4a*R*,6a*R*,7*R*,9*S*,10a*S*,10b*R*)-methyl 9-acetoxy-2-(benzo[d]isoxazol-3-yl)-6a,10b-dimethyl -4,10-dioxododecahydro-1*H*-benzo[*f*]isochromene-7-carboxylate (187).

Oxime **186** (0.101 g, 0.202 mmol) was dissolved in isopropyl acetate (10 mL) and cooled to 0°C under an argon atmosphere. Diisopropylethylamine (0.042 mL, 0.242 mmol) was added followed by dropwise addition of methanesulfonyl chloride (0.047 mL, 0.606 mmol). The reaction was maintained at 0°C for 30 minutes. Another 1.2 equivalents of diisopropylethylamine (0.042 mL, 0.242 mmol) was added and reaction was heated to 55°C and monitored by TLC. Upon completion, reaction was cooled to room temperature and quenched with 2N HCl. EtOAc (10 mL) was added and organic layer was collected. Organic layer was washed with saturated aqueous $NaHCO_3$ (3 × 15 mL), brine (15 mL) and dried (Na_2SO_4). The solvent was evaporated *in vacuo* and the resulting residue purified by flash column chromatography on silica gel using mixtures of EtOAc/*n*-hexanes and triturated in EtOAc/*n*-hexanes to afford desired product in 0.037 g (37.7%) as a white solid, mp = 114 – 117°C; ^{1}H NMR (500 MHz, $CDCl_3$) δ 7.84 (d, *J* = 8.0 Hz, 1H), 7.62 – 7.56 (m, 2H), 7.35 (ddd, *J* = 2.0, 5.9, 8.0 Hz, 1H), 6.02 (dd, *J* = 6.4, 9.6 Hz, 1H), 5.18 (dd, *J* = 8.7, 11.4 Hz, 1H), 3.73 (s, 3H), 2.83 –

2.72 (m, 2H), 2.35 – 2.29 (m, 3H), 2.27 – 2.09 (m, 6H), 1.79 (dt, *J* = 3.1, 13.3 Hz, 1H), 1.77 – 1.65 (m, 1H), 1.65 – 1.57 (m, 2H), 1.54 (s, 3H), 1.13 (s, 3H). ^{13}C NMR (126 MHz, $CDCl_3$) δ 202.05, 171.79, 170.81, 170.01, 163.98, 157.41, 130.65, 124.29, 122.40, 119.86, 110.30, 75.11, 71.74, 64.48, 53.63, 52.20, 51.00, 42.20, 40.18, 38.08, 35.73, 30.96, 20.79, 18.39, 16.51, 16.46. HRMS (*m/z*): [M+Na] calcd for $C_{26}H_{29}NO_8Na$, 506.1791; found, 506.1762. HPLC t_R = 11.12 min; purity = 99.67%.

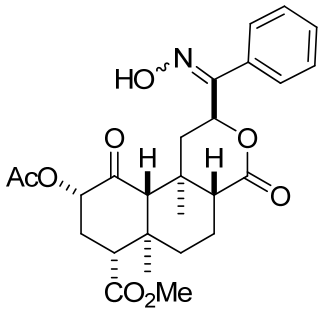

(2*S*,4a*R*,6a*R*,7*R*,9*S*,10a*S*,10b*R*)-methyl 9-acetoxy-2-((hydroxyimino)(phenyl)methyl)-6a,10b-dimethyl-4,10-dioxododecahydro-1*H*-benzo[*f*]isochromene-7-carboxylate (188).

Compound **188** was synthesized from **119** using **Procedure E** to afford 0.140 g (65.0%) as a white solid, mp 158 – 162 ºC; ^{1}H NMR (500 MHz, $CDCl_3$) δ 9.48 (s, 1H), 7.84 (s, 1H), 7.57 – 7.40 (m, 9H), 7.40 – 7.32 (m, 1H), 5.95 (dd, *J* = 5.7, 12.3, 1H), 5.51 – 5.44 (m, 1H), 5.34 (dd, *J* = 5.6, 11.6 Hz, 1H), 5.17 – 5.07 (m, 1H), 3.77 (s, 4H), 3.70 (s, 2H), 2.79 (dd, *J* = 5.6, 11.4 Hz, 1H), 2.73 – 2.65 (m, 2H), 2.38 – 2.21 (m, 9H), 2.17 (s, 2H), 2.10 – 2.02 (m, 2H), 1.95 (d, *J* = 11.2 Hz, 1H), 1.84 (s, 1H), 1.77 – 1.67 (m, 2H), 1.59 – 1.31 (m, 12H), 1.29 – 1.17 (m, 2H), 1.05 (d, *J* = 13.5 Hz, 6H). ^{13}C NMR (126 MHz, $CDCl_3$) δ 202.12, 201.61, 172.04, 171.78, 171.13, 171.00 (2C), 170.35, 157.39, 155.98, 133.50, 130.33, 129.90, 129.59, 128.88 (2C), 128.73 (2C), 128.61 (2C), 128.16 (2C), 78.53, 75.35, 75.17, 73.08, 64.03, 62.78, 53.51, 52.74, 52.25, 52.17,

51.77, 51.06, 42.13, 41.64, 39.62, 38.02, 37.89, 37.33, 35.41, 35.31, 30.89, 30.68, 21.07, 20.82, 18.24, 18.18, 16.61, 16.54, 15.56, 14.88. HRMS (*m/z*): [M+Na] calcd for $C_{26}H_{31}NO_8Na$, 508.1947; found, 508.1949. HPLC t_R = 13.52, 15.54 min; purity = 24.16, 75.44% as determined on a Phenomenex Luna column (250 × 4.5 mm, 5 μm) using 40 CH_3CN:60 H_2O as the mobile phase.

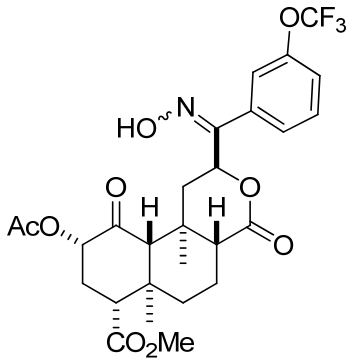

(2*S*,4a*R*,6a*R*,7*R*,9*S*,10a*S*,10b*R*)-methyl 9-acetoxy-2-((hydroxyimino)(3-(trifluoromethoxy) phenyl)methyl)-6a,10b-dimethyl-4,10-dioxododecahydro-1*H*-benzo[*f*]isochromene-7-carboxylate (189).

Compound **189** was synthesized from **177** using **Procedure E** to afford 0.221 g (52.6%) as a white solid, mp 139 – 145 ºC; ^{1}H NMR (500 MHz, $CDCl_3$) δ 8.76 (s, 1H), 7.89 (s, 1H), 7.49 – 7.43 (m, 2H), 7.38 (dd, *J* = 1.6, 4.9 Hz, 2H), 7.33 – 7.27 (m, 4H), 5.98 (dd, *J* = 5.8, 12.1 Hz, 1H), 5.34 (dd, *J* = 5.6, 11.7 Hz, 1H), 5.28 – 5.20 (m, 1H), 5.18 – 5.11 (m, 1H), 3.72 (d, *J* = 10.6 Hz, 6H), 2.71 (td, *J* = 6.5, 10.7 Hz, 2H), 2.60 (dd, *J* = 5.8, 13.3 Hz, 1H), 2.38 – 2.24 (m, 5H), 2.18 (d, *J* = 6.8 Hz, 6H), 2.07 (dd, *J* = 12.3, 22.8 Hz, 4H), 1.87 – 1.67 (m, 4H), 1.63 – 1.36 (m, 12H), 1.08 (d, *J* = 4.9 Hz, 6H). ^{13}C NMR (126 MHz, $CDCl_3$) δ 202.13, 201.85, 171.82, 171.76, 170.72, 170.70, 170.63, 170.39, 156.17, 154.27, 149.49 (d, *J* = 1.8 Hz), 149.28 (d, *J* = 1.8 Hz), 135.29, 132.17, 130.23, 130.20, 127.12, 126.42, 121.99, 121.94, 121.54, 120.72, 120.61 (q, *J* = 258.1

Hz, 2C), 78.24, 75.26, 75.19, 72.56, 64.07, 63.69, 53.53, 53.35, 52.19 (2C), 51.67, 51.21, 42.16, 42.04, 39.53, 38.08, 38.04, 37.96, 35.69, 35.35, 30.89, 30.87, 20.90, 20.82, 18.28, 18.24, 16.56 (2C), 15.55, 15.05. HRMS (*m/z*): [M+Na] calcd for $C_{27}H_{30}F_3NO_9Na$, 592.1770; found, 592.1767. HPLC t_R = 7.15, 7.69 min; purity = 27.16, 72.22% as determined on a Phenomenex Luna column (250 × 4.5 mm, 5 μm) using 55 CH_3CN:45 H_2O as the mobile phase.

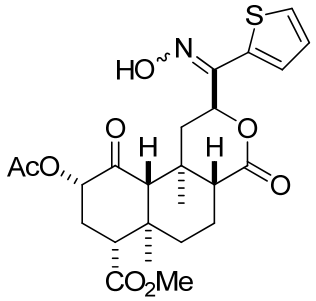

(2*S*,4a*R*,6a*R*,7*R*,9*S*,10a*S*,10b*R*)-methyl 9-acetoxy-2-((hydroxyimino)(thiophen-2-yl)methyl)-6a,10b-dimethyl-4,10-dioxododecahydro-1*H*-benzo[*f*]isochromene-7-carboxylate (190).

Compound **190** was synthesized from **117** using **Procedure E** to afford 0.178g (69.1%) as a white solid, mp 152 – 157 ºC; ^{1}H NMR (500 MHz, $CDCl_3$) δ 8.88 (s, 2H), 7.60 (dd, *J* = 1.0, 3.9 Hz, 1H), 7.56 (dd, *J* = 1.0, 5.1 Hz, 1H), 7.33 (dt, *J* = 3.4, 6.8 Hz, 1H), 7.20 – 7.16 (m, 1H), 7.12 (dd, *J* = 3.9, 5.1 Hz, 2H), 7.03 (dd, *J* = 3.7, 5.1 Hz, 1H), 6.03 (dd, *J* = 5.9, 12.0 Hz, 1H), 5.62 (dd, *J* = 6.0, 10.5 Hz, 1H), 5.17 (dd, *J* = 9.7, 20.1 Hz, 2H), 3.76 – 3.69 (m, 6H), 2.86 – 2.70 (m, 2H), 2.51 (dd, *J* = 5.9, 13.3 Hz, 1H), 2.39 (dd, *J* = 6.0, 13.7 Hz, 1H), 2.34 – 2.21 (m, 7H), 2.21 – 2.08 (m, 7H), 2.05 (dt, *J* = 3.6, 12.5 Hz, 1H), 1.98 (dd, *J* = 10.7, 13.6 Hz, 1H), 1.79 – 1.48 (m, 7H), 1.45 (d, *J* = 7.3 Hz, 6H), 1.10 (d, *J* = 4.2 Hz, 6H). ^{13}C NMR (126 MHz, $CDCl_3$) δ 202.48, 202.01, 171.91, 171.90, 171.36, 171.20, 170.56, 170.37, 152.62, 148.23, 135.07, 130.89 (2C), 130.46, 129.42, 127.93, 127.58, 126.50, 77.05, 75.28, 75.26, 72.41, 64.20, 63.48, 53.53, 53.36, 52.21, 52.18, 51.37, 50.72, 42.26, 42.13, 39.41, 38.11, 38.05, 37.93, 35.66, 35.56, 30.97, 30.90,

20.89, 20.85, 18.35, 18.31, 16.59, 16.54, 16.14, 15.07. HRMS (*m/z*): [M+Na] calcd for $C_{24}H_{29}NO_8SNa$, 514.1512; found, 514.1519. HPLC t_R = 15.93, 16.95 min; purity = 27.25, 69.83% as determined on a Phenomenex Luna column (250 × 4.5 mm, 5 μm) using 40 CH_3CN:60 H_2O as the mobile phase.

Binding and Activity Studies

Radioligand Binding Studies

MOP receptor binding sites were labeled using [^{3}H]D-Ala^2-MePhe^4,Gly-ol^5]-enkephalin ([^{3}H]DAMGO, SA = 44 – 48 Ci/mmol) while DOP receptor binding sides were labeled using [^{3}H][D-Ala^2, D-Leu^5]-enkephalin ([^{3}H]DADLE, SA = 40 – 50 Ci/mmol) in rat brain homogenates. KOP receptor binding sites were labeled using [^{3}H]*N*-methyl-2-phenyl-*N*-[(5*R*,7*S*,8*S*)-7-(pyrrolidin-1-yl)-1-oxaspiro[4.5]dec-8-yl]acetamide ([^{3}H]U69,593, SA = 50 Ci/mmol). On the day of the assay, Cell pellets were thawed on ice for 15 minutes followed by homogenization with a polytron in 10 mL/pellet of ice-cold 10mM Tris-HCl, pH 7.4. The membranes were centrifuged at 30,000 × g for 10 minutes, then resuspended in 10 mL/pellet ice-cold 10mM Tris-HCl, pH 7.4 followed again by centrifugation at 30,000 × g for 10 minutes. Membranes were then resuspended in 25°C 50 mM Tris-HCl, pH 7.4 (~100 mL/pellet hMOP-CHO, 50 mL/pellet hDOP-CHO, and 120 mL/pellet hKOP-CHO). All assays were performed in 50 mM Tris-HCl, pH 7.4 in a final assay volume of 1.0 mL, with a protease inhibitor cocktail: bacitracin (100 μg/mL), bestatin (10 μg/mL), leupeptin (4 μg/mL) and chymostatin (2 μg/mL). Drug dilution curves were determined with buffer containing 1 mg/mL BSA. 20 μM levallorphan ([^{3}H]DAMGO and [^{3}H]DADLE) or 10 μM (-)-U69,593 (for [^{3}H]U69,593 binding) was used to

account for nonspecific binding. [^{3}H]Radioligands were used at concentrations of approximately 2 nM. After 2 hours of incubation at 25°C, triplicate samples were filtered with Brandell Cell Harvesters (Biomedical Research & Development Inc., Gaithersburg, MD), over Whatman GF/B filters. The filters were the punched into 24-well plates in which 0.6 mL of LSC-cocktail (Cytoscint) was added. After an overnight extraction, the samples were counted in a Trilux liquid scintillation counter at 44% efficiency. Approximately 30 μg protein was in each assay tube for the opioid binding assays. The inhibition curves were determined by displacing a single concentration of radioligand by 10 concentrations of drug.

Functional Activity Studies

[^{35}S]GTPγS Assay

The [^{35}S]GTPγS assays were conducted previous described. Buffer A is is 50 mM Tris-HCl, pH 7.4, containing 100 mM NaCl, 10 mM $MgCl_2$, 1 mM EDTA and buffer B is buffer A with the addition of 1.67 mM dithiothreitol (DTT) and 0.15% bovine serum albumin (BSA). On the day of the assay, cells were thawed on ice for 15 min and homogenized using a polytron in 50 mM Tris-HCl, pH 7.4, containing a protease inhibitor cocktail: bacitracin (100 μg/mL), bestatin (10 μg/mL), leupeptin (4 μg/mL) and chymostatin (2 μg/mL). The homogenate was centrifuged at 30,000 × g for 10 minutes at 4°C, and the supernatant discarded. The membrane pellets were then resuspended in buffer B and used for [^{35}S]GTPγS binding assays. 50 μL of buffer A plus 0.1% BSA, 50 μL of GDP in buffer A/0.1% BSA (final concentration = 40 μM), 50 μL of drug in buffer A/0.1% bovine serum albumin, 50 μL of [^{35}S]GTPγS in buffer A/0.1% BSA (final concentration = 50 pM), and 300 μL of cell membranes (50 μg of protein) in buffer B were added in test tubes. Final concentration of reagents in assay were: 50 mM Tris-HCl, pH

7.4, containing 100 mM NaCl, 10 mM $MgCl_2$, 1 mM EDTA, 1 mM DTT, 40 μM GDP, and 0.1% BSA. Media was incubated at 55°C for 3 hours. Non-specific binding was accounted for and determined using GTPγS (40 μM). Vacuum filtration through Whatman GF/B filters separated bound and free [^{35}S]GTPγS. The filters were punched into 24-well plates followed by the addition of 0.6 mL of liquid scintillation media (Cytoscint). An overnight extraction was performed and samples were counted in a Trilux liquid scintillation counter at an efficiency of 27%.

FLIPR Assay

All cells were maintained in F-12 nutrient medium (Ham), supplemented with 10% fetal bovine serum (FBS), 1% penicillin and streptomycin (p/s), and 0.2% normocin. Cell culture supplies were from Invitrogen (Carlsbad, CA) unless otherwise specified. Chinese hamster ovary (CHO) cells stably expressing MOR- or KOR-Gαq16 were removed from their flasks using Versene and quenched with the Ham media, centrifuged and re-suspended in media. Cells were counted with a Cellometer Auto T4 (Nexcelom Bioscience, Lawrence, MA) and 30,000 cells were transferred to each well of a black Costar 96-well optical bottom plate (Corning Corporation, Corning, NY). Each plate was incubated at 37°C overnight to confluence. The culture media was removed from the plates and cells were subsequently loaded with a fluorescent calcium probe (Calcium 5 dye, Molecular Devices, Sunnyvale, CA) in an HBSS-based buffer containing 20 mM HEPES, 0.25% BSA, 1% DMSO, and 10 μM probenecid (Sigma) in a total volume of 225 μL. Cells were incubated at 37°C for 1 h and then stimulated with DAMGO, U69,593 or test compounds at various concentrations using a Flexstation 3 plate-reader, which automatically added 25 μL of the compounds at 10X concentration to each well

after reading baseline values for ~17 sec. Agonist-mediated change in fluorescence (485 nm excitation, 525 nm emission) was monitored in each well at 1.52 sec intervals for 60 sec and reported for each well. Data were collected using Softmax version 4.8 (MDS Analytical Technologies) and analyzed using Prism software (GraphPad, La Jolla, CA). Nonlinear regression analysis was performed to fit data and obtain maximum response (E_{max}), EC_{50}, correlation coefficient ($r2$) and other parameters. All experiments were performed at least 3 times to ensure reproducibility and data reported as mean ± standard error, unless noted otherwise.

Solubility Studies

Sample Preparation

Excess salvinorin A was added into duplicate 2 mL screw cap vials which contained approximately 1 mL of the Captisol® solution. The vials were sonicated in a Branson 1510 sonicator for 72 hours and then set at room temperature for 24 hours. Vials were then centrifuged at 7700 rpms for 10 minutes and HPLC analysis immediately followed. The samples were filtered with 0.45 µm, nylon, non-sterile Fisherbrand® syringe filters and analyzed without diluting for HPLC.

HPLC Measurements

HPLC was carried out on an Agilent 1100 Series capillary HPLC system with diode array detector. Peaks were detected at 209 and 214 nm. A Agilent Eclipse XDB-C18 column (250 × 10 mm, 5 µm) was used. Acetonitrile and water at the ratio of 60:40 was used as the mobile phase. The flow rate was 5.000 mL/min and the injection volume was 100 µL for all samples.

REFERENCES

(1) Grothaus, P. G.; Cragg, G. M.; Newman, D. J. Plant natural products in anticancer drug discovery. *Curr. Org. Chem.* **2010**, *14*, 1781 - 1791.

(2) Borchardt, J. K. The Beginnings of Drug Therapy: Ancient Mesopotamian Medicine. *Drug News Perspect.* **2002**, *15*, 187 - 192.

(3) Borchardt, J. K. Myrrh: an analgesic with a 4,000-year history. *Drug News Perspect.* **1996**, *9*, 554 - 557.

(4) Borchardt, J. K. Beginnings of drug therapy: drug therapy in ancient India. *Drug News Perspect.* **2003**, *16*, 403 - 408.

(5) Strohl, W. R. The role of natural products in a modern drug discovery program. *Drug Discov. Today* **2000**, *5*, 39 - 41.

(6) Li, J. W. H.; Vederas, J. C. Drug discovery and natural products end of an era or an endless frontier? *Science* **2009**, *325*, 161 - 165.

(7) Baker, D. D.; Chu, M.; Oza, U.; Rajgarhia, V. The value of natural products to future pharmaceutical discovery. *Nat. Prod. Rep.* **2007**, *24*, 1225 - 1244.

(8) Demain, A. L. Antibiotics: natural products essential to human health. *Med. Res. Rev.* **2009**, *29*, 821 - 842.

(9) Newman, D. J.; Cragg, G. M. Natural Products as Sources of New Drugs over the Last 25 Years. *J. Nat. Prod.* **2007**, *70*, 461 - 477.

(10) Harvey, A. L. Medicines from nature: are natural products still relevant to drug discovery? *Trends Pharmacol. Sci.* **1999**, *20*, 196 - 198.

(11) Lam, K. S. New aspects of natural products in drug discovery. *Trends Microbiol.* **2007**, *15*, 279 - 289.

(12) Lewis, R. J.; Garcia, M. L. Therapeutic potential of venom peptides. *Nat. Rev. Drug Discov.* **2003**, *2*, 790 - 802.

(13) Harvey, A. L. Natural products in drug discovery. *Drug Discov. Today* **2008**, *13*, 894 - 901.

(14) Bush, K. The coming of age of antibiotics: discovery and therapeutic value. *Ann. N.Y. Acad. Sci.* **2010**, *1213*, 1 - 4.

(15) Newman, D. J.; Cragg, G. M. Natural products as drugs and leads to drugs: the historical perspective. *Nat. Prod. Chem. Drug Discov.* **2010**, 3 - 27.

(16) Mitscher, L. A. Antibiotics and Antimicrobial Agents. In *Foye's Principles of Medicinal Chemistry*; 5th ed.; Troy, D., Ed.; Lippincott Williams & Wilkins: Philadelphia, 2002, p 819 - 864.

(17) Newman, D. J.; Cragg, G. M. Natural product scaffolds as leads to drugs. *Future Med. Chem.* **2009**, *1*, 1415 - 1427.

(18) Breslow, N. E.; Ou, S.-S.; Beckwith, J. B.; Haase, G. M.; Kalapurakal, J. A.; Ritchey, M. L.; Shamberger, R. C.; Thomas, P. R. M.; D'Angio, G. J.; Green, D. M. Doxorubicin for favorable histology, stage II-III Wilms tumor: results from the National Wilms Tumor Studies. *Cancer* **2004**, *101*, 1072 - 1080.

(19) Gore, M.; Huinink, W. t. B.; Carmichael, J.; Gordon, A.; Davidson, N.; Coleman, R.; Spaczynski, M.; Heron, J.-F.; Bolis, G.; Malmstrom, H.; Malfetano, J.; Scarabelli, C.; Vennin, P.; Ross, G.; Fields, S. Z. Clinical evidence for topotecan-paclitaxel non-cross-resistance in ovarian cancer. *J. Clin. Oncol.* **2001**, *19*, 1893 - 1900.

(20) Gruber, B. M.; Anuszewska, E. L.; Priebe, W. The effect of new anthracycline derivatives on the induction of apoptotic processes in human neoplastic cells. *Folia Histochem. Cytobiol.* **2004**, *42*, 127 - 130.

(21) Kepler, J. A.; Wani, M. C.; McNaull, J. N.; Wall, M. E.; Levine, S. G. Plant antitumor agents. IV. An approach toward the synthesis of camptothecin. *J. Org. Chem.* **1969**, *34*, 3853 - 3858.

(22) Pommier, Y. DNA Topoisomerase I Inhibitors: Chemistry, Biology, and Interfacial Inhibition. *Chem. Rev.* **2009**, *109*, 2894 - 2902.

(23) Redinbo, M. R.; Stewart, L.; Kuhn, P.; Champoux, J. J.; Hol, W. G. J. Crystal structures of human topoisomerase I in covalent and noncovalent complexes with DNA. *Science* **1998**, *279*, 1504 - 1513.

(24) Staker, B. L.; Hjerrild, K.; Feese, M. D.; Behnke, C. A.; Burgin, A. B., Jr.; Stewart, L. The mechanism of topoisomerase I poisoning by a camptothecin analog. *Proc. Natl. Acad. Sci. USA* **2002**, *99*, 15387 - 15392.

(25) Wani, M. C.; Ronman, P. E.; Lindley, J. T.; Wall, M. E. Plant antitumor agents. 18. Synthesis and biological activity of camptothecin analogs. *J. Med. Chem.* **1980**, *23*, 554 - 560.

(26) Newman, D. J.; Cragg, G. M.; Snader, K. M. Natural Products as Sources of New Drugs over the Period 1981-2002. *J. Nat. Prod.* **2003**, *66*, 1022 - 1037.

(27) Minotti, G.; Menna, P.; Salvatorelli, E.; Cairo, G.; Gianni, L. Anthracyclines: Molecular advances and pharmacologic developments in antitumor activity and cardiotoxicity. *Pharmacol. Rev.* **2004**, *56*, 185 - 229.

(28) Ferreira, S. H.; Bartelt, D. C.; Greene, L. J. Isolation of bradykinin-potentiating peptides from *Bothrops jararaca* venom. *Biochemistry* **1970**, *9*, 2583 - 2593.

(29) Ferreira, S. H.; Greene, L. J.; Alabaster, V. A.; Bakhle, Y. S.; Vane, J. R. Activity of various fractions of bradykinin potentiating factor against angiotensin I converting enzyme. *Nature (London)* **1970**, *225*, 379 - 380.

(30) Basso, N.; Terragno, N. A. History about the discovery of the renin-angiotensin system. *Hypertension* **2001**, *38*, 1246 - 1249.

(31) McMurray, J. J. V. Clinical practice. Systolic heart failure. *N. Engl. J. Med.* **2010**, *362*, 228 - 238.

(32) Pilote, L.; Abrahamowicz, M.; Eisenberg, M.; Humphries, K.; Behlouli, H.; Tu Jack, V. Effect of different angiotensin-converting-enzyme inhibitors on mortality among elderly patients with congestive heart failure. *Can. Med. Assoc. J.* **2008**, *178*, 1303 - 1311.

(33) Clark, A. M. Natural products as a resource for new drugs. *Pharm. Res.* **1996**, *13*, 1133 - 1141.

(34) Fernandez, L. S.; Jobling, M. F.; Andrews, K. T.; Avery, V. M. Antimalarial activity of natural product extracts from Papua New Guinean and Australian plants against *Plasmodium falciparum*. *Phytother. Res.* **2008**, *22*, 1409 - 1412.

(35) Borchardt, J. K. A short history of quinine. *Drug News Perspect.* **1996**, *9*, 116 - 120.

(36) Wellems, T. E.; Plowe, C. V. Chloroquine-resistant malaria. *J. Infect. Dis.* **2001**, *184*, 770 - 776.

(37) Mutai, C.; Rukunga, G.; Vagias, C.; Roussis, V. *In vivo* screening of antimalarial activity of *Acacia mellifera* (Benth) (Leguminosae) on *Plasmodium berghei* in mice. *Afr. J. Tradit., Complementary Altern. Med.* **2008**, *5*, 46 - 50.

(38) Kumar, S.; Misra, N.; Raj, K.; Srivastava, K.; Puri, S. K. Novel class of hybrid natural products derived from lupeol as antimalarial agents. *Nat. Prod. Res.* **2008**, *22*, 305 - 319.

(39) Haynes, R. K. Artemisinin and derivatives: the future for malaria treatment? *Curr. Opin. Infect. Dis.* **2001**, *14*, 719 - 726.

(40) Posner, G. H.; Ploypradith, P.; Parker, M. H.; O'Dowd, H.; Woo, S.-H.; Northrop, J.; Krasavin, M.; Dolan, P.; Kensler, T. W.; Xie, S.; Shapiro, T. A. Antimalarial, Antiproliferative, and Antitumor Activities of Artemisinin-Derived, Chemically Robust, Trioxane Dimers. *J. Med. Chem.* **1999**, *42*, 4275 - 4280.

(41) Posner, G. H.; Maxwell, J. P.; O'Dowd, H.; Krasavin, M.; Xie, S.; Shapiro, T. A. Antimalarial sulfide, sulfone, and sulfonamide trioxanes. *Bioorg. Med. Chem.* **2000**, *8*, 1361 - 1370.

(42) Itokawa, H.; Morris-Natschke, S. L.; Akiyama, T.; Lee, K.-H. Plant-derived natural product research aimed at new drug discovery. *J. Nat. Med.* **2008**, *62*, 263 - 280.

(43) Bachi, M. D.; Korshin, E. E.; Ploypradith, P.; Cumming, J. N.; Xie, S.; Shapiro, T. A.; Posner, G. H. Synthesis and *in vitro* antimalarial activity of sulfone endoperoxides. *Bioorg. Med. Chem. Lett.* **1998**, *8*, 903 - 908.

(44) Glaser, K. B.; Mayer, A. M. S. A renaissance in marine pharmacology: From preclinical curiosity to clinical reality. *Biochem. Pharmacol.* **2009**, *78*, 440 - 448.

(45) Miljanich, G. P. Ziconotide: Neuronal calcium channel blocker for treating severe chronic pain. *Curr. Med. Chem.* **2004**, *11*, 3029 - 3040.

(46) Prommer, E. Ziconotide: a new option for refractory pain. *Drugs Today* **2006**, *42*, 369 - 378.

(47) Williams, J. A.; Day, M.; Heavner, J. E. Ziconotide: an update and review. *Expert Opin. Pharmacother.* **2008**, *9*, 1575 - 1583.

(48) Olivera, B. M.; Teichert, R. W. Diversity of the neurotoxic Conus peptides: a model for concerted pharmacological discovery. *Mol. Interv.* **2007**, *7*, 251 - 260.

(49) Han, T. S.; Teichert, R. W.; Olivera, B. M.; Bulaj, G. Conus venoms - a rich source of peptide-based therapeutics. *Curr. Pharm. Des.* **2008**, *14*, 2462 - 2479.

(50) Terlau, H.; Olivera, B. M. Conus venoms: a rich source of novel ion channel-targeted peptides. *Physiol. Rev.* **2004**, *84*, 41 - 68.

(51) Terlau, H.; Shon, K.-J.; Grilley, M.; Stocker, M.; Stuehmer, W.; Olivera, B. M. Strategy for rapid immobilization of prey by a fish-hunting marine snail. *Nature (London)* **1996**, *381*, 148 - 151.

(52) Changeux, J.-P.; Taly, A. Nicotinic receptors, allosteric proteins and medicine. *Trends Mol. Med.* **2008**, *14*, 93 - 102.

(53) Galm, U.; Shen, B. Natural Product Drug Discovery: The Times Have Never Been Better. *Chem. Biol.* **2007**, *14*, 1098 - 1104.

(54) Soares, J. The nagoya protocol and natural product-based research. *ACS Chem. Biol.* **2011**, *6*, 289.

(55) Kennedy, J. Mutasynthesis, chemobiosynthesis, and back to semi-synthesis. Combining synthetic chemistry and biosynthetic engineering for diversifying natural products. *Nat. Prod. Rep.* **2008**, *25*, 25 - 34.

(56) Wilson, R. M.; Danishefsky, S. J. Small Molecule Natural Products in the Discovery of Therapeutic Agents: The Synthesis Connection. *J. Org. Chem.* **2006**, *71*, 8329 - 8351.

(57) Butler, M. S.; Buss, A. D. Natural products - the future scaffolds for novel antibiotics? *Biochem. Pharmacol.* **2006**, *71*, 919 - 929.

(58) Baker, D. D.; Chu, M.; Oza, U.; Rajgarhia, V. The value of natural products to future pharmaceutical discovery. *Nat. Prod. Rep.* **2007**, *24*, 1225 - 1244.

(59) Harvey, A. Strategies for discovering drugs from previously unexplored natural products. *Drug Discov. Today* **2000**, *5*, 294 - 300.

(60) McCurdy, C. R.; Prisinzano, T. E. Opioid Receptor Ligands. In *Burger's Medicinal Chemistry and Drug Discovery*; John Wiley & Sons, Inc.: 2010, p 1 - 168.

(61) Fries, D. S. Opioid Analgesics. In *Foye's Principles of Medicinal Chemistry*; 5th ed.; Troy, D., Ed.; Lippincott Williams & Wilkins: Philadelphia, 2002, p 453 - 479.

(62) Casy, A. F.; Parfitt, R. T. *Opioid Analgesics*; Plenum Press: New York, 1986.

(63) Gutstein, H. B.; Akil, H. Opioid Analagesics. In *Goodman LS, Hardman JG, Limbird LE, Gilman AG (eds) Goodman & Gilman's the pharmacological basis of therapeutics*; McGraw-Hill: New York, 2001, p 569 - 619.

(64) McNicol, E.; Horowicz-Mehler, N.; Fisk Ruth, A.; Bennett, K.; Gialeli-Goudas, M.; Chew Priscilla, W.; Lau, J.; Carr, D. Management of opioid side effects in cancer-related and chronic noncancer pain: a systematic review. *J. Pain* **2003**, *4*, 231 - 256.

(65) Mather, L. E.; Smith, M. T. Clinical Pharmacology and Adverse Effects. In *Opioids in Pain Control: Basic and Clinical Aspects*; Stein, Ed.; Cambridge University Press: Cambridge, 1999, p 188 - 211.

(66) Foss, J. F. A review of the potential role of methylnaltrexone in opioid bowel dysfunction. *Am. J. Surg.* **2001**, *182*, 19S - 26S.

(67) Friedman, J. D.; Dello Buono, F. A. Opioid antagonists in the treatment of opioid-induced constipation and pruritus. *Ann. Pharmacother.* **2001**, *35*, 85 - 91.

(68) Pappagallo, M. Incidence, prevalence, and management of opioid bowel dysfunction. *Am. J. Surg.* **2001**, *182*, 11S - 18S.

(69) Cherny, N. I. Opioid analgesics: comparative features and prescribing guidelines. *Drugs* **1996**, *51*, 713 - 737.

(70) Campora, E.; Merlini, L.; Pace, M.; Bruzzone, M.; Luzzani, M.; Gottlieb, A.; Rosso, R. The incidence of narcotic-induced emesis. *J. Pain Symptom Manage* **1991**, *6*, 428 - 430.

(71) Hampson, R. E.; Mu, J.; Deadwyler, S. A. Cannabinoid and kappa opioid receptors reduce potassium K current via activation of G(s) proteins in cultured hippocampal neurons. *J. Neurophysiol.* **2000**, *84*, 2356 - 2364.

(72) Wang, H. Y.; Burns, L. H. Gbetagamma that interacts with adenylyl cyclase in opioid tolerance originates from a G_s protein. *J. Neurobiol.* **2006**, *66*, 1302 - 1310.

(73) Kieffer, B. L.; Evans, C. J. Opioid tolerance-in search of the holy grail. *Cell* **2002**, *108*, 587 - 590.

(74) Maudsley, S.; Martin, B.; Luttrell, L. M. The origins of diversity and specificity in G protein-coupled receptor signaling. *J. Pharmacol. Exp. Ther.* **2005**, *314*, 485 - 494.

(75) Beckett, A. H.; Casy, A. F. Synthetic analgesics: stereochemical considerations. *J. Pharm. Pharmacol.* **1954**, *6*, 986 - 1001.

(76) Goldstein, A.; Lowney, L. I.; Pal, B. K. Stereospecific and nonspecific interactions of the morphine congener levorphanol in subcellular fractions of mouse brain. *Proc. Natl. Acad. Sci. USA* **1971**, *68*, 1742 - 1747.

(77) Pert, C. B.; Snyder, S. H. Opiate receptor: demonstration in nervous tissue. *Science* **1973**, *179*, 1011 - 1014.

(78) Gilbert, P. E.; Martin, W. R. The effects of morphine and nalorphine-like drugs in the nondependent, morphine-dependent and cyclazocine-dependent chronic spinal dog. *J. Pharmacol. Exp. Ther.* **1976**, *198*, 66 - 82.

(79) Martin, W. R.; Eades, C. G.; Thompson, J. A.; Huppler, R. E.; Gilbert, P. E. The effects of morphine- and nalorphine- like drugs in the nondependent and morphine-dependent chronic spinal dog. *J. Pharmacol. Exp. Ther.* **1976**, *197*, 517 - 532.

(80) Iwamoto, E. T.; Martin, W. R. Multiple opioid receptors. *Med. Res. Rev.* **1981**, *1*, 411 - 440.

(81) Aronoff, G. M. Opioids in chronic pain management: is there a significant risk of addiction? *Curr. Rev. Pain* **2000**, *4*, 112 - 121.

(82) Ko, M. C.; Lee, H.; Harrison, C.; Clark, M. J.; Song, H. F.; Naughton, N. N.; Woods, J. H.; Traynor, J. R. Studies of micro-, kappa-, and delta-opioid receptor density and G protein

activation in the cortex and thalamus of monkeys. *J. Pharmacol. Exp. Ther.* **2003**, *306*, 179 - 186.

(83) Hughes, J.; Smith, T. W.; Kosterlitz, H. W.; Fothergill, L. A.; Morgan, B. A.; Morris, H. R. Identification of two related pentapeptides from the brain with potent opiate agonist activity. *Nature* **1975**, *258*, 577 - 580.

(84) Li, C. H.; Chung, D. Isolation and structure of an untriakontapeptide with opiate activity from camel pituitary glands. *Proc. Natl. Acad. Sci. USA* **1976**, *73*, 1145 - 1148.

(85) Cox, B. M.; Opheim, K. E.; Teschemacher, H.; Goldstein, A. A peptide-like substance from pituitary that acts like morphine. 2. Purification and properties. *Life Sci.* **1975**, *16*, 1777 - 1782.

(86) Teschemacher, H.; Opheim, K. E.; Cox, B. M.; Goldstein, A. A peptide-like substance from pituitary that acts like morphine. I. Isolation. *Life Sci.* **1975**, *16*, 1771 - 1775.

(87) Ansonoff, M. A.; Zhang, J.; Czyzyk, T.; Rothman Richard, B.; Stewart, J.; Xu, H.; Zjwiony, J.; Siebert Daniel, J.; Yang, F.; Roth Bryan, L.; Pintar John, E. Antinociceptive and hypothermic effects of Salvinorin A are abolished in a novel strain of kappa-opioid receptor-1 knockout mice. *J. Pharmacol. Exp. Ther.* **2006**, *318*, 64 - 68.

(88) Pasternak, G. W. Multiple opiate receptors: deja vu all over again. *Neuropharmacology* **2004**, *47*, 312 - 323.

(89) Rothman, R. B. Evidence for heterogeneity of kappa-opioid binding sites: A review of data obtained using brain membranes depleted of mu and delta binding sites with irreversible agents. *Analgesia* **1994**, *1*, 27 - 49.

(90) Zaki, P. A.; Bilsky, E. J.; Vanderah, T. W.; Lai, J.; Evans, C. J.; Porreca, F. Opioid receptor types and subtypes: the delta receptor as a model. *Annu. Rev. Pharmacol. Toxicol.* **1996**, *36*, 379 - 401.

(91) Kieffer, B. L.; Befort, K.; Gaveriaux-Ruff, C.; Hirth, C. G. The delta-opioid receptor: isolation of a cDNA by expression cloning and pharmacological characterization. *Proc. Natl. Acad. Sci. USA* **1992**, *89*, 12048 - 12052.

(92) Wang, J. B.; Imai, Y.; Eppler, C. M.; Gregor, P.; Spivak, C. E.; Uhl, G. R. mu opiate receptor: cDNA cloning and expression. *Proc. Natl. Acad. Sci. USA* **1993**, *90*, 10230 - 10234.

(93) Xie, G. X.; Meng, F.; Mansour, A.; Thompson, R. C.; Hoversten, M. T.; Goldstein, A.; Watson, S. J.; Akil, H. Primary structure and functional expression of a guinea pig kappa opioid (dynorphin) receptor. *Proc. Natl. Acad. Sci. USA* **1994**, *91*, 3779 - 3783.

(94) Lovell, K. M.; Simpson, D. S.; Cunningham, C. W.; Prisinzano, T. E. Utilizing nature as a source of new probes for opioid pharmacology. *Future Med. Chem.* **2009**, *1*, 285 - 301.

(95) Prisinzano, T. E.; Rothman, R. B. Salvinorin A Analogs as Probes in Opioid Pharmacology. *Chem. Rev.* **2008**, *108*, 1732 - 1743.

(96) Prisinzano, T. E. Natural products as tools for neuroscience: discovery and development of novel agents to treat drug abuse. *J. Nat. Prod.* **2009**, *72*, 581 - 587.

(97) Carlezon, W. A., Jr.; Beguin, C.; DiNieri, J. A.; Baumann, M. H.; Richards, M. R.; Todtenkopf, M. S.; Rothman, R. B.; Ma, Z.; Lee, D. Y. W.; Cohen, B. M. Depressive-like effects of the k-opioid receptor agonist salvinorin A on behavior and neurochemistry in rats. *J. Pharmacol. Exp. Ther.* **2006**, *316*, 440 - 447.

(98) DeHaven-Hudkins, D. L.; Dolle, R. E. Peripherally restricted opioid agonists as novel analgesic agents. *Curr. Pharm. Des.* **2004**, *10*, 743 - 757.

(99) Kivell, B.; Prisinzano, T. E. Kappa opioids and the modulation of pain. *Psychopharmacology (Berlin)* **2010**, *210*, 109 - 119.

(100) Shippenberg, T. S.; Zapata, A.; Chefer, V. I. Dynorphin and the pathophysiology of drug addiction. *Pharmacol. Ther.* **2007**, *116*, 306 - 321.

(101) Schenk, S.; Partridge, B.; Shippenberg, T. S. U69593, a kappa-opioid agonist, decreases cocaine self-administration and decreases cocaine-produced drug-seeking. *Psychopharmacology (Berlin)* **1999**, *144*, 339 - 346.

(102) Mello, N. K.; Negus, S. S. Interactions between kappa opioid agonists and cocaine. Preclinical studies. *Ann. N.Y. Acad. Sci.* **2000**, *909*, 104 - 132.

(103) Crawford, C. A.; McDougall, S. A.; Bolanos, C. A.; Hall, S.; Berger, S. P. The effects of the kappa agonist U-50,488 on cocaine-induced conditioned and unconditioned behaviors and Fos immunoreactivity. *Psychopharmacology (Berlin)* **1995**, *120*, 392 - 399.

(104) Glick, S. D.; Maisonneuve, I. M.; Raucci, J.; Archer, S. Kappa opioid inhibition of morphine and cocaine self-administration in rats. *Brain Res.* **1995**, *681*, 147 - 152.

(105) Mello, N. K.; Negus, S. S. Effects of kappa opioid agonists on cocaine- and food-maintained responding by rhesus monkeys. *J. Pharmacol. Exp. Ther.* **1998**, *286*, 812 - 824.

(106) Negus, S. S.; Mello, N. K.; Portoghese, P. S.; Lin, C.-E. Effects of kappa opioids on cocaine self-administration by rhesus monkeys. *J. Pharmacol. Exp. Ther.* **1997**, *282*, 44 - 55.

(107) Schenk, S.; Partridge, B.; Shippenberg, T. S. Reinstatement of extinguished drug-taking behavior in rats: effect of the kappa-opioid receptor agonist, U69593. *Psychopharmacology (Berlin)* **2000**, *151*, 85 - 90.

(108) Wee, S.; Koob, G. F. The role of the dynorphin-kappa opioid system in the reinforcing effects of drugs of abuse. *Psychopharmacology (Berlin)* **2010**, *210*, 121 - 135.

(109) Schenk, S.; Partridge, B.; Shippenberg, T. S. Effects of the k-opioid receptor agonist U69593 on the development of sensitization and on the maintenance of cocaine self-administration. *Neuropsychopharmacology* **2001**, *24*, 441 - 450.

(110) Mori, T.; Nomura, M.; Nagase, H.; Narita, M.; Suzuki, T. Effects of a newly synthesized k-opioid receptor agonist, TRK-820, on the discriminative stimulus and rewarding effects of cocaine in rats. *Psychopharmacology (Berlin)* **2002**, *161*, 17 - 22.

(111) Zhang, Y.; Butelman, E. R.; Schlussman, S. D.; Ho, A.; Kreek, M. J. Effect of the endogenous k opioid agonist dynorphin A(1-17) on cocaine-evoked increases in striatal dopamine levels and cocaine-induced place preference in C57BL/6J mice. *Psychopharmacology (Berlin)* **2004**, *172*, 422 - 429.

(112) Mucha, R. F.; Herz, A. Motivational properties of kappa and mu opioid receptor agonists studied with place and taste preference conditioning. *Psychopharmacology (Berlin)* **1985**, *86*, 274 - 280.

(113) Shippenberg, T. S.; Herz, A. Influence of chronic lithium treatment upon the motivational effects of opioids: alteration in the effects of mu- but not kappa-opioid receptor ligands. *J. Pharmacol. Exp. Ther.* **1991**, *256*, 1101 - 1106.

(114) Carlezon, W. A., Jr.; Thome, J.; Olson, V. G.; Lane-Ladd, S. B.; Brodkin, E. S.; Hiroi, N.; Duman, R. S.; Neve, R. L.; Nestler, E. J. Regulation of cocaine reward by CREB. *Science* **1998**, *282*, 2272 - 2275.

(115) Pan, Z. Z. mu-Opposing actions of the kappa-opioid receptor. *Trends Pharmacol. Sci.* **1998**, *19*, 94 - 98.

(116) Friedman, R. N.; Bittner, G. D.; Blundon, J. A. Electrophysiological and behavioral effects of ethanol on crayfish. *J. Pharmacol. Exp. Ther.* **1988**, *246*, 125 - 131.

(117) Matthes, H. W. D.; Maldonado, R.; Simonin, F.; Valverde, O.; Slowe, S.; Kitchen, I.; Befort, K.; Dierich, A.; Le Meur, M.; et al. Loss of morphine-induced analgesia, reward effect and withdrawal symptoms in mice lacking the micro -opioid-receptor gene. *Nature (London)* **1996**, *383*, 819 - 823.

(118) Ramarao, P.; Jablonski, H. I., Jr.; Rehder, K. R.; Bhargava, H. N. Effect of k-opioid receptor agonists on morphine analgesia in morphine-naive and morphine-tolerant rats. *Eur. J. Pharmacol.* **1988**, *156*, 239 - 246.

(119) Sora, I.; Takahashi, N.; Funada, M.; Ujike, H.; Revay, R. S.; Donovan, D. M.; Miner, L. L.; Uhl, G. R. Opiate receptor knockout mice define micro receptor roles in endogenous

nociceptive responses and morphine-induced analgesia. *Proc. Natl. Acad. Sci. USA* **1997**, *94*, 1544 - 1549.

(120) Tao, P.-L.; Hwang, C.-L.; Chen, C.-Y. U-50,488 blocks the development of morphine tolerance and dependence at a very low dose in guinea pigs. *Eur. J. Pharmacol.* **1994**, *256*, 281 - 286.

(121) Tulunay, F. C.; Jen, M.-F.; Chang, J. K.; Loh, H. H.; Lee, N. M. Possible regulatory role of dynorphin on morphine- and beta -endorphin-induced analgesia. *J. Pharmacol. Exp. Ther.* **1981**, *219*, 296 - 298.

(122) Law, P. Y.; Hom, D. S.; Loh, H. H. Opiate receptor down-regulation and desensitization in neuroblastoma X glioma NG108-15 hybrid cells are two separate cellular adaptation processes. *Mol. Pharmacol.* **1983**, *24*, 413 - 424.

(123) He, L.; Fong, J.; von Zastrow, M.; Whistler, J. L. Regulation of opioid receptor trafficking and morphine tolerance by receptor oligomerization. *Cell* **2002**, *108*, 271 - 282.

(124) Gabra, B. H.; Bailey, C. P.; Kelly, E.; Sanders, A. V.; Henderson, G.; Smith, F. L.; Dewey, W. L. Evidence for an important role of protein phosphatases in the mechanism of morphine tolerance. *Brain Res.* **2007**, *1159*, 86 - 93.

(125) Lefkowitz, R. J.; Pitcher, J.; Krueger, K.; Daaka, Y. Mechanisms of beta-adrenergic receptor desensitization and resensitization. *Adv. Pharmacol.* **1998**, *42*, 416 - 420.

(126) Chang, K. J.; Eckel, R. W.; Blanchard, S. G. Opioid peptides induce reduction of enkephalin receptors in cultured neuroblastoma cells. *Nature* **1982**, *296*, 446 - 448.

(127) Tao, P. L.; Liu, C. F.; Tsai, H. C. Chronic intracerebroventricular administration of morphine down-regulates spinal adenosine A_1 receptors in rats. *Eur. J. Pharmacol.* **1995**, *278*, 233 - 237.

(128) Takahashi, M.; Senda, T.; Kaneto, H. Role of spinal k opioid receptors in the blockade of the development of antinociceptive tolerance to morphine. *Eur. J. Pharmacol.* **1991**, *200*, 293 - 297.

(129) Yamamoto, T.; Ohno, M.; Ueki, S. A selective k-opioid agonist, U-50,488H, blocks the development of tolerance to morphine analgesia in rats. *Eur. J. Pharmacol.* **1988**, *156*, 173 - 176.

(130) Bolanos, C. A.; Garmsen, G. M.; Clair, M. A.; McDougall, S. A. Effects of the k-opioid receptor agonist U-50,488 on morphine-induced place preference conditioning in the developing rat. *Eur. J. Pharmacol.* **1996**, *317*, 1 - 8.

(131) Funada, M.; Suzuki, T.; Narita, M.; Misawa, M.; Nagase, H. Blockade of morphine reward through the activation of k-opioid receptors in mice. *Neuropharmacology* **1993**, *32*, 1315 - 1323.

(132) Kuzmin, A. V.; Semenova, S.; Gerrits, A. F. M.; Zvartau, E. E.; Van Ree, J. M. k-Opioid receptor agonist U50488H modulates cocaine and morphine self-administration in drug-naive rats and mice. *Eur. J. Pharmacol.* **1997**, *321*, 265 - 271.

(133) Epstein, D. H.; Preston, K. L.; Stewart, J.; Shaham, Y. Toward a model of drug relapse: an assessment of the validity of the reinstatement procedure. *Psychopharmacology (Berlin)* **2006**, *189*, 1 - 16.

(134) Gawin, F.; Kleber, H. Pharmacologic treatments of cocaine abuse. *Psychiatr. Clin. North Am.* **1986**, *9*, 573 - 583.

(135) Beardsley, P. M.; Howard, J. L.; Shelton, K. L.; Carroll, F. I. Differential effects of the novel kappa opioid receptor antagonist, JDTic, on reinstatement of cocaine-seeking induced by footshock stressors vs cocaine primes and its antidepressant-like effects in rats. *Psychopharmacology (Berlin)* **2005**, *183*, 118 - 126.

(136) Vanderah, T. W. Delta and kappa opioid receptors as suitable drug targets for pain. *Clin. J. Pain.* **2010**, *26 Suppl 10*, S10 - 15.

(137) Roth, B. L.; Baner, K.; Westkaemper, R.; Siebert, D.; Rice, K. C.; Steinberg, S.; Ernsberger, P.; Rothman, R. B. Salvinorin A: A potent naturally occurring nonnitrogenous kappa opioid selective agonist. *Proc. Natl. Acad. Sci. USA* **2002**, *99*, 11934 - 11939.

(138) Kumor, K. M.; Haertzen, C. A.; Johnson, R. E.; Kocher, T.; Jasinski, D. Human psychopharmacology of ketocyclazocine as compared with cyclazocine, morphine and placebo. *J. Pharmacol. Exp. Ther.* **1986**, *238*, 960 - 968.

(139) Martin, W. R.; Fraser, H. F.; Gorodetzky, C. W.; Rosenberg, D. E. Dependence-producing potential of the narcotic antagonist 2 - cyclopropylmethyl - 2' - hydroxy - 5,9 - dimethyl - 6,7 - benzomorphan (cyclazocine, Win-20,740, ARC II-C-3). *J. Pharmacol. Exp. Ther.* **1965**, *150*, 426 - 436.

(140) Pfeiffer, A.; Brantl, V.; Herz, A.; Emrich, H. M. Psychotomimesis mediated by k opiate receptors. *Science* **1986**, *233*, 774-776.

(141) Rimoy, G. H.; Wright, D. M.; Bhaskar, N. K.; Rubin, P. C. The cardiovascular and central nervous system effects in the human of U-62066E - A selective opioid receptor agonist. *Eur. J. Clin. Pharmacol.* **1994**, *46*, 203 - 207.

(142) Walsh, S. L.; Strain, E. C.; Abreu, M. E.; Bigelow, G. E. Enadoline, a selective kappa opioid agonist: comparison with butorphanol and hydromorphone in humans. *Psychopharmacology (Berlin)* **2001**, *157*, 151 - 162.

(143) Burton, M. B.; Gebhart, G. F. Effects of kappa-opioid receptor agonists on responses to colorectal distension in rats with and without acute colonic inflammation. *J. Pharmacol. Exp. Ther.* **1998**, *285*, 707 - 715.

(144) Herrero, J. F.; Headley, P. M. The effects of sham and full spinalization on the systemic potency of micro - and k-opioids on spinal nociceptive reflexes in rats. *Br. J. Pharmacol.* **1991**, *104*, 166 - 170.

(145) Schepers, R. J.; Mahoney, J. L.; Gehrke, B. J.; Shippenberg, T. S. Endogenous kappa-opioid receptor systems inhibit hyperalgesia associated with localized peripheral inflammation. *Pain* **2008**, *138*, 423 - 439.

(146) Vanderah, T. W.; Largent-Milnes, T.; Lai, J.; Porreca, F.; Houghten, R. A.; Menzaghi, F.; Wisniewski, K.; Stalewski, J.; Sueiras-Diaz, J.; Galyean, R.; Schteingart, C.; Junien, J.-L.; Trojnar, J.; Riviere, P. J. M. Novel D-amino acid tetrapeptides produce potent antinociception by selectively acting at peripheral k-opioid receptors. *Eur. J. Pharmacol.* **2008**, *583*, 62 - 72.

(147) Cole, R. L.; Konradi, C.; Douglass, J.; Hyman, S. E. Neuronal adaptation to amphetamine and dopamine: molecular mechanisms of prodynorphin gene regulation in rat striatum. *Neuron* **1995**, *14*, 813 - 823.

(148) Daunais, J. B.; Roberts, D. C.; McGinty, J. F. Short-term cocaine self administration alters striatal gene expression. *Brain Res. Bull.* **1995**, *37*, 523 - 527.

(149) Douglass, J.; McKinzie, A. A.; Pollock, K. M. Identification of multiple DNA elements regulating basal and protein kinase A-induced transcriptional expression of the rat prodynorphin gene. *Mol. Endocrinol.* **1994**, *8*, 333 - 344.

(150) Carlezon, W. A., Jr.; Beguin, C.; Knoll, A. T.; Cohen, B. M. Kappa-opioid ligands in the study and treatment of mood disorders. *Pharmacol. Ther.* **2009**, *123*, 334 - 343.

(151) Bals-Kubik, R.; Herz, A.; Shippenberg, T. S. Evidence that the aversive effects of opioid antagonists and kappa-agonists are centrally mediated. *Psychopharmacology (Berlin)* **1989**, *98*, 203 - 206.

(152) Pfeiffer, A.; Brantl, V.; Herz, A.; Emrich, H. M. Psychotomimesis mediated by kappa opiate receptors. *Science* **1986**, *233*, 774 - 776.

(153) Kendler, K. S.; Karkowski, L. M.; Prescott, C. A. Causal relationship between stressful life events and the onset of major depression. *Am. J. Psychiatry* **1999**, *156*, 837 - 841.

(154) Pliakas, A. M.; Carlson, R. R.; Neve, R. L.; Konradi, C.; Nestler, E. J.; Carlezon, W. A., Jr. Altered responsiveness to cocaine and increased immobility in the forced swim test associated with elevated cAMP response element-binding protein expression in nucleus accumbens. *J. Neurosci.* **2001**, *21*, 7397 - 7403.

(155) Newton, S. S.; Thome, J.; Wallace, T. L.; Shirayama, Y.; Schlesinger, L.; Sakai, N.; Chen, J.; Neve, R.; Nestler, E. J.; Duman, R. S. Inhibition of cAMP response element-binding protein or dynorphin in the nucleus accumbens produces an antidepressant-like effect. *J. Neurosci.* **2002**, *22*, 10883 - 10890.

(156) Mague, S. D.; Pliakas, A. M.; Todtenkopf, M. S.; Tomasiewicz, H. C.; Zhang, Y.; Stevens, W. C., Jr.; Jones, R. M.; Portoghese, P. S.; Carlezon, W. A., Jr. Antidepressant-like effects of kappa-opioid receptor antagonists in the forced swim test in rats. *J. Pharmacol. Exp. Ther.* **2003**, *305*, 323 - 330.

(157) McLaughlin, J. P.; Marton-Popovici, M.; Chavkin, C. Kappa opioid receptor antagonism and prodynorphin gene disruption block stress-induced behavioral responses. *J. Neurosci.* **2003**, *23*, 5674 - 5683.

(158) Shirayama, Y.; Ishida, H.; Iwata, M.; Hazama, G. I.; Kawahara, R.; Duman, R. S. Stress increases dynorphin immunoreactivity in limbic brain regions and dynorphin antagonism produces antidepressant-like effects. *J. Neurochem.* **2004**, *90*, 1258 - 1268.

(159) Di Chiara, G.; Imperato, A. Drugs abused by humans preferentially increase synaptic dopamine concentrations in the mesolimbic system of freely moving rats. *Proc. Natl. Acad. Sci. USA* **1988**, *85*, 5274 - 5278.

(160) Wise, R. A.; Bozarth, M. A. A psychomotor stimulant theory of addiction. *Psychol. Rev.* **1987**, *94*, 469 - 492.

(161) Todtenkopf, M. S.; Marcus, J. F.; Portoghese, P. S.; Carlezon, W. A., Jr. Effects of kappa-opioid receptor ligands on intracranial self-stimulation in rats. *Psychopharmacology (Berlin)* **2004**, *172*, 463 - 470.

(162) Maisonneuve, I. M.; Archer, S.; Glick, S. D. U50,488, a kappa opioid receptor agonist, attenuates cocaine-induced increases in extracellular dopamine in the nucleus accumbens of rats. *Neurosci. Lett.* **1994**, *181*, 57 - 60.

(163) Peters, M. F.; Zacco, A.; Gordon, J.; Maciag, C. M.; Litwin, L. C.; Thompson, C.; Schroeder, P.; Sygowski, L. A.; Piser, T. M.; Brugel, T. A. Identification of short-acting kappa-opioid receptor antagonists with anxiolytic-like activity. *Eur. J. Pharmacol.* **2011**, *661*, 27 - 34.

(164) Bidlack, J. M.; Khimich, M.; Parkhill, A. L.; Sumagin, S.; Sun, B.; Tipton, C. M. Opioid receptors and signaling on cells from the immune system. *J. Neuroimmune Pharmacol.* **2006**, *1*, 260 - 269.

(165) Chao, C. C.; Gekker, G.; Hu, S.; Sheng, W. S.; Shark, K. B.; Bu, D. F.; Archer, S.; Bidlack, J. M.; Peterson, P. K. kappa opioid receptors in human microglia downregulate human immunodeficiency virus 1 expression. *Proc. Natl. Acad. Sci. USA* **1996**, *93*, 8051 - 8056.

(166) Bidlack, J. M.; Abraham, M. K. Mitogen-induced activation of mouse T cells increases kappa opioid receptor expression. *Adv. Exp. Med. Biol.* **2001**, *493*, 103 - 110.

(167) Tortella, F. C.; DeCoster, M. A. Kappa opioids: therapeutic considerations in epilepsy and CNS injury. *Clin. Neuropharmacol.* **1994**, *17*, 403 - 416.

(168) Berman, E. F.; Adler, M. W. The anticonvulsant effect of opioids and opioid peptides against maximal electroshock seizures in rats. *Neuropharmacology* **1984**, *23*, 367 - 371.

(169) Perry, D. C.; Lyeth, B. G.; Miller, L. P.; Getz, R. L.; Jenkins, L. W.; Hayes, R. L. Effects of traumatic brain injury in rats on binding to forebrain opiate receptor subtypes. *Mol Chem Neuropathol* **1992**, *16*, 95 - 107.

(170) Scavini, C.; Rozza, A.; Bo, P.; Lanza, E.; Favalli, L.; Savoldi, F.; Racagni, G. k-Opioid receptor changes and neurophysiological alterations during cerebral ischemia in rabbits. *Stroke* **1990**, *21*, 943 - 947.

(171) Negus, S. S.; Mello, N. K.; Linsenmayer, D. C.; Jones, R. M.; Portoghese, P. S. Kappa opioid antagonist effects of the novel kappa antagonist 5'-guanidinonaltrindole (GNTI) in an assay of schedule-controlled behavior in rhesus monkeys. *Psychopharmacology (Berlin)* **2002**, *163*, 412 - 419.

(172) Butelman, E. R.; Negus, S. S.; Ai, Y.; de Costa, B. R.; Woods, J. H. Kappa opioid antagonist effects of systemically administered nor-binaltorphimine in a thermal antinociception assay in rhesus monkeys. *J. Pharmacol. Exp. Ther.* **1993**, *267*, 1269 - 1276.

(173) Broadbear, J. H.; Negus, S. S.; Butelman, E. R.; de Costa, B. R.; Woods, J. H. Differential effects of systemically administered nor-binaltorphimine (nor-BNI) on kappa-opioid agonists in the mouse writhing assay. *Psychopharmacology (Berlin)* **1994**, *115*, 311 - 319.

(174) Jones, D. N.; Holtzman, S. G. Long term kappa-opioid receptor blockade following *nor*-binaltorphimine. *Eur. J. Pharmacol.* **1992**, *215*, 345 - 348.

(175) Horan, P.; Taylor, J.; Yamamura, H. I.; Porreca, F. Extremely long-lasting antagonistic actions of *nor*-binaltorphimine (*nor*-BNI) in the mouse tail-flick test. *J. Pharmacol. Exp. Ther.* **1992**, *260*, 1237 - 1243.

(176) Jewett, D. C.; Woods, J. H. *Nor*-binaltorphimine: an ultra-long acting kappa-opioid antagonist in pigeons. *Behav. Pharmacol.* **1995**, *6*, 815 - 820.

(177) Ko, M. C.; Johnson, M. D.; Butelman, E. R.; Willmont, K. J.; Mosberg, H. I.; Woods, J. H. Intracisternal *nor*-binaltorphimine distinguishes central and peripheral kappa-opioid antinociception in rhesus monkeys. *J. Pharmacol. Exp. Ther.* **1999**, *291*, 1113 - 1120.

(178) Bruchas, M. R.; Yang, T.; Schreiber, S.; Defino, M.; Kwan, S. C.; Li, S.; Chavkin, C. Long-acting kappa opioid antagonists disrupt receptor signaling and produce noncompetitive effects by activating c-Jun N-terminal kinase. *J. Biol. Chem.* **2007**, *282*, 29803 - 29811.

(179) Ruzicka, L. Isoprene rule and the biogenesis of terpenic compounds. *Experientia* **1953**, *9*, 357 - 367.

(180) Chinou, I. Labdanes of natural origin-biological activities (1981-2004). *Curr. Med. Chem.* **2005**, *12*, 1295 - 1317.

(181) Breitmaier *Terpenes: Flavors, Fragrances, Pharmaca, Pheromones*; Wiley-VCH: Weinheim, 2006.

(182) Wang, F. P.; Chen, Q. H.; Liu, X. Y. Diterpenoid alkaloids. *Nat. Prod. Rep.* **2010**, *27*, 529 - 570.

(183) Peters, R. J. Two rings in them all: the labdane-related diterpenoids. *Nat. Prod. Rep.* **2010**, *27*, 1521 - 1530.

(184) Ambrosio, S. R.; Tirapelli, C. R.; da Costa, F. B.; de Oliveira, A. M. Kaurane and pimarane-type diterpenes from the *Viguiera species* inhibit vascular smooth muscle contractility. *Life Sci.* **2006**, *79*, 925 - 933.

(185) Mitscher, L. A.; Rao, G. S.; Veysoglu, T.; Drake, S.; Haas, T. Isolation and identification of trachyloban-19-oic and (-)-kaur-16-en-19-oic acids as antimicrobial agents from the prairie sunflower, *Helianthus annuus*. *J. Nat. Prod.* **1983**, *46*, 745 - 746.

(186) Slimestad, R.; Marston, A.; Mavi, S.; Hostettmann, K. Larvicidal constituents of *Melantheria albinervia*. *Planta Med.* **1995**, *61*, 562 - 563.

(187) Chen, B. J. Triptolide, a novel immunosuppressive and anti-inflammatory agent purified from a Chinese herb *Tripterygium wilfordii* Hook F. *Leuk Lymphoma* **2001**, *42*, 253 - 265.

(188) Matta, R.; Wang, X.; Ge, H.; Ray, W.; Nelin, L. D.; Liu, Y. Triptolide induces anti-inflammatory cellular responses. *Am. J. Transl. Res.* **2009**, *1*, 267 - 282.

(189) Jiang, X. H.; Wong, B. C.; Lin, M. C.; Zhu, G. H.; Kung, H. F.; Jiang, S. H.; Yang, D.; Lam, S. K. Functional p53 is required for triptolide-induced apoptosis and AP-1 and nuclear factor-kappaB activation in gastric cancer cells. *Oncogene* **2001**, *20*, 8009 - 8018.

(190) Qiu, D.; Zhao, G.; Aoki, Y.; Shi, L.; Uyei, A.; Nazarian, S.; Ng, J. C.; Kao, P. N. Immunosuppressant PG490 (triptolide) inhibits T-cell interleukin-2 expression at the level of purine-box/nuclear factor of activated T-cells and NF-kappaB transcriptional activation. *J. Biol. Chem.* **1999**, *274*, 13443 - 13450.

(191) Schroeder, F. C.; Gonzalez, A.; Eisner, T.; Meinwald, J. Miriamin, a defensive diterpene from the eggs of a land slug (*Arion sp.*). *Proc. Natl. Acad. Sci. USA* **1999**, *96*, 13620 - 13625.

(192) Tokoroyama, T. Synthesis of clerodane diterpenoids and related compounds - stereoselective construction of the decalin skeleton with multiple contiguous stereogenic centers. *Synthesis* **2000**, 611 - 633.

(193) Kohno, H.; Maeda, M.; Tanino, M.; Tsukio, Y.; Ueda, N.; Wada, K.; Sugie, S.; Mori, H.; Tanaka, T. A bitter diterpenoid furanolactone columbin from *Calumbae Radix* inhibits azoxymethane-induced rat colon carcinogenesis. *Cancer Lett.* **2002**, *183*, 131 - 139.

(194) Moody, J. O.; Robert, V. A.; Connolly, J. D.; Houghton, P. J. Anti-inflammatory activities of the methanol extracts and an isolated furanoditerpene constituent of *Sphenocentrum jollyanum* Pierre (Menispermaceae). *J Ethnopharmacol* **2006**, *104*, 87 - 91.

(195) Shi, Q.; Liang, M.; Zhang, W.; Zhang, C.; Liu, R.; Shen, Y.; Li, H.; Wang, X.; Wang, X.; Pan, Q.; Chen, C. Quantitative LC/MS/MS method and pharmacokinetic studies of columbin, an anti-inflammation furanoditerpen isolated from *Radix Tinosporae*. *Biomed. Chromatogr.* **2007**, *21*, 642 - 648.

(196) Bruno, M.; Fazio, C.; Arnold, N. A. Neo-clerodane diterpenoids from *Scutellaria cypria*. *Phytochem.* **1996**, *42*, 555 - 557.

(197) Lallemand, J.-Y.; Six, Y.; Ricard, L. A concise synthesis of an advanced clerodin intermediate through a Vaultier tandem reaction. *Eur. J. Org. Chem.* **2002**, 503 - 513.

(198) Ley, S. V.; Denholm, A. A.; Wood, A. The chemistry of azadirachtin. *Nat. Prod. Rep.* **1993**, *10*, 109 - 157.

(199) Merritt, A. T.; Ley, S. V. Clerodane diterpenoids. *Nat. Prod. Rep.* **1992**, *9*, 243 - 287.

(200) Rogers, D.; Unal, G. G.; Williams, D. J.; Ley, S. V.; Sim, G. A.; Joshi, B. S.; Ravindranath, K. R. The crystal structure of 3-epicaryoptin and the reversal of the currently accepted absolute configuration of clerodin. *J. Chem. Soc., Chem. Commun.* **1979**, 97 - 99.

(201) Valdes, L. J., 3rd. *Salvia divinorum* and the unique diterpene hallucinogen, Salvinorin (*divinorin*) A. *J Psychoactive Drugs* **1994**, *26*, 277 - 283.

(202) Hagiwara, H.; Suka, Y.; Nojima, T.; Hoshi, T.; Suzuki, T. Second-generation synthesis of salvinorin A. *Tetrahedron* **2009**, *65*, 4820 - 4825.

(203) Nozawa, M.; Suka, Y.; Hoshi, T.; Suzuki, T.; Hagiwara, H. Total Synthesis of the Hallucinogenic Neoclerodane Diterpenoid Salvinorin A. *Org. Lett.* **2008**, *10*, 1365 - 1368.

(204) Scheerer, J. R.; Lawrence, J. F.; Wang, G. C.; Evans, D. A. Asymmetric synthesis of salvinorin A, a potent kappa opioid receptor agonist. *J Am Chem Soc* **2007**, *129*, 8968 - 8969.

(205) Lozama, A.; Prisinzano, T. E. Chemical methods for the synthesis and modification of neoclerodane diterpenes. *Bioorg. Med. Chem. Lett.* **2009**, *19*, 5490 - 5495.

(206) Valdes, L. J.; Butler, W. M.; Hatfield, G. M.; Paul, A. G.; Koreeda, M. Divinorin A, a psychotropic terpenoid, and divinorin B from the hallucinogenic Mexican mint, *Salvia divinorum*. *J. Org. Chem.* **1984**, *49*, 4716 - 4720.

(207) Valdes, L. J., 3rd; Diaz, J. L.; Paul, A. G. Ethnopharmacology of ska Maria Pastora (*Salvia divinorum*, Epling and Jativa-M.). *J. Ethnopharmacol.* **1983**, *7*, 287 - 312.

(208) Lange, J. E.; Daniel, J.; Homer, K.; Reed, M. B.; Clapp, J. D. *Salvia divinorum*: effects and use among YouTube users. *Drug Alcohol Depend.* **2010**, *108*, 138 - 140.

(209) Lange, J. E.; Reed, M. B.; Croff, J. M.; Clapp, J. D. College student use of *Salvia divinorum*. *Drug Alcohol Depend.* **2008**, *94*, 263 - 266.

(210) Siebert, D. J. *Salvia divinorum* and salvinorin A: New pharmacologic findings. *J. Ethnopharmacol.* **1994**, *43*, 53 - 56.

(211) Ortega, A.; Blount, J. F.; Manchand, P. S. Salvinorin, a new *trans*-neoclerodane diterpene from *Salvia divinorum* (Labiatae). *J. Chem. Soc., Perkin Trans. 1* **1982**, 2505 - 2508.

(212) Prisinzano, T. E. Psychopharmacology of the hallucinogenic sage *Salvia divinorum*. *Life Sci.* **2005**, *78*, 527 - 531.

(213) Rees, D. C.; Hunter, J. C. Opioid Receptors. In *Comprehensive Medicinal Chemistry*; Emmet, J. C., Ed.; Pergamon Press: New York, 1990, p 805 - 846.

(214) Aldrich, J.; Vigil-Cruz, S. Narcotic Analgesics. In *Burger's Medicinal Chemistry and Drug Discovery*; 6th ed.; Abraham, D. A., Ed.; John Wiley: New York, 2003, p 329 - 441.

(215) Eguchi, M. Recent advances in selective opioid receptor agonists and antagonists. *Med. Res. Rev.* **2004**, *24*, 182 - 212.

(216) Kaczor, A.; Matosiuk, D. Non-peptide opioid receptor ligands - recent advances. Part II. Antagonists. *Curr. Med. Chem.* **2002**, *9*, 1591 - 1603.

(217) Kaczor, A.; Matosiuk, D. Non-peptide opioid receptor ligands - recent advances. Part I. Agonists. *Curr. Med. Chem.* **2002**, *9*, 1567 - 1589.

(218) Lu, Y.; Weltrowska, G.; Lemieux, C.; Chung, N. N.; Schiller, P. W. Stereospecific synthesis of (2S)-2-methyl-3-(2',6'-dimethyl-4'-hydroxyphenyl)propionic acid (Mdp) and its incorporation into an opioid peptide. *Bioorg. Med. Chem. Lett.* **2001**, *11*, 323 - 325.

(219) Surratt, C. K.; Johnson, P. S.; Moriwaki, A.; Seidleck, B. K.; Blaschak, C. J.; Wang, J. B.; Uhl, G. R. Micro Opiate receptor. Charged transmembrane domain amino acids are critical for agonist recognition and intrinsic activity. *J. Biol. Chem.* **1994**, *269*, 20548 - 20553.

(220) Weltrowska, G.; Chung, N. N.; Lemieux, C.; Guo, J.; Lu, Y.; Wilkes, B. C.; Schiller, P. W. "Carba"-Analogues of Fentanyl are Opioid Receptor Agonists. *J. Med. Chem.* **2010**.

(221) Chavkin, C.; Sud, S.; Jin, W.; Stewart, J.; Zjawiony, J. K.; Siebert, D. J.; Toth, B. A.; Hufeisen, S. J.; Roth, B. L. Salvinorin A, an active component of the hallucinogenic sage *Salvia divinorum* is a highly efficacious k-opioid receptor agonist: Structural and functional considerations. *J. Pharmacol. Exp. Ther.* **2004**, *308*, 1197 - 1203.

(222) Iyengar, S.; Kim, H. S.; Wood, P. L. Effects of kappa opiate agonists on neurochemical and neuroendocrine indices: evidence for kappa receptor subtypes. *Life Sci.* **1986**, *39*, 637 - 644.

(223) Rothman, R. B.; Bykov, V.; de Costa, B. R.; Jacobson, A. E.; Rice, K. C.; Brady, L. S. Interaction of endogenous opioid peptides and other drugs with four kappa opioid binding sites in guinea pig brain. *Peptides* **1990**, *11*, 311 - 331.

(224) Zukin, R. S.; Eghbali, M.; Olive, D.; Unterwald, E. M.; Tempel, A. Characterization and visualization of rat and guinea pig brain kappa opioid receptors: evidence for kappa 1 and kappa 2 opioid receptors. *Proc. Natl. Acad. Sci. USA* **1988**, *85*, 4061 - 4065.

(225) Wang, Y.; Tang, K.; Inan, S.; Siebert, D.; Holzgrabe, U.; Lee, D. Y. W.; Huang, P.; Li, J.-G.; Cowan, A.; Liu-Chen, L.-Y. Comparison of pharmacological activities of three distinct k ligands (salvinorin A, TRK-820 and 3FLB) on k opioid receptors in vitro and their antipruritic and antinociceptive activities *in vivo*. *J. Pharmacol. Exp. Ther.* **2005**, *312*, 220 - 230.

(226) Li, J. G.; Benovic, J. L.; Liu-Chen, L. Y. Mechanisms of agonist-induced down-regulation of the human kappa-opioid receptor: internalization is required for down-regulation. *Mol. Pharmacol.* **2000**, *58*, 795 - 801.

(227) Li, J. G.; Luo, L. Y.; Krupnick, J. G.; Benovic, J. L.; Liu-Chen, L. Y. U50,488H-induced internalization of the human kappa opioid receptor involves a beta-arrestin- and dynamin-dependent mechanism. Kappa receptor internalization is not required for mitogen-activated protein kinase activation. *J. Biol. Chem.* **1999**, *274*, 12087 - 12094.

(228) Li, J. G.; Zhang, F.; Jin, X. L.; Liu-Chen, L. Y. Differential regulation of the human kappa opioid receptor by agonists: etorphine and levorphanol reduced dynorphin A- and U50,488H-induced internalization and phosphorylation. *J. Pharmacol. Exp. Ther.* **2003**, *305*, 531 - 540.

(229) Bohn, L. M.; Dykstra, L. A.; Lefkowitz, R. J.; Caron, M. G.; Barak, L. S. Relative opioid efficacy is determined by the complements of the G protein-coupled receptor desensitization machinery. *Mol. Pharmacol.* **2004**, *66*, 106 - 112.

(230) Johnson, M. W.; Maclean, K. A.; Reissig, C. J.; Prisinzano, T. E.; Griffiths, R. R. Human psychopharmacology and dose-effects of salvinorin A, a kappa opioid agonist hallucinogen present in the plant *Salvia divinorum*. *Drug Alcohol Depend.* **2011**, *115*, 150 - 155.

(231) Mendelson, J. E.; Coyle, J. R.; Lopez, J. C.; Baggott, M. J.; Flower, K.; Everhart, E. T.; Munro, T. A.; Galloway, G. P.; Cohen, B. M. Lack of effect of sublingual salvinorin A, a naturally occurring kappa opioid, in humans: a placebo-controlled trial. *Psychopharmacology (Berlin)* **2011**, *214*, 933 - 939.

(232) Hooker, J. M.; Xu, Y.; Schiffer, W.; Shea, C.; Carter, P.; Fowler, J. S. Pharmacokinetics of the potent hallucinogen, salvinorin A in primates parallels the rapid onset and short duration of effects in humans. *Neuroimage* **2008**, *41*, 1044 - 1050.

(233) Schmidt, M. S.; Prisinzano, T. E.; Tidgewell, K.; Harding, W.; Butelman, E. R.; Kreek, M. J.; Murry, D. J. Determination of Salvinorin A in body fluids by high performance liquid chromatography-atmospheric pressure chemical ionization. *J Chromatogr B Analyt Technol Biomed Life Sci* **2005**, *818*, 221 - 225.

(234) Schmidt, M. D.; Schmidt, M. S.; Butelman, E. R.; Harding, W. W.; Tidgewell, K.; Murry, D. J.; Kreek, M. J.; Prisinzano, T. E. Pharmacokinetics of the plant-derived kappa-opioid hallucinogen salvinorin A in nonhuman primates. *Synapse* **2005**, *58*, 208 - 210.

(235) Pichini, S.; Abanades, S.; Farre, M.; Pellegrini, M.; Marchei, E.; Pacifici, R.; Torre Rde, L.; Zuccaro, P. Quantification of the plant-derived hallucinogen Salvinorin A in conventional and non-conventional biological fluids by gas chromatography/mass spectrometry after *Salvia divinorum* smoking. *Rapid Commun Mass Spectrom* **2005**, *19*, 1649 - 1656.

(236) Tsujikawa, K.; Kuwayama, K.; Miyaguchi, H.; Kanamori, T.; Iwata, Y. T.; Inoue, H. *In vitro* stability and metabolism of salvinorin A in rat plasma. *Xenobiotica* **2009**, *39*, 391 - 398.

(237) Teksin, Z. S.; Lee, I. J.; Nemieboka, N. N.; Othman, A. A.; Upreti, V. V.; Hassan, H. E.; Syed, S. S.; Prisinzano, T. E.; Eddington, N. D. Evaluation of the transport, *in vitro* metabolism and pharmacokinetics of Salvinorin A, a potent hallucinogen. *Eur. J. Pharm. Biopharm.* **2009**, *72*, 471 - 477.

(238) Coffman, B. L.; King, C. D.; Rios, G. R.; Tephly, T. R. The glucuronidation of opioids, other xenobiotics, and androgens by human UGT2B7Y(268) and UGT2B7H(268). *Drug Metab. Dispos.* **1998**, *26*, 73 - 77.

(239) Coffman, B. L.; Rios, G. R.; King, C. D.; Tephly, T. R. Human UGT2B7 catalyzes morphine glucuronidation. *Drug Metab. Dispos.* **1997**, *25*, 1 - 4.

(240) King, C. D.; Green, M. D.; Rios, G. R.; Coffman, B. L.; Owens, I. S.; Bishop, W. P.; Tephly, T. R. The glucuronidation of exogenous and endogenous compounds by stably expressed rat and human UDP-glucuronosyltransferase 1.1. *Arch. Biochem. Biophys.* **1996**, *332*, 92 - 100.

(241) Mowry, M.; Mosher, M.; Briner, W. Acute physiologic and chronic histologic changes in rats and mice exposed to the unique hallucinogen salvinorin A. *J. Psychoactive Drugs* **2003**, *35*, 379 - 382.

(242) Butelman, E. R.; Mandau, M.; Tidgewell, K.; Prisinzano, T. E.; Yuferov, V.; Kreek, M. J. Effects of salvinorin A, a k-opioid hallucinogen, on a neuroendocrine biomarker assay in nonhuman primates with high k-receptor homology to humans. *J. Pharmacol. Exp. Ther.* **2007**, *320*, 300 - 306.

(243) Butelman, E. R.; Prisinzano, T. E.; Deng, H.; Rus, S.; Kreek, M. J. Unconditioned behavioral effects of the powerful k-opioid hallucinogen salvinorin A in nonhuman primates: fast onset and entry into cerebrospinal fluid. *J. Pharmacol. Exp. Ther.* **2009**, *328*, 588 - 597.

(244) Butelman, E. R.; Rus, S.; Prisinzano, T. E.; Kreek, M. J. The discriminative effects of the kappa-opioid hallucinogen salvinorin A in nonhuman primates: dissociation from classic hallucinogen effects. *Psychopharmacology (Berlin)* **2010**, *210*, 253 - 262.

(245) Butelman, E. R.; Harris, T. J.; Kreek, M. J. The plant-derived hallucinogen, salvinorin A, produces kappa-opioid agonist-like discriminative effects in rhesus monkeys. *Psychopharmacology (Berlin)* **2004**, *172*, 220 - 224.

(246) Willmore-Fordham, C. B.; Krall, D. M.; McCurdy, C. R.; Kinder, D. H. The hallucinogen derived from *Salvia divinorum*, salvinorin A, has k-opioid agonist discriminative stimulus effects in rats. *Neuropharmacology* **2007**, *53*, 481 - 486.

(247) Baker, L. E.; Panos, J. J.; Killinger, B. A.; Peet, M. M.; Bell, L. M.; Haliw, L. A.; Walker, S. L. Comparison of the discriminative stimulus effects of salvinorin A and its derivatives to U69,593 and U50,488 in rats. *Psychopharmacology (Berlin)* **2009**, *203*, 203 - 211.

(248) Li, J. X.; Rice, K. C.; France, C. P. Discriminative stimulus effects of 1-(2,5-dimethoxy-4-methylphenyl)-2-aminopropane in rhesus monkeys. *J. Pharmacol. Exp. Ther.* **2008**, *324*, 827 - 833.

(249) Killinger, B. A.; Peet, M. M.; Baker, L. E. Salvinorin A fails to substitute for the discriminative stimulus effects of LSD or ketamine in Sprague-Dawley rats. *Pharmacol. Biochem. Behav.* **2010**, *96*, 260 - 265.

(250) McCurdy, C. R.; Sufka, K. J.; Smith, G. H.; Warnick, J. E.; Nieto, M. J. Antinociceptive profile of salvinorin A, a structurally unique kappa opioid receptor agonist. *Pharmacol. Biochem. Behav.* **2006**, *83*, 109 - 113.

(251) John, T. F.; French, L. G.; Erlichman, J. S. The antinociceptive effect of Salvinorin A in mice. *Eur. J. Pharmacol.* **2006**, *545*, 129 - 133.

(252) Capasso, R.; Borrelli, F.; Capasso, F.; Siebert, D. J.; Stewart, D. J.; Zjawiony, J. K.; Izzo, A. A. The hallucinogenic herb *Salvia divinorum* and its active ingredient salvinorin A inhibit enteric cholinergic transmission in the guinea-pig ileum. *Neurogastroenterol. Motil.* **2006**, *18*, 69 - 75.

(253) Capasso, R.; Borrelli, F.; Zjawiony, J.; Kutrzeba, L.; Aviello, G.; Sarnelli, G.; Capasso, F.; Izzo, A. A. The hallucinogenic herb *Salvia divinorum* and its active ingredient salvinorin a reduce inflammation-induced hypermotility in mice. *Neurogastroenterol. Motil.* **2008**, *20*, 142 - 148.

(254) Morani, A. S.; Kivell, B.; Prisinzano, T. E.; Schenk, S. Effect of kappa-opioid receptor agonists U69593, U50488H, spiradoline and salvinorin A on cocaine-induced drug-seeking in rats. *Pharmacol. Biochem. Behav.* **2009**, *94*, 244 - 249.

(255) Chartoff, E. H.; Potter, D.; Damez-Werno, D.; Cohen, B. M.; Carlezon, W. A., Jr. Exposure to the Selective k-Opioid Receptor Agonist Salvinorin A Modulates the Behavioral and Molecular Effects of Cocaine in Rats. *Neuropsychopharmacology* **2008**, *33*, 2676 - 2687.

(256) Shippenberg, T. S.; Herz, A. Place preference conditioning reveals the involvement of D_1-dopamine receptors in the motivational properties of mu- and kappa-opioid agonists. *Brain Res.* **1987**, *436*, 169 - 172.

(257) Detke, M. J.; Rickels, M.; Lucki, I. Active behaviors in the rat forced swimming test differentially produced by serotonergic and noradrenergic antidepressants. *Psychopharmacology (Berlin)* **1995**, *121*, 66 - 72.

(258) Zhang, Y.; Butelman, E. R.; Schlussman, S. D.; Ho, A.; Kreek, M. J. Effects of the plant-derived hallucinogen salvinorin A on basal dopamine levels in the caudate putamen and in a conditioned place aversion assay in mice: agonist actions at kappa opioid receptors. *Psychopharmacology (Berlin)* **2005**, *179*, 551 - 558.

(259) Ebner, S. R.; Roitman, M. F.; Potter, D. N.; Rachlin, A. B.; Chartoff, E. H. Depressive-like effects of the kappa opioid receptor agonist salvinorin A are associated with decreased phasic dopamine release in the nucleus accumbens. *Psychopharmacology (Berlin)* **2010**, *210*, 241 - 252.

(260) Fantegrossi, W. E.; Kugle, K. M.; Valdes, L. J. I. I. I.; Koreeda, M.; Woods, J. H. Kappa-opioid receptor-mediated effects of the plant-derived hallucinogen, salvinorin A, on inverted screen performance in the mouse. *Behav. Pharmacol.* **2005**, *16*, 627 - 633.

(261) Braida, D.; Limonta, V.; Pegorini, S.; Zani, A.; Guerini-Rocco, C.; Gori, E.; Sala, M. Hallucinatory and rewarding effect of salvinorin A in zebrafish: kappa-opioid and CB_1-cannabinoid receptor involvement. *Psychopharmacology (Berlin)* **2007**, *190*, 441 - 448.

(262) Braida, D.; Limonta, V.; Capurro, V.; Fadda, P.; Rubino, T.; Mascia, P.; Zani, A.; Gori, E.; Fratta, W.; Parolaro, D.; Sala, M. Involvement of kappa-opioid and endocannabinoid system on Salvinorin A-induced reward. *Biol. Psychiatry* **2008**, *63*, 286 - 292.

(263) Braida, D.; Capurro, V.; Zani, A.; Rubino, T.; Vigano, D.; Parolaro, D.; Sala, M. Potential anxiolytic- and antidepressant-like effects of salvinorin A, the main active ingredient of *Salvia divinorum*, in rodents. *Br. J. Pharmacol.* **2009**, *157*, 844 - 853.

(264) Walentiny, D. M.; Vann, R. E.; Warner, J. A.; King, L. S.; Seltzman, H. H.; Navarro, H. A.; Twine, C. E., Jr.; Thomas, B. F.; Gilliam, A. F.; Gilmour, B. P.; Carroll, F. I.; Wiley, J. L. Kappa opioid mediation of cannabinoid effects of the potent hallucinogen, salvinorin A, in rodents. *Psychopharmacology (Berlin)* **2010**, *210*, 275 - 284.

(265) Kane, B. E.; McCurdy, C. R.; Ferguson, D. M. Toward a Structure-Based Model of Salvinorin A Recognition of the k-Opioid Receptor. *J. Med. Chem.* **2008**, *51*, 1824 - 1830.

(266) Kane, B. E.; Nieto, M. J.; McCurdy, C. R.; Ferguson, D. M. A unique binding epitope for salvinorin A, a non-nitrogenous kappa opioid receptor agonist. *Febs J.* **2006**, *273*, 1966 - 1974.

(267) Vortherms, T. A.; Mosier, P. D.; Westkaemper, R. B.; Roth, B. L. Differential helical orientations among related G protein-coupled receptors provide a novel mechanism for selectivity. studies with Salvinorin A and the k-opioid receptor. *J. Biol. Chem.* **2007**, *282*, 3146 - 3156.

(268) Yan, F.; Bikbulatov, R. V.; Mocanu, V.; Dicheva, N.; Parker, C. E.; Wetsel, W. C.; Mosier, P. D.; Westkaemper, R. B.; Allen, J. A.; Zjawiony, J. K.; Roth, B. L. Structure-Based Design, Synthesis, and Biochemical and Pharmacological Characterization of Novel Salvinorin A Analogues as Active State Probes of the k-Opioid Receptor. *Biochemistry* **2009**, *48*, 6898 - 6908.

(269) Yan, F.; Mosier Philip, D.; Westkaemper Richard, B.; Stewart, J.; Zjawiony Jordan, K.; Vortherms Timothy, A.; Sheffler Douglas, J.; Roth Bryan, L. Identification of the molecular mechanisms by which the diterpenoid salvinorin A binds to kappa-opioid receptors. *Biochemistry* **2005**, *44*, 8643 - 8651.

(270) Cunningham, C. W.; Rothman, R. B.; Prisinzano, T. E. Neuropharmacology of the Naturally Occurring k-Opioid Hallucinogen Salvinorin A. *Pharmacol Rev* **2011**, *63*, 316 - 347.

(271) Munro, T. A.; Duncan, K. K.; Xu, W.; Wang, Y.; Liu-Chen, L.-Y.; Carlezon, W. A.; Cohen, B. M.; Beguin, C. Standard protecting groups create potent and selective k opioids: Salvinorin B alkoxymethyl ethers. *Bioorg. Med. Chem.* **2008**, *16*, 1279 - 1286.

(272) Holden, K. G.; Tidgewell, K.; Marquam, A.; Rothman, R. B.; Navarro, H.; Prisinzano, T. E. Synthetic studies of neoclerodane diterpenes from *Salvia divinorum*: Exploration of the 1-position. *Bioorg. Med. Chem. Lett.* **2007**, *17*, 6111 - 6115.

(273) Valdes, L. J.; Chang, H.-M.; Visger, D. C.; Koreeda, M. Salvinorin C, a New Neoclerodane Diterpene from a Bioactive Fraction of the Hallucinogenic Mexican Mint *Salvia divinorum*. *Org. Lett.* **2001**, *3*, 3935 - 3937.

(274) Harding, W. W.; Tidgewell, K.; Byrd, N.; Cobb, H.; Dersch, C. M.; Butelman, E. R.; Rothman, R. B.; Prisinzano, T. E. Neoclerodane Diterpenes as a Novel Scaffold for micro Opioid Receptor Ligands. *J. Med. Chem.* **2005**, *48*, 4765 - 4771.

(275) Lee, D. Y. W.; Karnati, V. V. R.; He, M.; Liu-Chen, L.-Y.; Kondaveti, L.; Ma, Z.; Wang, Y.; Chen, Y.; Beguin, C.; Carlezon, J. W. A.; Cohen, B. Synthesis and *in vitro* pharmacological studies of new C(2) modified salvinorin A analogues. *Bioorg. Med. Chem. Lett.* **2005**, *15*, 3744 - 3747.

(276) Tidgewell, K.; Harding, W. W.; Schmidt, M.; Holden, K. G.; Murry, D. J.; Prisinzano, T. E. A facile method for the preparation of deuterium labeled salvinorin A: synthesis of [2,2,2-2H3]-salvinorin A. *Bioorg. Med. Chem. Lett.* **2004**, *14*, 5099 - 5102.

(277) Koreeda, M.; Brown, L.; Valdes, L. J., III. The absolute stereochemistry of salvinorins. *Chem. Lett.* **1990**, 2015 - 2018.

(278) Munro, T. A.; Goetchius, G. W.; Roth, B. L.; Vortherms, T. A.; Rizzacasa, M. A. Autoxidation of salvinorin A under basic conditions. *J. Org. Chem.* **2005**, *70*, 10057 - 10061.

(279) Bikbulatov, R. V.; Stewart, J.; Jin, W.; Yan, F.; Roth, B. L.; Ferreira, D.; Zjawiony, J. K. Short synthesis of a novel class of salvinorin A analogs with hemiacetalic structure. *Tetrahedron Lett.* **2008**, *49*, 937 - 940.

(280) Bikbulatov, R. V.; Yan, F.; Roth, B. L.; Zjawiony, J. K. Convenient synthesis and in vitro pharmacological activity of 2-thioanalogs of salvinorins A and B. *Bioorg. Med. Chem. Lett.* **2007**, *17*, 2229 - 2232.

(281) Munro, T. A.; Rizzacasa, M. A.; Roth, B. L.; Toth, B. A.; Yan, F. Studies toward the Pharmacophore of Salvinorin A, a Potent Kappa Opioid Receptor Agonist. *J. Med. Chem.* **2005**, *48*, 345 - 348.

(282) Tidgewell, K.; Groer, C. E.; Harding, W. W.; Lozama, A.; Schmidt, M.; Marquam, A.; Hiemstra, J.; Partilla, J. S.; Dersch, C. M.; Rothman, R. B.; Bohn, L. M.; Prisinzano, T. E. Herkinorin Analogues with Differential beta -Arrestin-2 Interactions. *J. Med. Chem.* **2008**, *51*, 2421 - 2431.

(283) Tidgewell, K.; Harding, W. W.; Lozama, A.; Cobb, H.; Shah, K.; Kannan, P.; Dersch, C. M.; Parrish, D.; Deschamps, J. R.; Rothman, R. B.; Prisinzano, T. E. Synthesis of Salvinorin A Analogues as Opioid Receptor Probes. *J. Nat. Prod.* **2006**, *69*, 914 - 918.

(284) Lee, D. Y. W.; He, M.; Kondaveti, L.; Liu-Chen, L.-Y.; Ma, Z.; Wang, Y.; Chen, Y.; Li, J.-G.; Beguin, C.; Carlezon, W. A.; Cohen, B. Synthesis and *in vitro* pharmacological studies of C(4) modified salvinorin A analogues. *Bioorg. Med. Chem. Lett.* **2005**, *15*, 4169 - 4173.

(285) Lee, D. Y. W.; He, M.; Liu-Chen, L.-Y.; Wang, Y.; Li, J.-G.; Xu, W.; Ma, Z.; Carlezon, W. A.; Cohen, B. Synthesis and *in vitro* pharmacological studies of new C(4)-modified salvinorin A analogs. *Bioorg. Med. Chem. Lett.* **2006**, *16*, 5498 - 5502.

(286) Béguin, C.; Duncan Katharine, K.; Munro Thomas, A.; Ho Douglas, M.; Xu, W.; Liu-Chen, L.-Y.; Carlezon William, A., Jr.; Cohen Bruce, M. Modification of the furan ring of salvinorin A: identification of a selective partial agonist at the kappa opioid receptor. *Bioorg. Med. Chem.* **2009**, *17*, 1370 - 1380.

(287) Harding, W. W.; Schmidt, M.; Tidgewell, K.; Kannan, P.; Holden, K. G.; Dersch, C. M.; Rothman, R. B.; Prisinzano, T. E. Synthetic studies of neoclerodane diterpenes from *Salvia divinorum*: Selective modification of the furan ring. *Bioorg. Med. Chem. Lett.* **2006**, *16*, 3170 - 3174.

(288) Shirota, O.; Nagamatsu, K.; Sekita, S. Neo-clerodane diterpenes from the hallucinogenic sage *Salvia divinorum*. *J. Nat. Prod.* **2006**, *69*, 1782 - 1786.

(289) Simpson, D. S.; Katavic, P. L.; Lozama, A.; Harding, W. W.; Parrish, D.; Deschamps, J. R.; Dersch, C. M.; Partilla, J. S.; Rothman, R. B.; Navarro, H.; Prisinzano, T. E. Synthetic Studies of Neoclerodane Diterpenes from *Salvia divinorum*: Preparation and Opioid Receptor Activity of Salvinicin Analogues. *J. Med. Chem.* **2007**, *50*, 3596 - 3603.

(290) Harding, W. W.; Schmidt, M.; Tidgewell, K.; Kannan, P.; Holden, K. G.; Gilmour, B.; Navarro, H.; Rothman, R. B.; Prisinzano, T. E. Synthetic Studies of Neoclerodane Diterpenes from *Salvia divinorum*: Semisynthesis of Salvinicins A and B and Other Chemical Transformations of Salvinorin A. *J. Nat. Prod.* **2006**, *69*, 107 - 112.

(291) Harding, W. W.; Tidgewell, K.; Schmidt, M.; Shah, K.; Dersch, C. M.; Snyder, J.; Parrish, D.; Deschamps, J. R.; Rothman, R. B.; Prisinzano, T. E. Salvinicins A and B, new neoclerodane diterpenes from *Salvia divinorum*. *Org. Lett.* **2005**, *7*, 3017 - 3020.

(292) Simpson, D. S.; Lovell, K. M.; Lozama, A.; Han, N.; Day, V. W.; Dersch, C. M.; Rothman, R. B.; Prisinzano, T. E. Synthetic studies of neoclerodane diterpenes from *Salvia divinorum*: role of the furan in affinity for opioid receptors. *Org. Biomol. Chem.* **2009**, *7*, 3748 - 3756.

(293) Yang, L.; Xu, W.; Chen, F.; Liu-Chen, L.-Y.; Ma, Z.; Lee, D. Y. W. Synthesis and biological evaluation of C-12 triazole and oxadiazole analogs of salvinorin A. *Bioorg. Med. Chem. Lett.* **2009**, *19*, 1301 - 1304.

(294) Lozama, A.; Cunningham, C. W.; Caspers, M. J.; Douglas, J. T.; Dersch, C. M.; Rothman, R. B.; Prisinzano, T. E. Opioid receptor probes derived from cycloaddition of the hallucinogen natural product salvinorin A. *J. Nat. Prod.* **2011**, *74*, 718 - 726.

(295) Dalvie, D. K.; Kalgutkar, A. S.; Khojasteh-Bakht, S. C.; Obach, R. S.; O'Donnell, J. P. Biotransformation reactions of five-membered aromatic heterocyclic rings. *Chem. Res. Toxicol.* **2002**, *15*, 269 - 299.

(296) Peterson, L. A. Electrophilic intermediates produced by bioactivation of furan. *Drug Metab. Rev.* **2006**, *38*, 615 - 626.

(297) Zhou, S.; Koh, H. L.; Gao, Y.; Gong, Z. Y.; Lee, E. J. Herbal bioactivation: the good, the bad and the ugly. *Life Sci.* **2004**, *74*, 935 - 968.

(298) Kouzi, S. A.; McMurtry, R. J.; Nelson, S. D. Hepatotoxicity of Germander (*Teucrium chamaedrys* L.) and One of Its Constituent Neoclerodane Diterpenes Teucrin A in the Mouse. *Chem. Res. Toxicol.* **1994**, *7*, 850 - 856.

(299) Druckova, A.; Marnett, L. J. Characterization of the amino acid adducts of the enedial derivative of teucrin A. *Chem. Res. Toxicol.* **2006**, *19*, 1330 - 1340.

(300) Druckova, A.; Mernaugh, R. L.; Ham, A. J.; Marnett, L. J. Identification of the protein targets of the reactive metabolite of teucrin A *in vivo* in the rat. *Chem. Res. Toxicol.* **2007**, *20*, 1393 - 1408.

(301) Guengerich, F. P. Cytochrome P450s and other enzymes in drug metabolism and toxicity. *Aaps J.* **2006**, *8*, E101 - 111.

(302) Castro, C. A.; Hogan, J. B.; Benson, K. A.; Shehata, C. W.; Landauer, M. R. Behavioral effects of vehicles: DMSO, ethanol, Tween-20, Tween-80, and emulphor-620. *Pharmacol. Biochem. Behav.* **1995**, *50*, 521 - 526.

(303) Fossum, E. N.; Lisowski, M. J.; Macey, T. A.; Ingram, S. L.; Morgan, M. M. Microinjection of the vehicle dimethyl sulfoxide (DMSO) into the periaqueductal gray modulates morphine antinociception. *Brain Res.* **2008**, *1204*, 53 - 58.

(304) Haigler, H. J.; Spring, D. D. DMSO (dimethyl sulfoxide), morphine and analgesia. *Life Sci.* **1981**, *29*, 1545 - 1553.

(305) Gintzler, A. R.; Scalisi, J. A. Opioid-mediated acute responses to alcohol: ethanol potentiates opioid actions on the guinea pig ileum. *Brain Res.* **1983**, *269*, 391 - 394.

(306) Park, K. Efficient oral delivery of paclitaxel using cyclodextrin complexes. *J. Control Release* **2010**, *145*, 1.

(307) Hamada, H.; Ishihara, K.; Masuoka, N.; Mikuni, K.; Nakajima, N. Enhancement of water-solubility and bioactivity of paclitaxel using modified cyclodextrins. *J. Biosci. Bioeng.* **2006**, *102*, 369 - 371.

(308) Results not Published.

(309) Prokopcova, H.; Kappe, C. O. Copper-catalyzed C-C coupling of thiol esters and boronic acids under aerobic conditions. *Angew. Chem. Int. Ed.* **2008**, *47*, 3674 - 3676.

(310) Liebeskind, L. S.; Srogl, J. Thiol Ester-Boronic Acid Coupling. A Mechanistically Unprecedented and General Ketone Synthesis. *J Am Chem Soc* **2000**, *122*, 11260 - 11261.

(311) Yang, H.; Li, H.; Wittenberg, R.; Egi, M.; Huang, W.; Liebeskind, L. S. Ambient temperature synthesis of high enantiopurity N-protected peptidyl ketones by peptidyl thiol ester-boronic acid cross-coupling. *J Am Chem Soc* **2007**, *129*, 1132 - 1140.

(312) Yang, H.; Liebeskind, L. S. A concise and scalable synthesis of high enantiopurity (-)-D-erythro-sphingosine using peptidyl thiol ester-boronic acid cross-coupling. *Org. Lett.* **2007**, *9*, 2993 - 2995.

(313) Pace, P.; Spieser, S. A.; Summa, V. 4-Hydroxy-5-pyrrolinone-3-carboxamide HIV-1 integrase inhibitors. *Bioorg. Med. Chem. Lett.* **2008**, *18*, 3865 - 3869.

(314) Rao, H. S.; Jothilingam, S. Facile microwave-mediated transformations of 2-butene-1,4-diones and 2-butyne-1,4-diones to furan derivatives. *J. Org. Chem.* **2003**, *68*, 5392 - 5394.

(315) Frankowski, K. J.; Ghosh, P.; Setola, V.; Tran, T. B.; Roth, B. L.; Aube, J. N-Alkyl-octahydroisoquinolin-1-one-8-carboxamides: a Novel Class of Selective, Nonbasic, Nitrogen-Containing kappa-Opioid Receptor Ligands. *ACS Med. Chem. Lett.* **2010**, *1*, 189 - 193.

(316) Wentland, M. P.; Lou, R.; Ye, Y.; Cohen, D. J.; Richardson, G. P.; Bidlack, J. M. 8-Carboxamidocyclazocine analogues: redefining the structure-activity relationships of 2,6-methano-3-benzazocines. *Bioorg. Med. Chem. Lett.* **2001**, *11*, 623 - 626.

(317) Wentland, M. P.; Lou, R.; Lu, Q.; Bu, Y.; VanAlstine, M. A.; Cohen, D. J.; Bidlack, J. M. Syntheses and opioid receptor binding properties of carboxamido-substituted opioids. *Bioorg. Med. Chem. Lett.* **2009**, *19*, 203 - 208.

(318) Harrison, C.; Traynor, J. R. The [^{35}S]GTPgammaS binding assay: approaches and applications in pharmacology. *Life Sci.* **2003**, *74*, 489 - 508.

(319) Liu, A. M.; Ho, M. K.; Wong, C. S.; Chan, J. H.; Pau, A. H.; Wong, Y. H. Galpha(16/z) chimeras efficiently link a wide range of G protein-coupled receptors to calcium mobilization. *J Biomol Screen* **2003**, *8*, 39 - 49.

(320) Coward, P.; Chan, S. D.; Wada, H. G.; Humphries, G. M.; Conklin, B. R. Chimeric G proteins allow a high-throughput signaling assay of Gi-coupled receptors. *Anal. Biochem.* **1999**, *270*, 242 - 248.

(321) Singh, N.; Cheve, G.; Ferguson, D. M.; McCurdy, C. R. A combined ligand-based and target-based drug design approach for G-protein coupled receptors: application to salvinorin A, a selective kappa opioid receptor agonist. *J. Comput. Aided Mol. Des.* **2006**, 471–493.

(322) Santos, N. C.; Figueira-Coelho, J.; Martins-Silva, J.; Saldanha, C. Multidisciplinary utilization of dimethyl sulfoxide: pharmacological, cellular, and molecular aspects. *Biochem. Pharmacol.* **2003**, *65*, 1035 - 1041.

(323) Okimoto, K.; Rajewski, R. A.; Stella, V. J. Release of testosterone from an osmotic pump tablet utilizing $(SBE)_{7m}$-beta-cyclodextrin as both a solubilizing and an osmotic pump agent. *J. Control Release* **1999**, *58*, 29 - 38.

(324) Bouquet, W.; Ceelen, W.; Fritzinger, B.; Pattyn, P.; Peeters, M.; Remon, J. P.; Vervaet, C. Paclitaxel/beta-cyclodextrin complexes for hyperthermic peritoneal perfusion - formulation and stability. *Eur. J. Pharm. Biopharm.* **2007**, *66*, 391 - 397.

(325) Uekama, K.; Hirayama, F.; Irie, T. Cyclodextrin Drug Carrier Systems. *Chem. Rev.* **1998**, *98*, 2045 - 2076.

(326) Stella, V. J.; Rao, V. M.; Zannou, E. A.; Zia, V. V. Mechanisms of drug release from cyclodextrin complexes. *Adv. Drug Deliv. Rev.* **1999**, *36*, 3 - 16.

(327) Ma, D. Q.; Rajewski, R. A.; Vander Velde, D.; Stella, V. J. Comparative effects of $(SBE)_{7m}$-beta-CD and HP-beta-CD on the stability of two anti-neoplastic agents, melphalan and carmustine. *J. Pharm. Sci.* **2000**, *89*, 275 - 287.

(328) Johnson, M. D.; Hoesterey, B. L.; Anderson, B. D. Solubilization of a tripeptide HIV protease inhibitor using a combination of ionization and complexation with chemically modified cyclodextrins. *J. Pharm. Sci.* **1994**, *83*, 1142 - 1146.

(329) Zia, V.; Rajewski, R. A.; Bornancini, E. R.; Luna, E. A.; Stella, V. J. Effect of alkyl chain length and degree of substitution on the complexation of sulfoalkyl ether beta-cyclodextrins with steroids. *J. Pharm. Sci.* **1997**, *86*, 220 - 224.

(330) Stella, V. J.; Lee, H. K.; Thompson, D. O. The Effect of SBE_4-beta-CD on i.v. Methylprednisolone Pharmacokinetics in Rats: Comparison to a Co-Solvent Solution and Two Water-Soluble Prodrugs *Int. J. Pharm.* **1995**, *120*, 197 - 204.

(331) Rajewski, R. A.; Traiger, G.; Bresnahan, J.; Jaberaboansari, P.; Stella, V. J.; Thompson, D. O. Preliminary safety evaluation of parenterally administered sulfoalkyl ether beta-cyclodextrin derivatives. *J. Pharm. Sci.* **1995**, *84*, 927 - 932.

(332) Okimoto, K.; Rajewski, R. A.; Uekama, K.; Jona, J. A.; Stella, V. J. The interaction of charged and uncharged drugs with neutral (HP-beta-CD) and anionically charged (SBE7-beta-CD) beta-cyclodextrins. *Pharm. Res.* **1996**, *13*, 256 - 264.

(333) Okimoto, K.; Miyake, M.; Ohnishi, N.; Rajewski, R. A.; Stella, V. J.; Irie, T.; Uekama, K. Design and evaluation of an osmotic pump tablet (OPT) for prednisolone, a poorly water soluble drug, using $(SBE)_{7m}$-beta-CD. *Pharm. Res.* **1998**, *15*, 1562 - 1568.

(334) McIntosh, M. P.; Schwarting, N.; Rajewski, R. A. *In vitro* and *in vivo* evaluation of a sulfobutyl ether beta-cyclodextrin enabled etomidate formulation. *J. Pharm. Sci.* **2004**, *93*, 2585 - 2594.

APPENDIX A: ^{1}H NMR SPECTRA

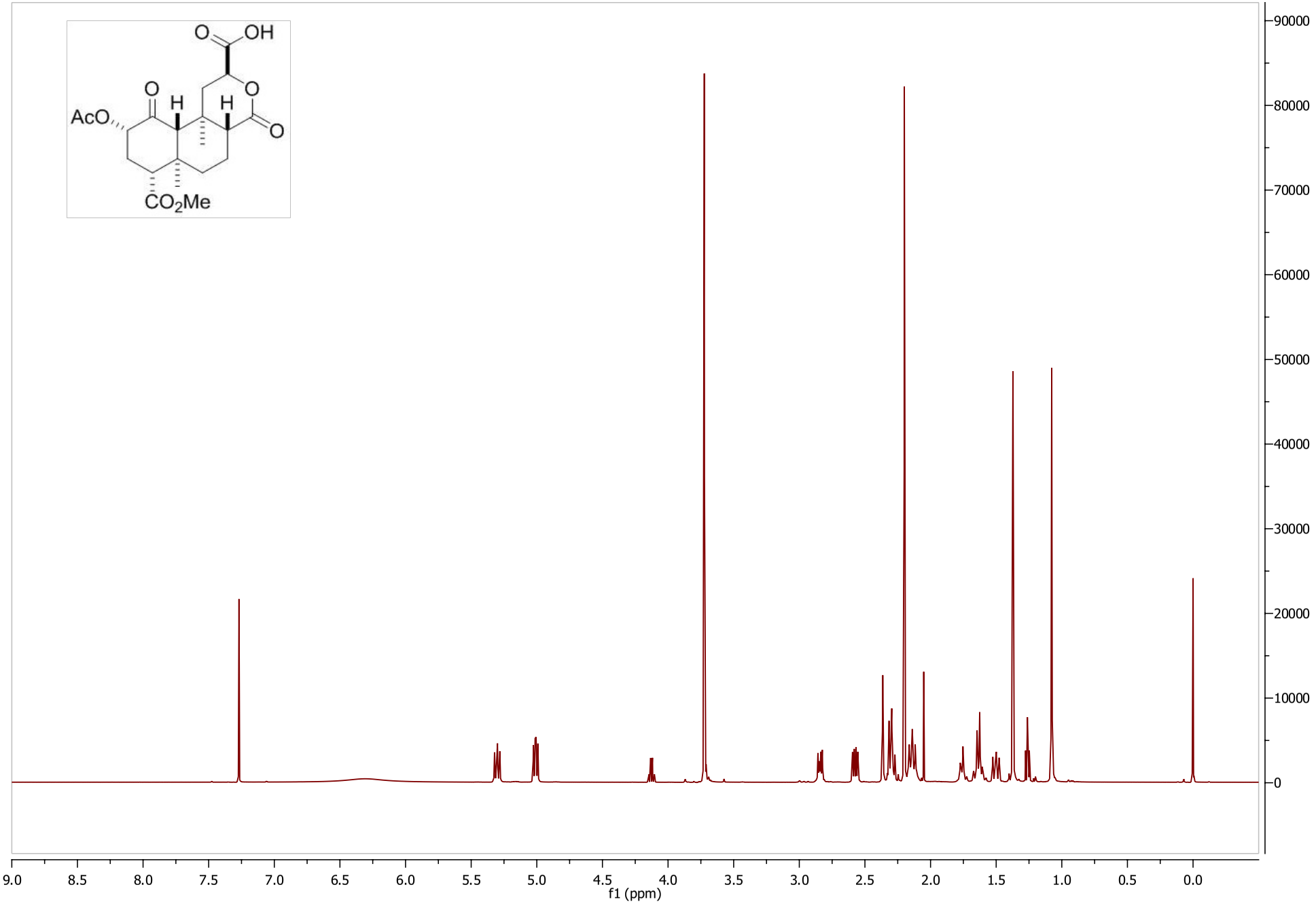
O
OH
O
H
H
O
AcO
O
CO2Me
90000
80000
70000
60000
50000
40000
30000
20000
10000
0
9.0
8.5
8.0
7.5
7.0
6.5
6.0
5.5
5.0
4.5
4.0
3.5
3.0
2.5
2.0
1.5
1.0
0.5
0.0
f1 (ppm)

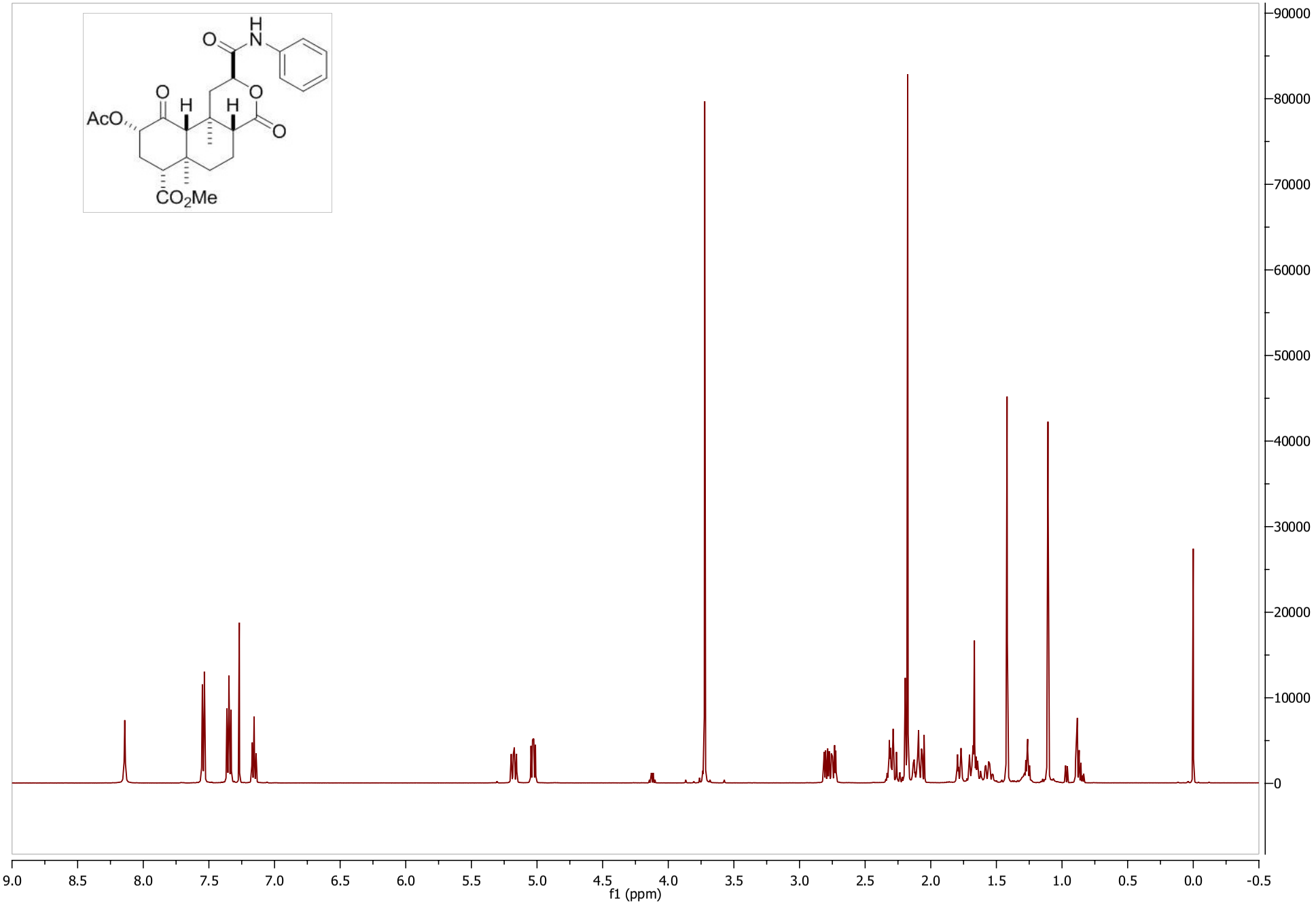
AcO
O
H
H
O
O
O
H
N
O
CO2Me
90000
80000
70000
60000
50000
40000
30000
20000
10000
0
9.0
8.5
8.0
7.5
7.0
6.5
6.0
5.5
5.0
4.5
4.0
3.5
3.0
2.5
2.0
1.5
1.0
0.5
0.0
-0.5
f1 (ppm)

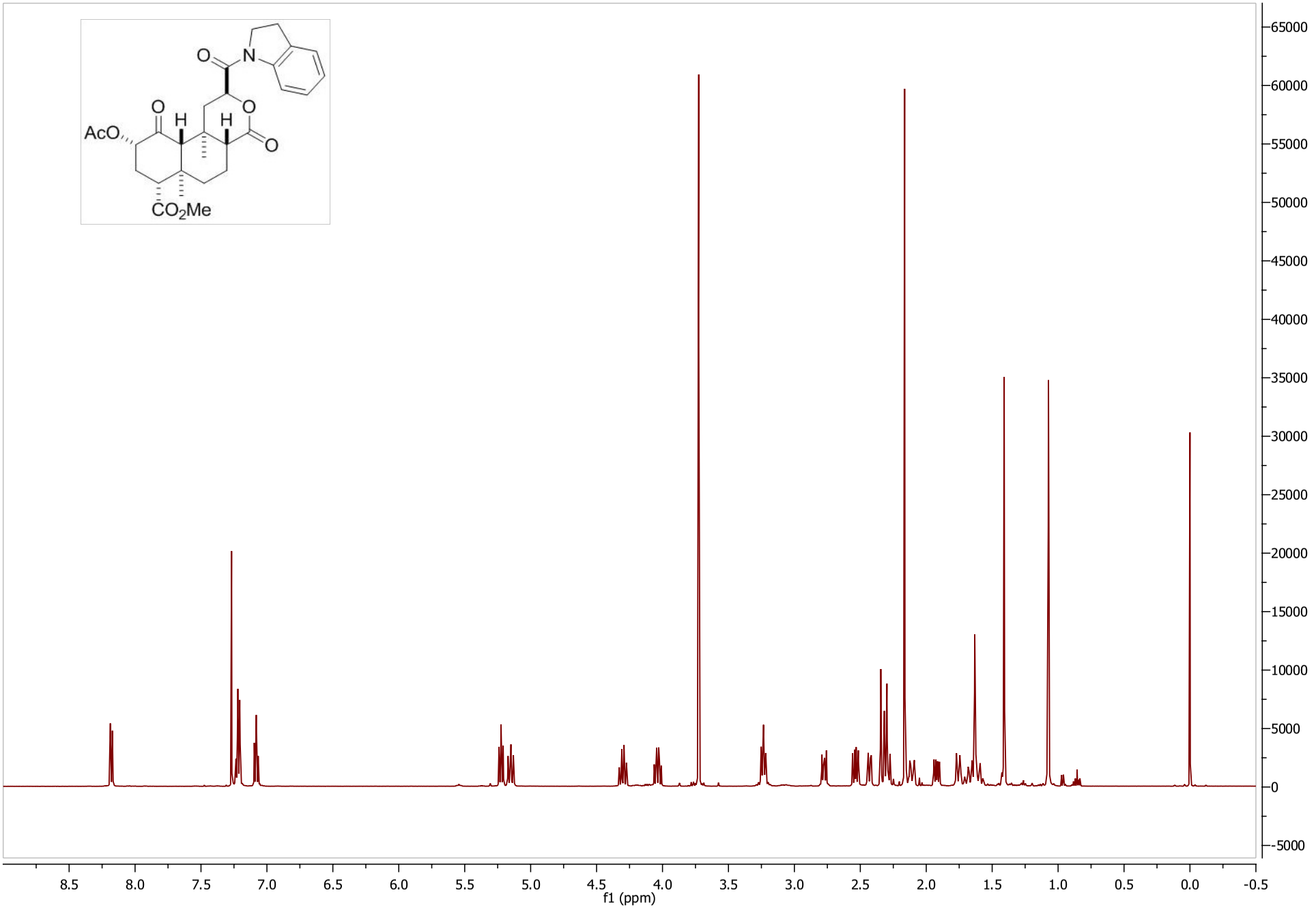
O
N
O
O
H
H
AcO
O
CO2Me
65000
60000
55000
50000
45000
40000
35000
30000
25000
20000
15000
10000
5000
0
-5000
8.5
8.0
7.5
7.0
6.5
6.0
5.5
5.0
4.5
4.0
3.5
3.0
2.5
2.0
1.5
1.0
0.5
0.0
-0.5
f1 (ppm)

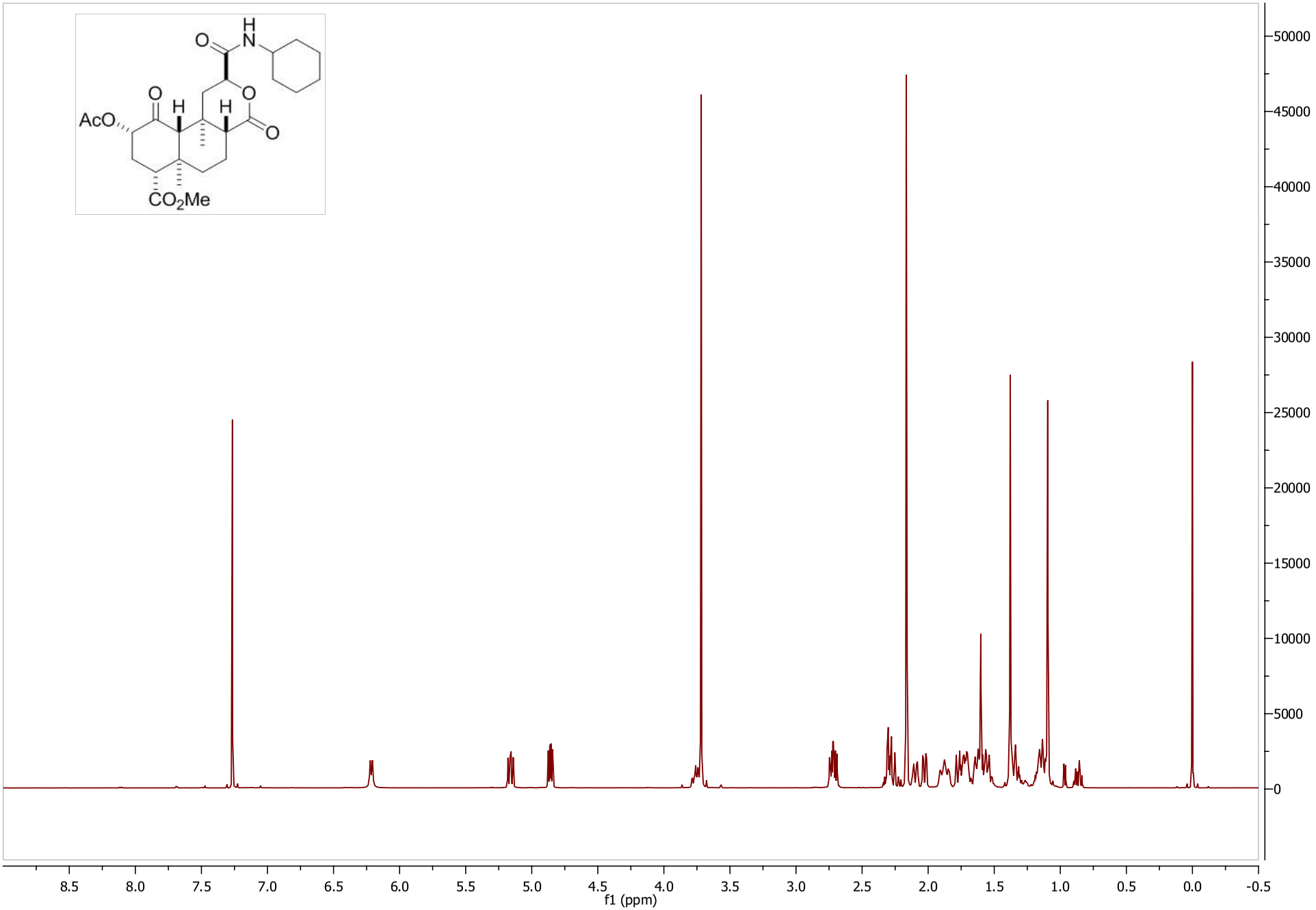
H
N
O
O
H
H
O
AcO
O
CO2Me
50000
45000
40000
35000
30000
25000
20000
15000
10000
5000
0
8.5
8.0
7.5
7.0
6.5
6.0
5.5
5.0
4.5
4.0
3.5
3.0
2.5
2.0
1.5
1.0
0.5
0.0
-0.5
f1 (ppm)

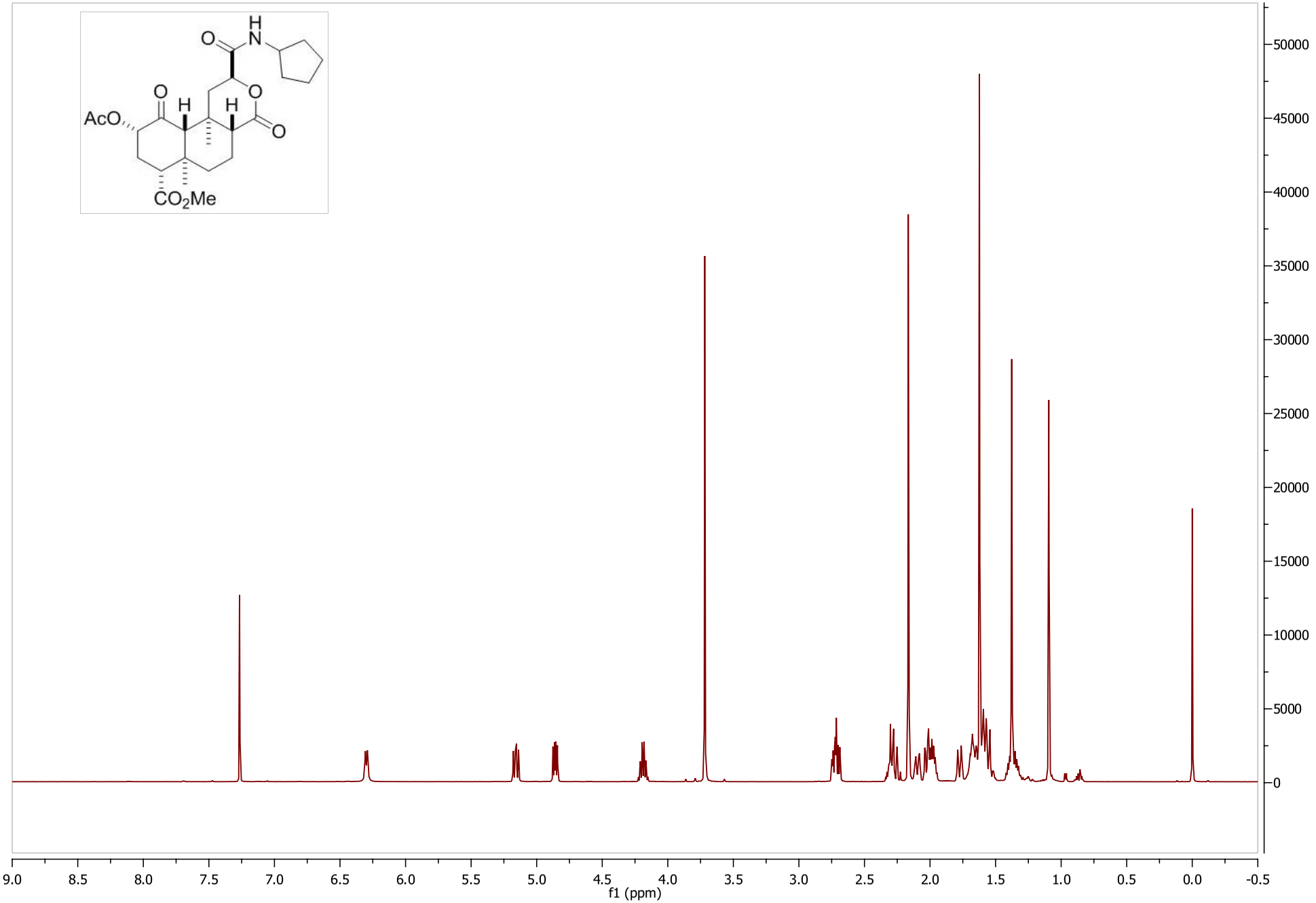
H
N
O
O
O
H
H
O
AcO
O
CO2Me
50000
45000
40000
35000
30000
25000
20000
15000
10000
5000
0
9.0
8.5
8.0
7.5
7.0
6.5
6.0
5.5
5.0
4.5
4.0
3.5
3.0
2.5
2.0
1.5
1.0
0.5
0.0
-0.5
f1 (ppm)

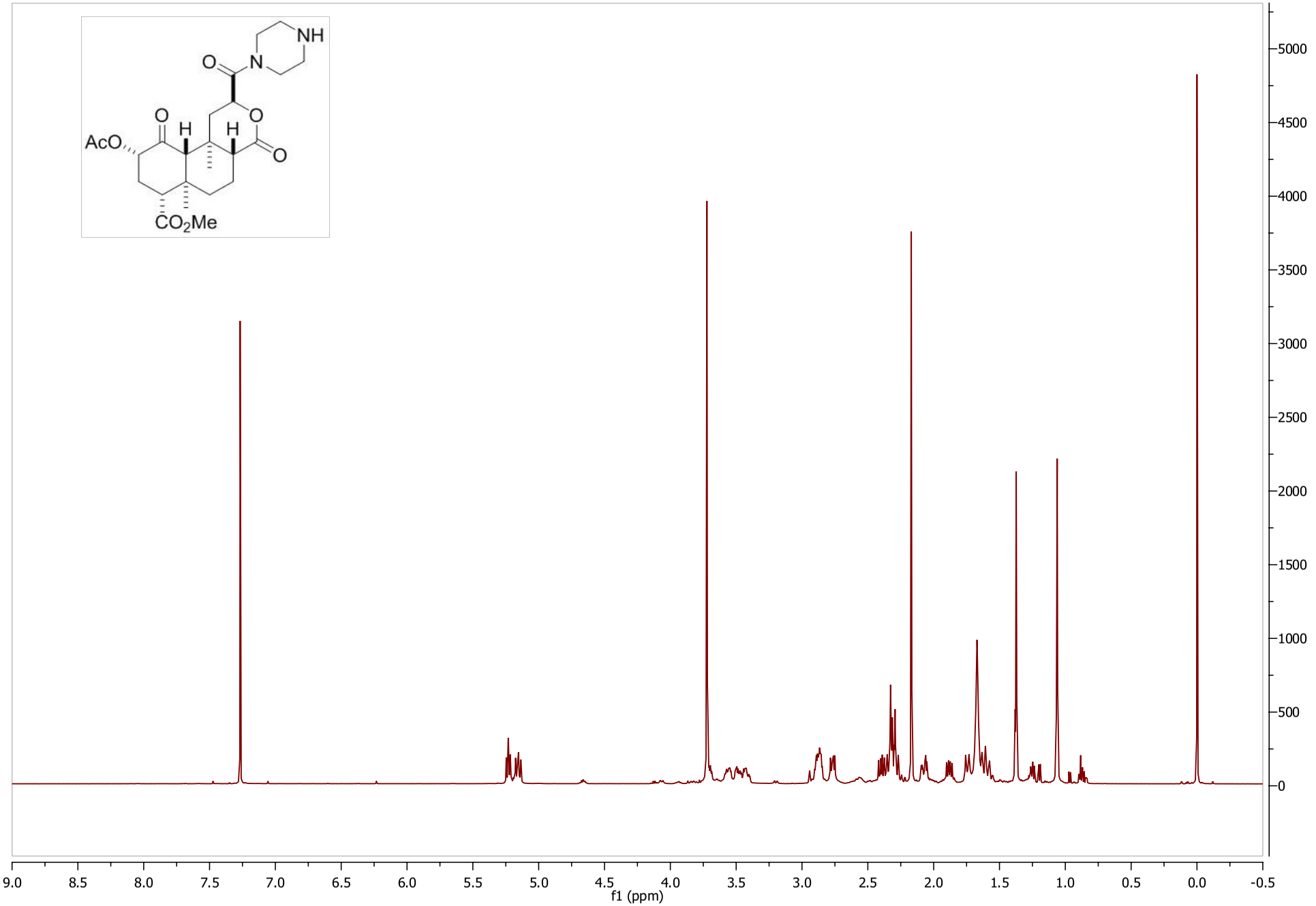
NH
O
N
O
H
H
O
AcO
O
CO2Me
5000
4500
4000
3500
3000
2500
2000
1500
1000
500
0
9.0
8.5
8.0
7.5
7.0
6.5
6.0
5.5
5.0
4.5
4.0
3.5
3.0
2.5
2.0
1.5
1.0
0.5
0.0
-0.5
f1 (ppm)

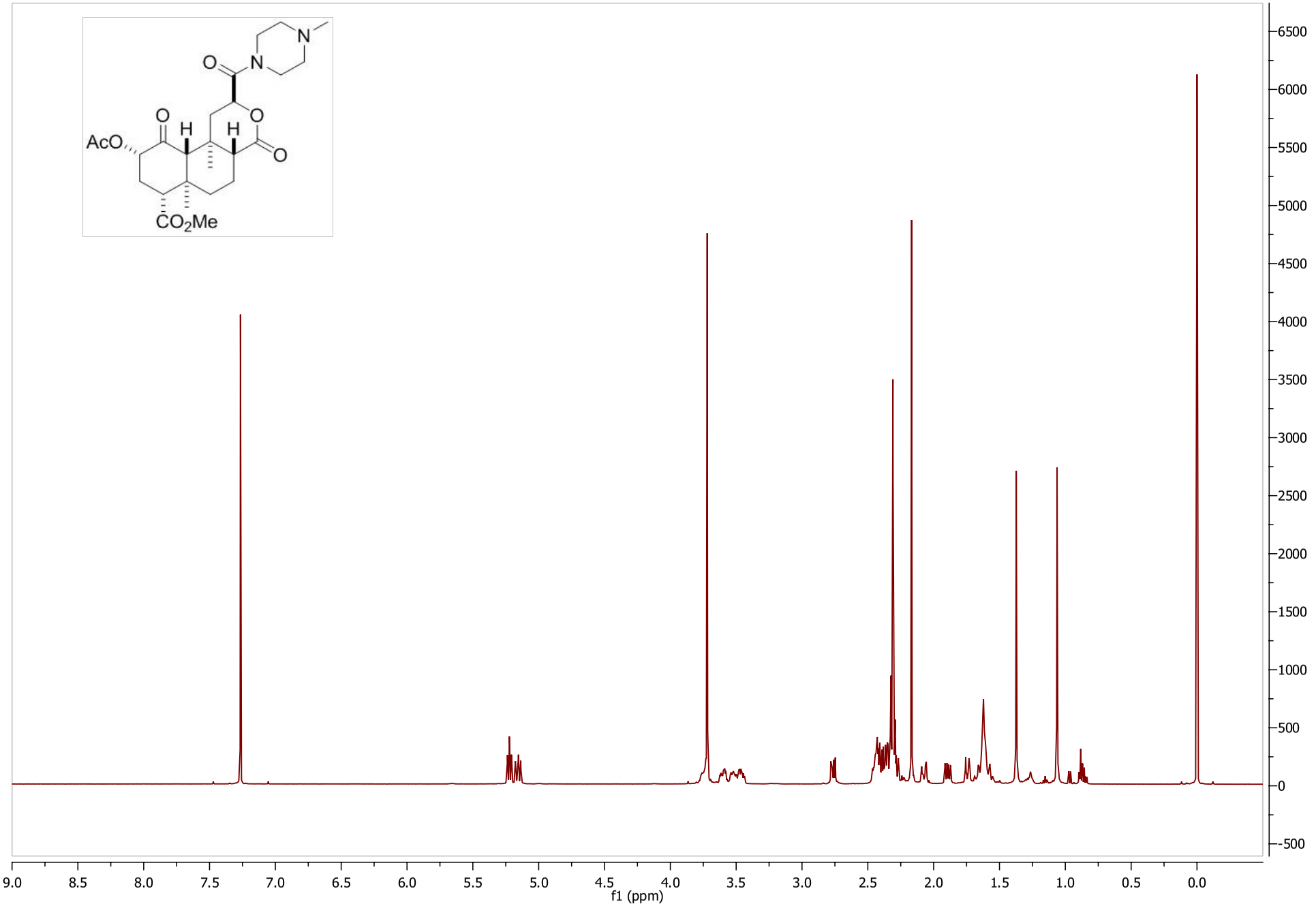
AcO
O
H
H
O
O
O
N
N
CO2Me
6500
6000
5500
5000
4500
4000
3500
3000
2500
2000
1500
1000
500
0
-500
9.0
8.5
8.0
7.5
7.0
6.5
6.0
5.5
5.0
4.5
4.0
3.5
3.0
2.5
2.0
1.5
1.0
0.5
0.0
f1 (ppm)

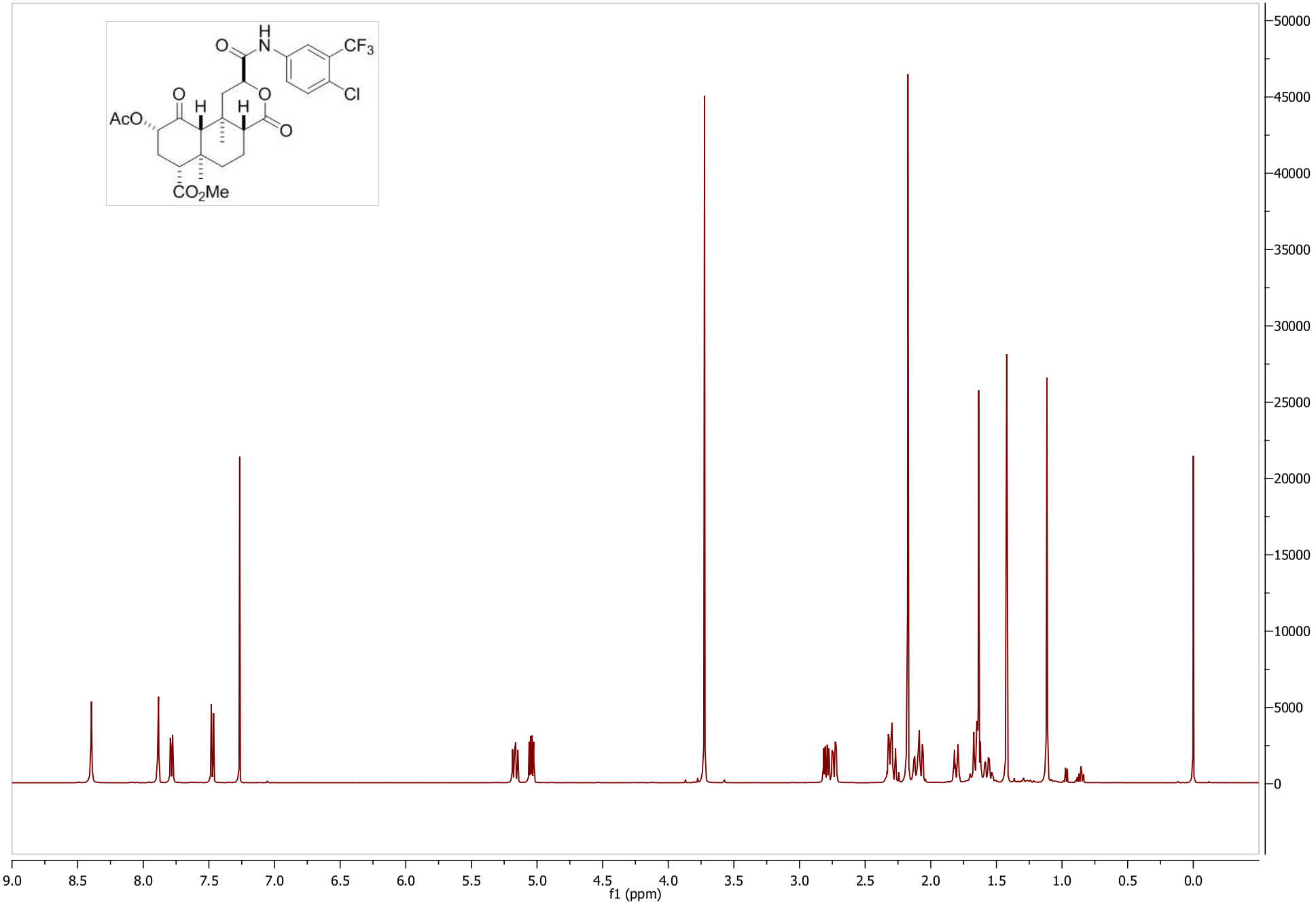
H
O
N
CF3
Cl
O
H
H
O
AcO
O
CO2Me
50000
45000
40000
35000
30000
25000
20000
15000
10000
5000
0
9.0
8.5
8.0
7.5
7.0
6.5
6.0
5.5
5.0
4.5
4.0
3.5
3.0
2.5
2.0
1.5
1.0
0.5
0.0
f1 (ppm)

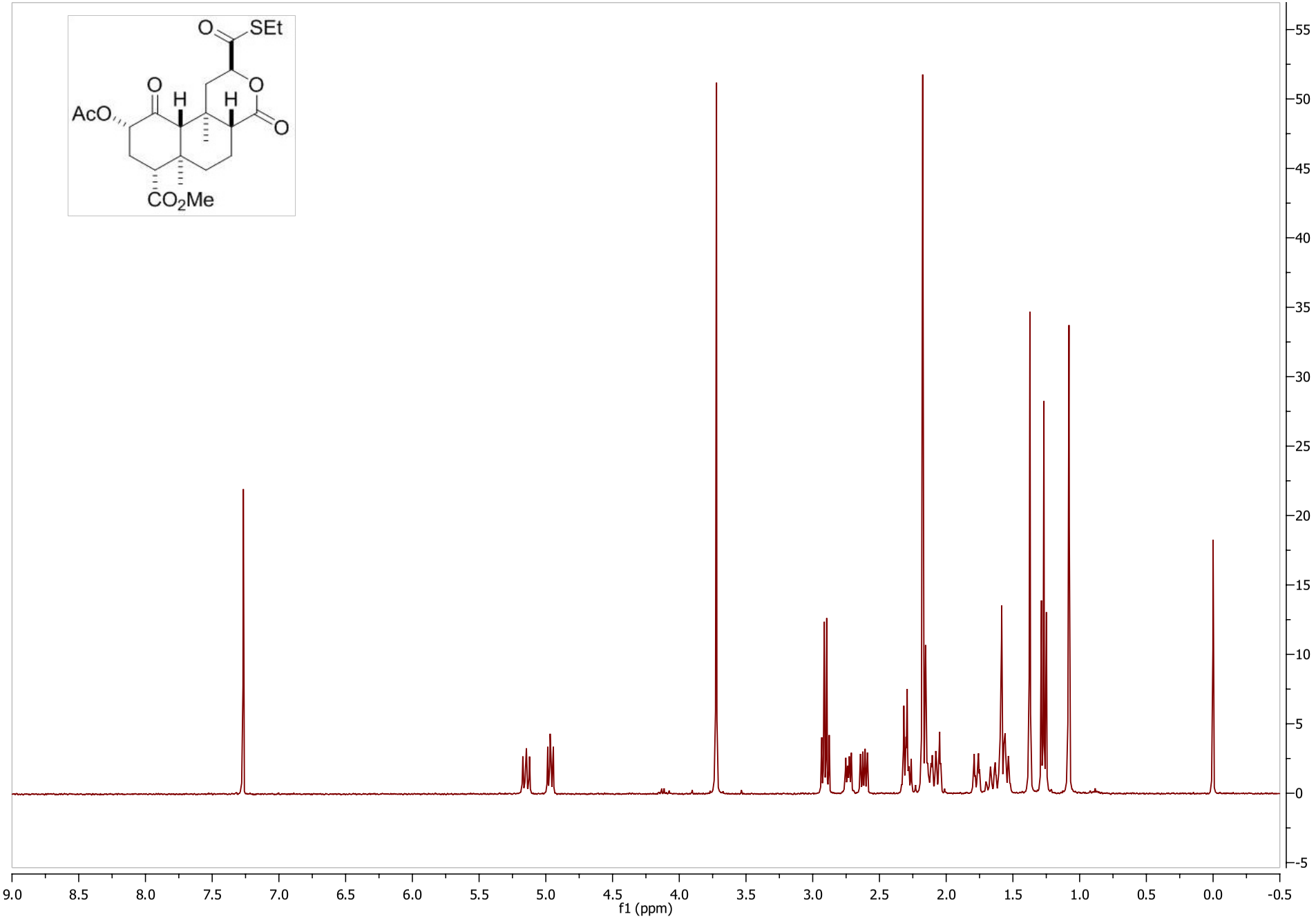
O
SEt
O
H
H
O
AcO
O
CO2Me
55
50
45
40
35
30
25
20
15
10
5
0
-5
9.0
8.5
8.0
7.5
7.0
6.5
6.0
5.5
5.0
4.5
4.0
3.5
3.0
2.5
2.0
1.5
1.0
0.5
0.0
-0.5
f1 (ppm)

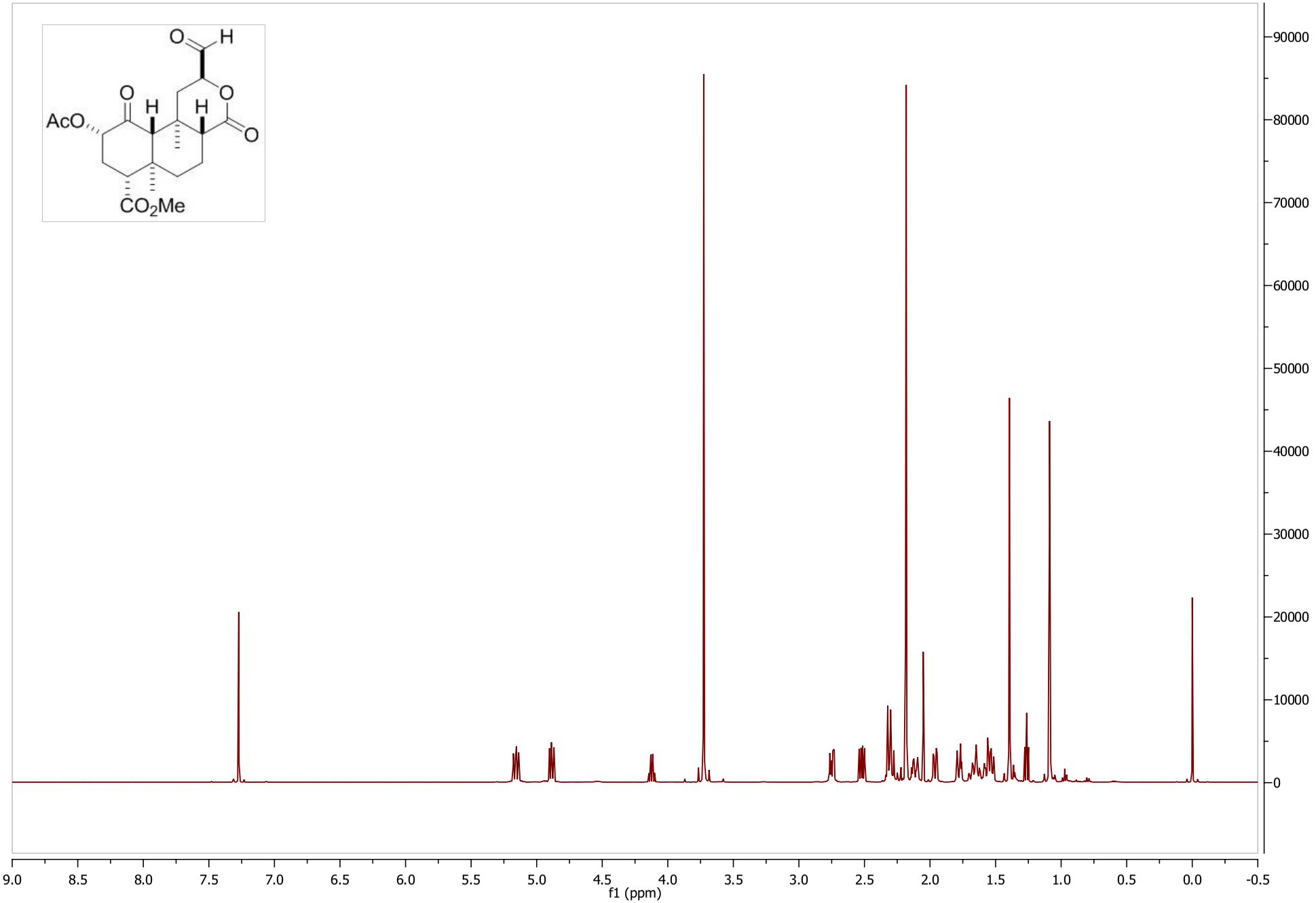
O
H
O
H
H
O
AcO
O
CO2Me
90000
80000
70000
60000
50000
40000
30000
20000
10000
0
9.0
8.5
8.0
7.5
7.0
6.5
6.0
5.5
5.0
4.5
4.0
3.5
3.0
2.5
2.0
1.5
1.0
0.5
0.0
-0.5
f1 (ppm)

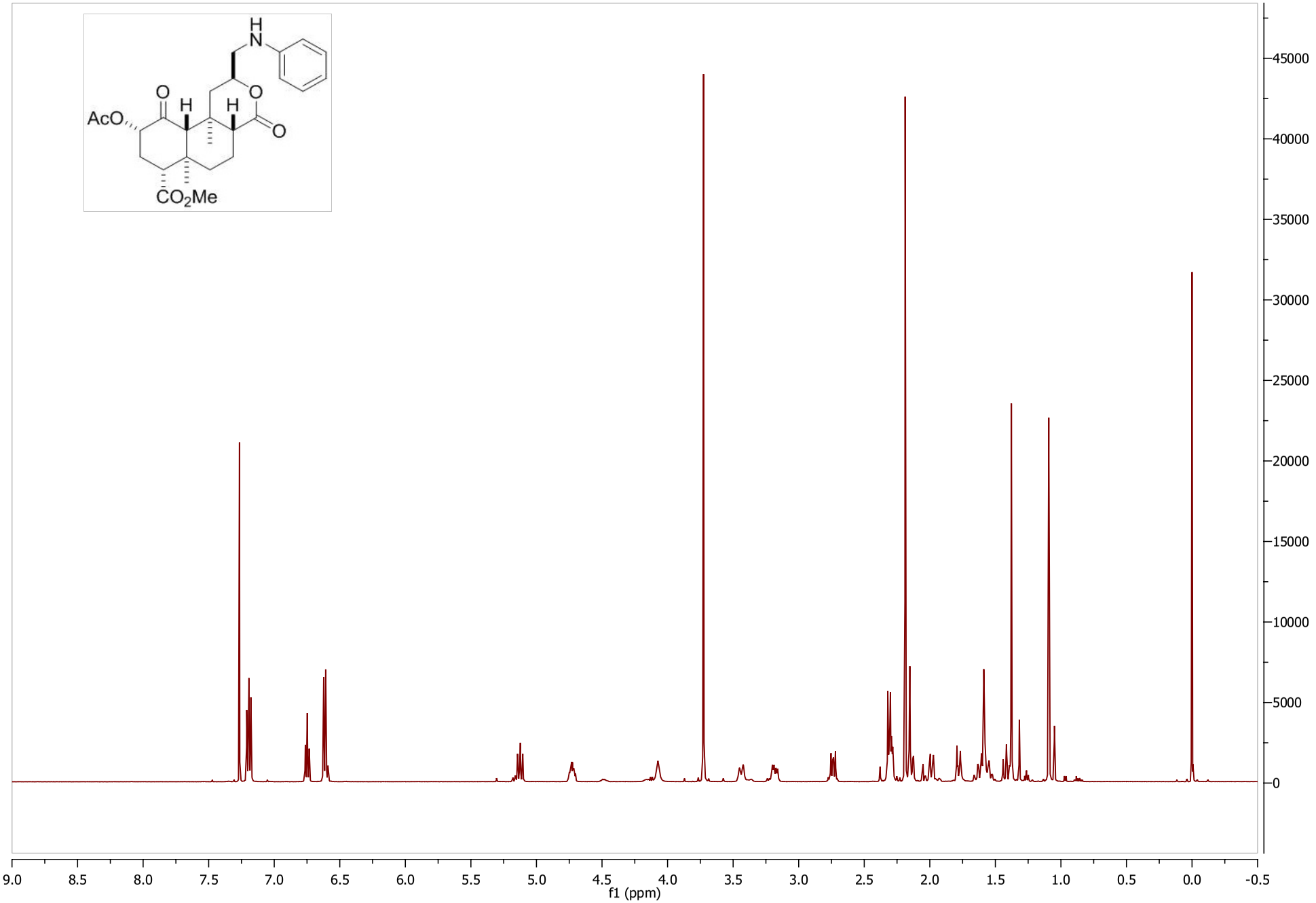
H
N
O
H
H
O
AcO
O
CO2Me
45000
40000
35000
30000
25000
20000
15000
10000
5000
0
9.0
8.5
8.0
7.5
7.0
6.5
6.0
5.5
5.0
4.5
4.0
3.5
3.0
2.5
2.0
1.5
1.0
0.5
0.0
-0.5
f1 (ppm)

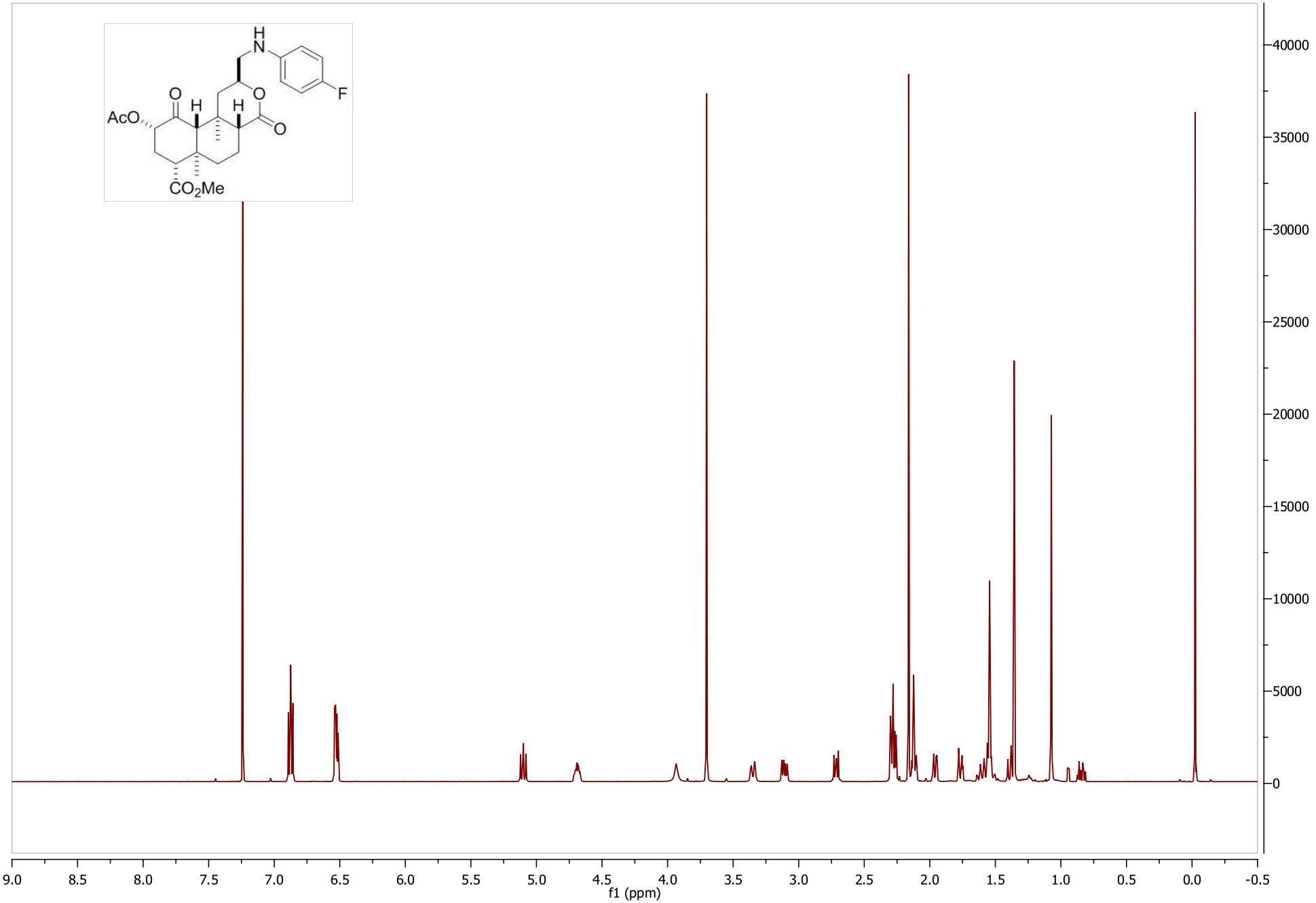
H
N
F
O
H
H
O
AcO
O
CO2Me
40000
35000
30000
25000
20000
15000
10000
5000
0
9.0
8.5
8.0
7.5
7.0
6.5
6.0
5.5
5.0
4.5
4.0
3.5
3.0
2.5
2.0
1.5
1.0
0.5
0.0
-0.5
f1 (ppm)

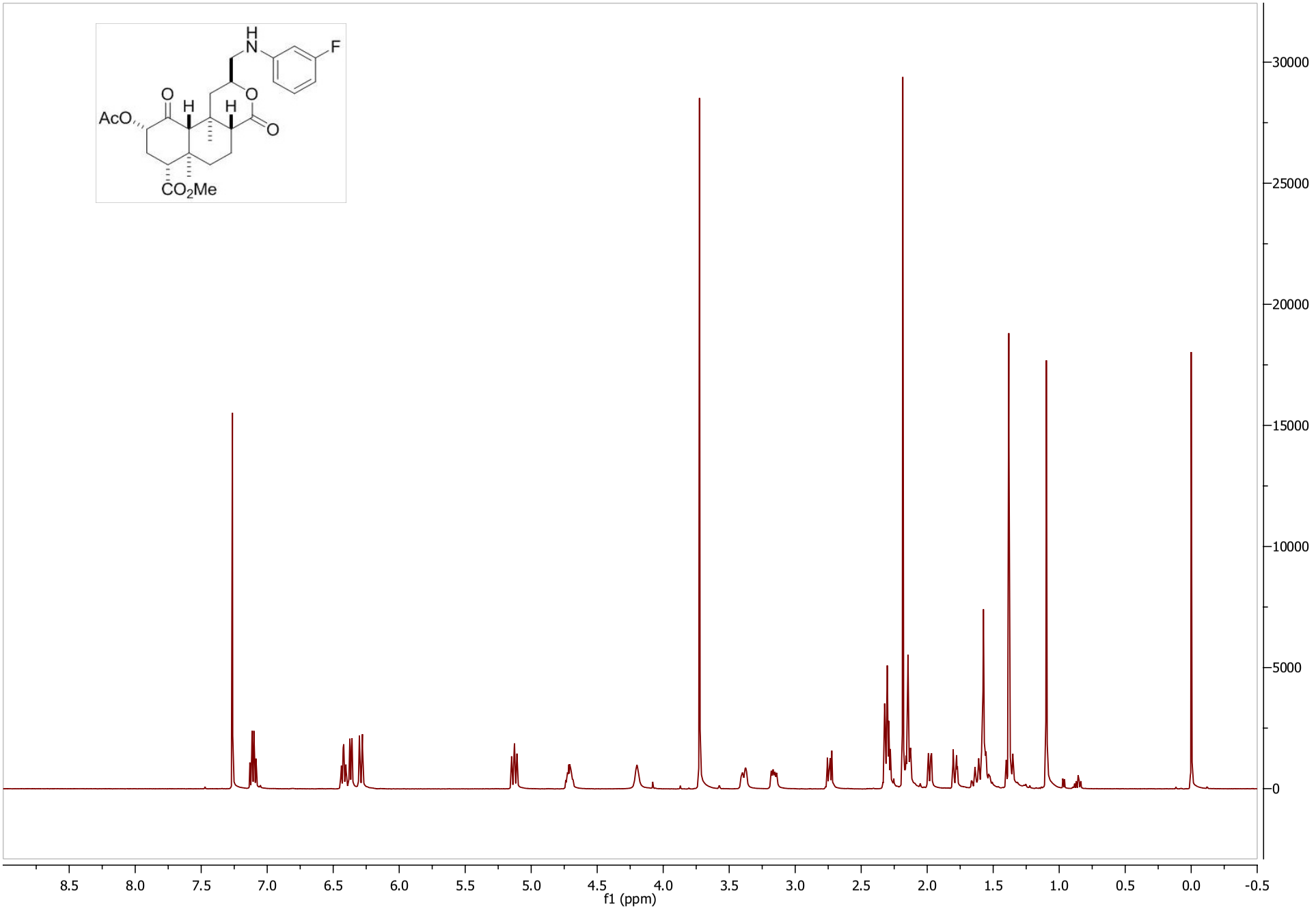
H
N
F
O
H
H
O
AcO
O
CO2Me
30000
25000
20000
15000
10000
5000
0
8.5
8.0
7.5
7.0
6.5
6.0
5.5
5.0
4.5
4.0
3.5
3.0
2.5
2.0
1.5
1.0
0.5
0.0
-0.5
f1 (ppm)

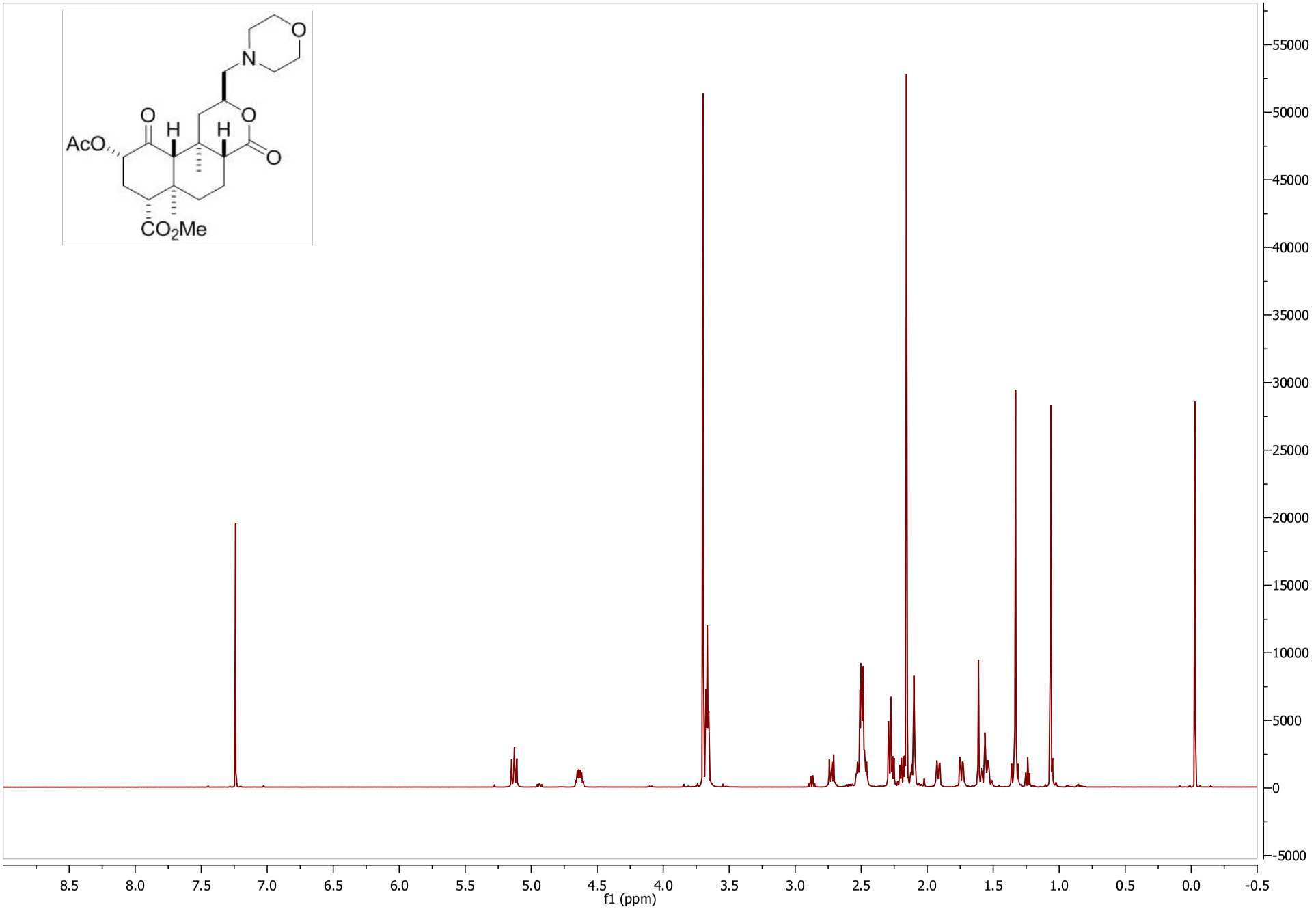
AcO
O
H
H
O
O
N
O
CO2Me
55000
50000
45000
40000
35000
30000
25000
20000
15000
10000
5000
0
-5000
8.5
8.0
7.5
7.0
6.5
6.0
5.5
5.0
4.5
4.0
3.5
3.0
2.5
2.0
1.5
1.0
0.5
0.0
-0.5
f1 (ppm)

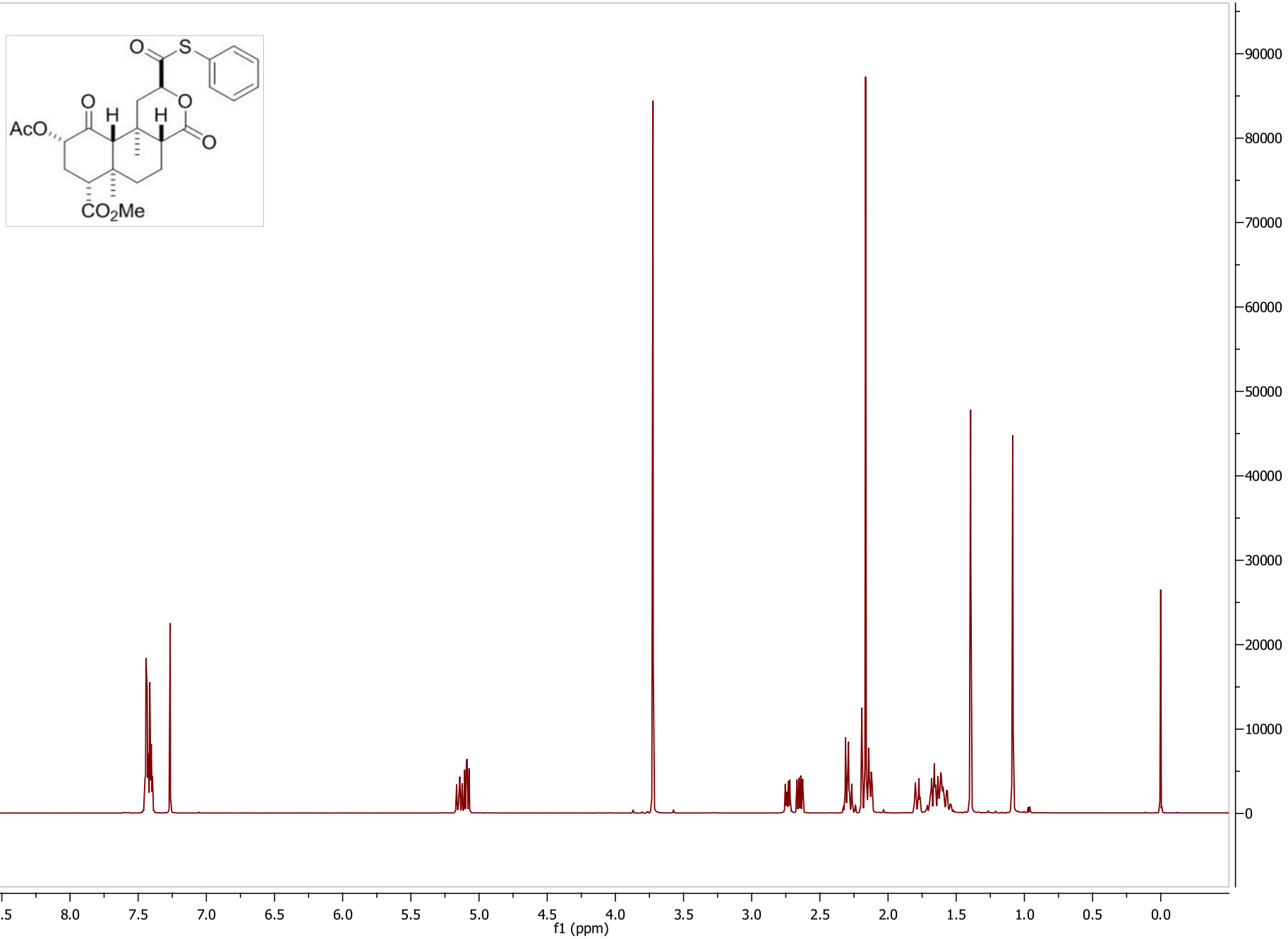
O
S
O
H
H
O
AcO
O
CO2Me
90000
80000
70000
60000
50000
40000
30000
20000
10000
0
9.0
8.5
8.0
7.5
7.0
6.5
6.0
5.5
5.0
4.5
4.0
3.5
3.0
2.5
2.0
1.5
1.0
0.5
0.0
f1 (ppm)

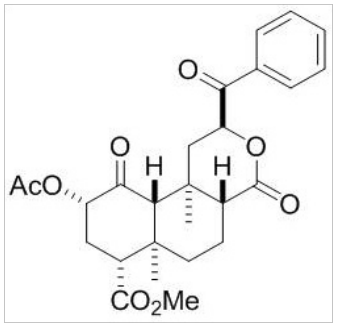
O
O
H
H
O
AcO
O
CO2Me

34000
32000
30000
28000
26000
24000
22000
20000
18000
16000
14000
12000
10000
8000
6000
4000
2000
0
-2000
9.0
8.5
8.0
7.5
7.0
6.5
6.0
5.5
5.0
4.5
4.0
3.5
3.0
2.5
2.0
1.5
1.0
0.5
0.0
-0.5
f1 (ppm)

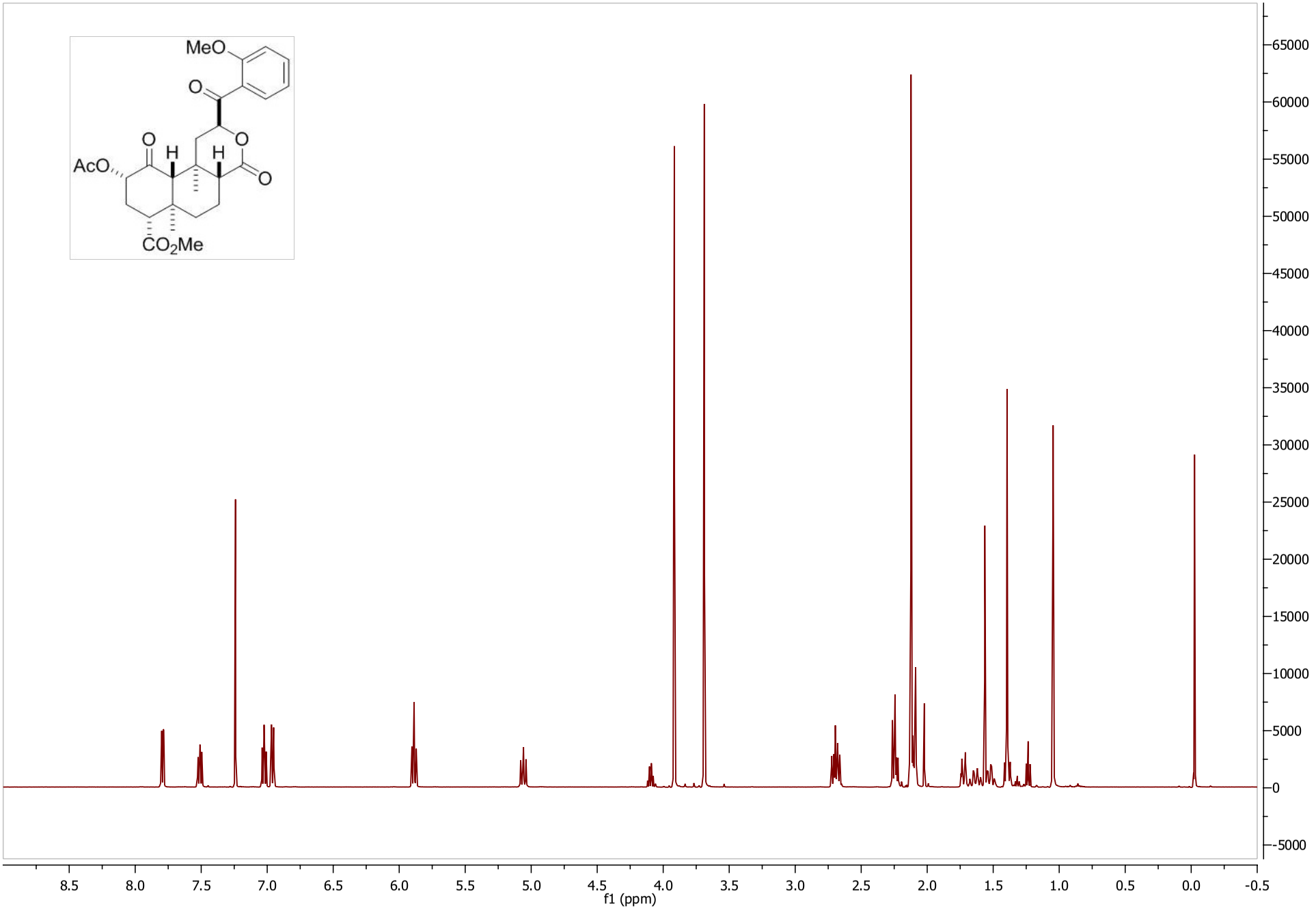
MeO
O
O
H
H
O
AcO
O
CO2Me
65000
60000
55000
50000
45000
40000
35000
30000
25000
20000
15000
10000
5000
0
-5000
8.5
8.0
7.5
7.0
6.5
6.0
5.5
5.0
4.5
4.0
3.5
3.0
2.5
2.0
1.5
1.0
0.5
0.0
-0.5
f1 (ppm)

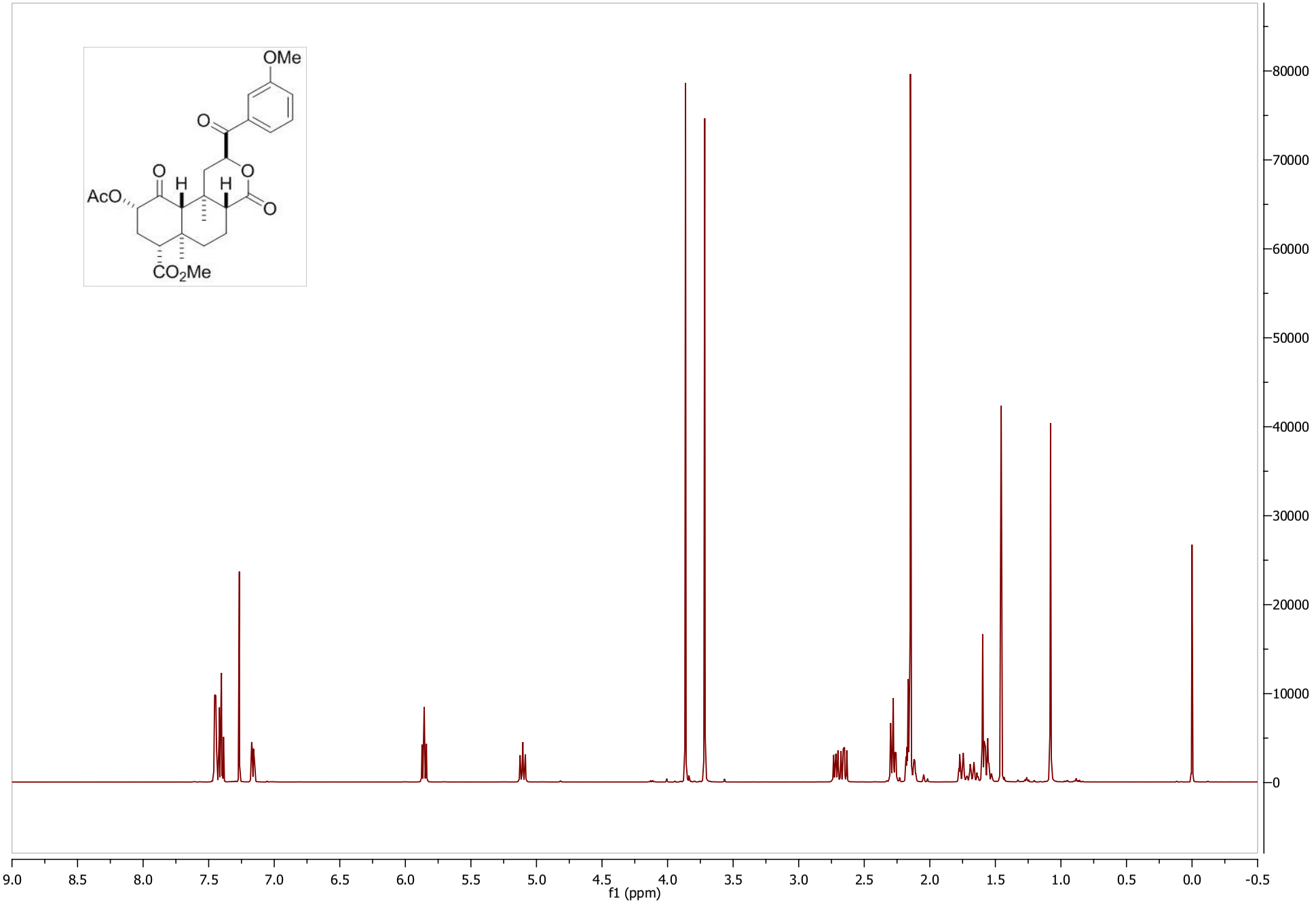
OMe
O
O
H
H
O
AcO
O
CO2Me
80000
70000
60000
50000
40000
30000
20000
10000
0
9.0
8.5
8.0
7.5
7.0
6.5
6.0
5.5
5.0
4.5
4.0
3.5
3.0
2.5
2.0
1.5
1.0
0.5
0.0
-0.5
f1 (ppm)

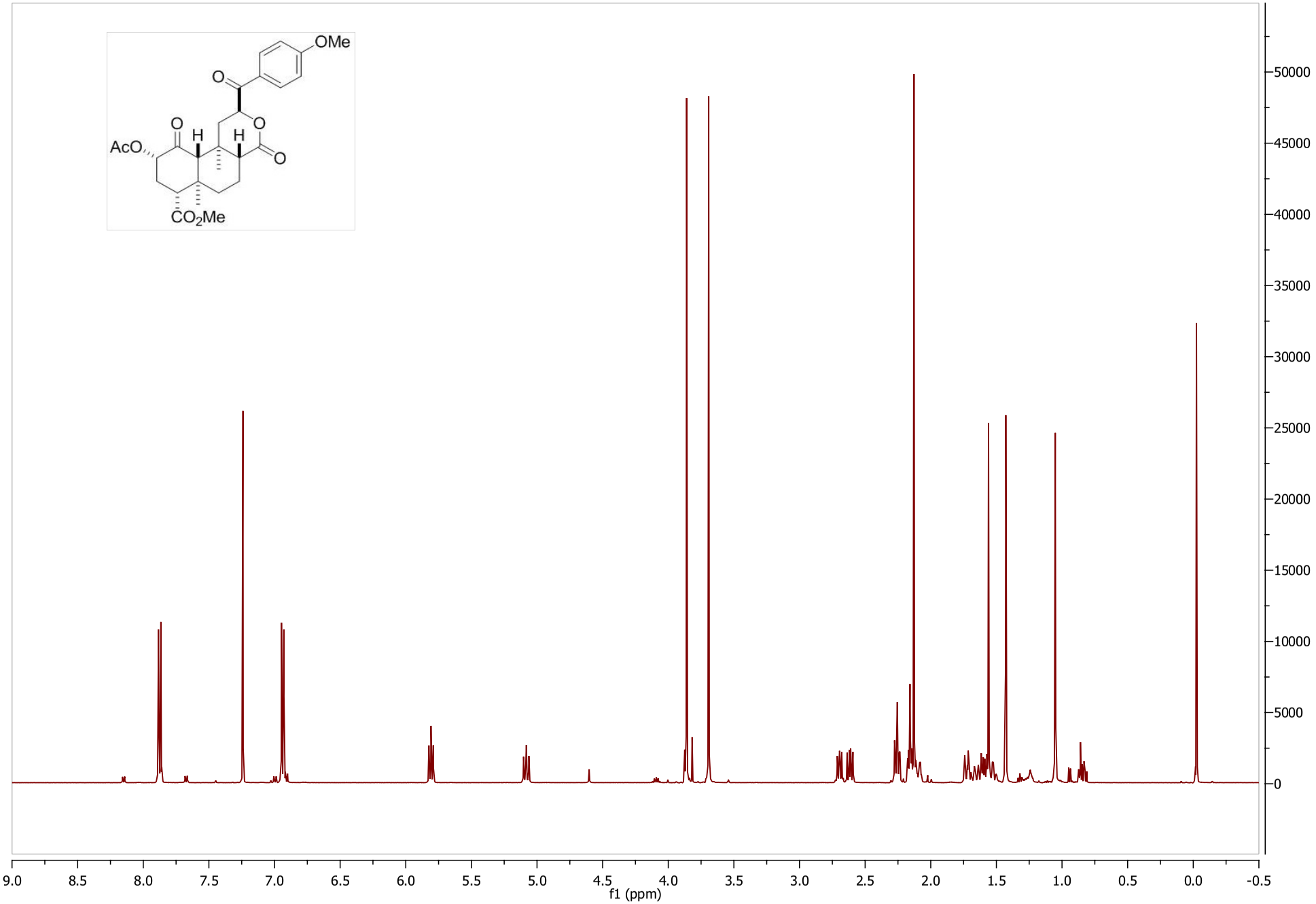
OMe
O
O
H
H
O
AcO
O
CO2Me
50000
45000
40000
35000
30000
25000
20000
15000
10000
5000
0
9.0
8.5
8.0
7.5
7.0
6.5
6.0
5.5
5.0
4.5
4.0
3.5
3.0
2.5
2.0
1.5
1.0
0.5
0.0
-0.5
f1 (ppm)

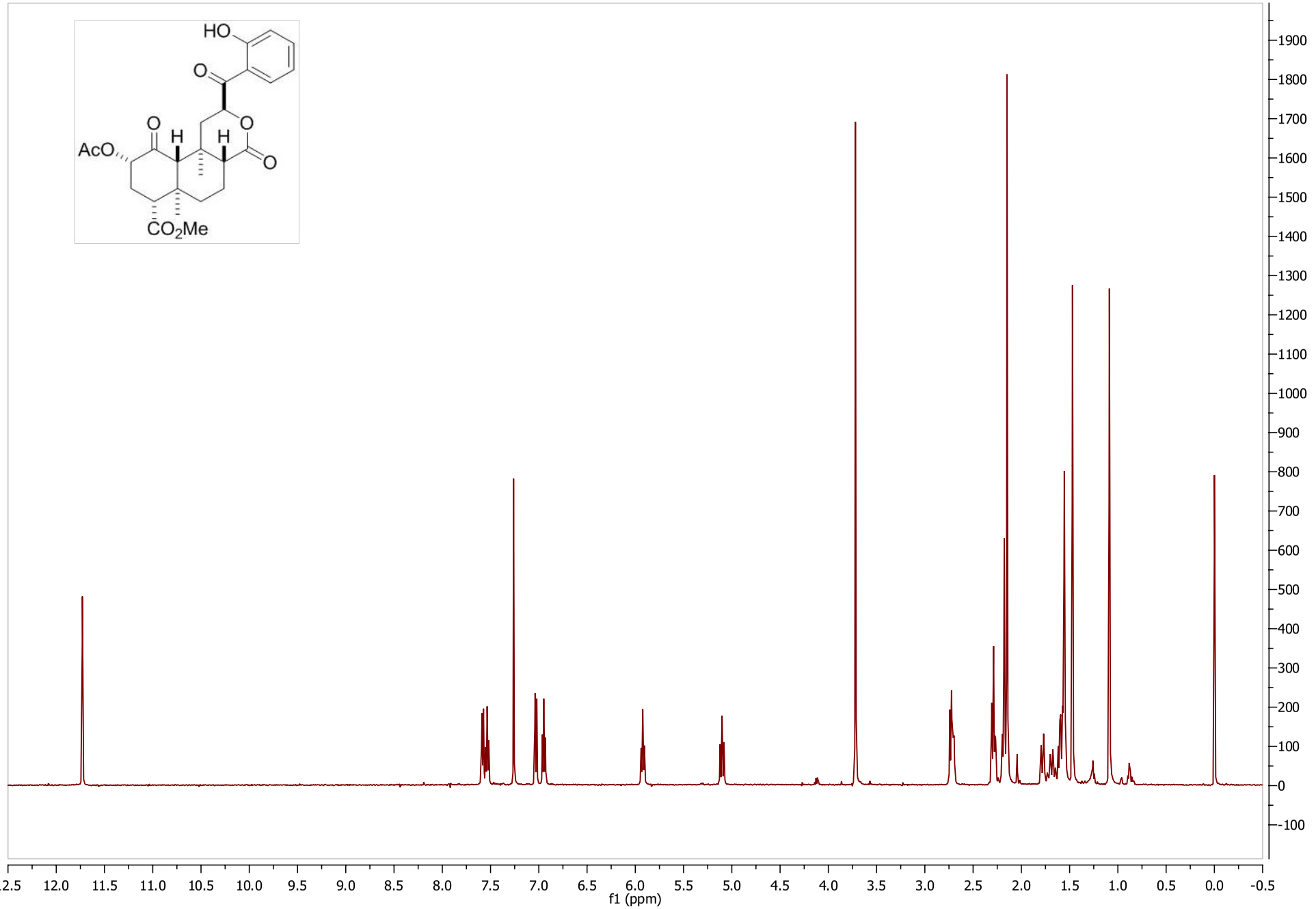
HO
O
O
H
H
O
AcO
O
CO2Me
1900
1800
1700
1600
1500
1400
1300
1200
1100
1000
900
800
700
600
500
400
300
200
100
0
-100
12.5
12.0
11.5
11.0
10.5
10.0
9.5
9.0
8.5
8.0
7.5
7.0
6.5
6.0
5.5
5.0
4.5
4.0
3.5
3.0
2.5
2.0
1.5
1.0
0.5
0.0
-0.5
f1 (ppm)

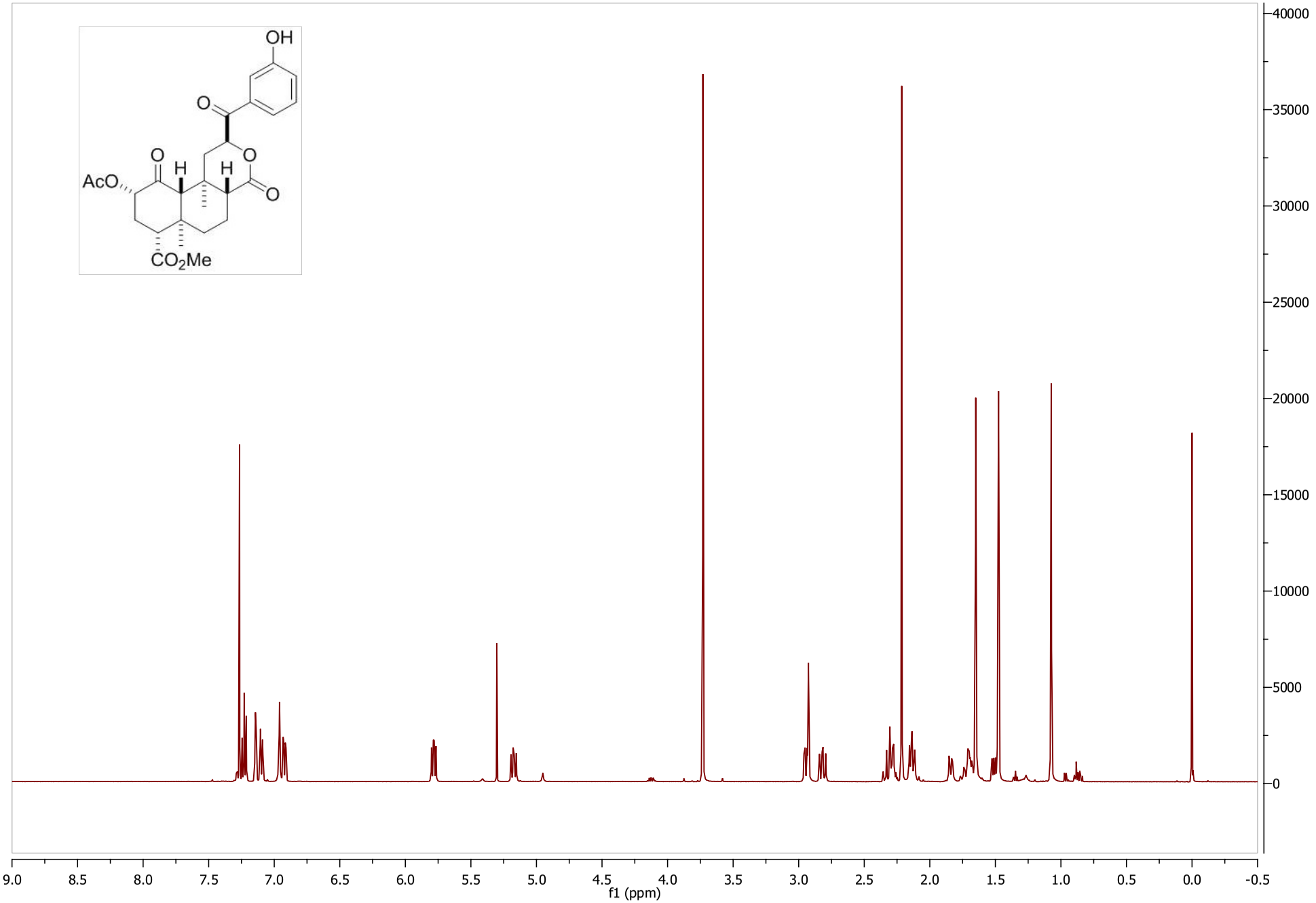
OH
O
O
H
H
O
AcO
O
CO2Me
40000
35000
30000
25000
20000
15000
10000
5000
0
9.0
8.5
8.0
7.5
7.0
6.5
6.0
5.5
5.0
4.5
4.0
3.5
3.0
2.5
2.0
1.5
1.0
0.5
0.0
-0.5
f1 (ppm)

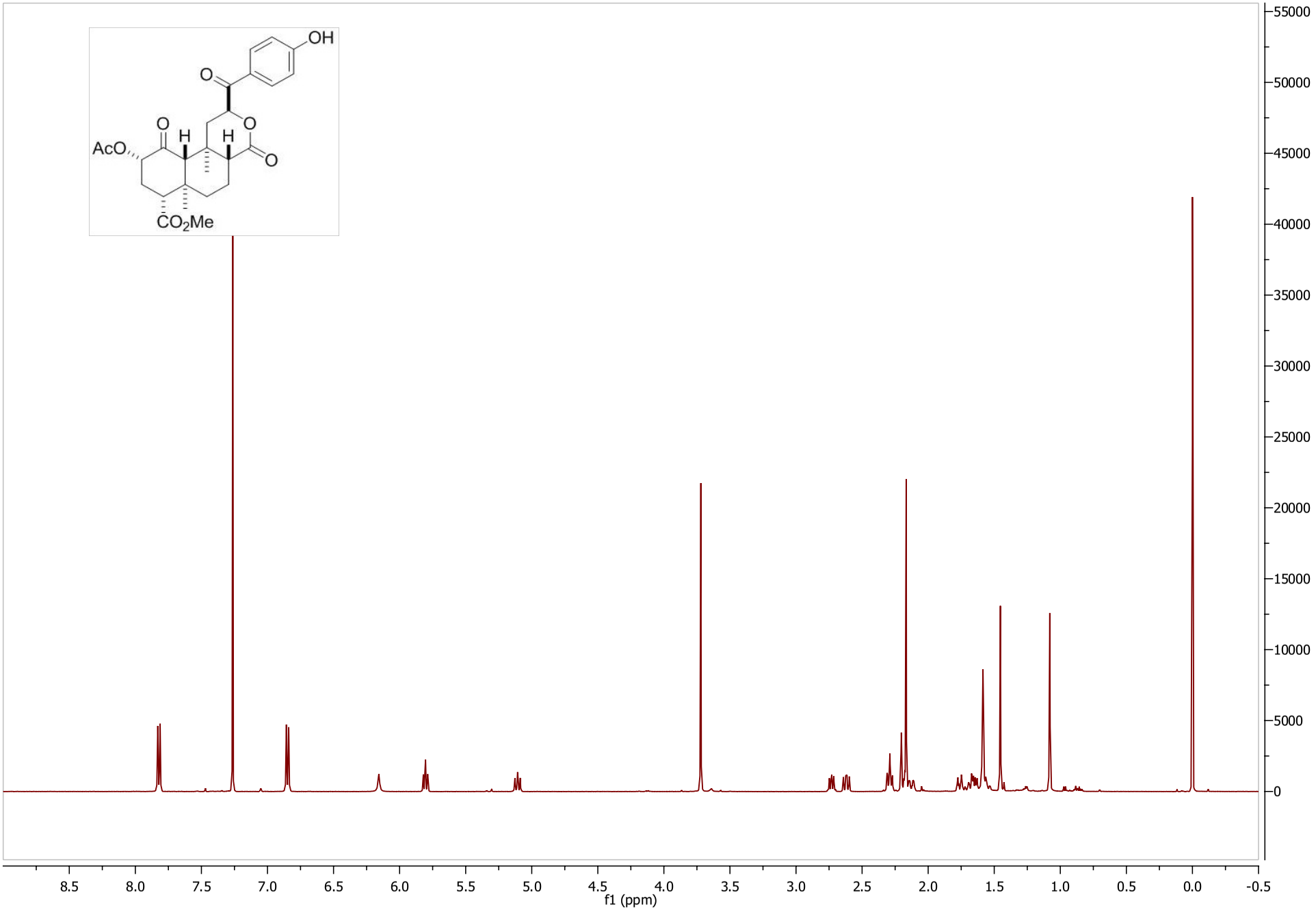
OH
O
O
H
H
O
AcO
O
CO2Me
55000
50000
45000
40000
35000
30000
25000
20000
15000
10000
5000
0
8.5
8.0
7.5
7.0
6.5
6.0
5.5
5.0
4.5
4.0
3.5
3.0
2.5
2.0
1.5
1.0
0.5
0.0
-0.5
f1 (ppm)

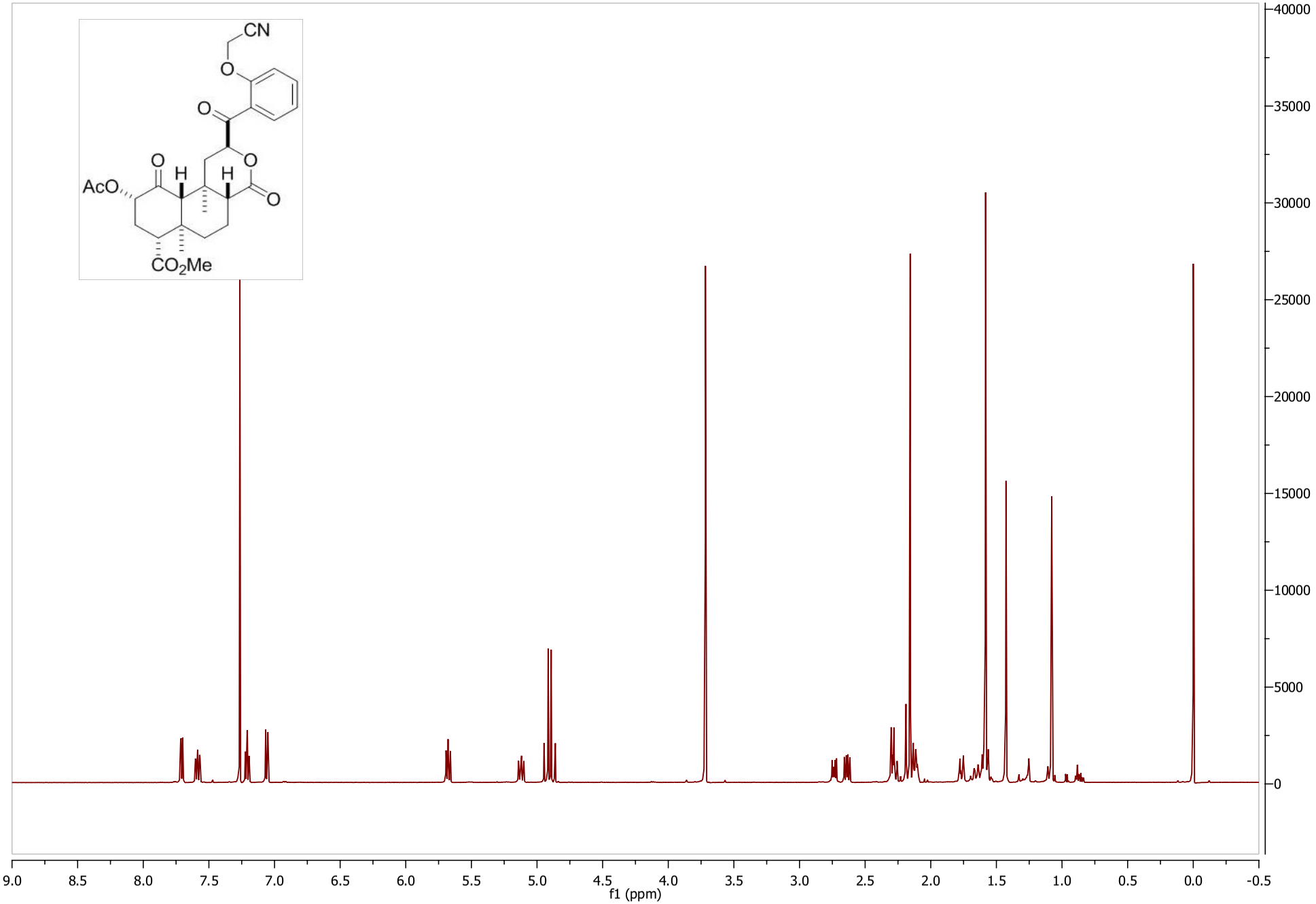
CN
O
O
O
H
H
O
O
AcO
CO2Me
40000
35000
30000
25000
20000
15000
10000
5000
0
9.0
8.5
8.0
7.5
7.0
6.5
6.0
5.5
5.0
4.5
4.0
3.5
3.0
2.5
2.0
1.5
1.0
0.5
0.0
-0.5
f1 (ppm)

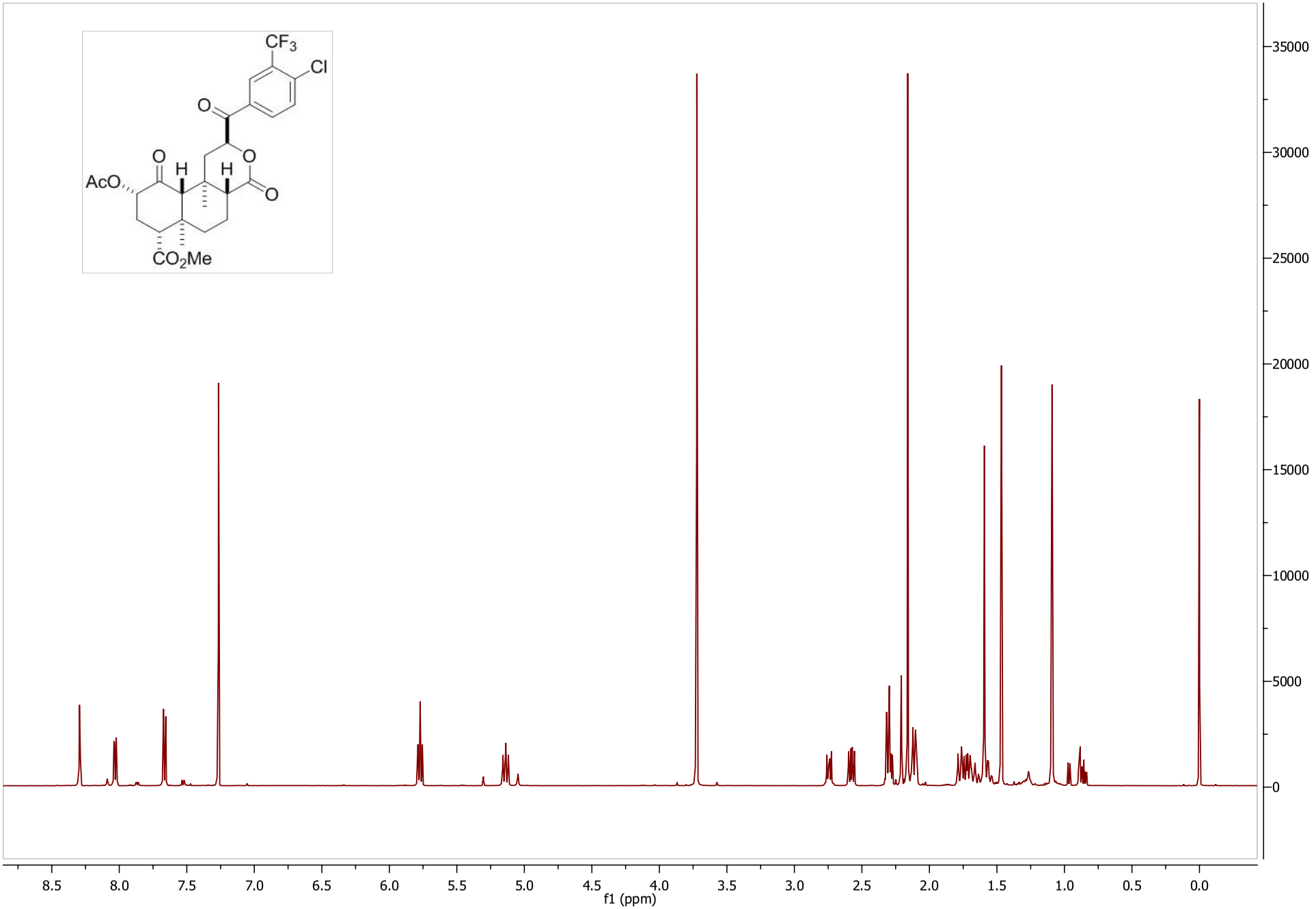
CF3
Cl
O
O
H
H
O
AcO
O
CO2Me
35000
30000
25000
20000
15000
10000
5000
0
8.5
8.0
7.5
7.0
6.5
6.0
5.5
5.0
4.5
4.0
3.5
3.0
2.5
2.0
1.5
1.0
0.5
0.0
f1 (ppm)

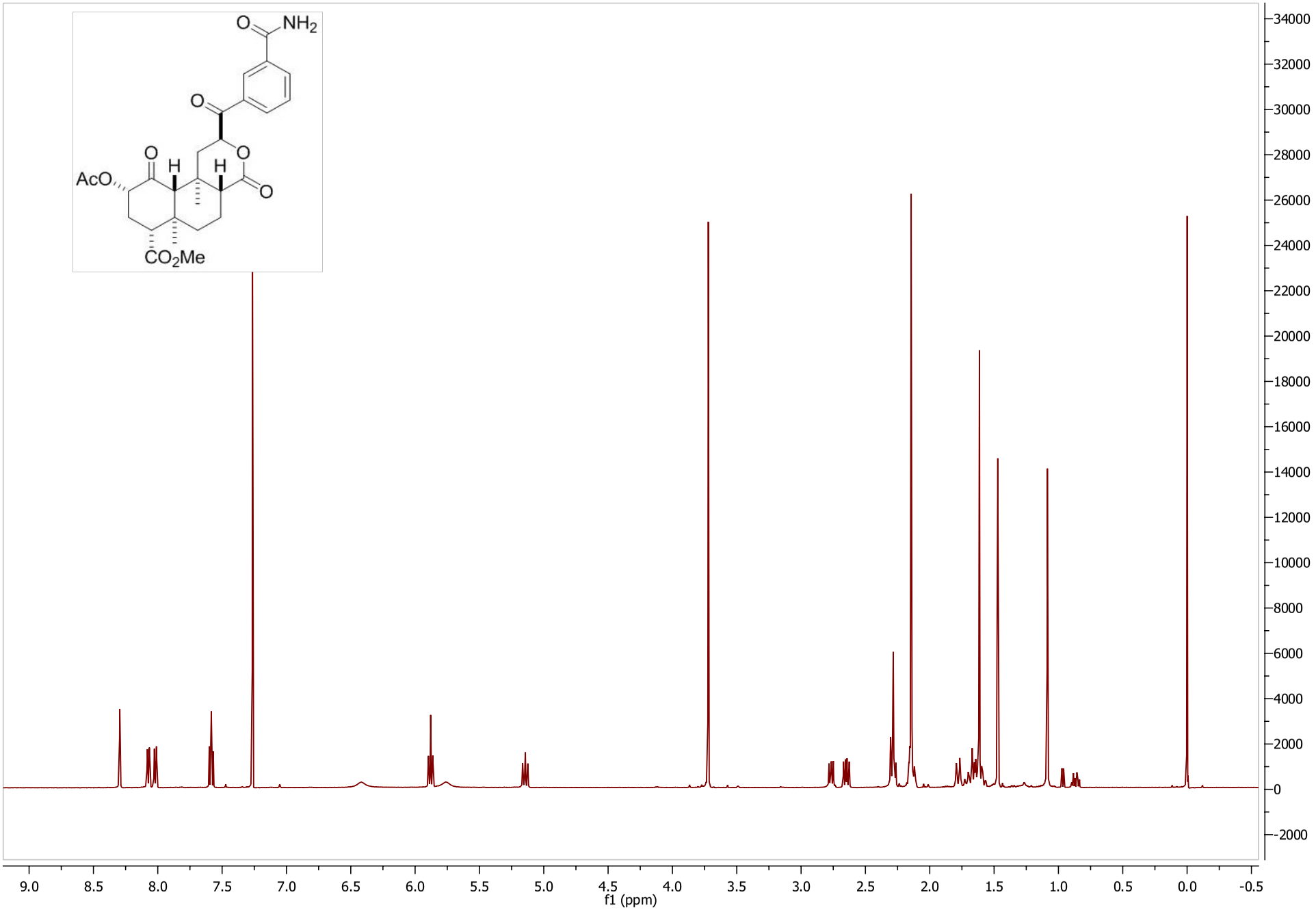
O
NH2
O
O
H
H
O
AcO
O
CO2Me
34000
32000
30000
28000
26000
24000
22000
20000
18000
16000
14000
12000
10000
8000
6000
4000
2000
0
-2000
9.0
8.5
8.0
7.5
7.0
6.5
6.0
5.5
5.0
4.5
4.0
3.5
3.0
2.5
2.0
1.5
1.0
0.5
0.0
-0.5
f1 (ppm)

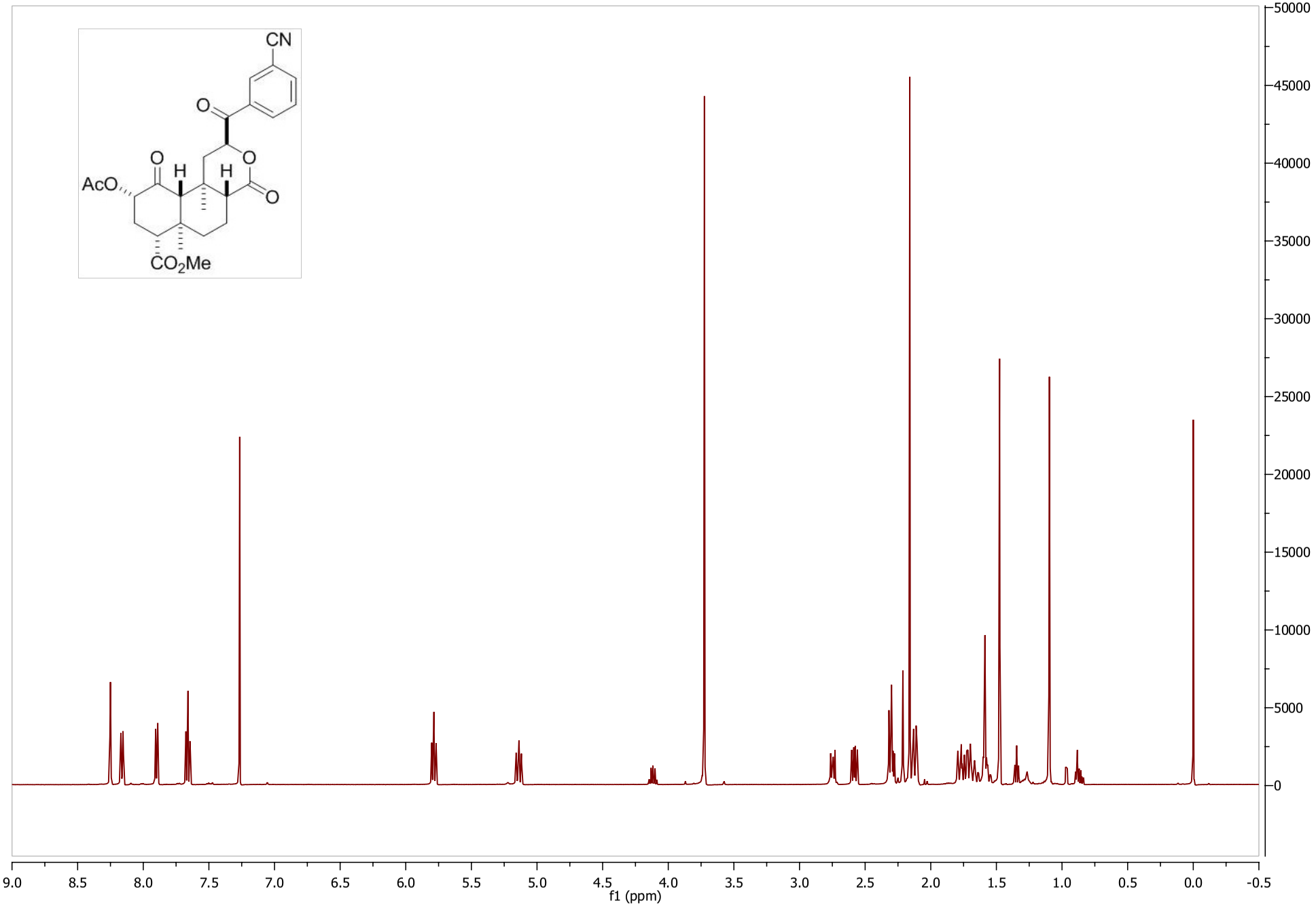
CN
O
O
H
H
O
AcO
O
CO2Me
50000
45000
40000
35000
30000
25000
20000
15000
10000
5000
0
9.0
8.5
8.0
7.5
7.0
6.5
6.0
5.5
5.0
4.5
4.0
3.5
3.0
2.5
2.0
1.5
1.0
0.5
0.0
-0.5
f1 (ppm)

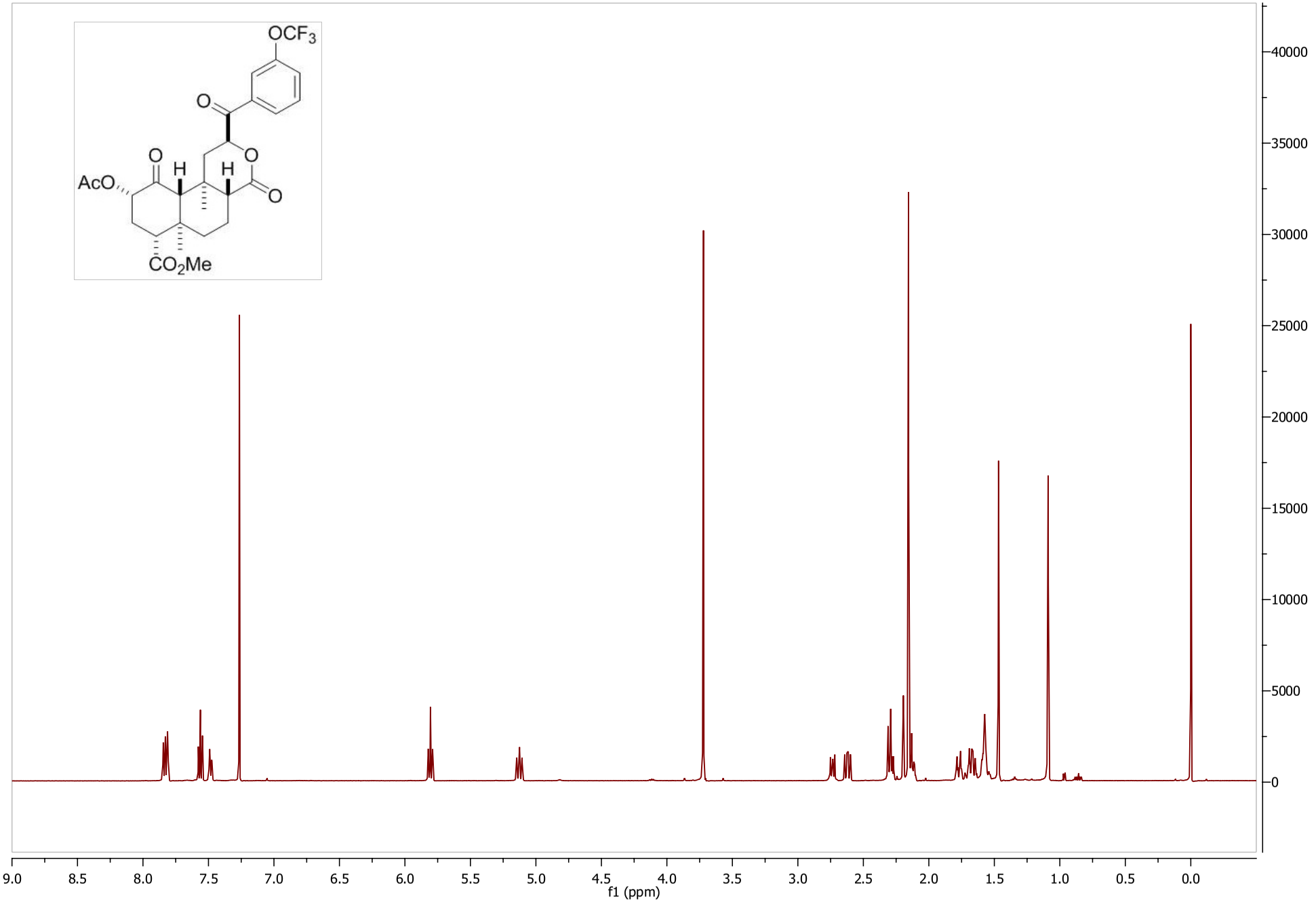
OCF3
O
O
H
H
O
AcO
O
CO2Me
40000
35000
30000
25000
20000
15000
10000
5000
0
9.0
8.5
8.0
7.5
7.0
6.5
6.0
5.5
5.0
4.5
4.0
3.5
3.0
2.5
2.0
1.5
1.0
0.5
0.0
f1 (ppm)

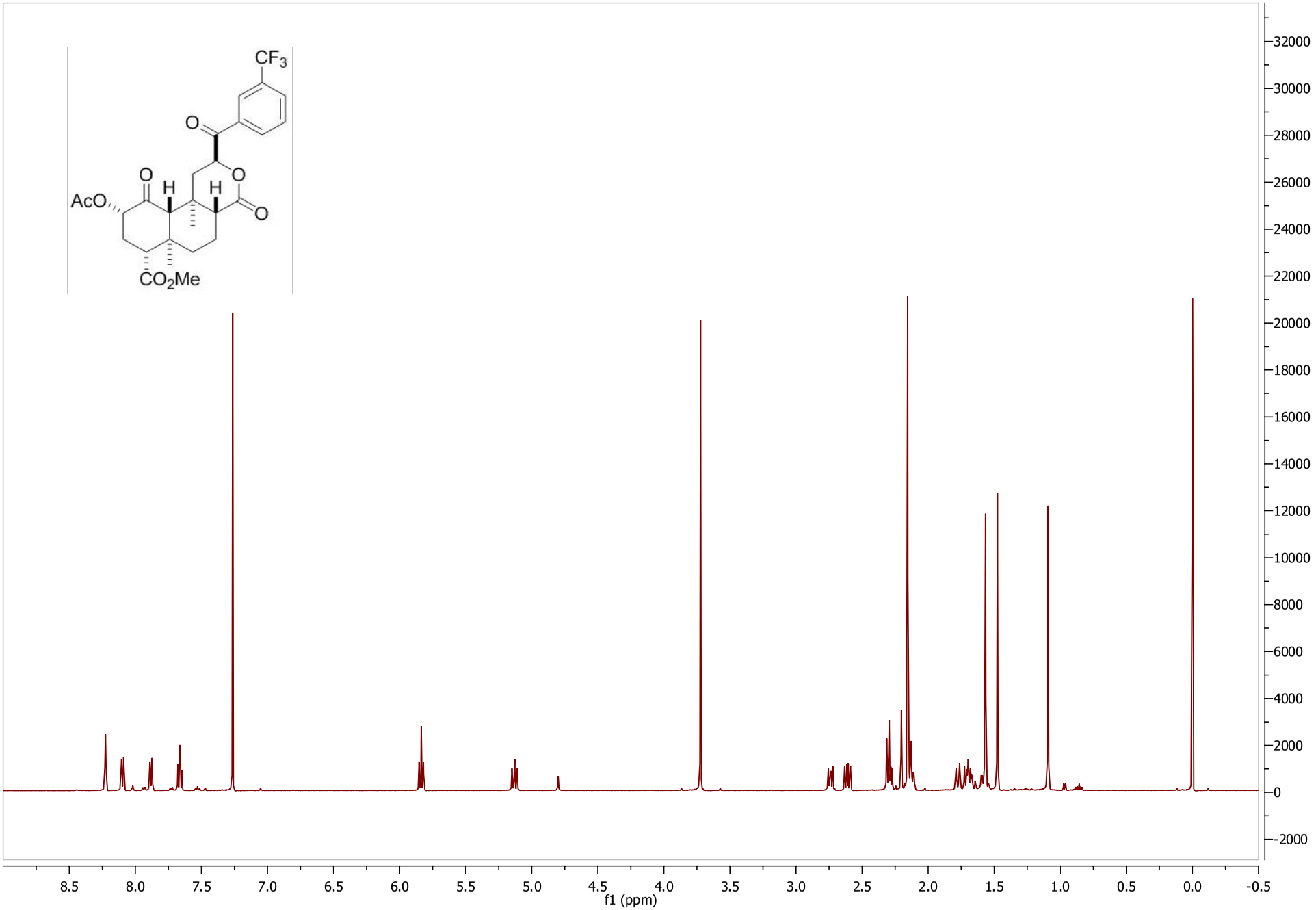
CF3
O
O
H
H
O
AcO
O
CO2Me
32000
30000
28000
26000
24000
22000
20000
18000
16000
14000
12000
10000
8000
6000
4000
2000
0
-2000
8.5
8.0
7.5
7.0
6.5
6.0
5.5
5.0
4.5
4.0
3.5
3.0
2.5
2.0
1.5
1.0
0.5
0.0
-0.5
f1 (ppm)

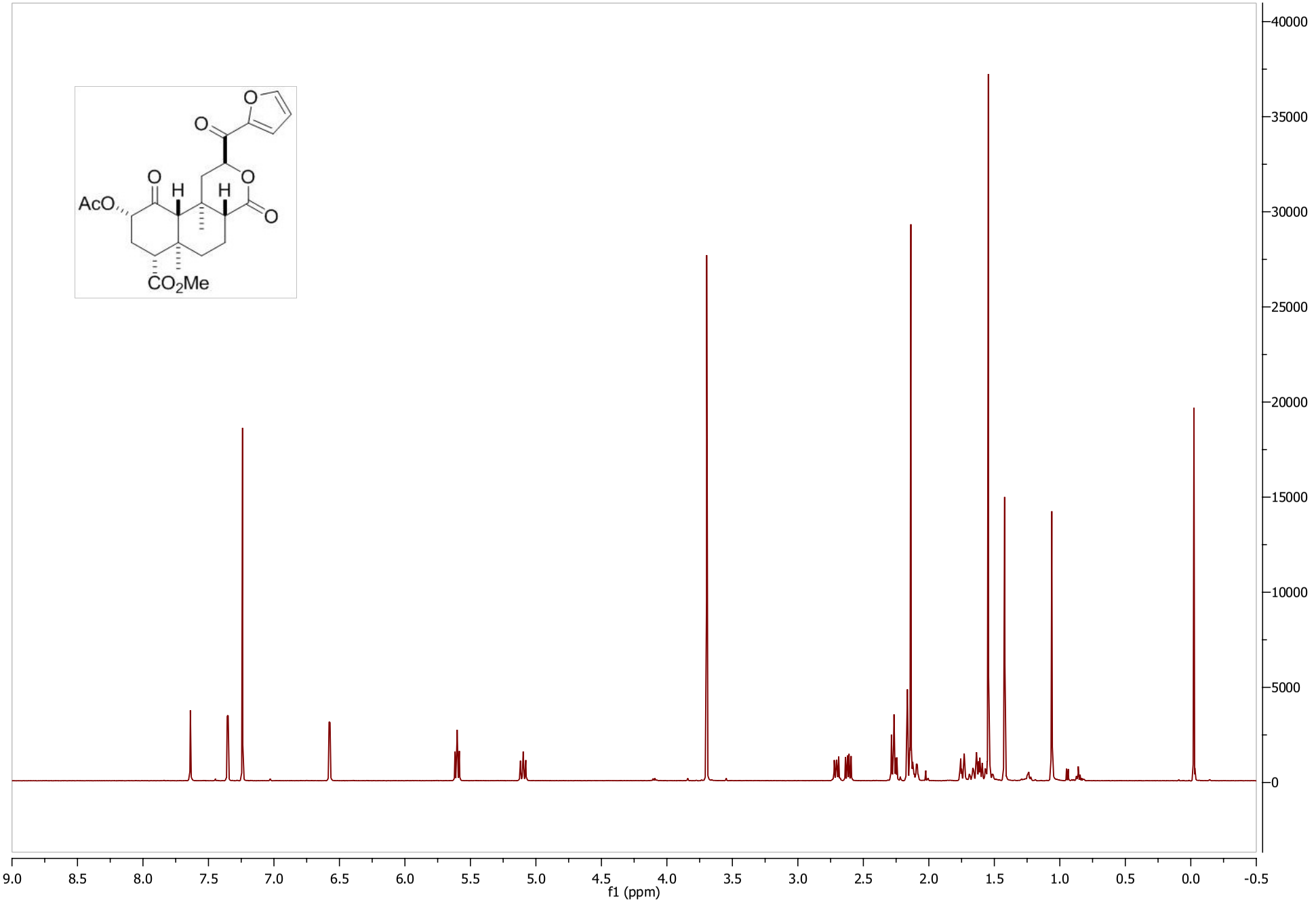
AcO
H
H
O
O
O
O
O
O
CO2Me
40000
35000
30000
25000
20000
15000
10000
5000
0
9.0
8.5
8.0
7.5
7.0
6.5
6.0
5.5
5.0
4.5
4.0
3.5
3.0
2.5
2.0
1.5
1.0
0.5
0.0
-0.5
f1 (ppm)

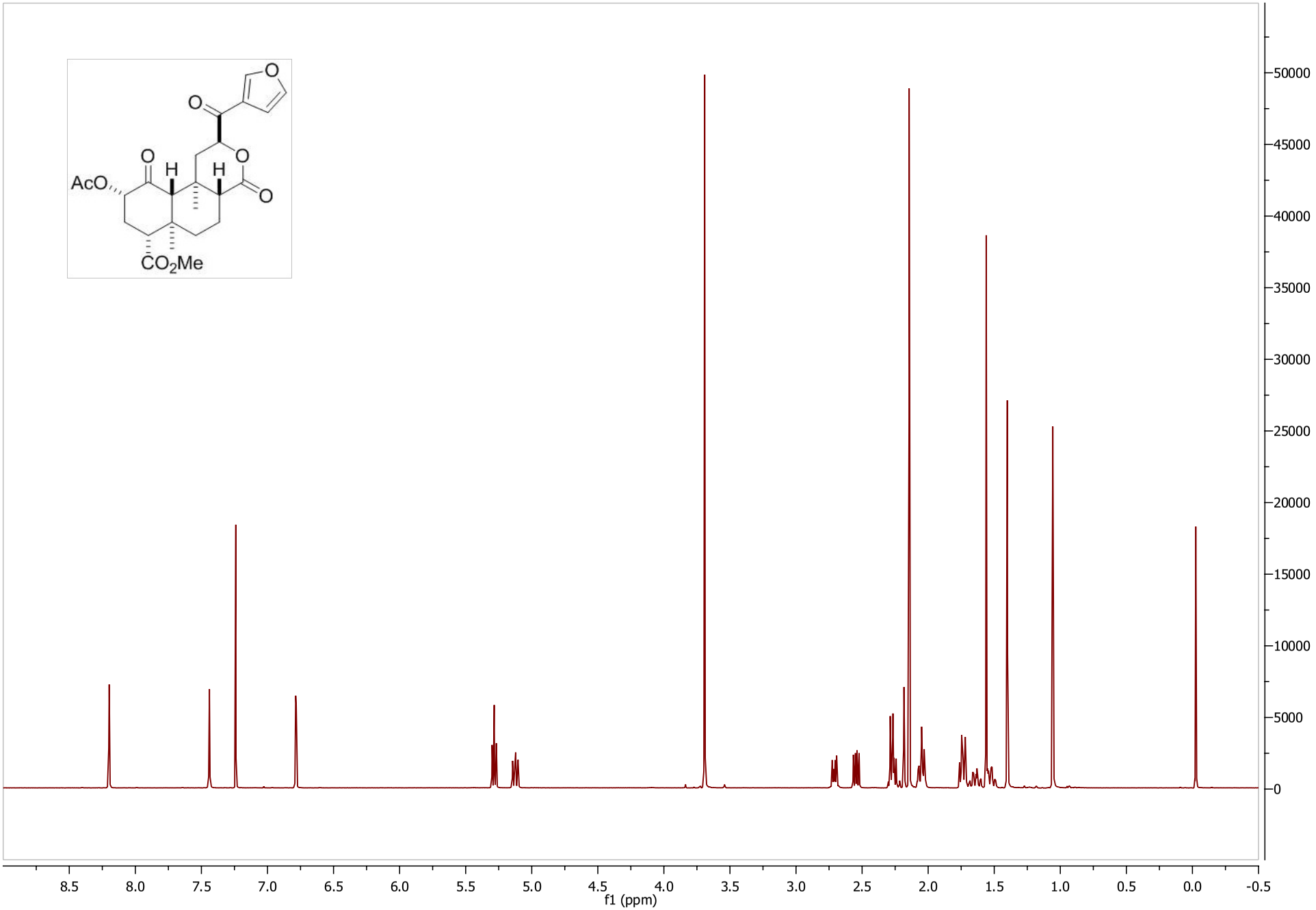
AcO
H
H
O
O
O
O
O
O
CO2Me
50000
45000
40000
35000
30000
25000
20000
15000
10000
5000
0
8.5
8.0
7.5
7.0
6.5
6.0
5.5
5.0
4.5
4.0
3.5
3.0
2.5
2.0
1.5
1.0
0.5
0.0
-0.5
f1 (ppm)

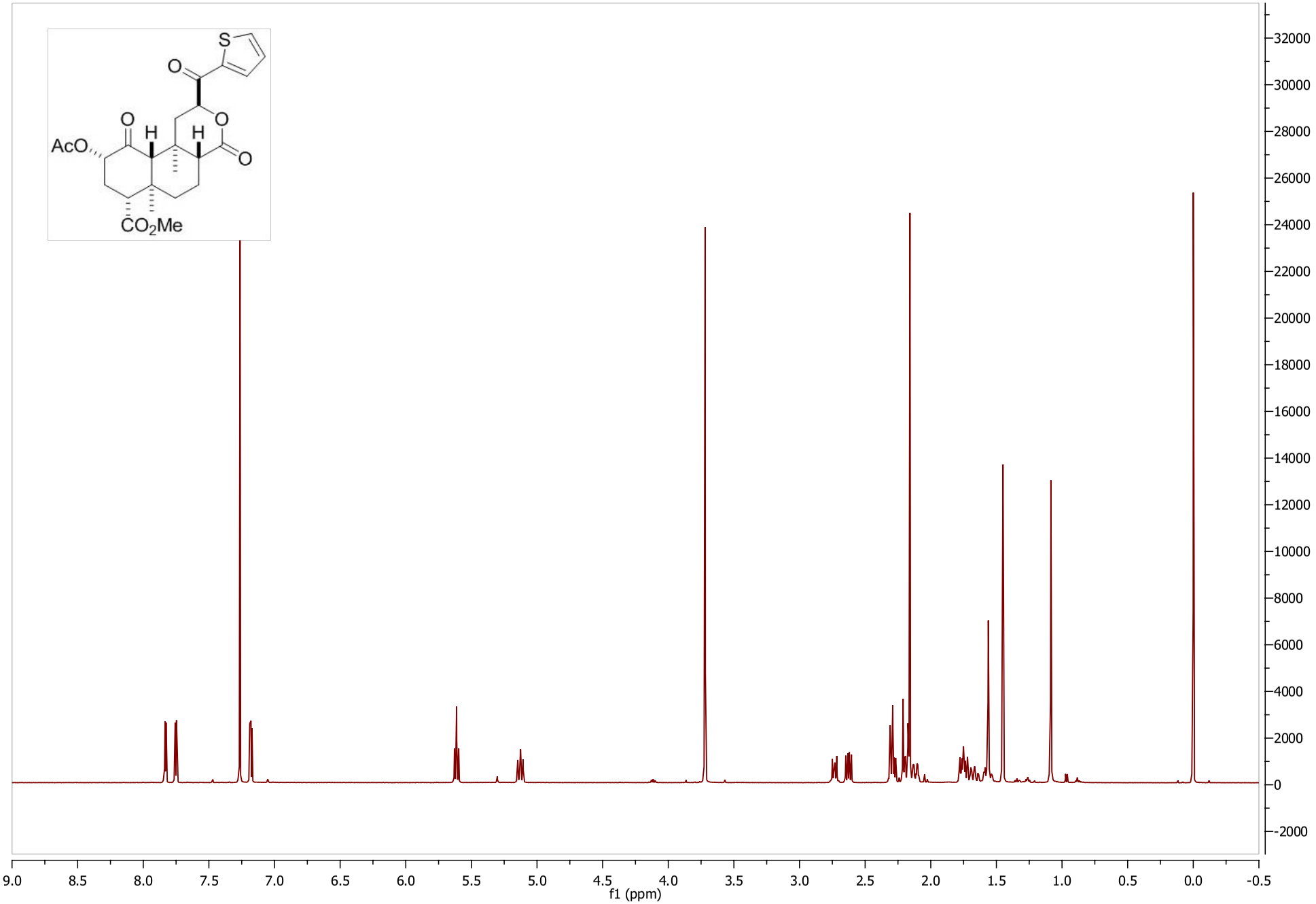
S
O
O
H
H
O
AcO
O
CO2Me
32000
30000
28000
26000
24000
22000
20000
18000
16000
14000
12000
10000
8000
6000
4000
2000
0
-2000
9.0
8.5
8.0
7.5
7.0
6.5
6.0
5.5
5.0
4.5
4.0
3.5
3.0
2.5
2.0
1.5
1.0
0.5
0.0
-0.5
f1 (ppm)

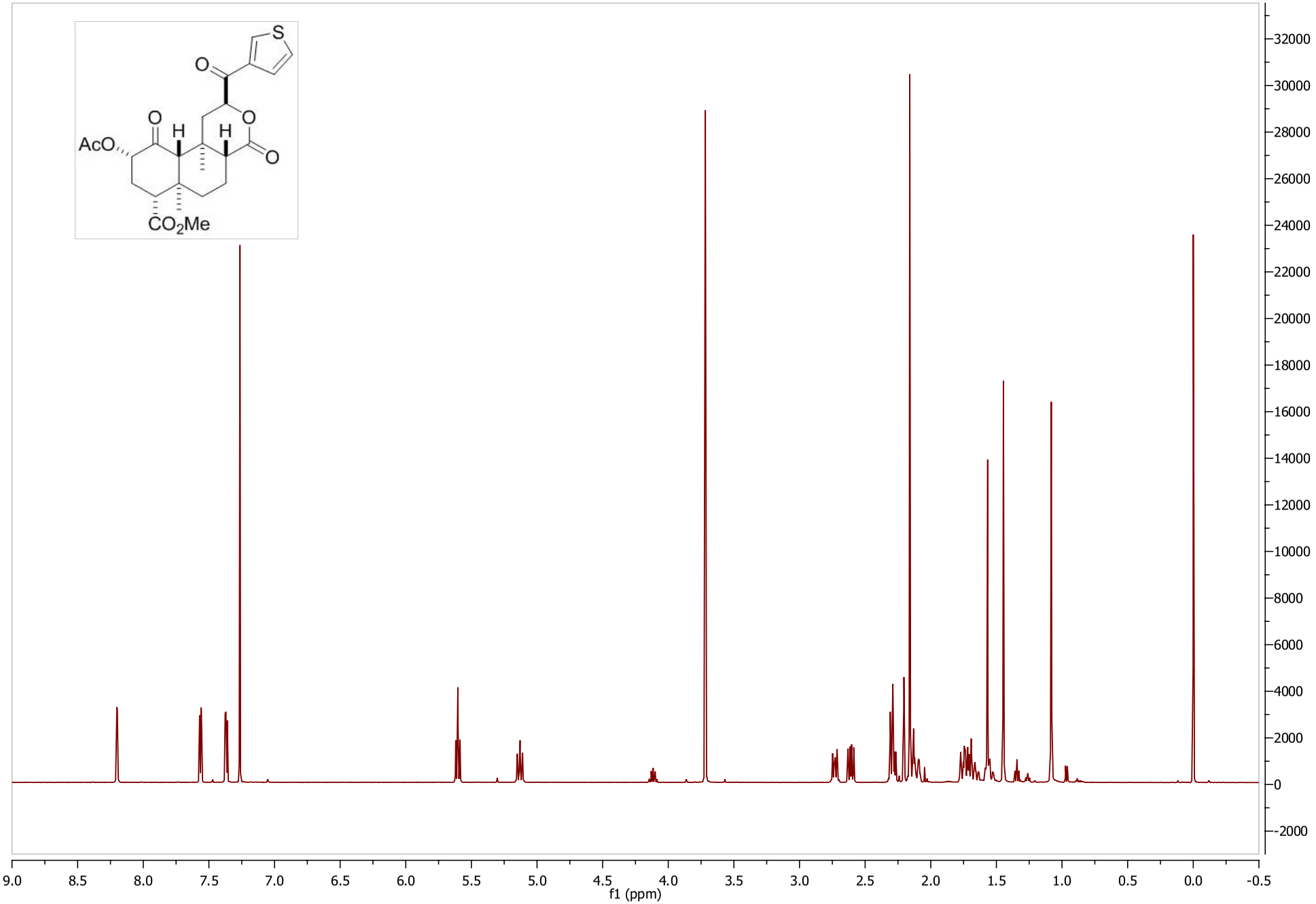
S
O
O
H
H
O
AcO
O
CO2Me
32000
30000
28000
26000
24000
22000
20000
18000
16000
14000
12000
10000
8000
6000
4000
2000
0
-2000
9.0
8.5
8.0
7.5
7.0
6.5
6.0
5.5
5.0
4.5
4.0
3.5
3.0
2.5
2.0
1.5
1.0
0.5
0.0
-0.5
f1 (ppm)

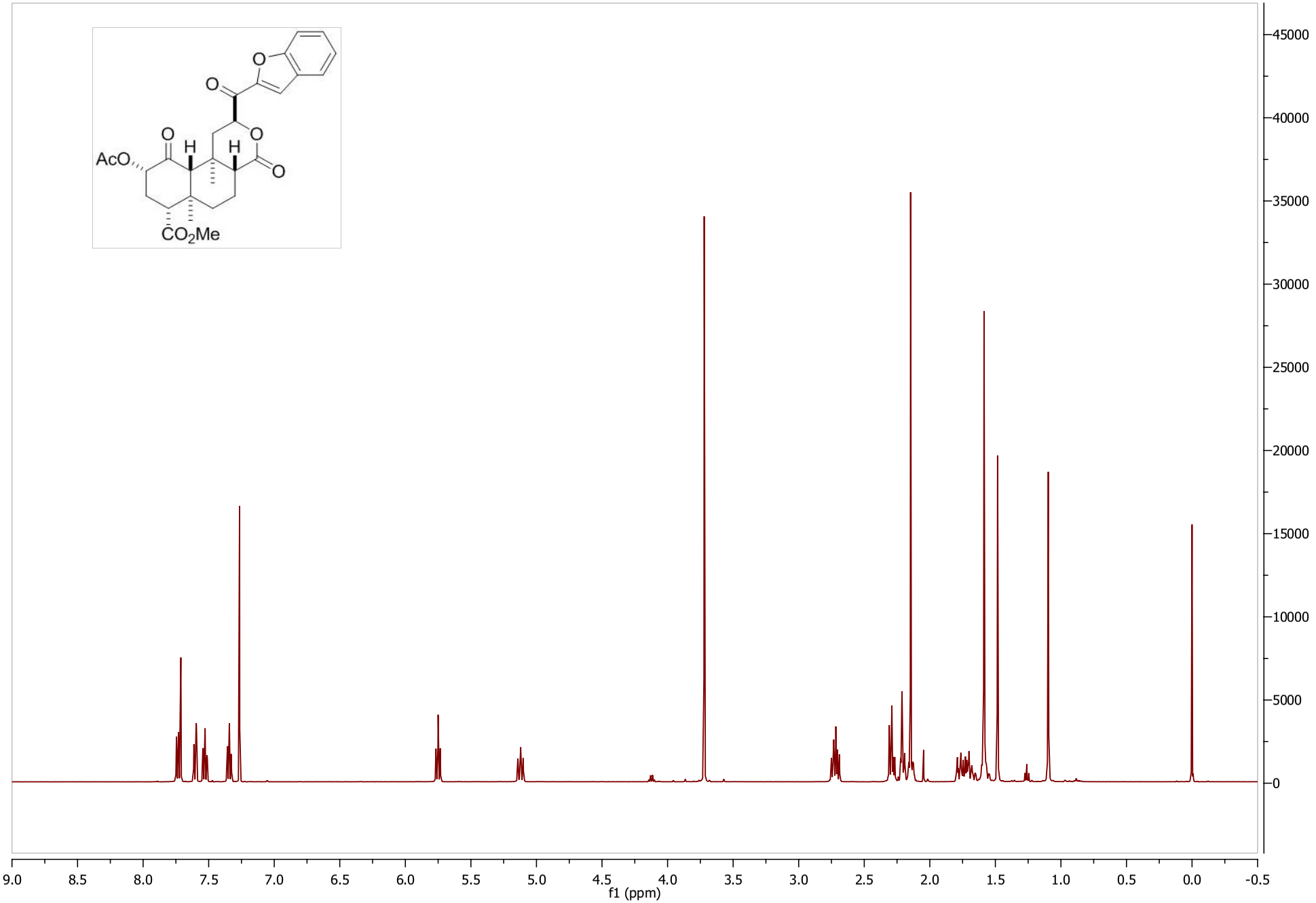
O
O
O
H
H
O
AcO
O
CO2Me
45000
40000
35000
30000
25000
20000
15000
10000
5000
0
9.0
8.5
8.0
7.5
7.0
6.5
6.0
5.5
5.0
4.5
4.0
3.5
3.0
2.5
2.0
1.5
1.0
0.5
0.0
-0.5
f1 (ppm)

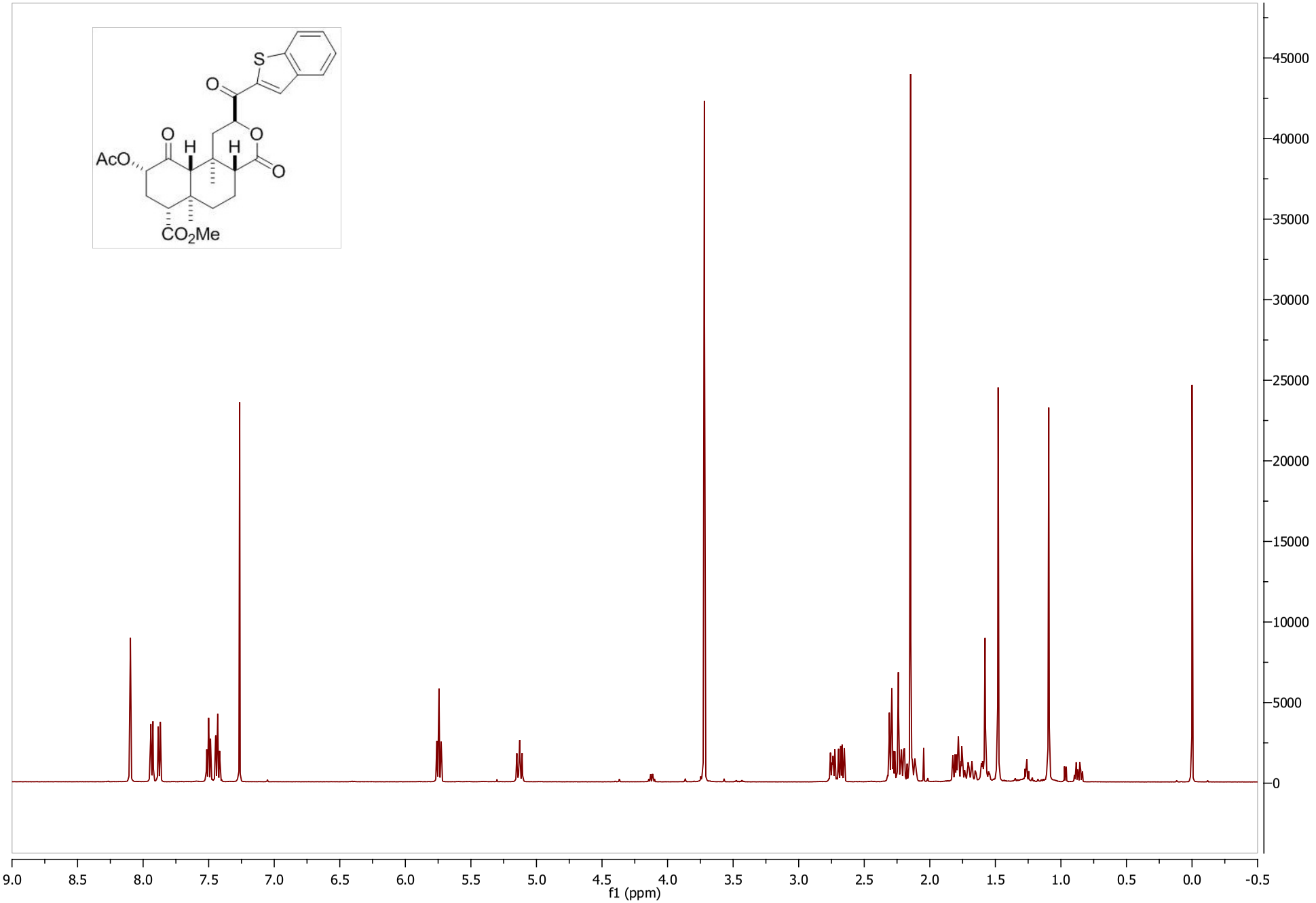
S
O
O
H
H
O
AcO
O
CO2Me
45000
40000
35000
30000
25000
20000
15000
10000
5000
0
9.0
8.5
8.0
7.5
7.0
6.5
6.0
5.5
5.0
4.5
4.0
3.5
3.0
2.5
2.0
1.5
1.0
0.5
0.0
-0.5
f1 (ppm)

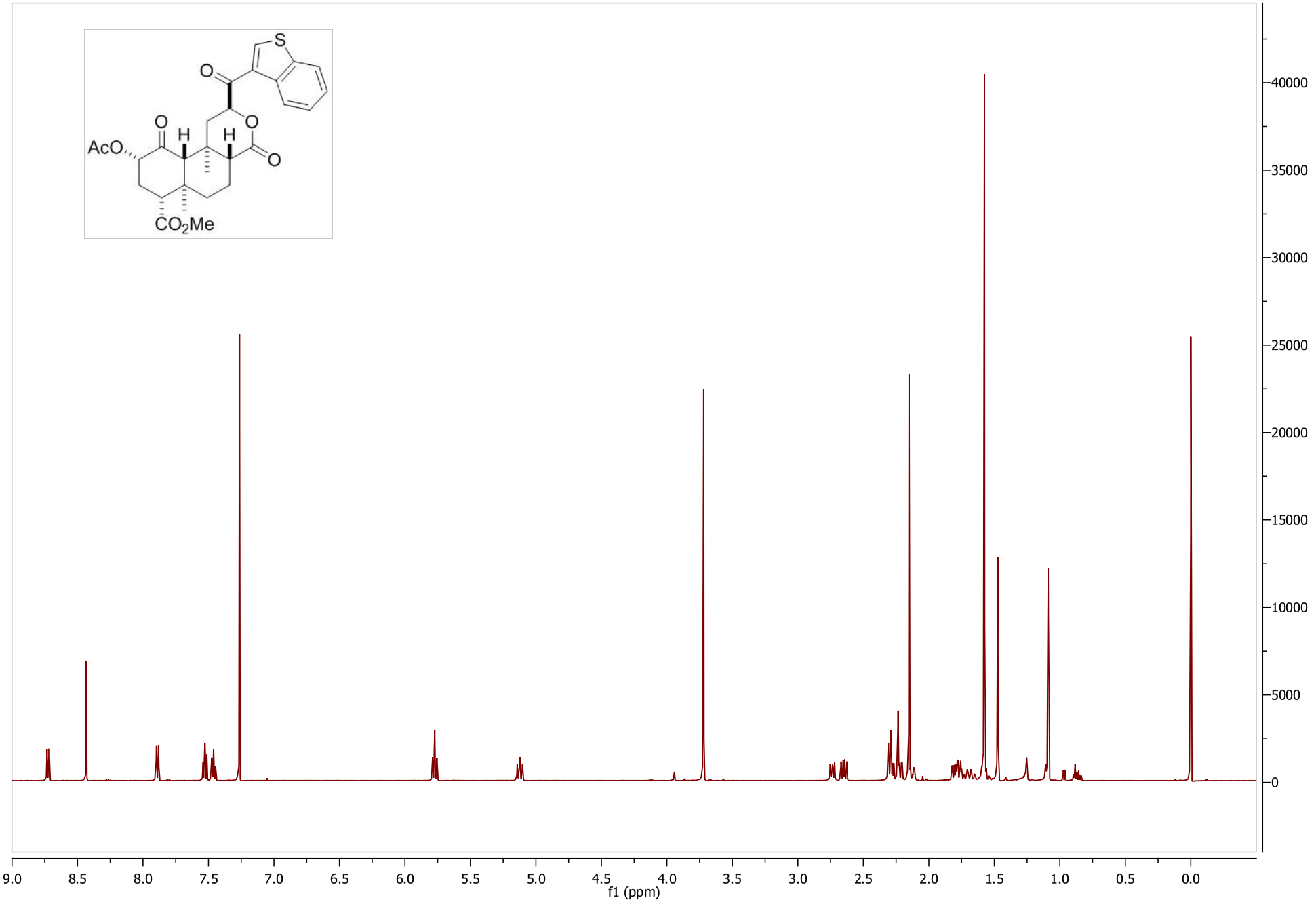
S
O
O
H
H
O
AcO
O
CO2Me
40000
35000
30000
25000
20000
15000
10000
5000
0
9.0
8.5
8.0
7.5
7.0
6.5
6.0
5.5
5.0
4.5
4.0
3.5
3.0
2.5
2.0
1.5
1.0
0.5
0.0
f1 (ppm)

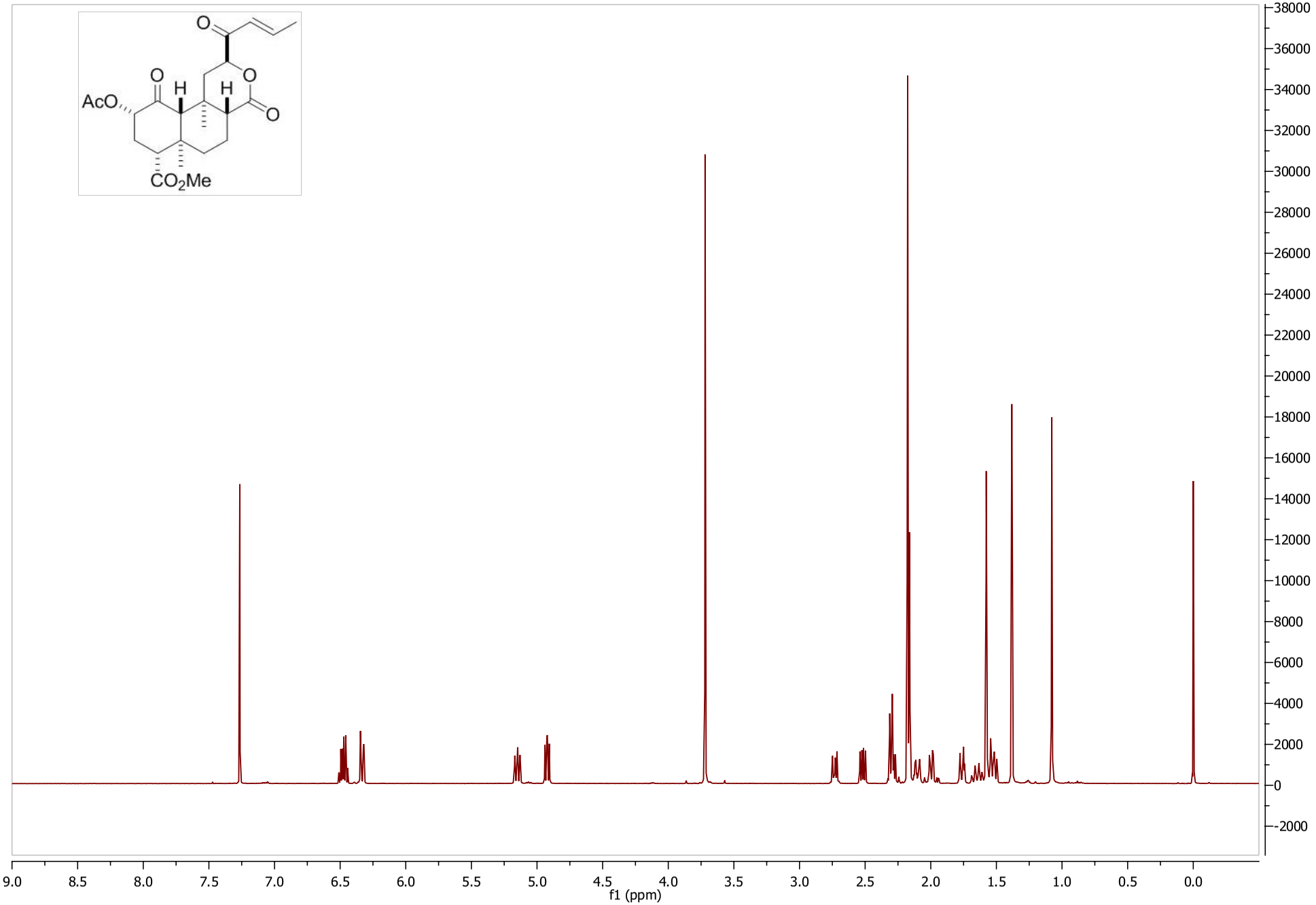
AcO
O
H
H
O
O
O
CO2Me
38000
36000
34000
32000
30000
28000
26000
24000
22000
20000
18000
16000
14000
12000
10000
8000
6000
4000
2000
0
-2000
9.0
8.5
8.0
7.5
7.0
6.5
6.0
5.5
5.0
4.5
4.0
3.5
3.0
2.5
2.0
1.5
1.0
0.5
0.0
f1 (ppm)

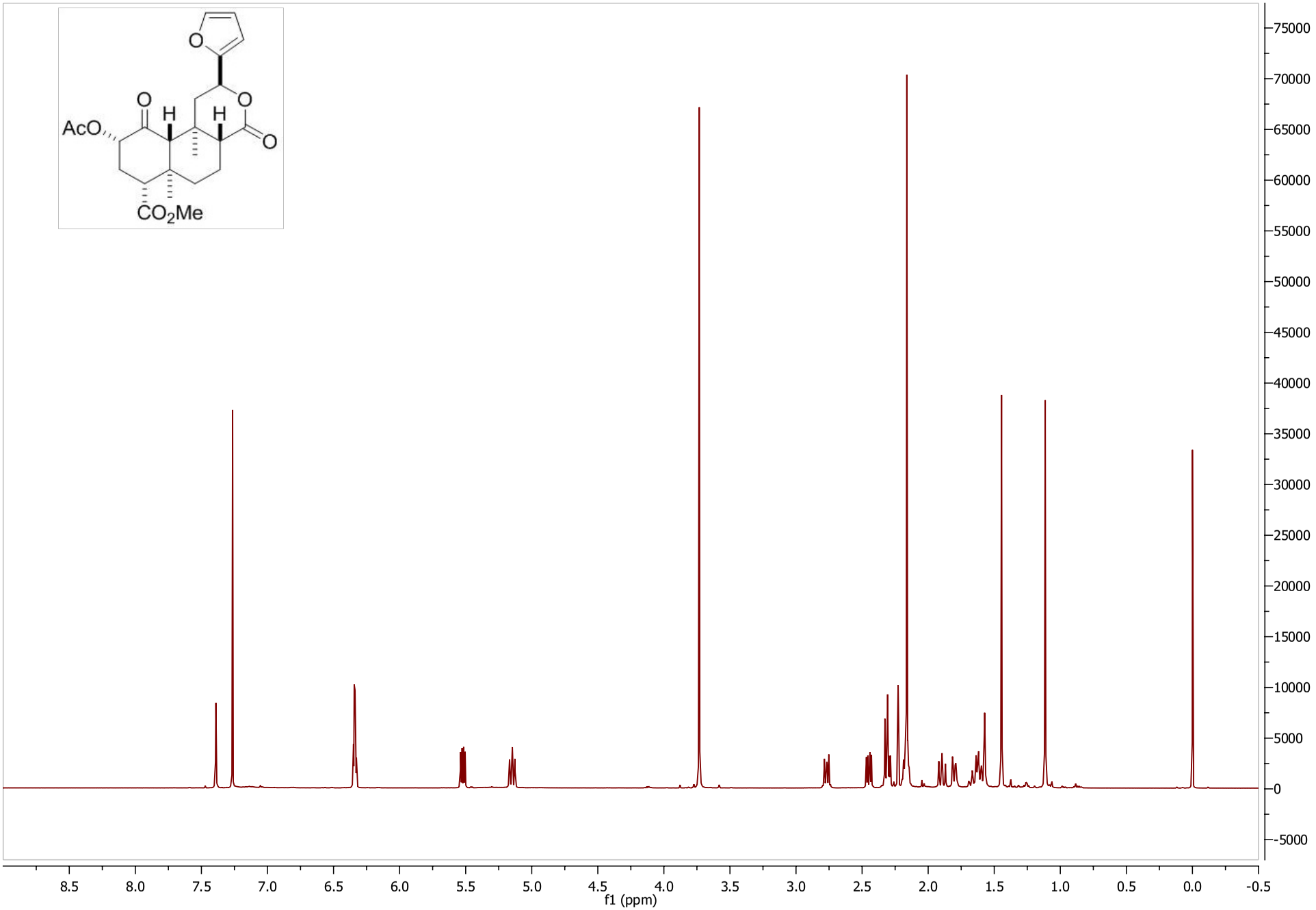
AcO
O
H
H
O
O
O
CO2Me
75000
70000
65000
60000
55000
50000
45000
40000
35000
30000
25000
20000
15000
10000
5000
0
-5000
8.5
8.0
7.5
7.0
6.5
6.0
5.5
5.0
4.5
4.0
3.5
3.0
2.5
2.0
1.5
1.0
0.5
0.0
-0.5
f1 (ppm)

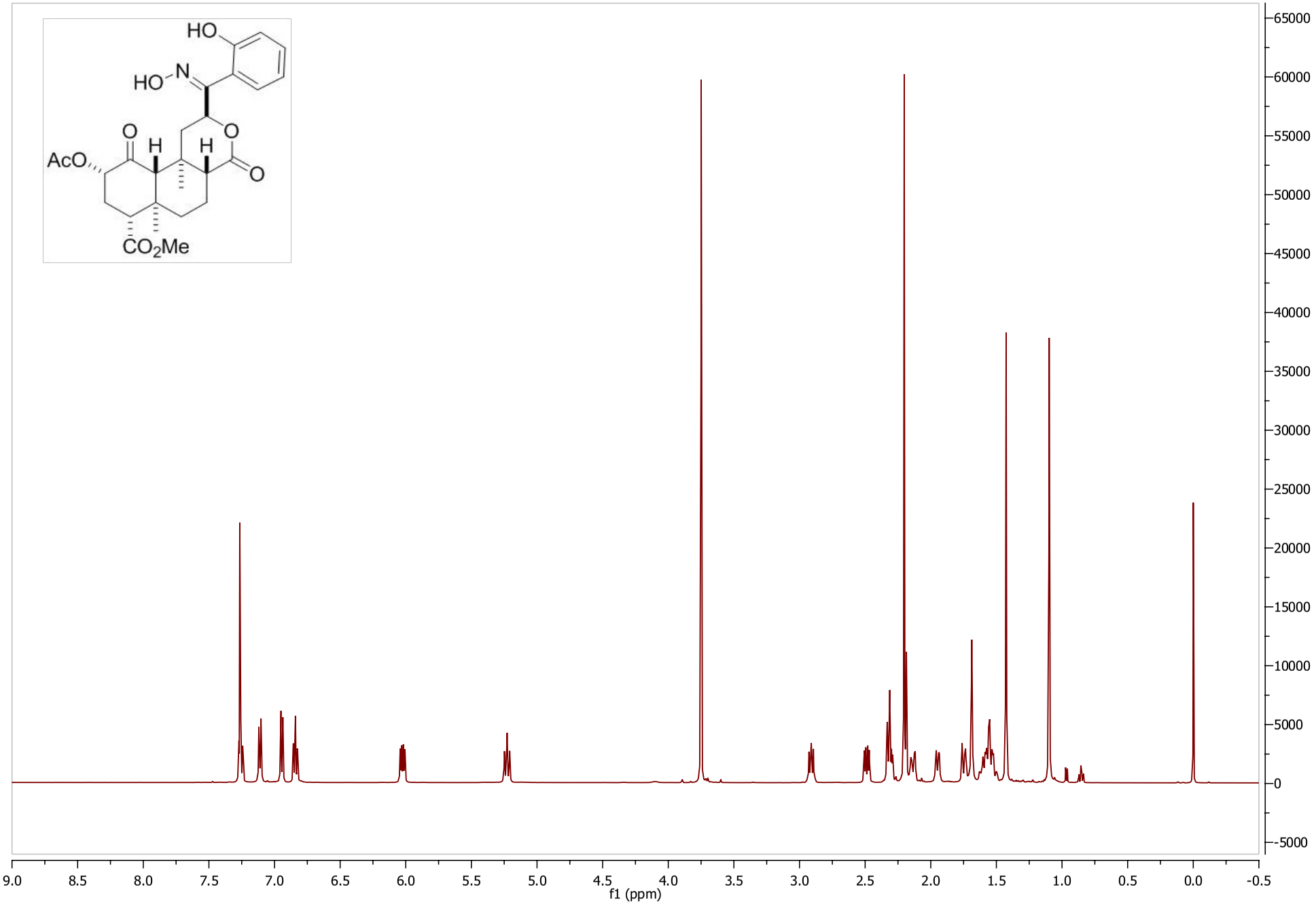
HO
HO
N
O
H
H
O
AcO
O
CO2Me
65000
60000
55000
50000
45000
40000
35000
30000
25000
20000
15000
10000
5000
0
-5000
9.0
8.5
8.0
7.5
7.0
6.5
6.0
5.5
5.0
4.5
4.0
3.5
3.0
2.5
2.0
1.5
1.0
0.5
0.0
-0.5
f1 (ppm)

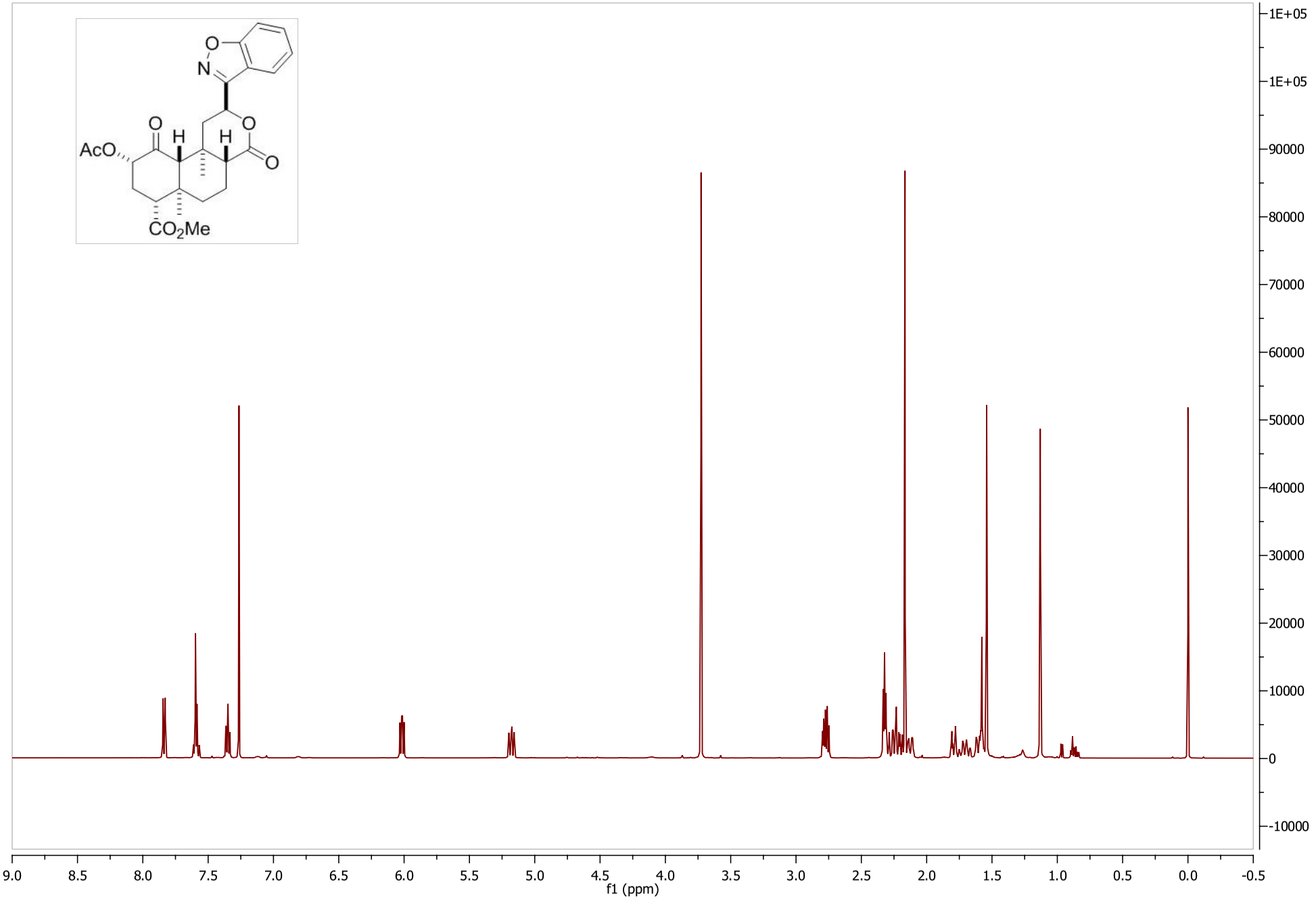
O
N
O
H
H
O
AcO
O
CO2Me
1E+05
1E+05
90000
80000
70000
60000
50000
40000
30000
20000
10000
0
-10000
9.0
8.5
8.0
7.5
7.0
6.5
6.0
5.5
5.0
4.5
4.0
3.5
3.0
2.5
2.0
1.5
1.0
0.5
0.0
-0.5
f1 (ppm)

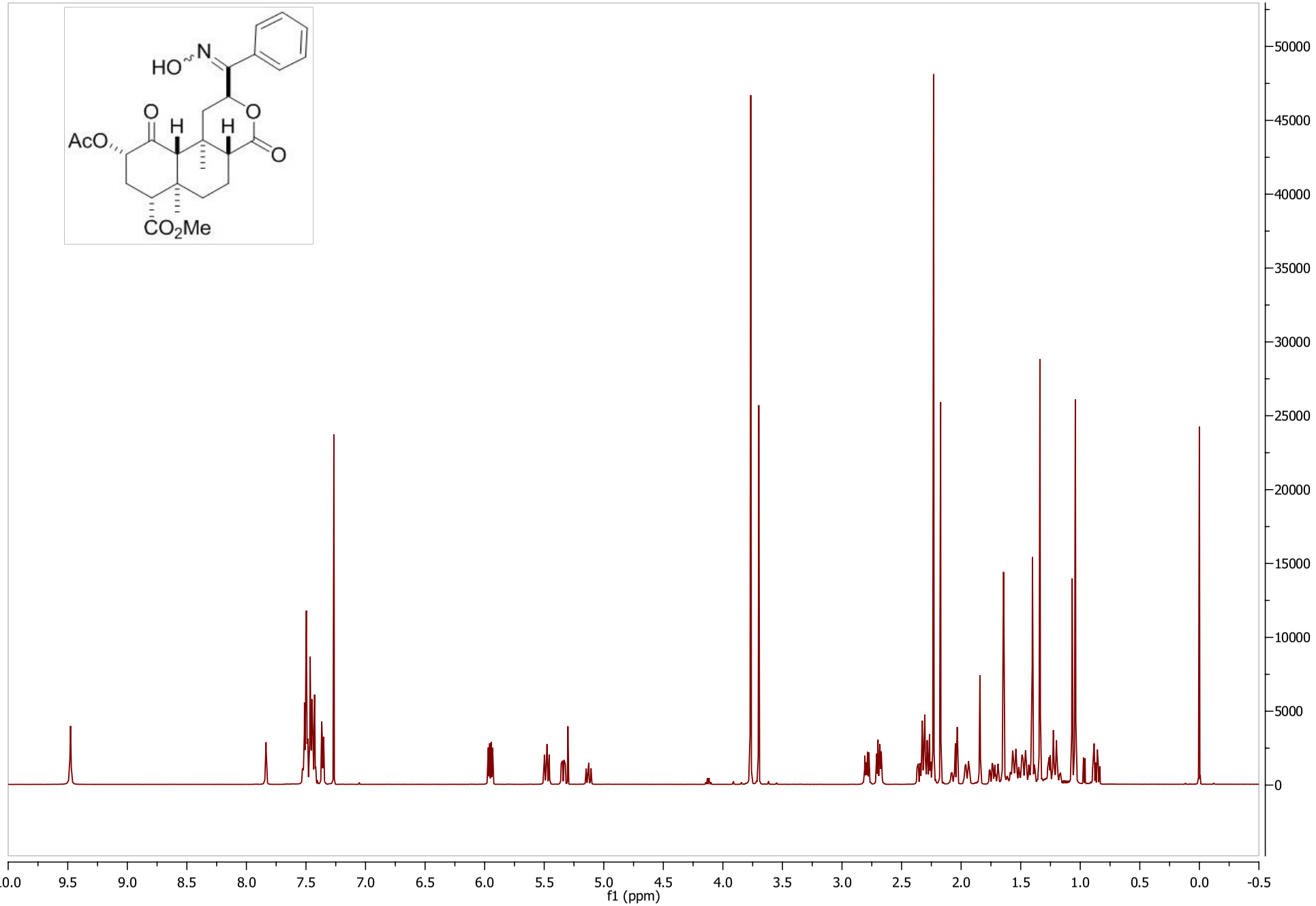
HO
N
O
H
H
O
AcO
O
CO2Me
50000
45000
40000
35000
30000
25000
20000
15000
10000
5000
0
10.0
9.5
9.0
8.5
8.0
7.5
7.0
6.5
6.0
5.5
5.0
4.5
4.0
3.5
3.0
2.5
2.0
1.5
1.0
0.5
0.0
-0.5
f1 (ppm)

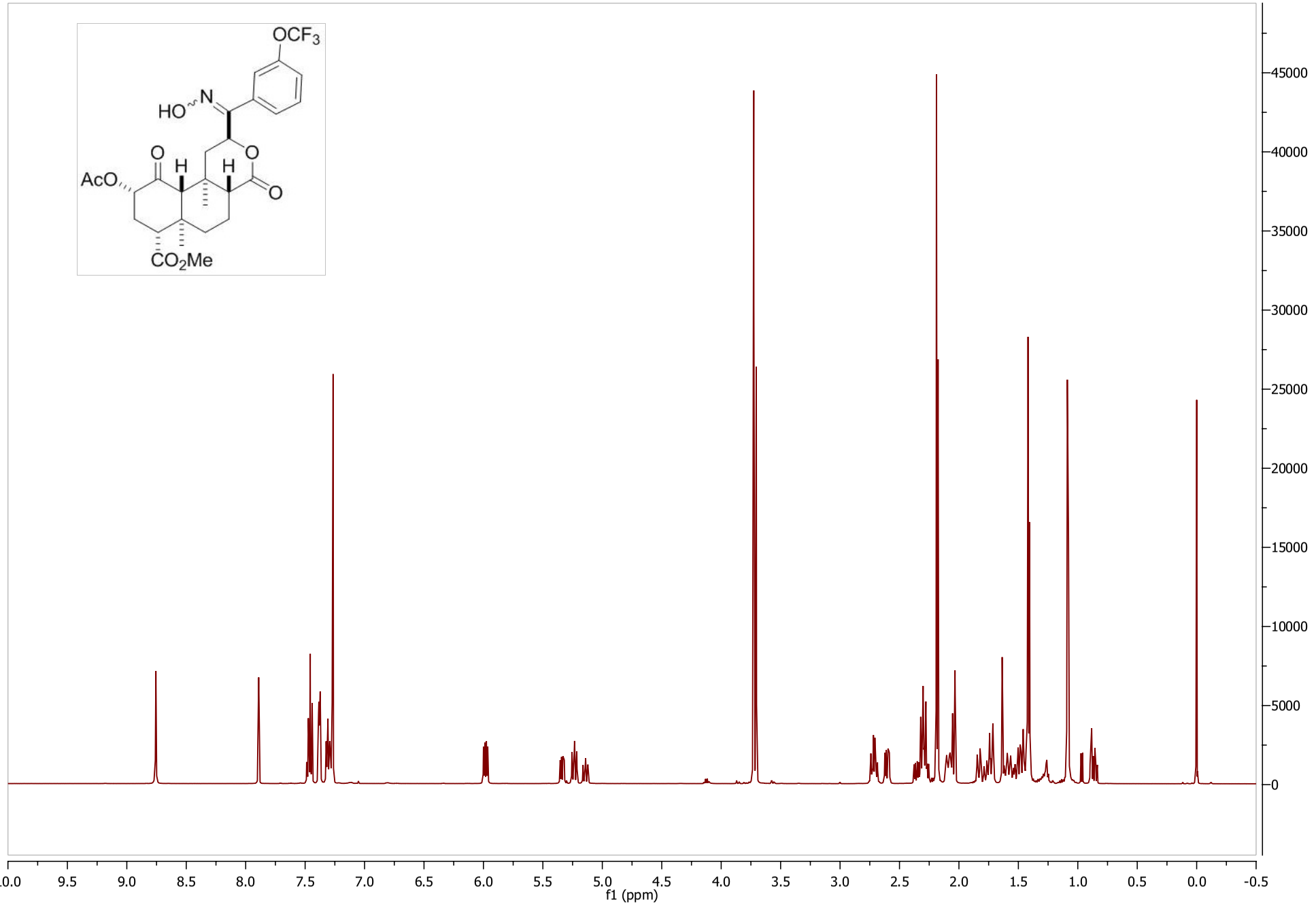
OCF3
HO
N
O
H
H
O
AcO
O
CO2Me
45000
40000
35000
30000
25000
20000
15000
10000
5000
0
10.0
9.5
9.0
8.5
8.0
7.5
7.0
6.5
6.0
5.5
5.0
4.5
4.0
3.5
3.0
2.5
2.0
1.5
1.0
0.5
0.0
-0.5
f1 (ppm)

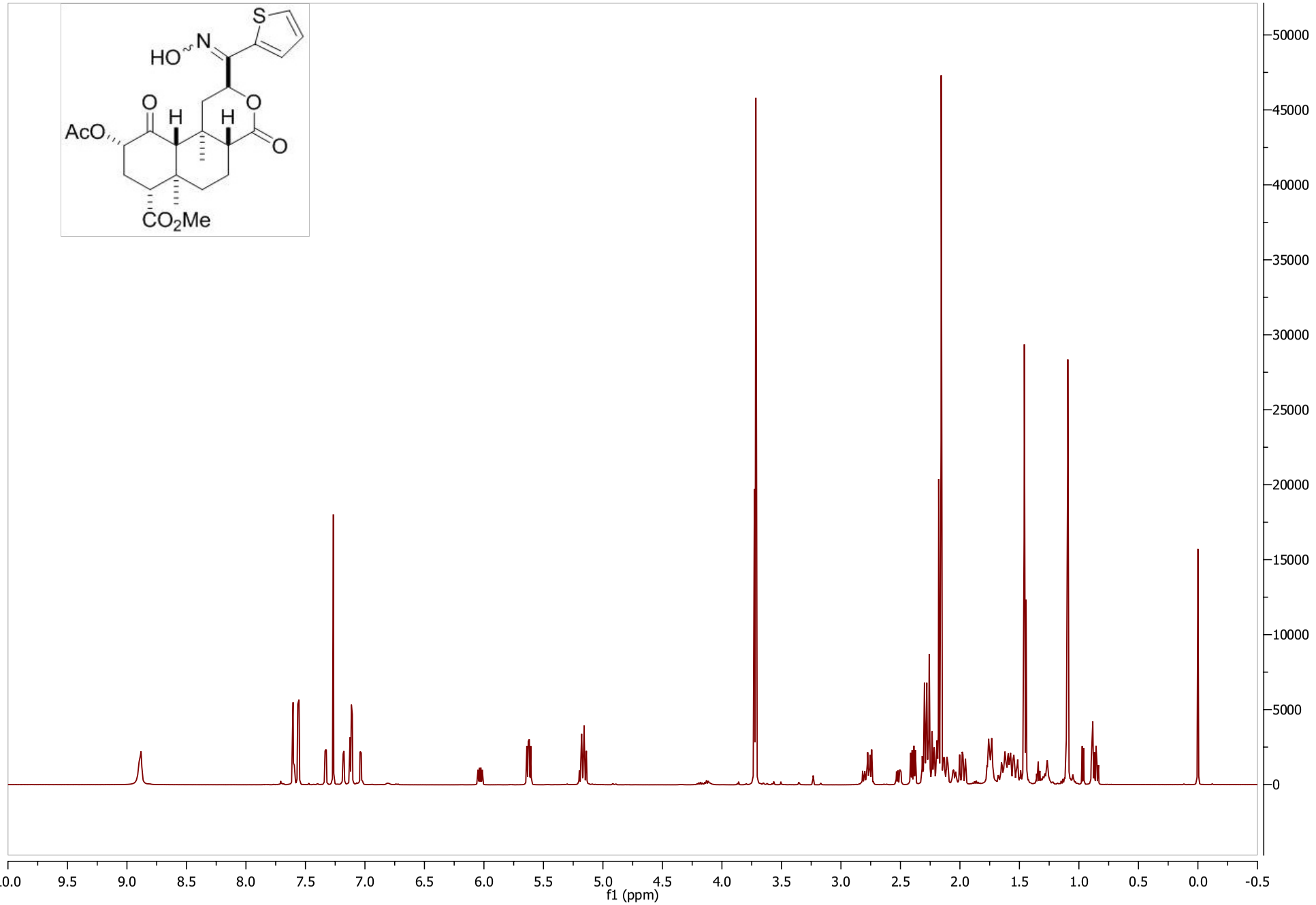
S
HO
N
O
H
H
O
AcO
O
CO2Me
50000
45000
40000
35000
30000
25000
20000
15000
10000
5000
0
10.0
9.5
9.0
8.5
8.0
7.5
7.0
6.5
6.0
5.5
5.0
4.5
4.0
3.5
3.0
2.5
2.0
1.5
1.0
0.5
0.0
-0.5
f1 (ppm)

APPENDIX B: HPLC CHROMATOGRAMS

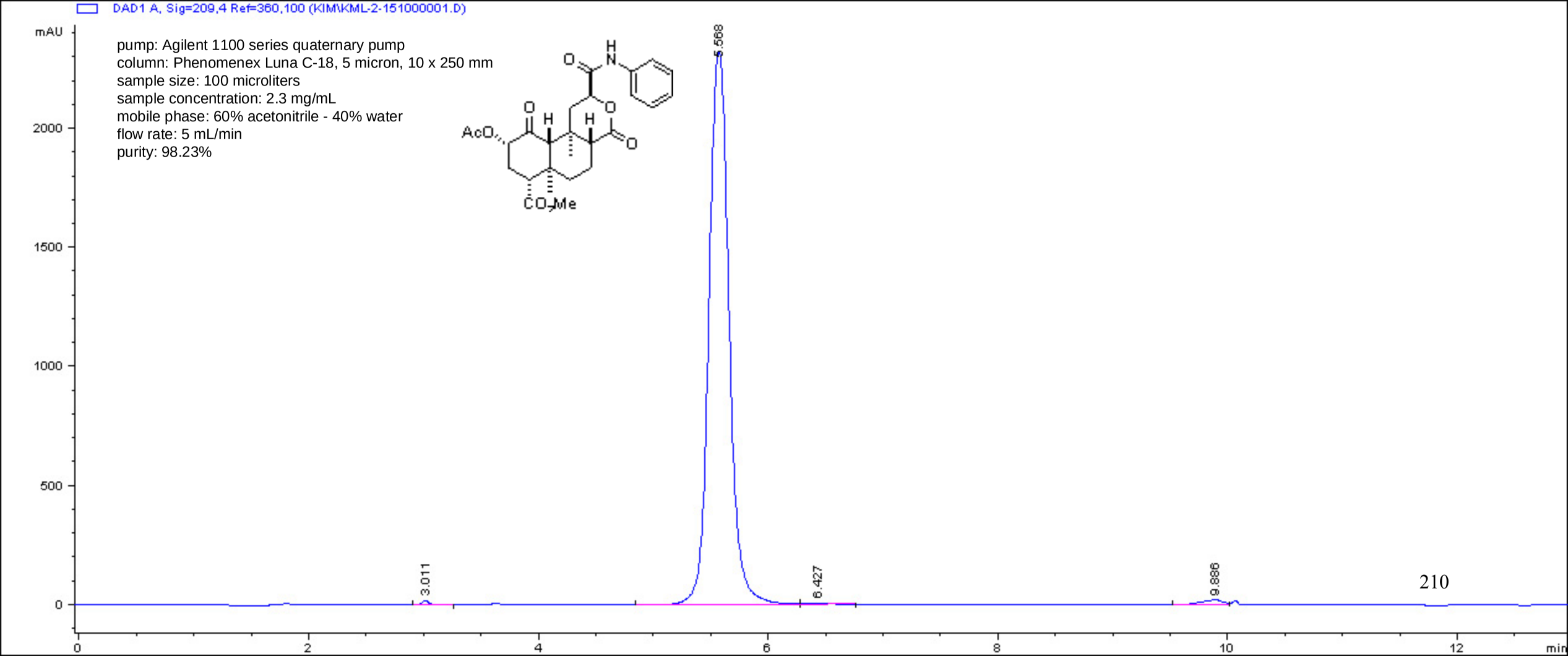
DAD1 A, Sig=209,4 Ref=360,100 (KIM\KML-2-151000001.D)
mAU
pump: Agilent 1100 series quaternary pump
column: Phenomenex Luna C-18, 5 micron, 10 x 250 mm
sample size: 100 microliters
sample concentration: 2.3 mg/mL
mobile phase: 60% acetonitrile - 40% water
flow rate: 5 mL/min
purity: 98.23%
AcO
CO2Me
3.011
5.568
6.427
9.886
2000
1500
1000
500
0
0
2
4
6
8
10
12
min

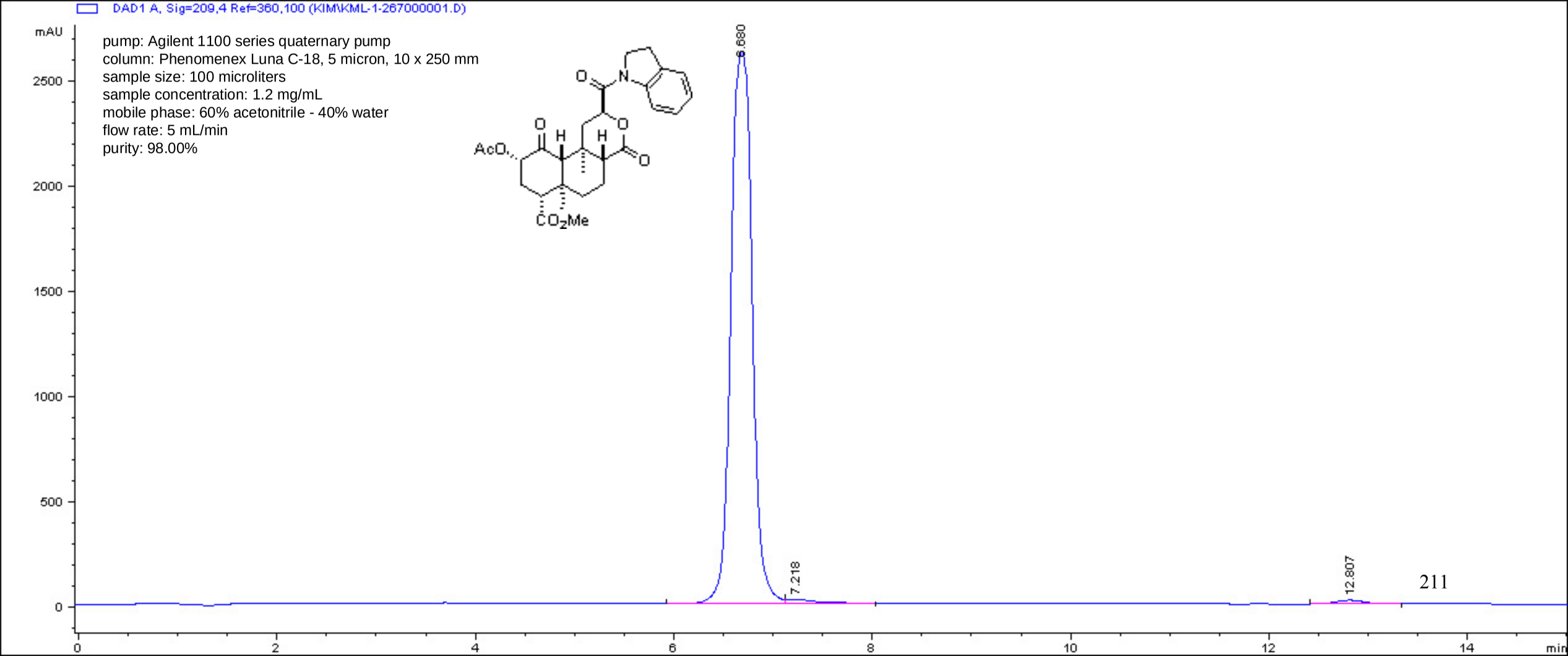
DAD1 A, Sig=209,4 Ref=360,100 (KIM\KML-1-267000001.D)
mAU
2500
2000
1500
1000
500
0
pump: Agilent 1100 series quaternary pump
column: Phenomenex Luna C-18, 5 micron, 10 x 250 mm
sample size: 100 microliters
sample concentration: 1.2 mg/mL
mobile phase: 60% acetonitrile - 40% water
flow rate: 5 mL/min
purity: 98.00%
AcO
H
H
O
N
O
O
O
O
CO2Me
6.680
7.218
12.807
0
2
4
6
8
10
12
14
min

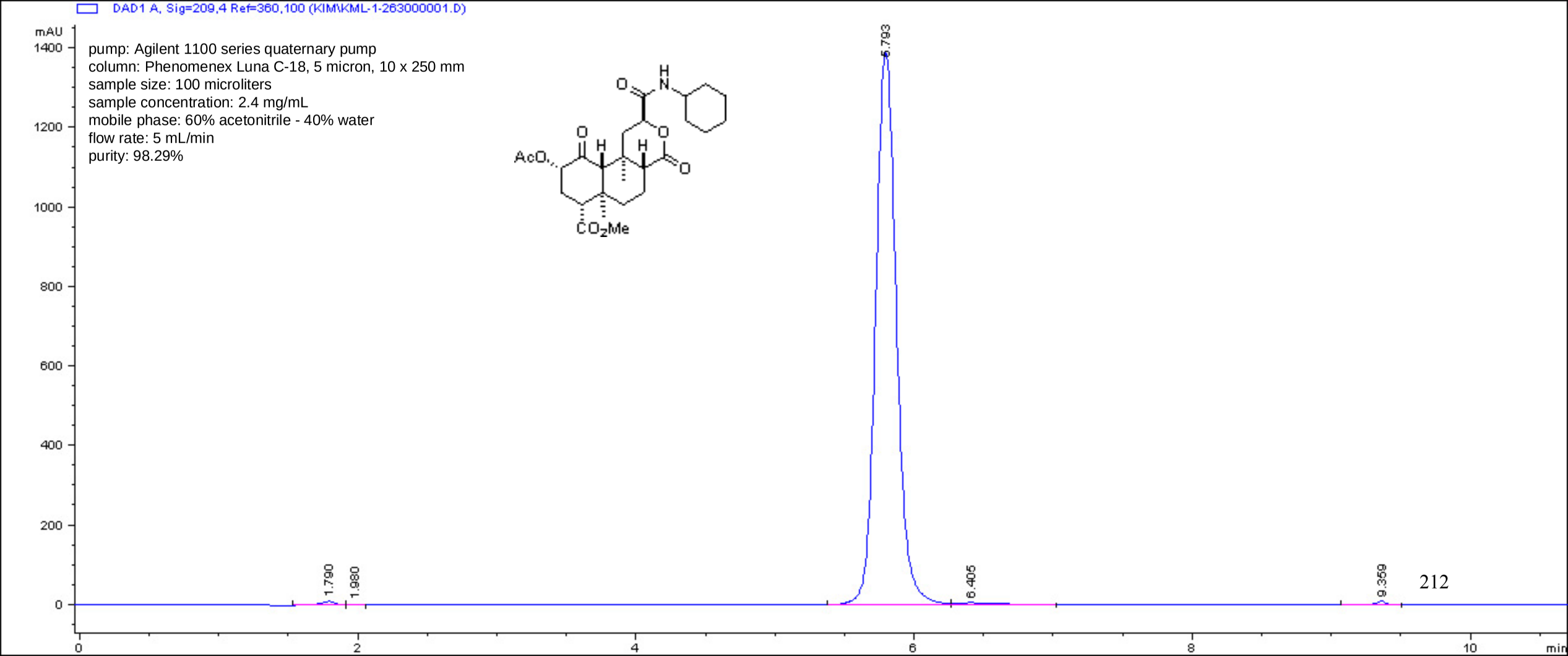
DAD1 A, Sig=209,4 Ref=360,100 (KIM\KML-1-263000001.D)
mAU
1400
1200
1000
800
600
400
200
0
pump: Agilent 1100 series quaternary pump
column: Phenomenex Luna C-18, 5 micron, 10 x 250 mm
sample size: 100 microliters
sample concentration: 2.4 mg/mL
mobile phase: 60% acetonitrile - 40% water
flow rate: 5 mL/min
purity: 98.29%
AcO
CO2Me
1.790
1.980
5.793
6.405
9.359
0
2
4
6
8
10
min

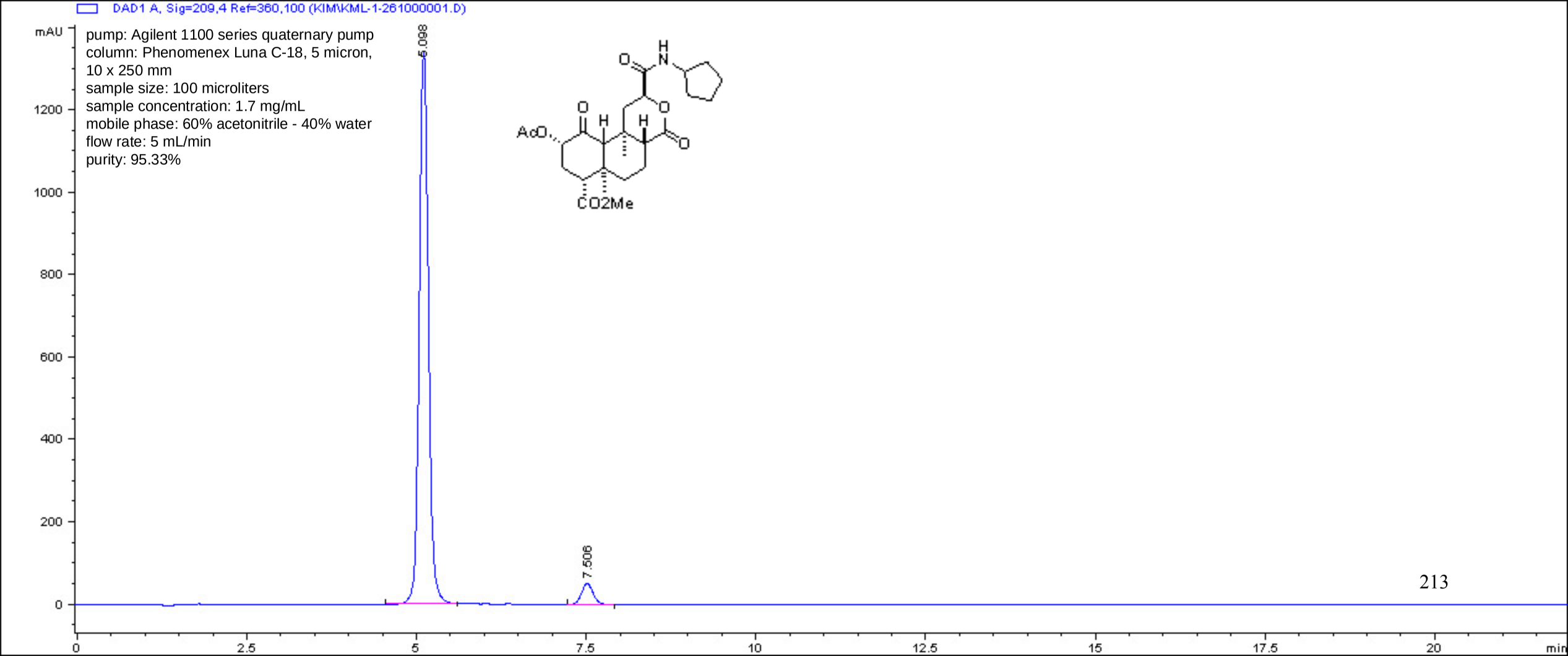
DAD1 A, Sig=209,4 Ref=360,100 (KIM\KML-1-261000001.D)
mAU
pump: Agilent 1100 series quaternary pump
column: Phenomenex Luna C-18, 5 micron, 10 x 250 mm
sample size: 100 microliters
sample concentration: 1.7 mg/mL
mobile phase: 60% acetonitrile - 40% water
flow rate: 5 mL/min
purity: 95.33%
5.098
7.506
AcO
CO2Me
1200
1000
800
600
400
200
0
2.5
5
7.5
10
12.5
15
17.5
20
min

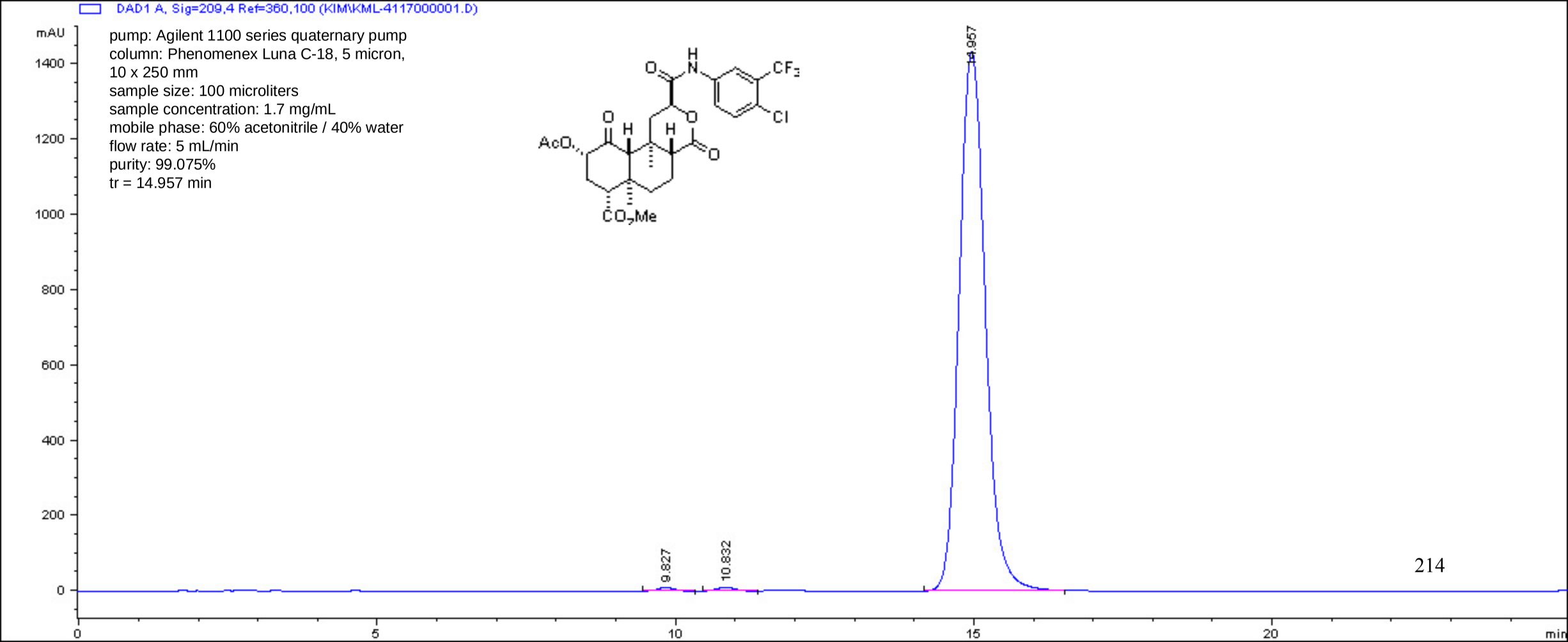
DAD1 A, Sig=209,4 Ref=360,100 (KIM\KML-4117000001.D)
pump: Agilent 1100 series quaternary pump
column: Phenomenex Luna C-18, 5 micron,
10 x 250 mm
sample size: 100 microliters
sample concentration: 1.7 mg/mL
mobile phase: 60% acetonitrile / 40% water
flow rate: 5 mL/min
purity: 99.075%
tr = 14.957 min
mAU
1400
1200
1000
800
600
400
200
0
9.827
10.832
14.957
0
5
10
15
20
min
214

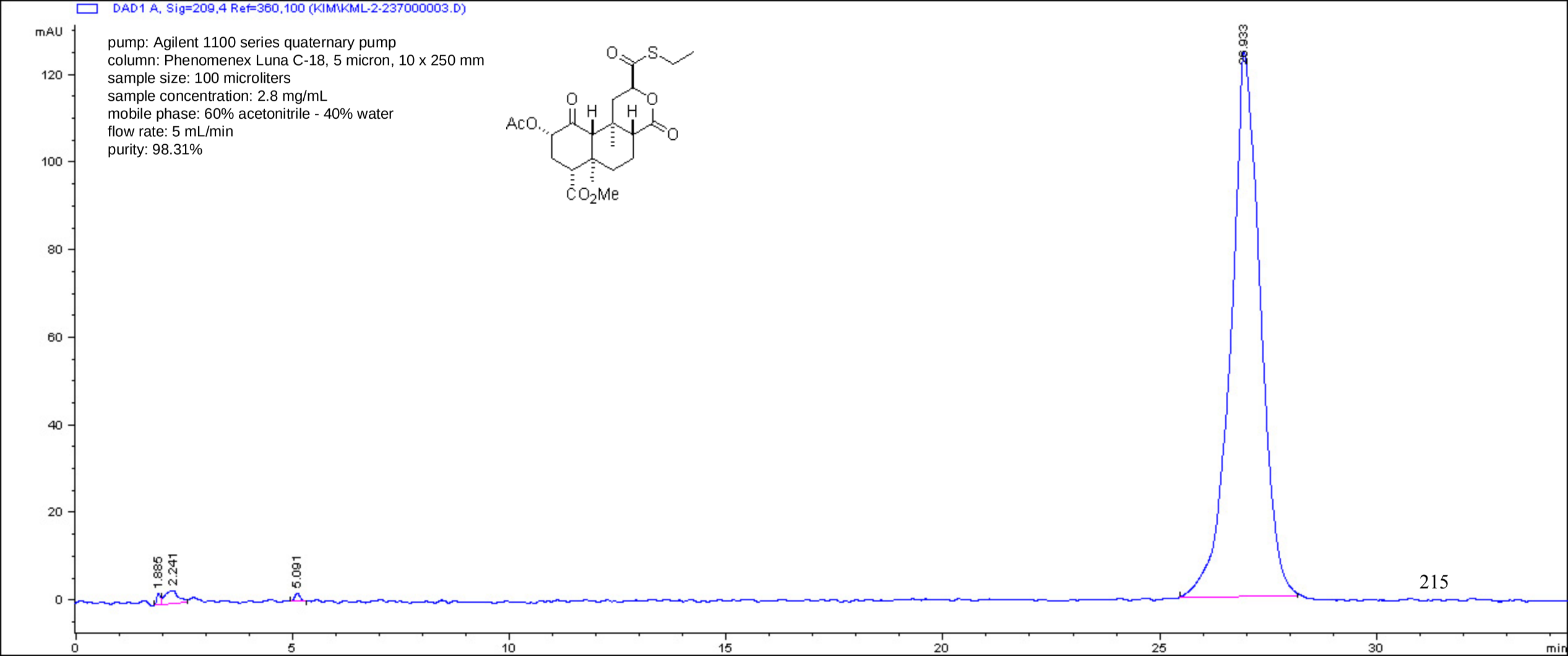
DAD1 A, Sig=209,4 Ref=360,100 (KIM\KML-2-237000003.D)
mAU
pump: Agilent 1100 series quaternary pump
column: Phenomenex Luna C-18, 5 micron, 10 x 250 mm
sample size: 100 microliters
sample concentration: 2.8 mg/mL
mobile phase: 60% acetonitrile - 40% water
flow rate: 5 mL/min
purity: 98.31%
AcO
H
H
CO2Me
1.885
2.241
5.091
26.933
215
min

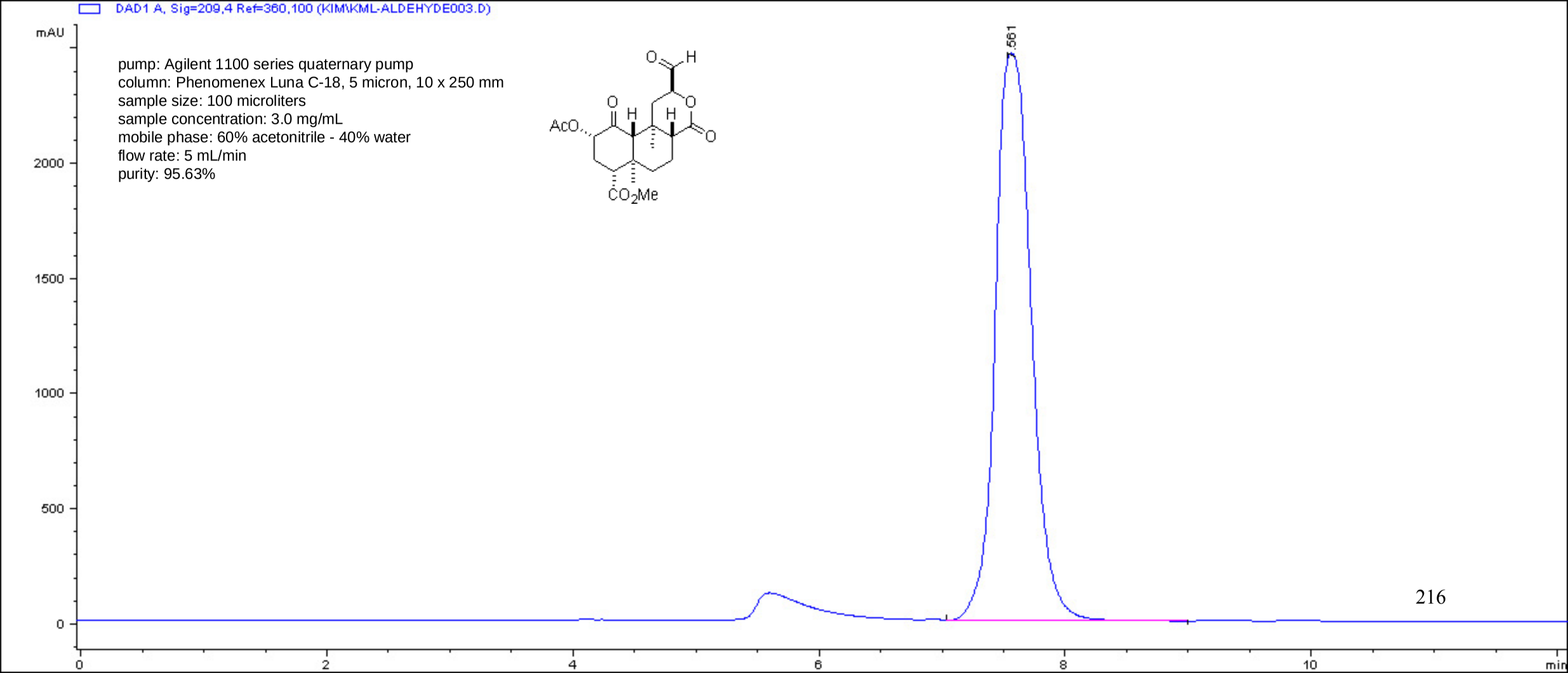
DAD1 A, Sig=209,4 Ref=360,100 (KIM\KML-ALDEHYDE003.D)
mAU
pump: Agilent 1100 series quaternary pump
column: Phenomenex Luna C-18, 5 micron, 10 x 250 mm
sample size: 100 microliters
sample concentration: 3.0 mg/mL
mobile phase: 60% acetonitrile - 40% water
flow rate: 5 mL/min
purity: 95.63%
AcO
CO2Me
7.561
2000
1500
1000
500
0
0
2
4
6
8
10
min

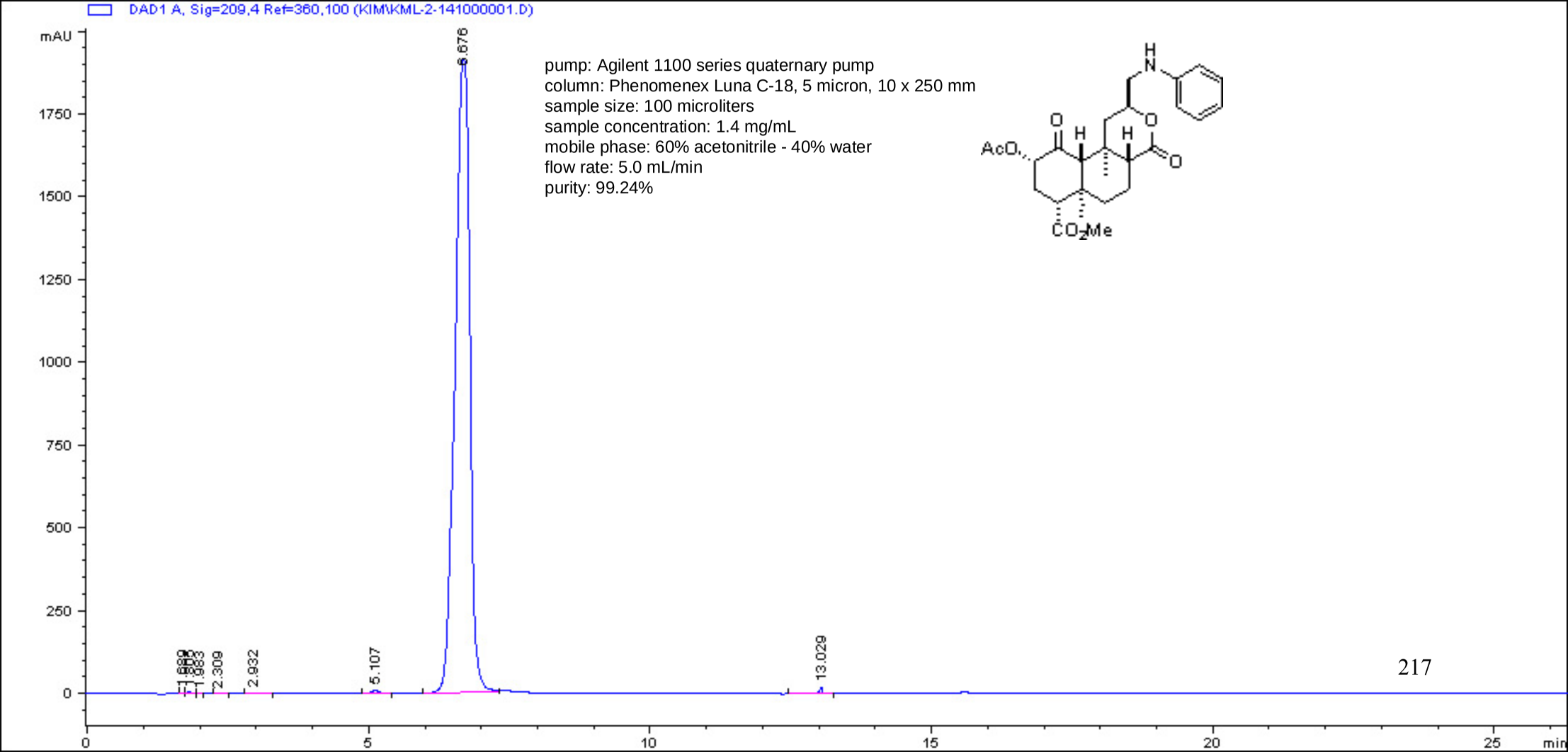
DAD1 A, Sig=209,4 Ref=360,100 (KIM\KML-2-141000001.D)
mAU
1750
1500
1250
1000
750
500
250
0
6.676
2.309
2.932
5.107
13.029
0
5
10
15
20
25
min
pump: Agilent 1100 series quaternary pump
column: Phenomenex Luna C-18, 5 micron, 10 x 250 mm
sample size: 100 microliters
sample concentration: 1.4 mg/mL
mobile phase: 60% acetonitrile - 40% water
flow rate: 5.0 mL/min
purity: 99.24%
H
N
O
O
H
H
O
AcO
O
CO2Me

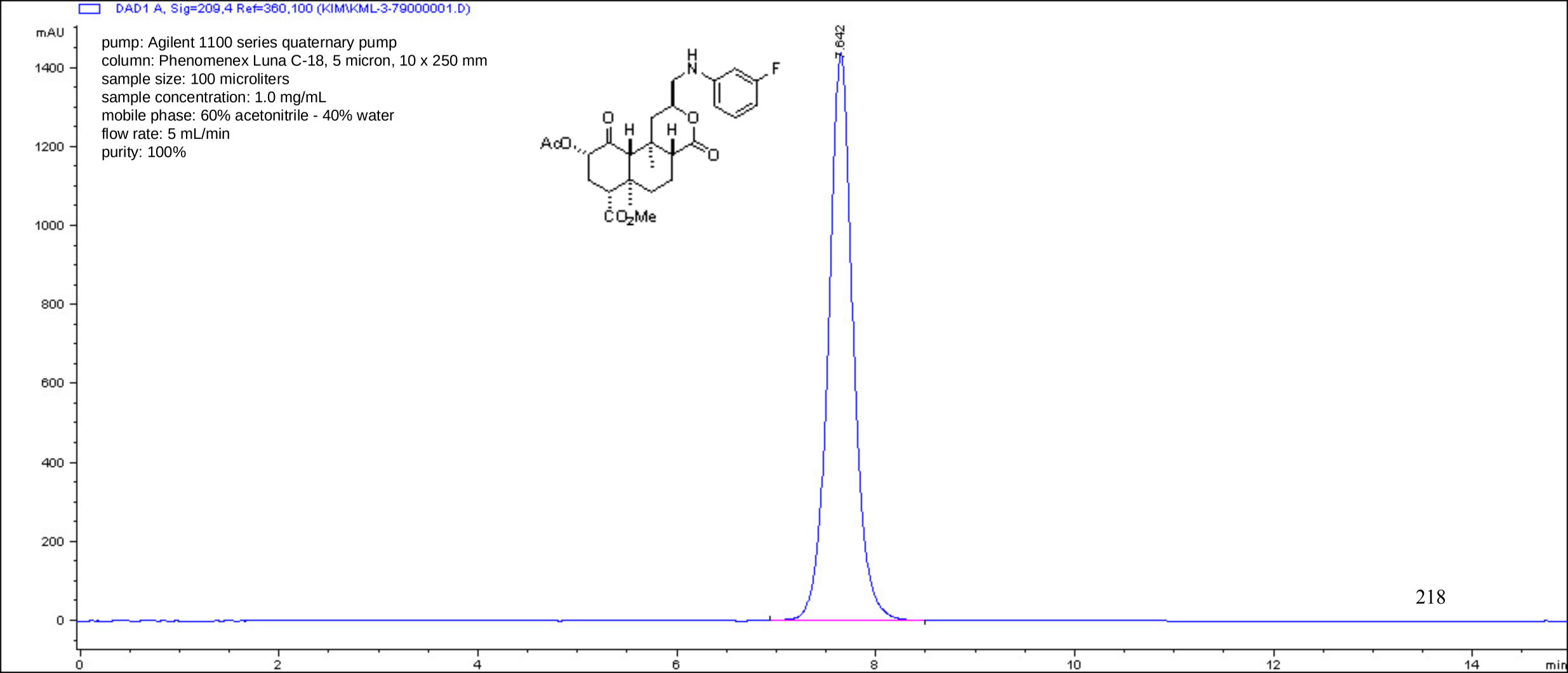
DAD1 A, Sig=209,4 Ref=360,100 (KIM\KML-3-79000001.D)
mAU
1400
1200
1000
800
600
400
200
0
pump: Agilent 1100 series quaternary pump
column: Phenomenex Luna C-18, 5 micron, 10 x 250 mm
sample size: 100 microliters
sample concentration: 1.0 mg/mL
mobile phase: 60% acetonitrile - 40% water
flow rate: 5 mL/min
purity: 100%
7.642
AcO
O
H
H
O
O
H
N
F
CO2Me
0
2
4
6
8
10
12
14
min

DAD1 A, Sig=209,4 Ref=360,100 (KIM\KML-3-61000001.D)

pump: Agilent 1100 series quaternary pump
column: Phenomenex Luna C-18, 5 micron, 10 x 250 mm
sample size: 100 microliters
sample concentration: 1.0 mg/mL
mobile phase: 60% acetonitrile - 40% water
flow rate: 5 mL/min
purity: 100%

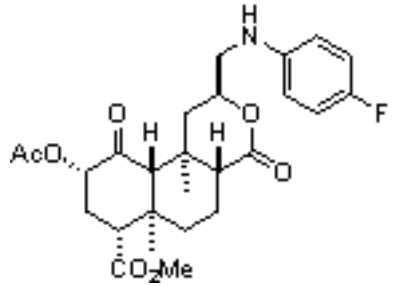

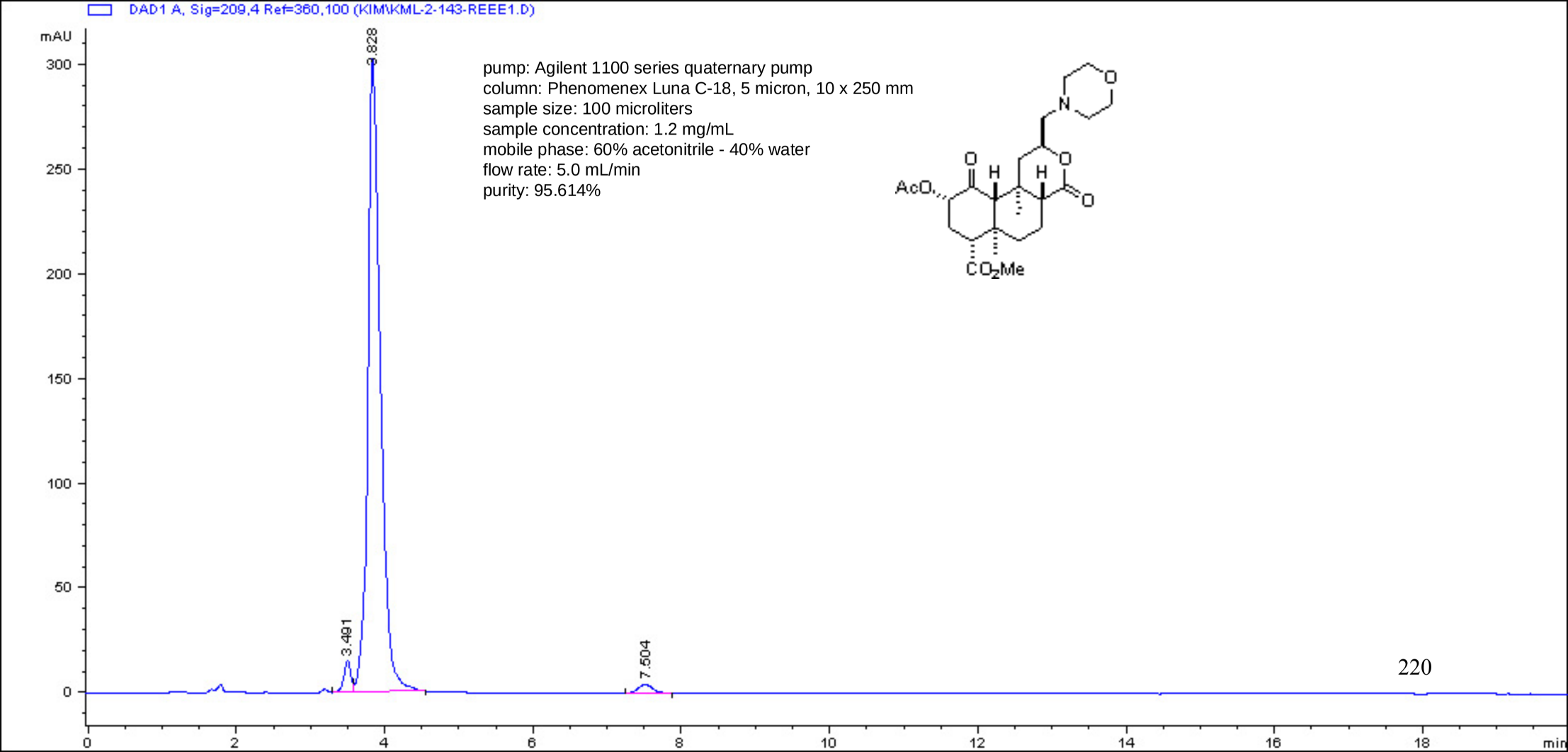
DAD1 A, Sig=209,4 Ref=360,100 (KIM\KML-2-143-REEE1.D)
mAU
300
250
200
150
100
50
0
3.828
3.491
7.504
0
2
4
6
8
10
12
14
16
18
min
pump: Agilent 1100 series quaternary pump
column: Phenomenex Luna C-18, 5 micron, 10 x 250 mm
sample size: 100 microliters
sample concentration: 1.2 mg/mL
mobile phase: 60% acetonitrile - 40% water
flow rate: 5.0 mL/min
purity: 95.614%
AcO
O
H
H
N
O
O
O
O
CO2Me

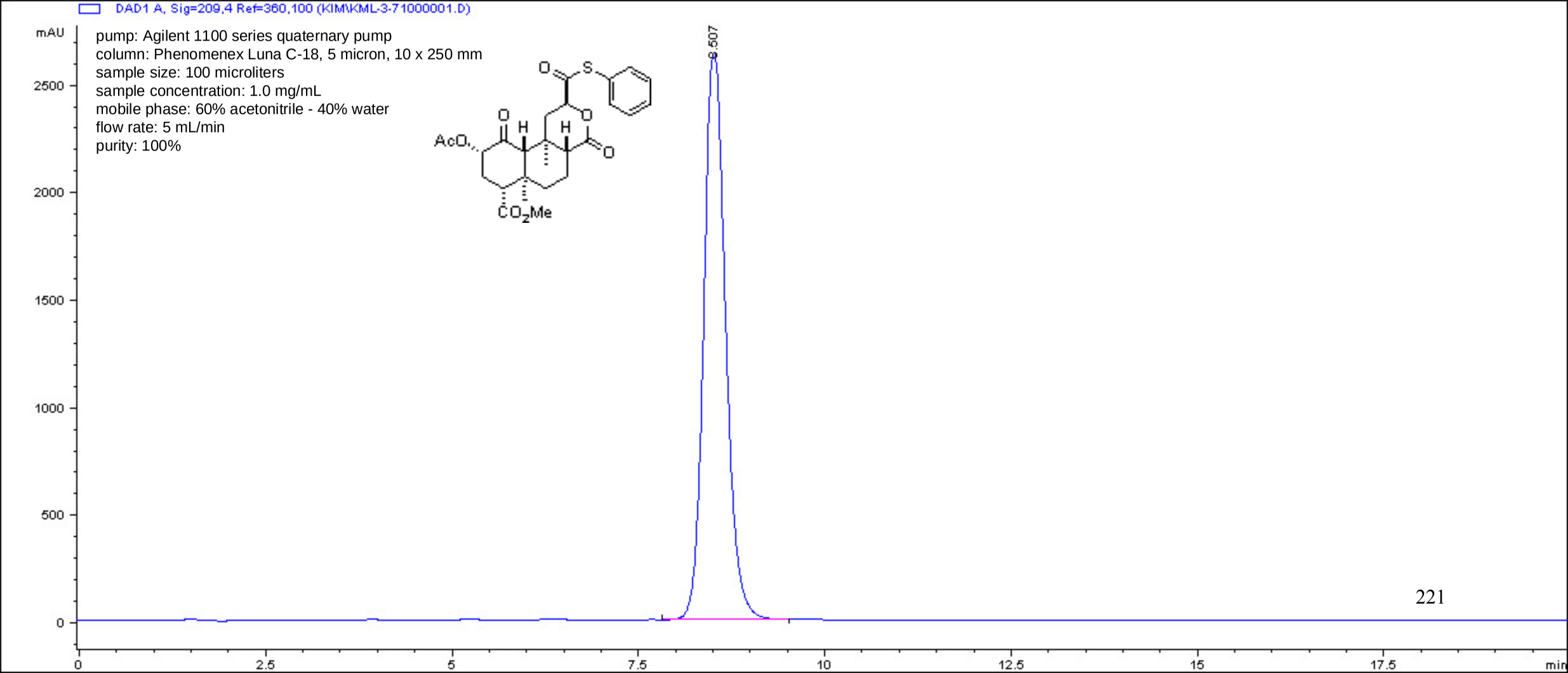
DAD1 A, Sig=209,4 Ref=360,100 (KIM\KML-3-71000001.D)
mAU
pump: Agilent 1100 series quaternary pump
column: Phenomenex Luna C-18, 5 micron, 10 x 250 mm
sample size: 100 microliters
sample concentration: 1.0 mg/mL
mobile phase: 60% acetonitrile - 40% water
flow rate: 5 mL/min
purity: 100%
9.507
2500
2000
1500
1000
500
0
0
2.5
5
7.5
10
12.5
15
17.5
min

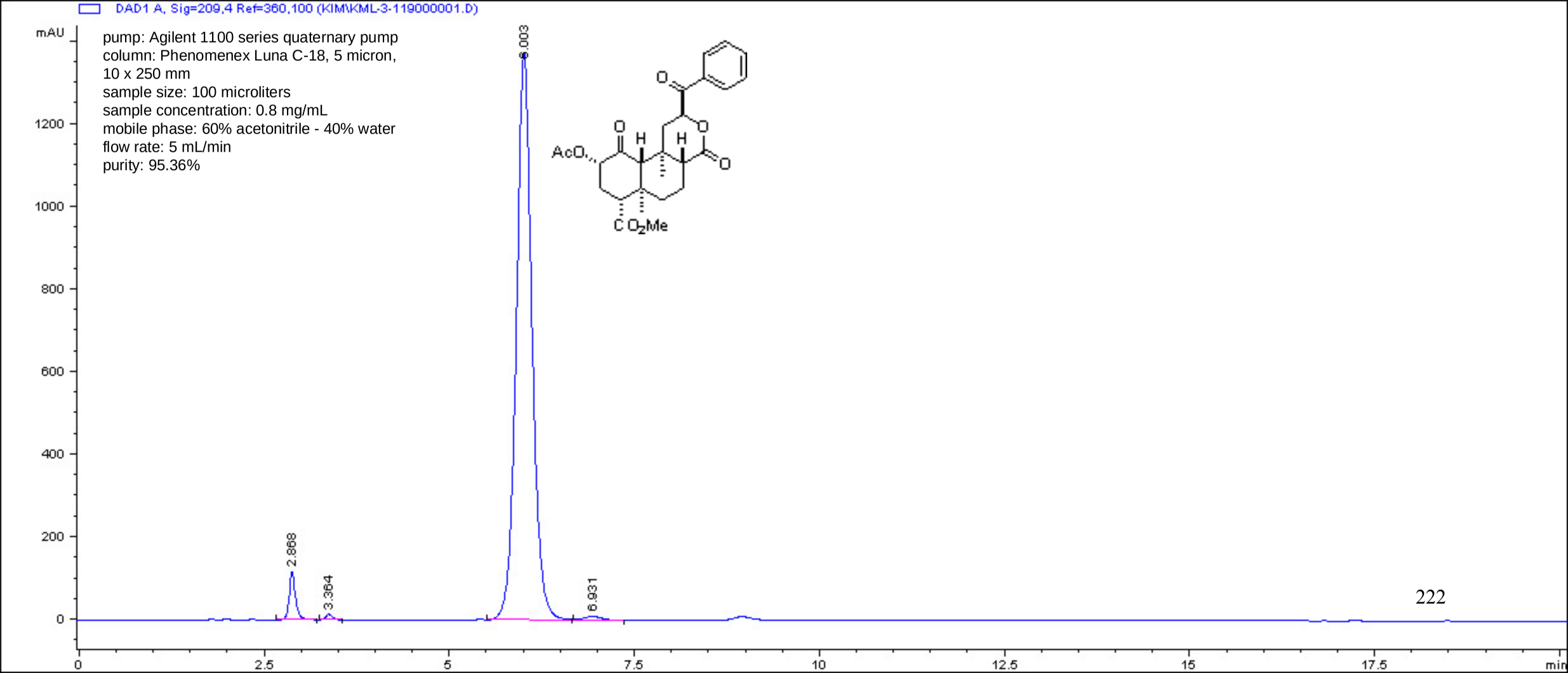
DAD1 A, Sig=209,4 Ref=360,100 (KIM\KML-3-119000001.D)
mAU
pump: Agilent 1100 series quaternary pump
column: Phenomenex Luna C-18, 5 micron,
10 x 250 mm
sample size: 100 microliters
sample concentration: 0.8 mg/mL
mobile phase: 60% acetonitrile - 40% water
flow rate: 5 mL/min
purity: 95.36%
6.003
2.868
3.364
6.931
AcO
CO2Me
1200
1000
800
600
400
200
0
2.5
5
7.5
10
12.5
15
17.5
min

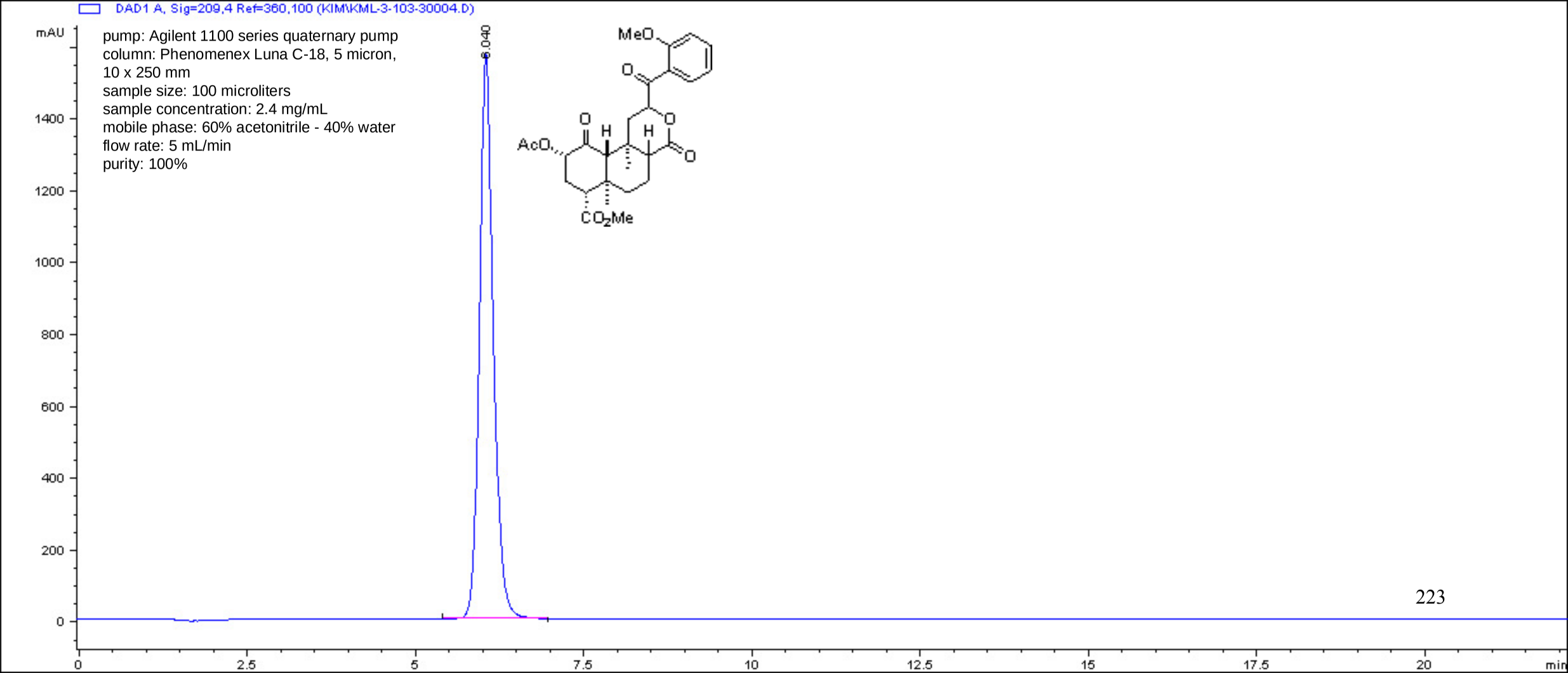
DAD1 A, Sig=209,4 Ref=360,100 (KIM\KML-3-103-30004.D)
mAU
pump: Agilent 1100 series quaternary pump
column: Phenomenex Luna C-18, 5 micron, 10 x 250 mm
sample size: 100 microliters
sample concentration: 2.4 mg/mL
mobile phase: 60% acetonitrile - 40% water
flow rate: 5 mL/min
purity: 100%
6.040
MeO
O
O
O
H
H
O
AcO
O
CO2Me
1400
1200
1000
800
600
400
200
0
0
2.5
5
7.5
10
12.5
15
17.5
20
min

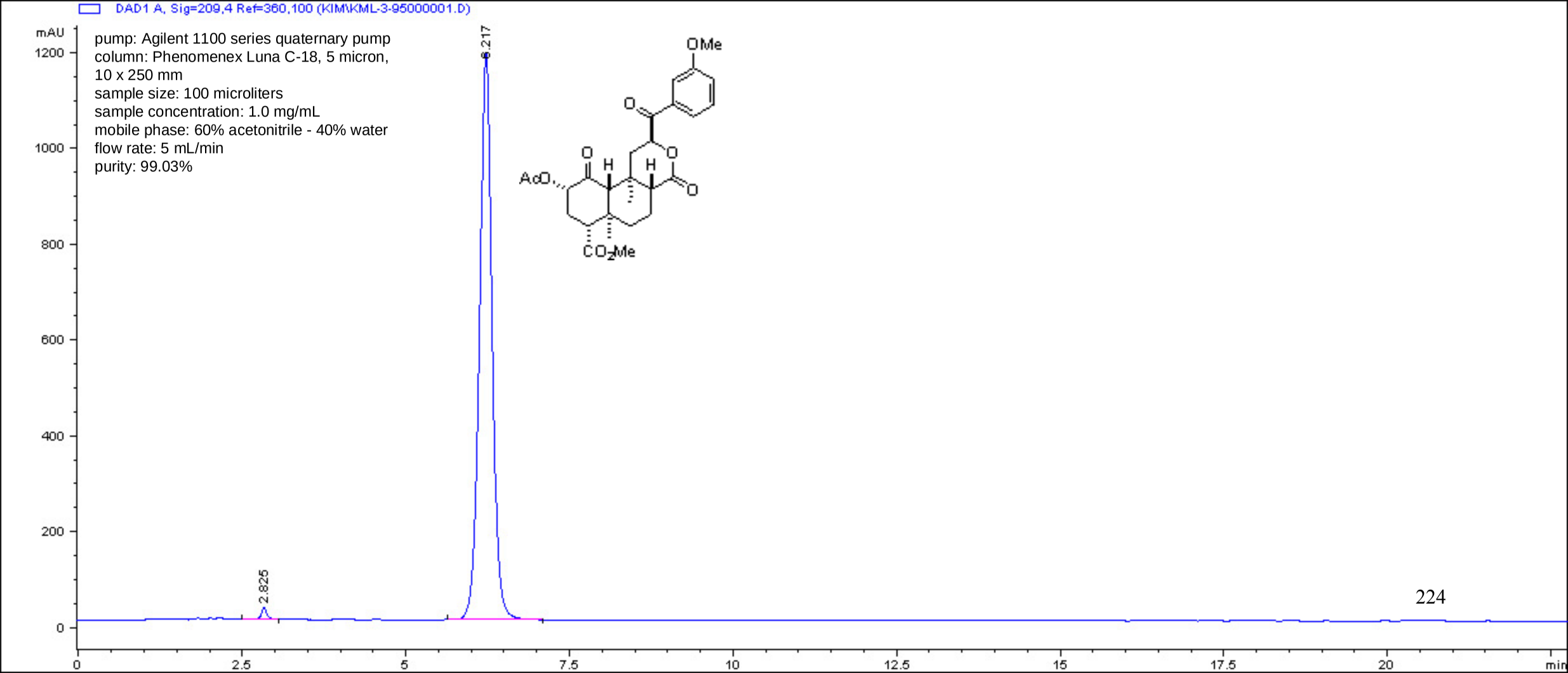
DAD1 A, Sig=209,4 Ref=360,100 (KIM\KML-3-95000001.D)
mAU
1200
1000
800
600
400
200
0
pump: Agilent 1100 series quaternary pump
column: Phenomenex Luna C-18, 5 micron,
10 x 250 mm
sample size: 100 microliters
sample concentration: 1.0 mg/mL
mobile phase: 60% acetonitrile - 40% water
flow rate: 5 mL/min
purity: 99.03%
6.217
2.825
OMe
O
O
H
H
O
O
AcO
O
CO2Me
0
2.5
5
7.5
10
12.5
15
17.5
20
min

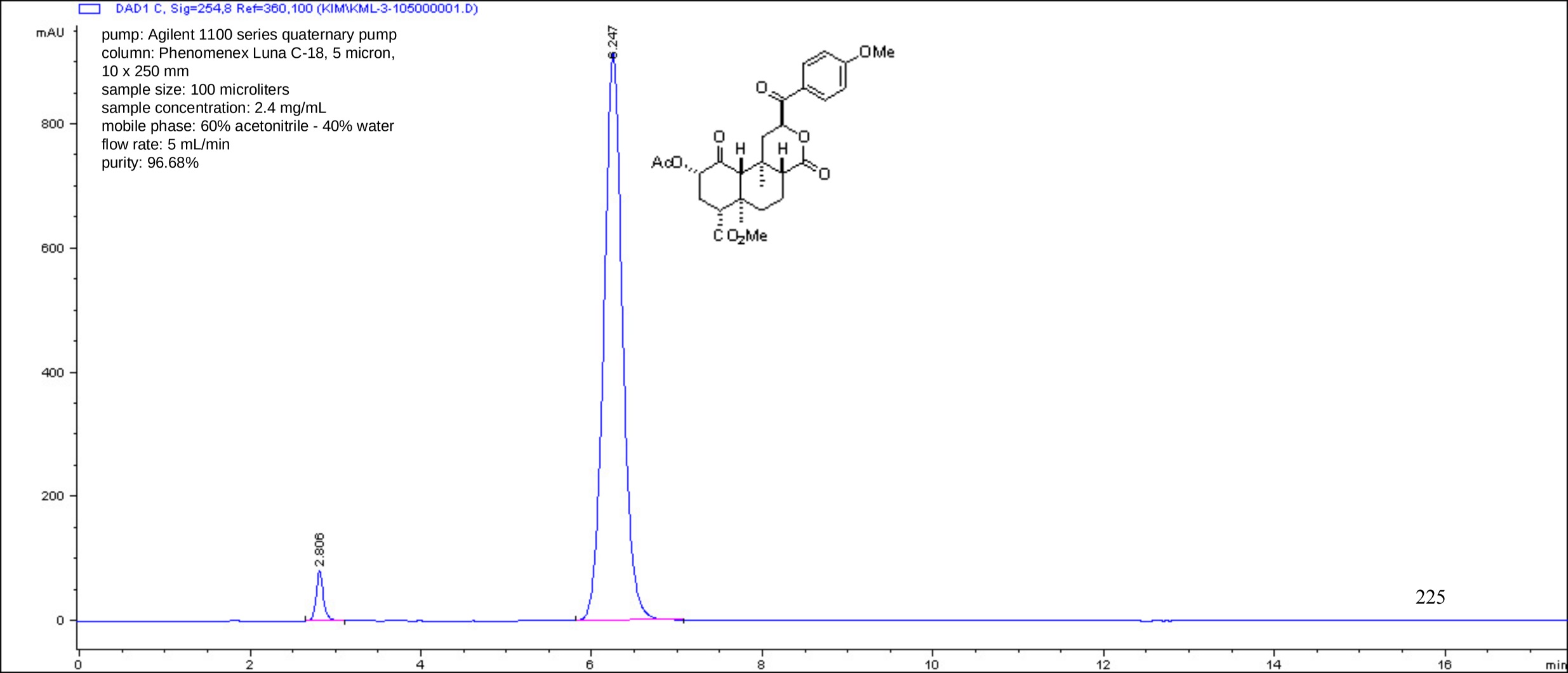
DAD1 C, Sig=254,8 Ref=360,100 (KIM\KML-3-105000001.D)
mAU
pump: Agilent 1100 series quaternary pump
column: Phenomenex Luna C-18, 5 micron,
10 x 250 mm
sample size: 100 microliters
sample concentration: 2.4 mg/mL
mobile phase: 60% acetonitrile - 40% water
flow rate: 5 mL/min
purity: 96.68%
6.247
2.806
OMe
O
O
H
H
O
O
AcO
O
CO2Me
800
600
400
200
0
0
2
4
6
8
10
12
14
16
min

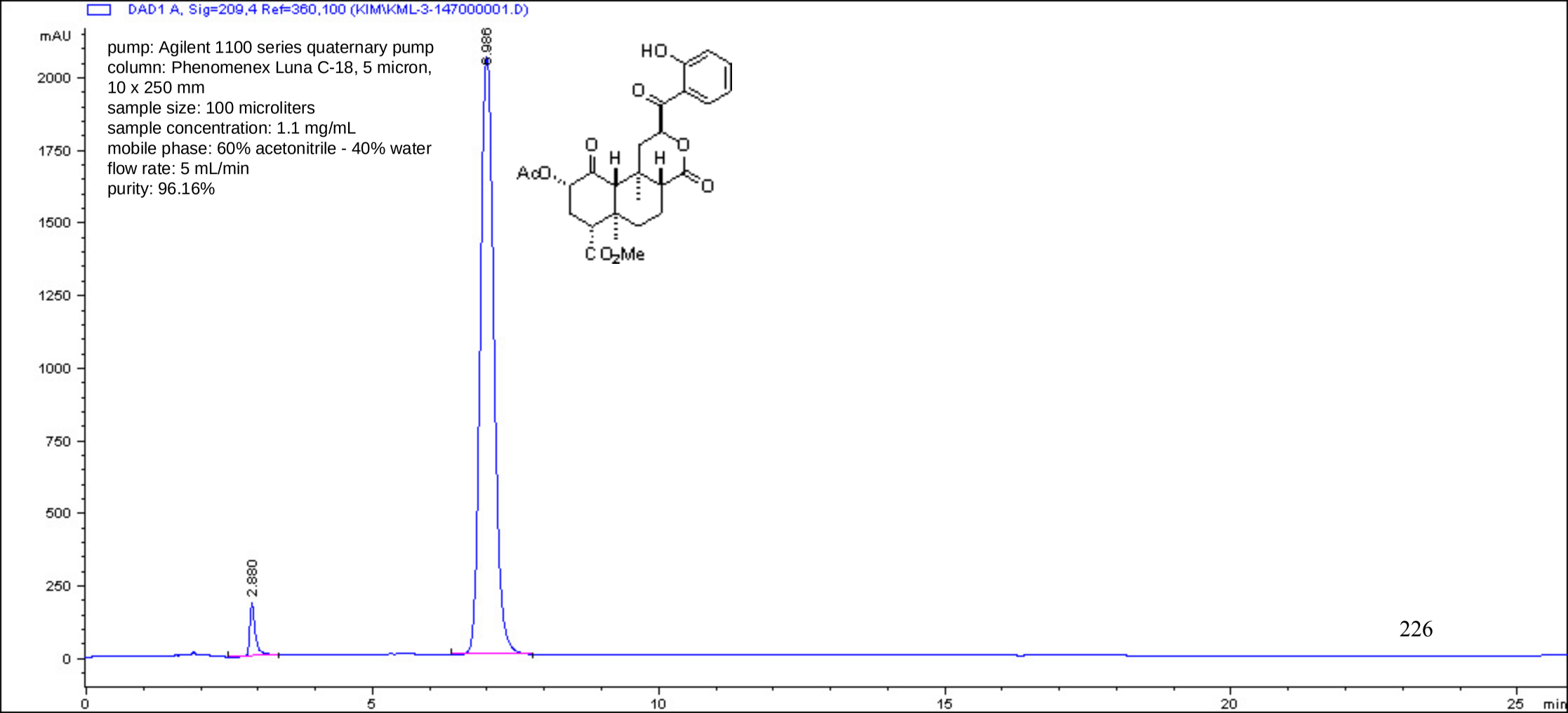
DAD1 A, Sig=209,4 Ref=360,100 (KIM\KML-3-147000001.D)
mAU
pump: Agilent 1100 series quaternary pump
column: Phenomenex Luna C-18, 5 micron, 10 x 250 mm
sample size: 100 microliters
sample concentration: 1.1 mg/mL
mobile phase: 60% acetonitrile - 40% water
flow rate: 5 mL/min
purity: 96.16%
6.986
2.880
HO
O
O
H
H
O
AcO
O
O
CO2Me
2000
1750
1500
1250
1000
750
500
250
0
0
5
10
15
20
25
min

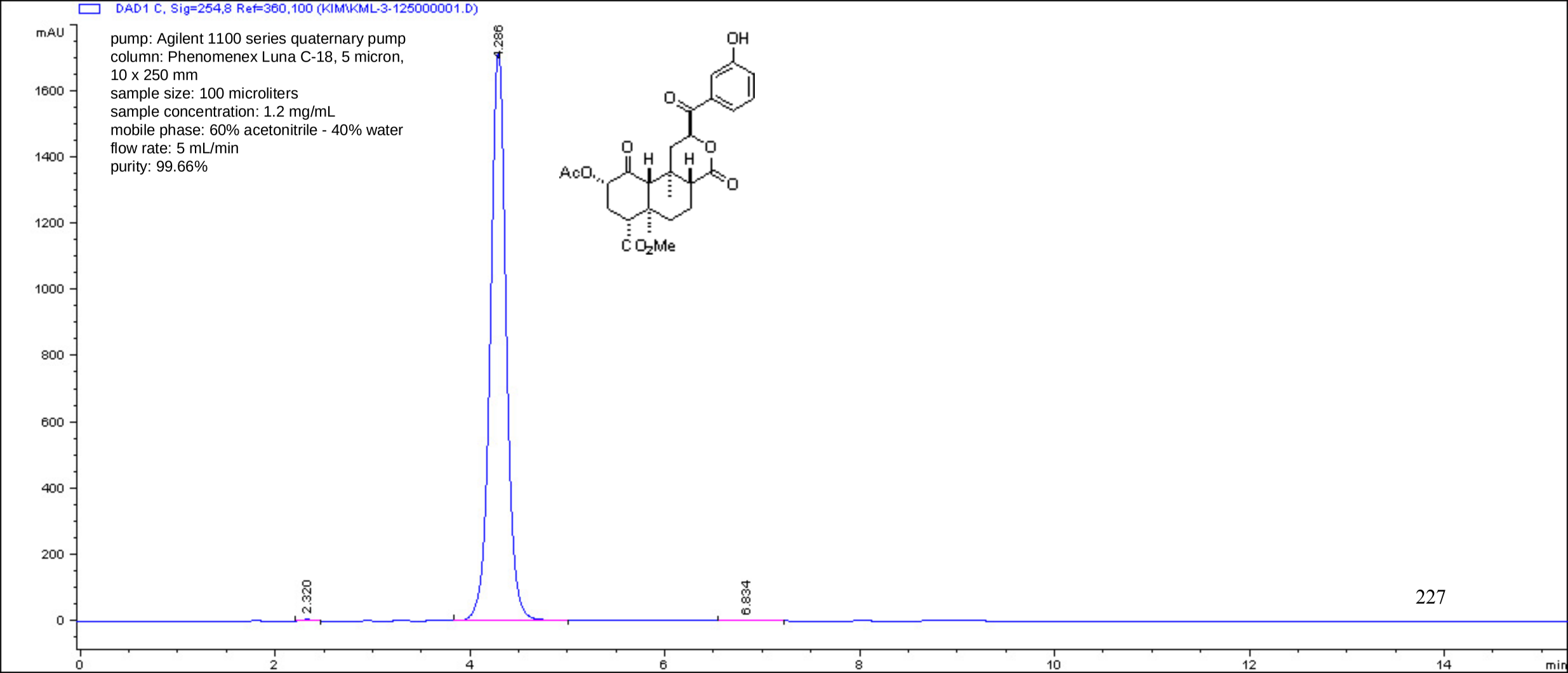
DAD1 C, Sig=254,8 Ref=360,100 (KIM\KML-3-125000001.D)
mAU
pump: Agilent 1100 series quaternary pump
column: Phenomenex Luna C-18, 5 micron,
10 x 250 mm
sample size: 100 microliters
sample concentration: 1.2 mg/mL
mobile phase: 60% acetonitrile - 40% water
flow rate: 5 mL/min
purity: 99.66%
4.286
2.320
6.834
OH
O
O
H
H
O
O
AcO
O
CO2Me
1600
1400
1200
1000
800
600
400
200
0
0
2
4
6
8
10
12
14
min

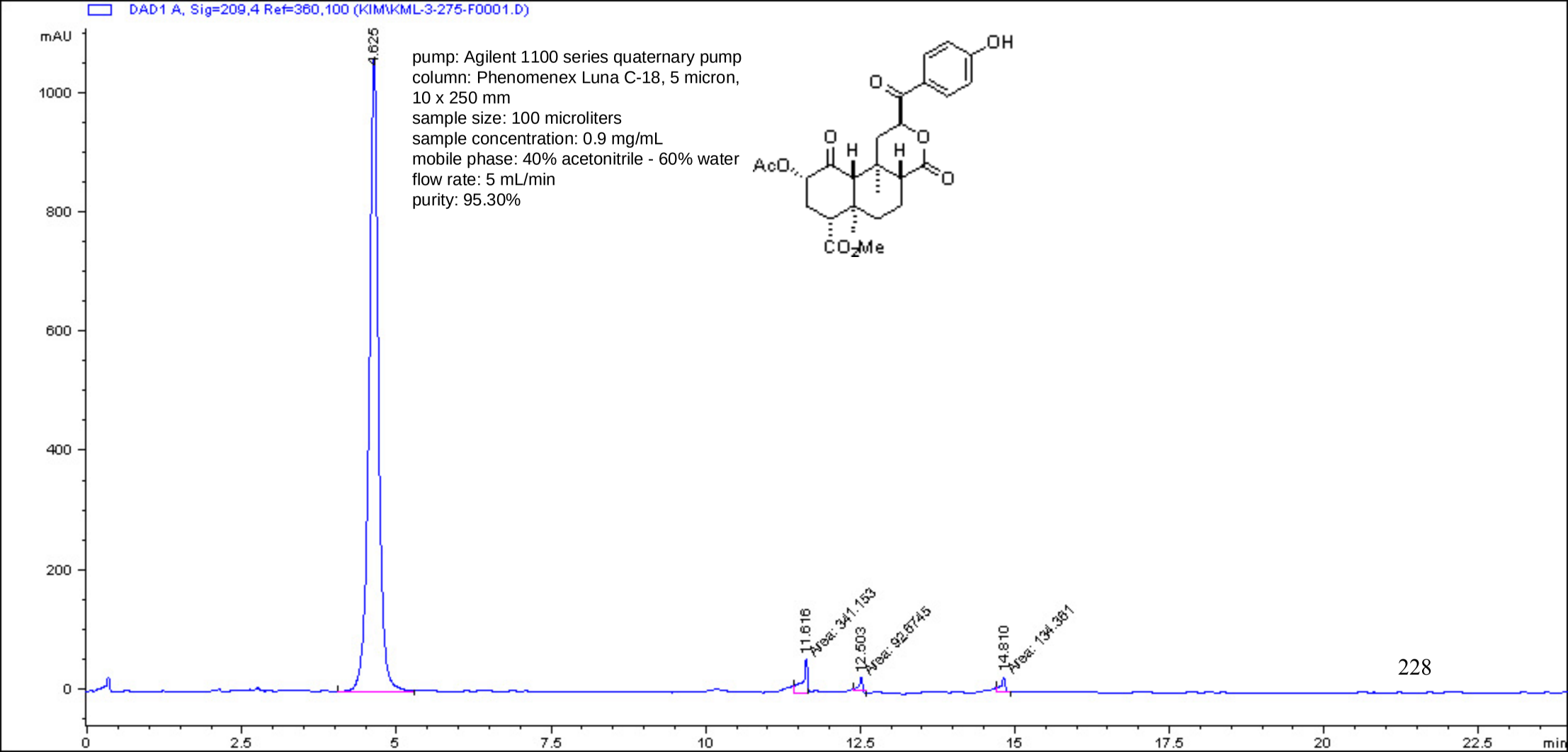
DAD1 A, Sig=209,4 Ref=360,100 (KIM\KML-3-275-F0001.D)
mAU
1000
800
600
400
200
0
4.625
pump: Agilent 1100 series quaternary pump
column: Phenomenex Luna C-18, 5 micron, 10 x 250 mm
sample size: 100 microliters
sample concentration: 0.9 mg/mL
mobile phase: 40% acetonitrile - 60% water
flow rate: 5 mL/min
purity: 95.30%
OH
O
O
H
H
O
AcO
O
CO2Me
11.616
Area: 341.153
12.503
Area: 92.6745
14.810
Area: 134.381
0
2.5
5
7.5
10
12.5
15
17.5
20
22.5
min

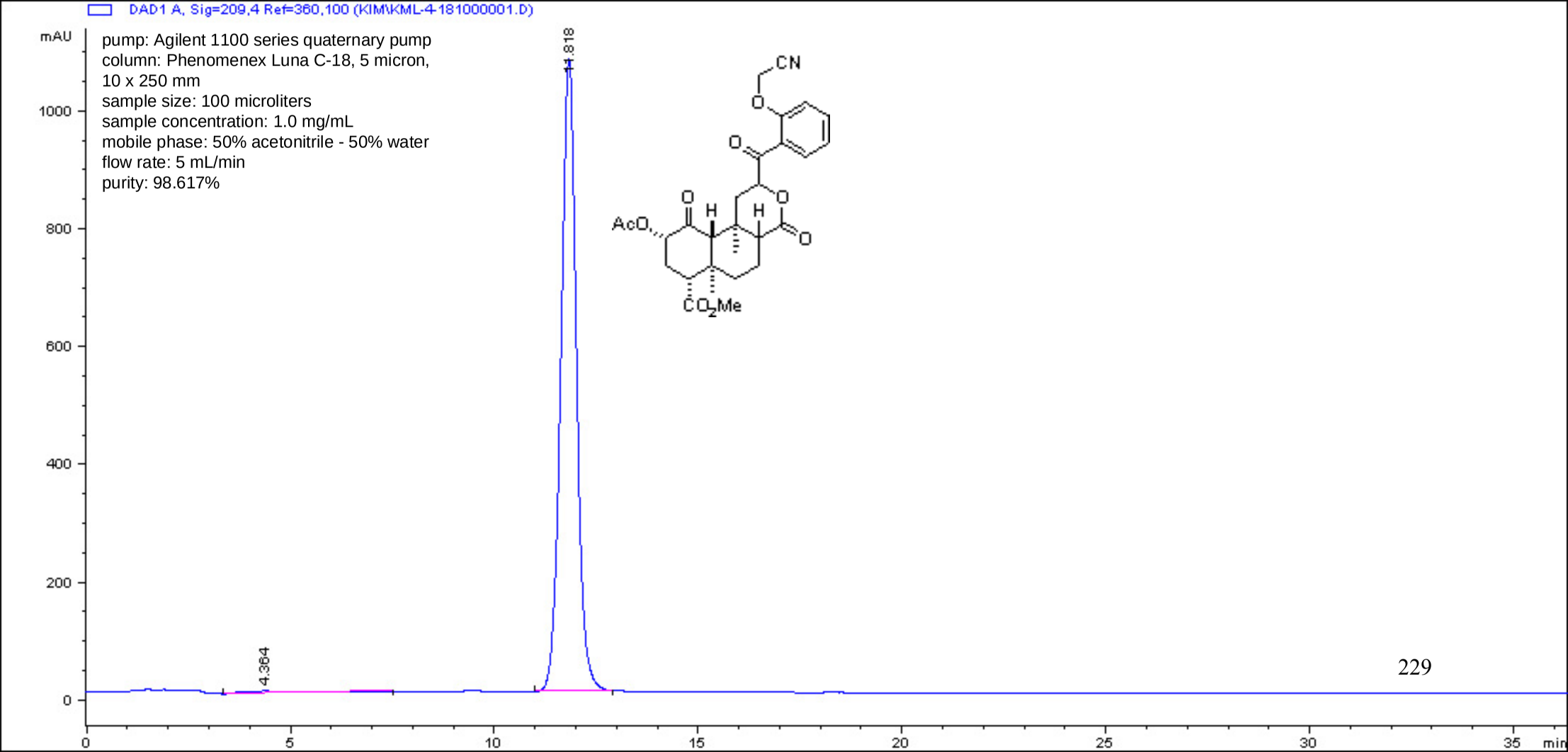
DAD1 A, Sig=209,4 Ref=360,100 (KIM\KML-4-181000001.D)
mAU
pump: Agilent 1100 series quaternary pump
column: Phenomenex Luna C-18, 5 micron,
10 x 250 mm
sample size: 100 microliters
sample concentration: 1.0 mg/mL
mobile phase: 50% acetonitrile - 50% water
flow rate: 5 mL/min
purity: 98.617%
11.818
4.364
CN
O
O
O
O
H
H
O
O
AcO
CO2Me
1000
800
600
400
200
0
0
5
10
15
20
25
30
35
min

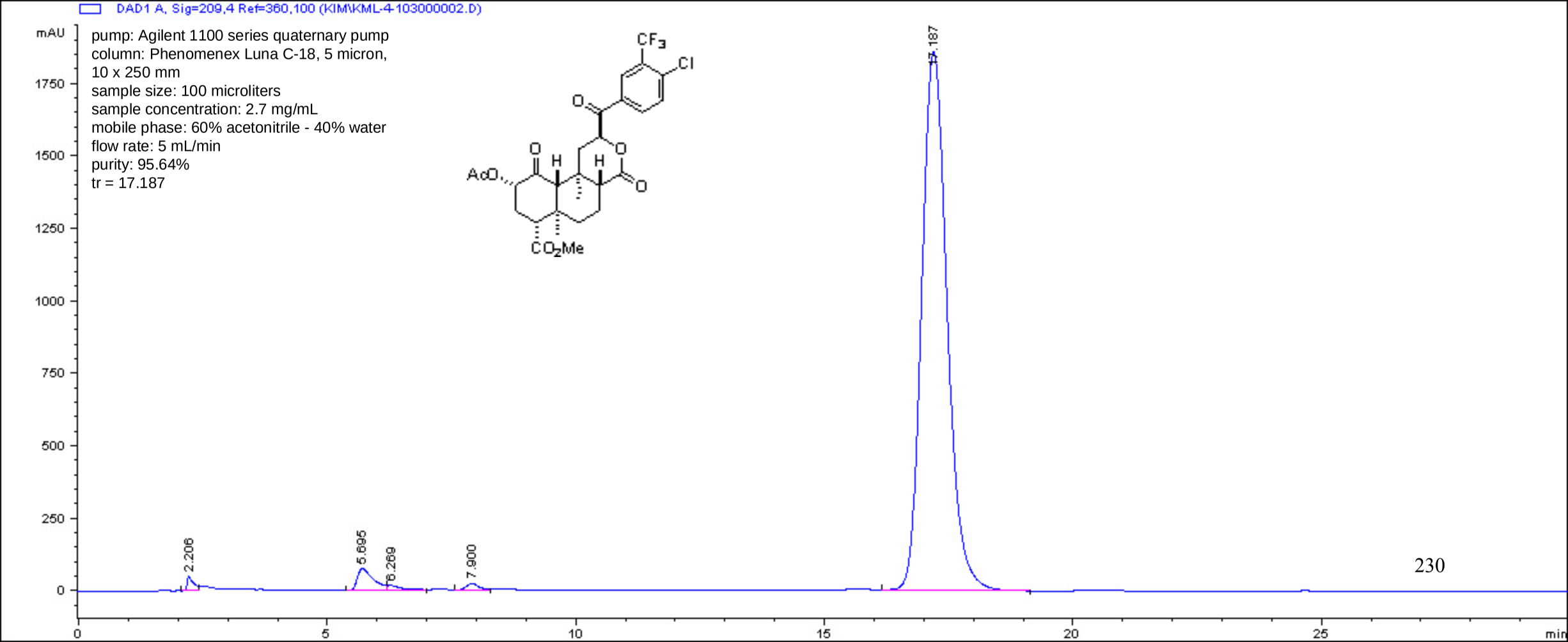
DAD1 A, Sig=209,4 Ref=360,100 (KIM\KML-4-103000002.D)
mAU
pump: Agilent 1100 series quaternary pump
column: Phenomenex Luna C-18, 5 micron,
10 x 250 mm
sample size: 100 microliters
sample concentration: 2.7 mg/mL
mobile phase: 60% acetonitrile - 40% water
flow rate: 5 mL/min
purity: 95.64%
tr = 17.187
CF3
Cl
O
O
H
H
O
O
AcO
O
CO2Me
17.187
2.206
5.695
6.269
7.900
1750
1500
1250
1000
750
500
250
0
0
5
10
15
20
25
min

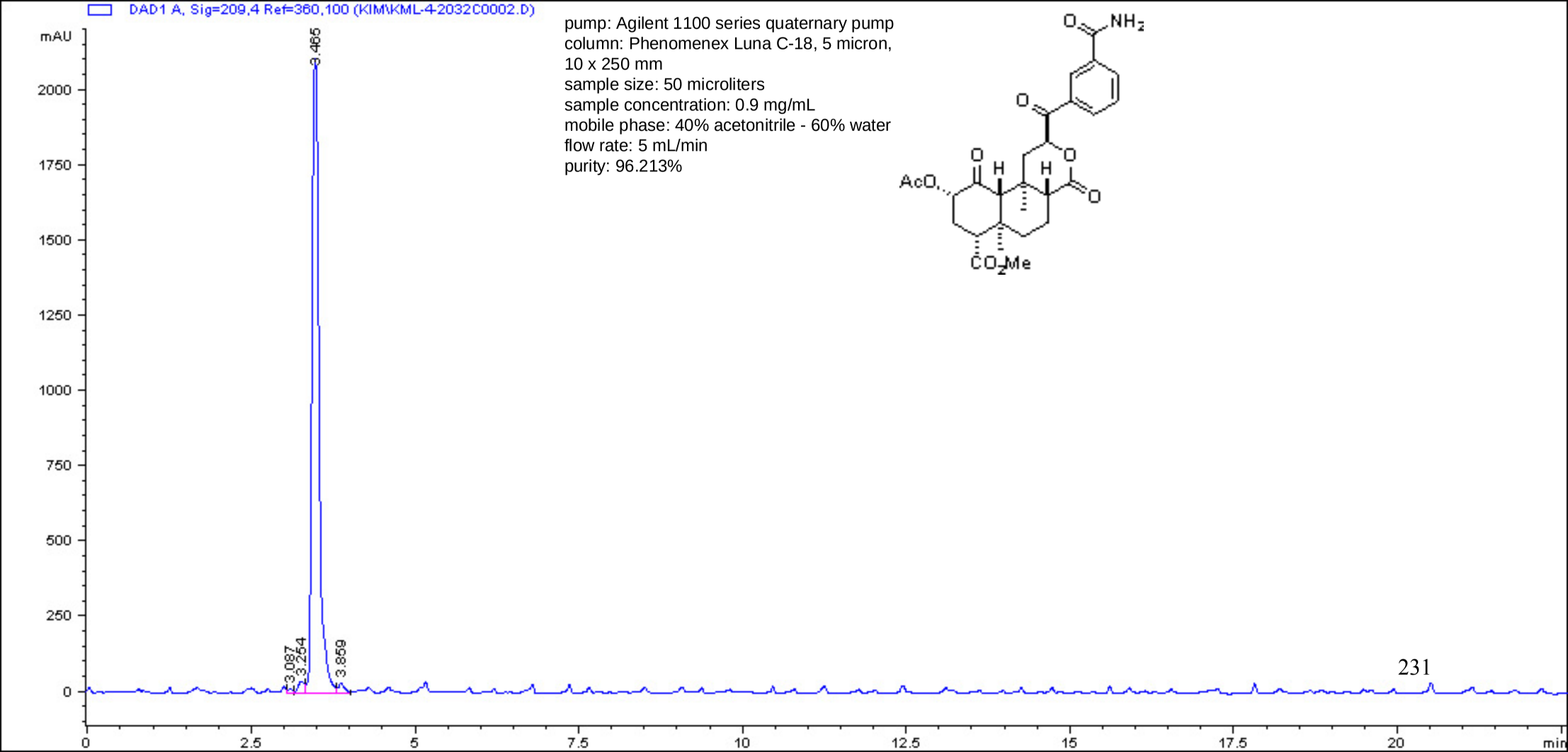
DAD1 A, Sig=209,4 Ref=360,100 (KIM\KML-4-2032C0002.D)
mAU
2000
1750
1500
1250
1000
750
500
250
0
3.465
3.087
3.254
3.859
0
2.5
5
7.5
10
12.5
15
17.5
20
min
pump: Agilent 1100 series quaternary pump
column: Phenomenex Luna C-18, 5 micron, 10 x 250 mm
sample size: 50 microliters
sample concentration: 0.9 mg/mL
mobile phase: 40% acetonitrile - 60% water
flow rate: 5 mL/min
purity: 96.213%
O
NH2
O
O
H
H
O
O
AcO
O
CO2Me

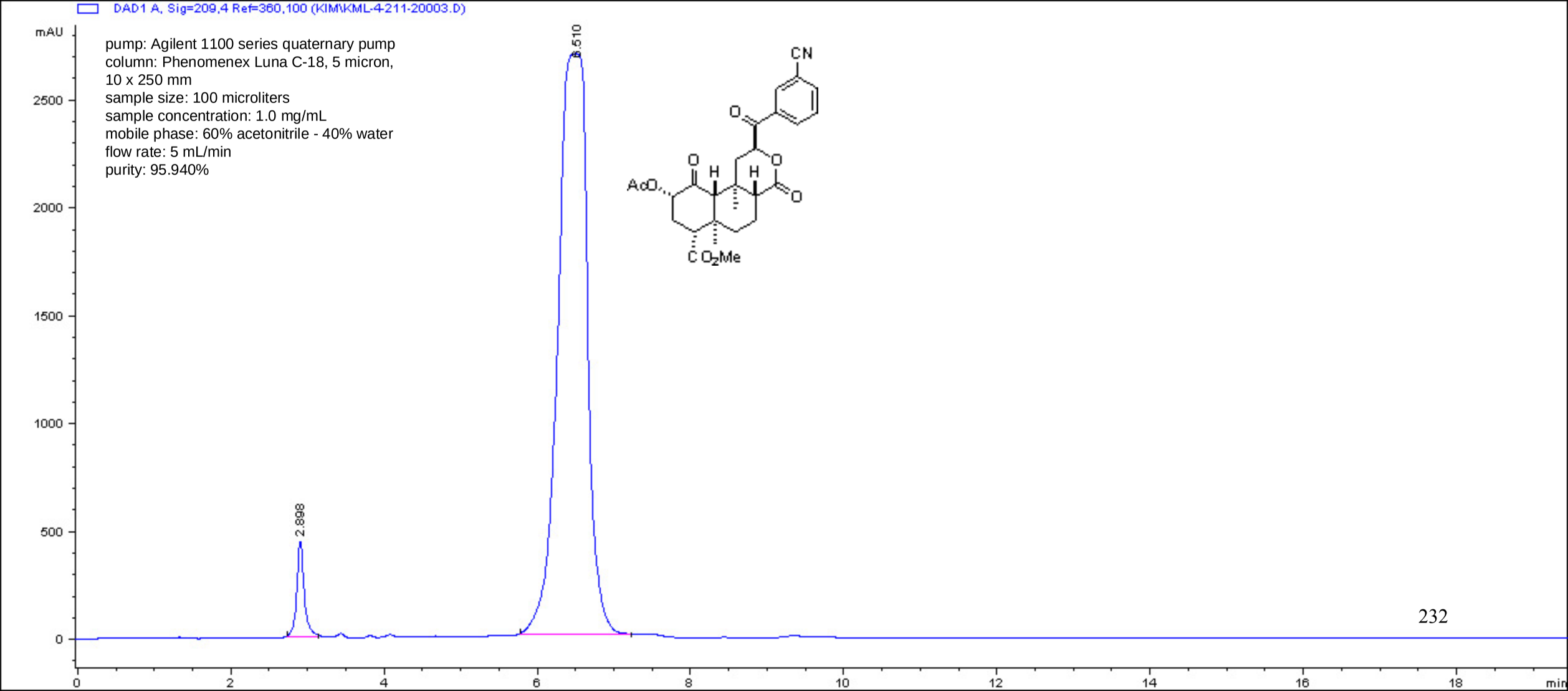
DAD1 A, Sig=209,4 Ref=360,100 (KIM\KML-4-211-20003.D)
mAU
pump: Agilent 1100 series quaternary pump
column: Phenomenex Luna C-18, 5 micron,
10 x 250 mm
sample size: 100 microliters
sample concentration: 1.0 mg/mL
mobile phase: 60% acetonitrile - 40% water
flow rate: 5 mL/min
purity: 95.940%
6.510
2.898
CN
O
O
H
H
O
O
AcO
O
C O2Me
2500
2000
1500
1000
500
0
0
2
4
6
8
10
12
14
16
18
min

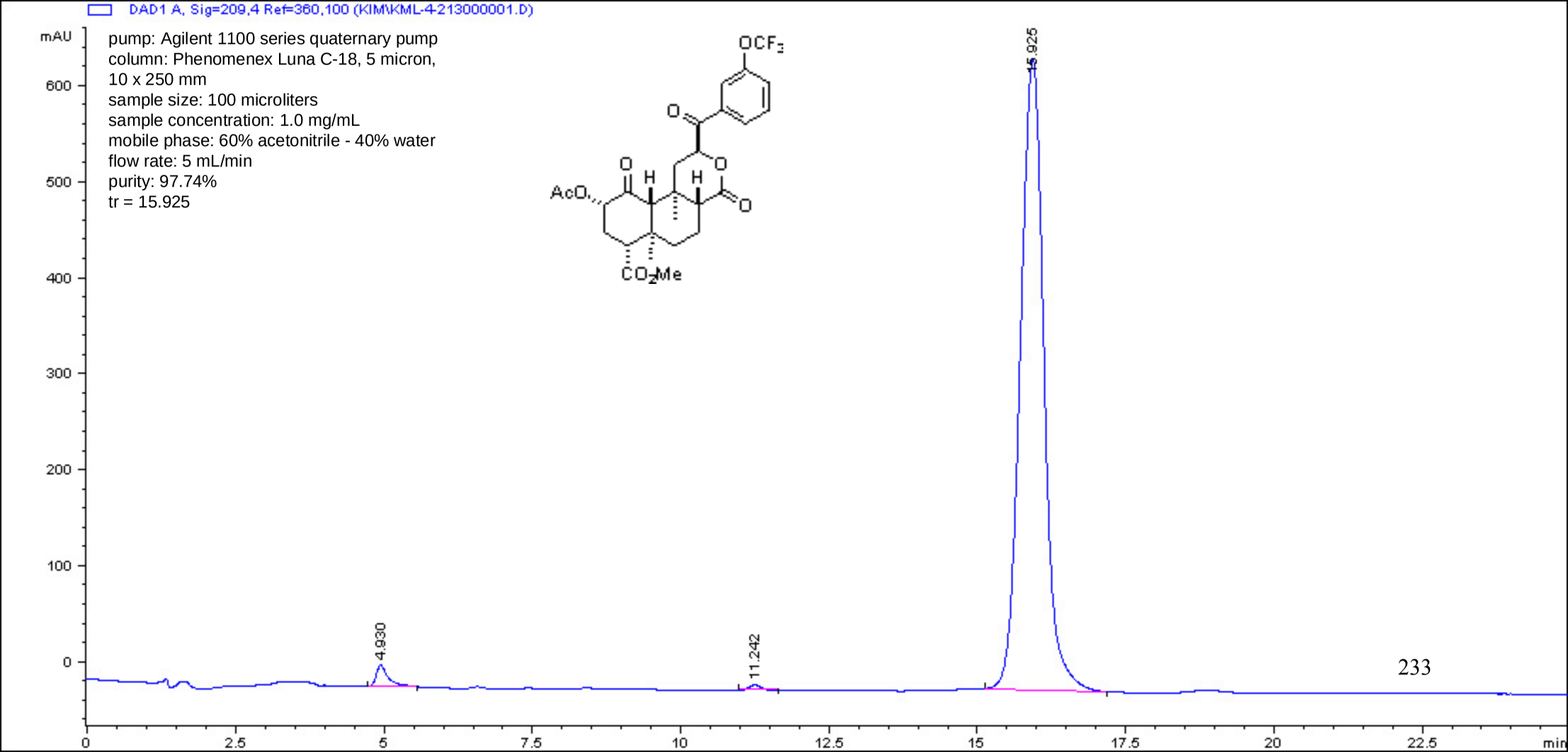
DAD1 A, Sig=209,4 Ref=360,100 (KIM\KML-4-213000001.D)
mAU
pump: Agilent 1100 series quaternary pump
column: Phenomenex Luna C-18, 5 micron, 10 x 250 mm
sample size: 100 microliters
sample concentration: 1.0 mg/mL
mobile phase: 60% acetonitrile - 40% water
flow rate: 5 mL/min
purity: 97.74%
tr = 15.925
OCF3
O
O
H
H
O
AcO
O
CO2Me
15.925
4.930
11.242
600
500
400
300
200
100
0
0
2.5
5
7.5
10
12.5
15
17.5
20
22.5
min

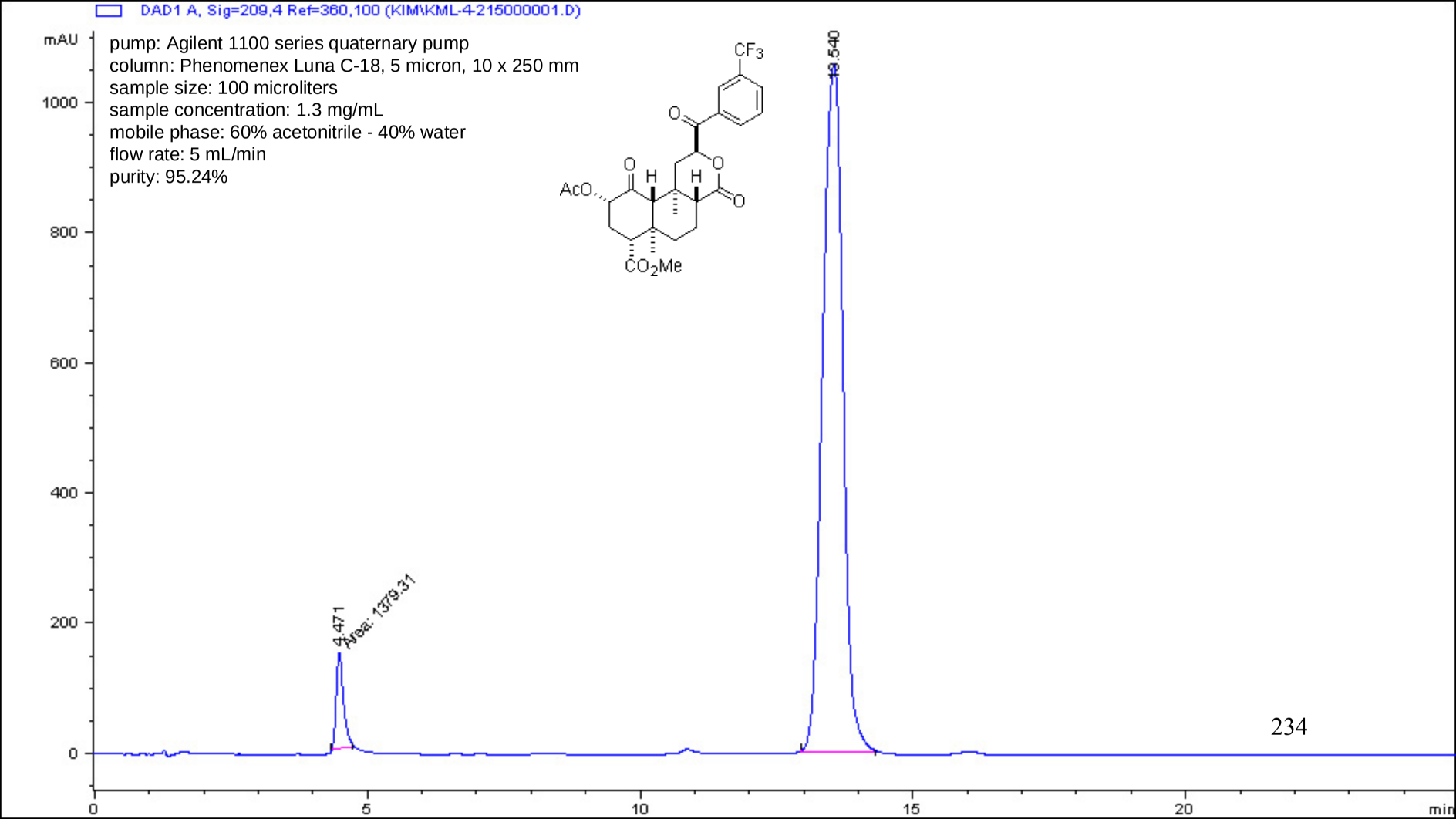
DAD1 A, Sig=209,4 Ref=360,100 (KIM\KML-4-215000001.D)
mAU
pump: Agilent 1100 series quaternary pump
column: Phenomenex Luna C-18, 5 micron, 10 x 250 mm
sample size: 100 microliters
sample concentration: 1.3 mg/mL
mobile phase: 60% acetonitrile - 40% water
flow rate: 5 mL/min
purity: 95.24%
CF3
O
O
H
H
O
AcO
O
CO2Me
13.540
4.471
Area: 1379.31
1000
800
600
400
200
0
0
5
10
15
20
min

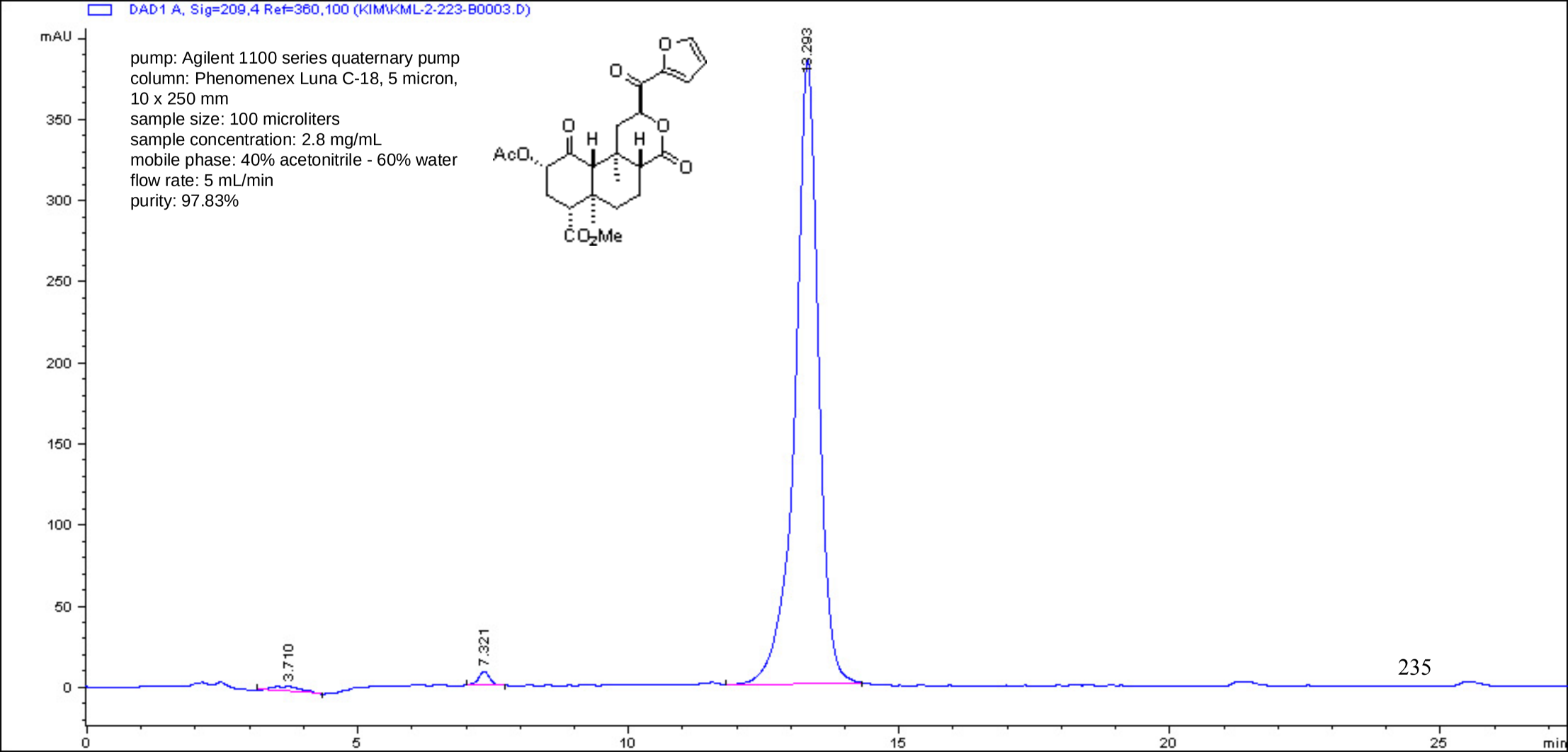
DAD1 A, Sig=209,4 Ref=360,100 (KIM\KML-2-223-B0003.D)
mAU
pump: Agilent 1100 series quaternary pump
column: Phenomenex Luna C-18, 5 micron, 10 x 250 mm
sample size: 100 microliters
sample concentration: 2.8 mg/mL
mobile phase: 40% acetonitrile - 60% water
flow rate: 5 mL/min
purity: 97.83%
AcO
H
H
CO2Me
3.710
7.321
13.293
235
min

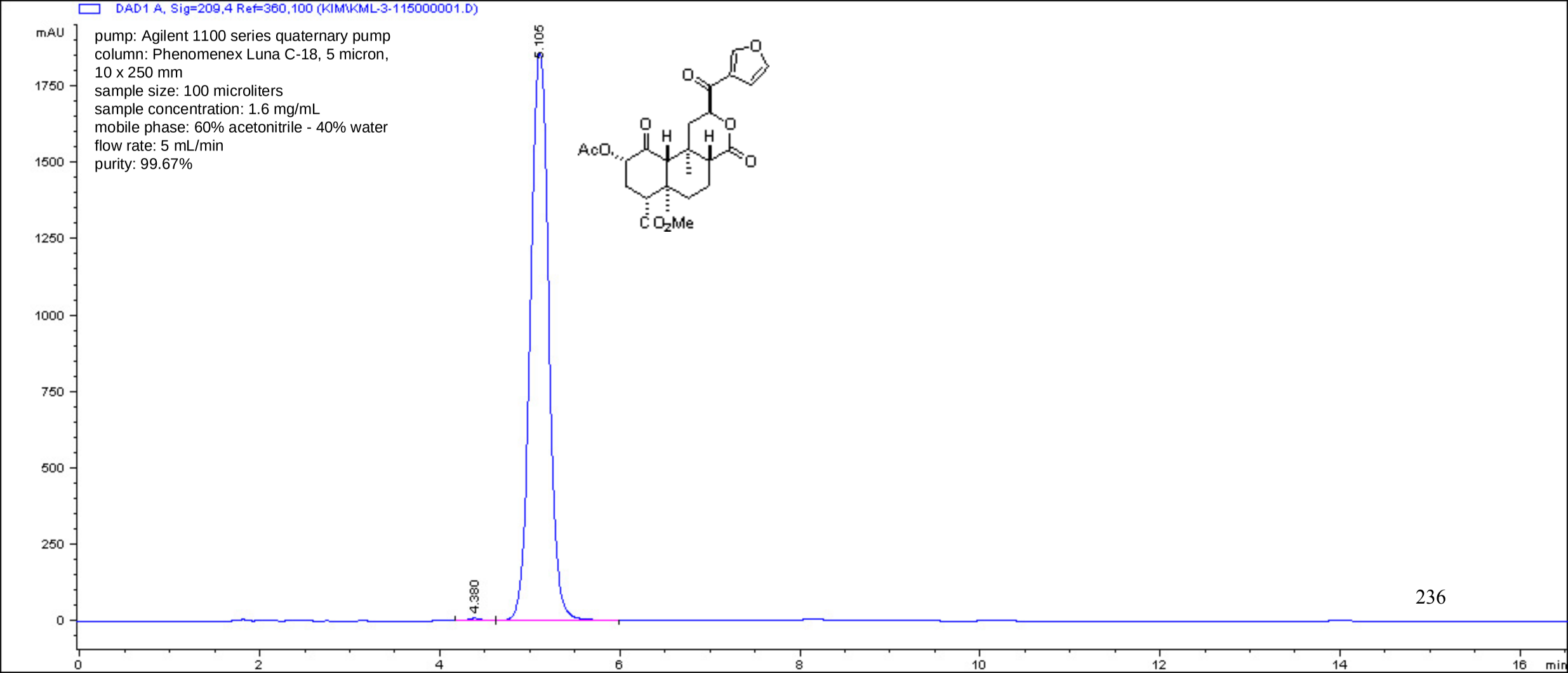
DAD1 A, Sig=209,4 Ref=360,100 (KIM\KML-3-115000001.D)
mAU
pump: Agilent 1100 series quaternary pump
column: Phenomenex Luna C-18, 5 micron,
10 x 250 mm
sample size: 100 microliters
sample concentration: 1.6 mg/mL
mobile phase: 60% acetonitrile - 40% water
flow rate: 5 mL/min
purity: 99.67%
5.105
4.380
AcO
H
H
O
CO2Me
1750
1500
1250
1000
750
500
250
0
2
4
6
8
10
12
14
16
min

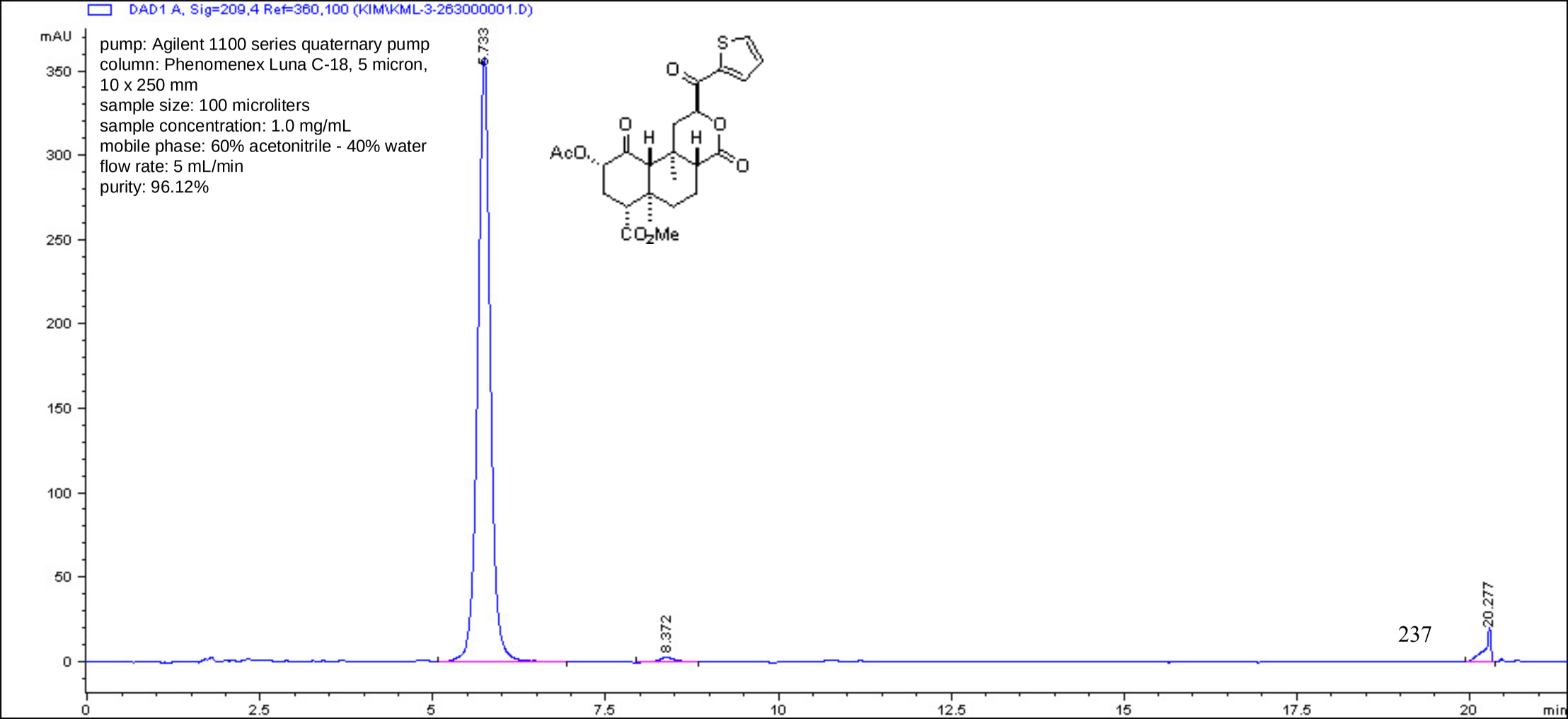
DAD1 A, Sig=209,4 Ref=360,100 (KIM\KML-3-263000001.D)
mAU
pump: Agilent 1100 series quaternary pump
column: Phenomenex Luna C-18, 5 micron, 10 x 250 mm
sample size: 100 microliters
sample concentration: 1.0 mg/mL
mobile phase: 60% acetonitrile - 40% water
flow rate: 5 mL/min
purity: 96.12%
6.733
8.372
20.277
AcO
H
H
O
O
O
O
S
CO2Me
350
300
250
200
150
100
50
0
0
2.5
5
7.5
10
12.5
15
17.5
20
min

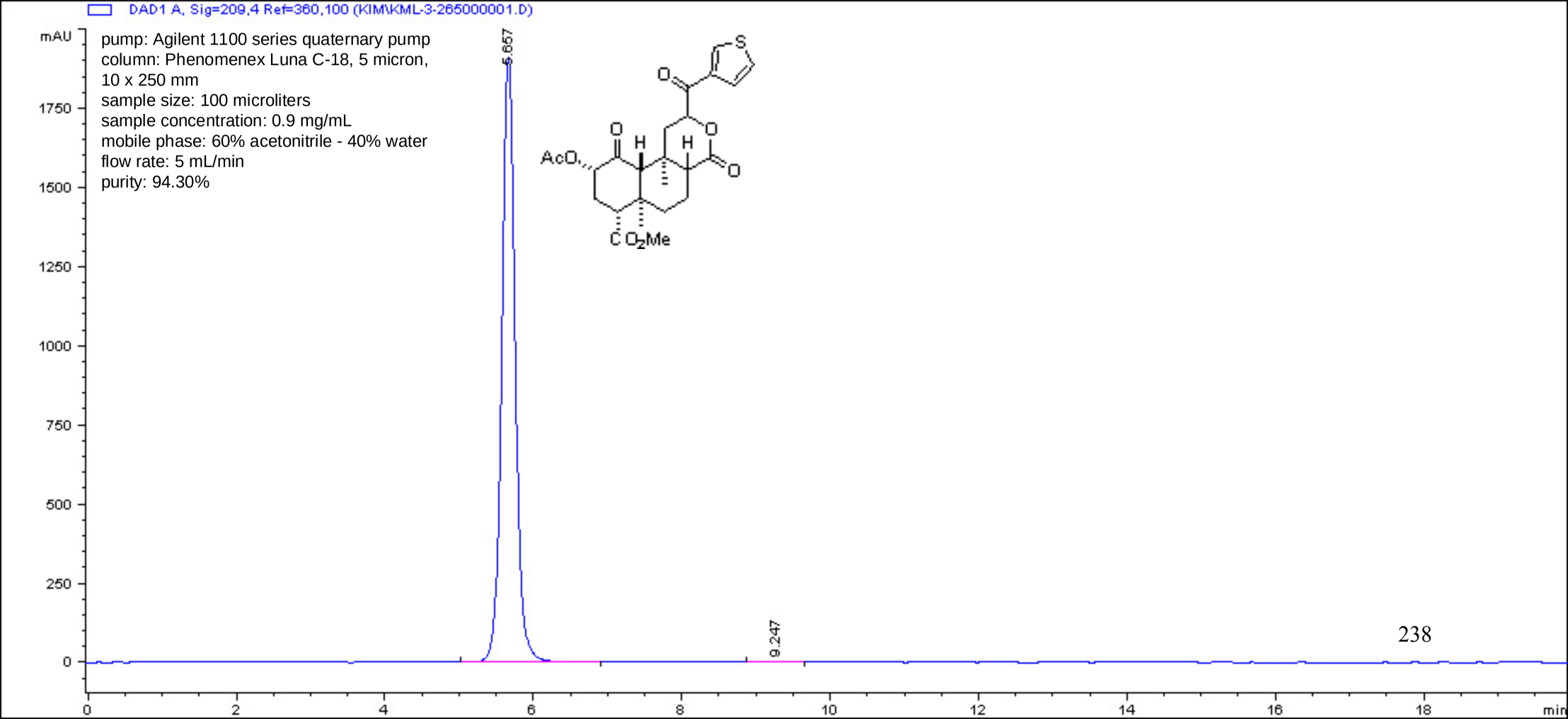
DAD1 A, Sig=209,4 Ref=360,100 (KIM\KML-3-265000001.D)
mAU
pump: Agilent 1100 series quaternary pump
column: Phenomenex Luna C-18, 5 micron,
10 x 250 mm
sample size: 100 microliters
sample concentration: 0.9 mg/mL
mobile phase: 60% acetonitrile - 40% water
flow rate: 5 mL/min
purity: 94.30%
5.657
9.247
AcO
H
H
O
O
O
O
S
CO2Me
1750
1500
1250
1000
750
500
250
0
0
2
4
6
8
10
12
14
16
18
min

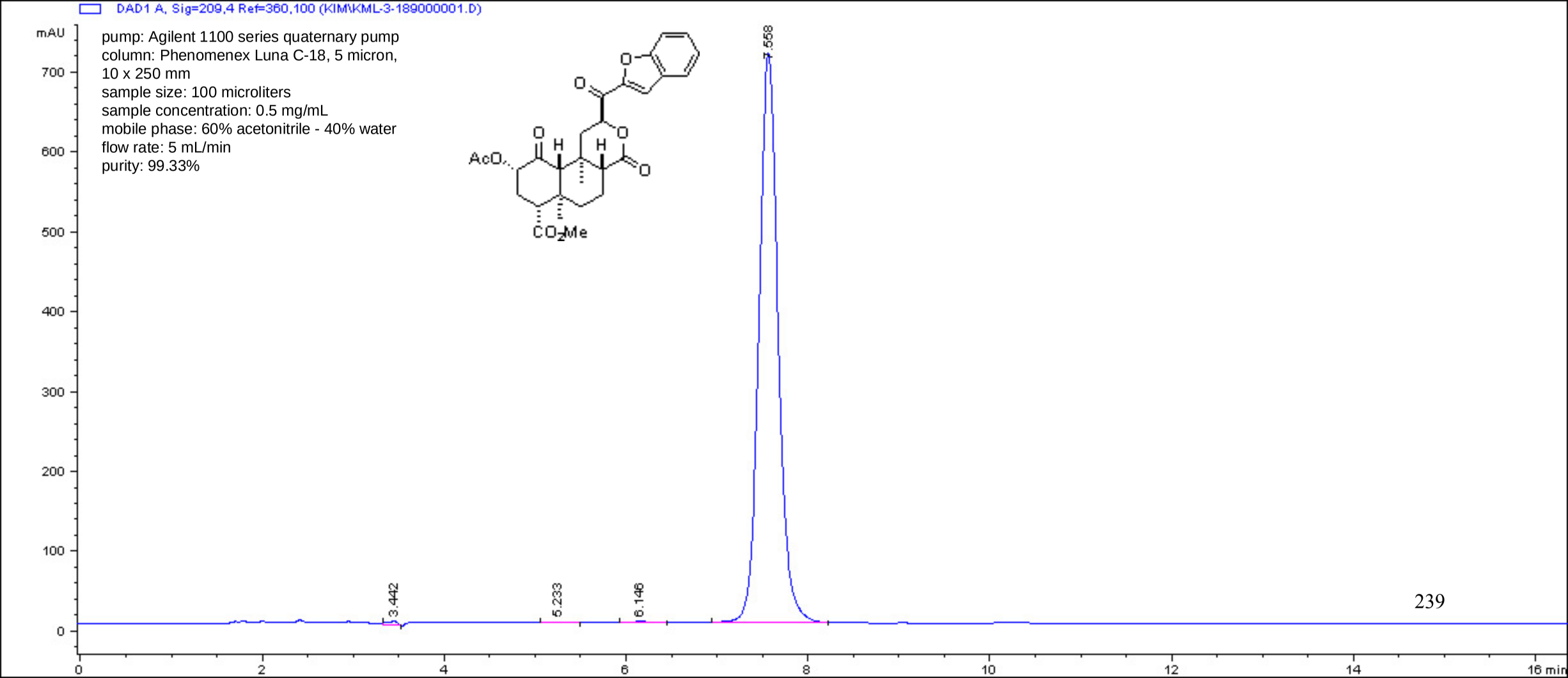
DAD1 A, Sig=209,4 Ref=360,100 (KIM\KML-3-189000001.D)
mAU
pump: Agilent 1100 series quaternary pump
column: Phenomenex Luna C-18, 5 micron, 10 x 250 mm
sample size: 100 microliters
sample concentration: 0.5 mg/mL
mobile phase: 60% acetonitrile - 40% water
flow rate: 5 mL/min
purity: 99.33%
AcO
CO2Me
3.442
5.233
6.146
7.568
0
100
200
300
400
500
600
700
0
2
4
6
8
10
12
14
16 min

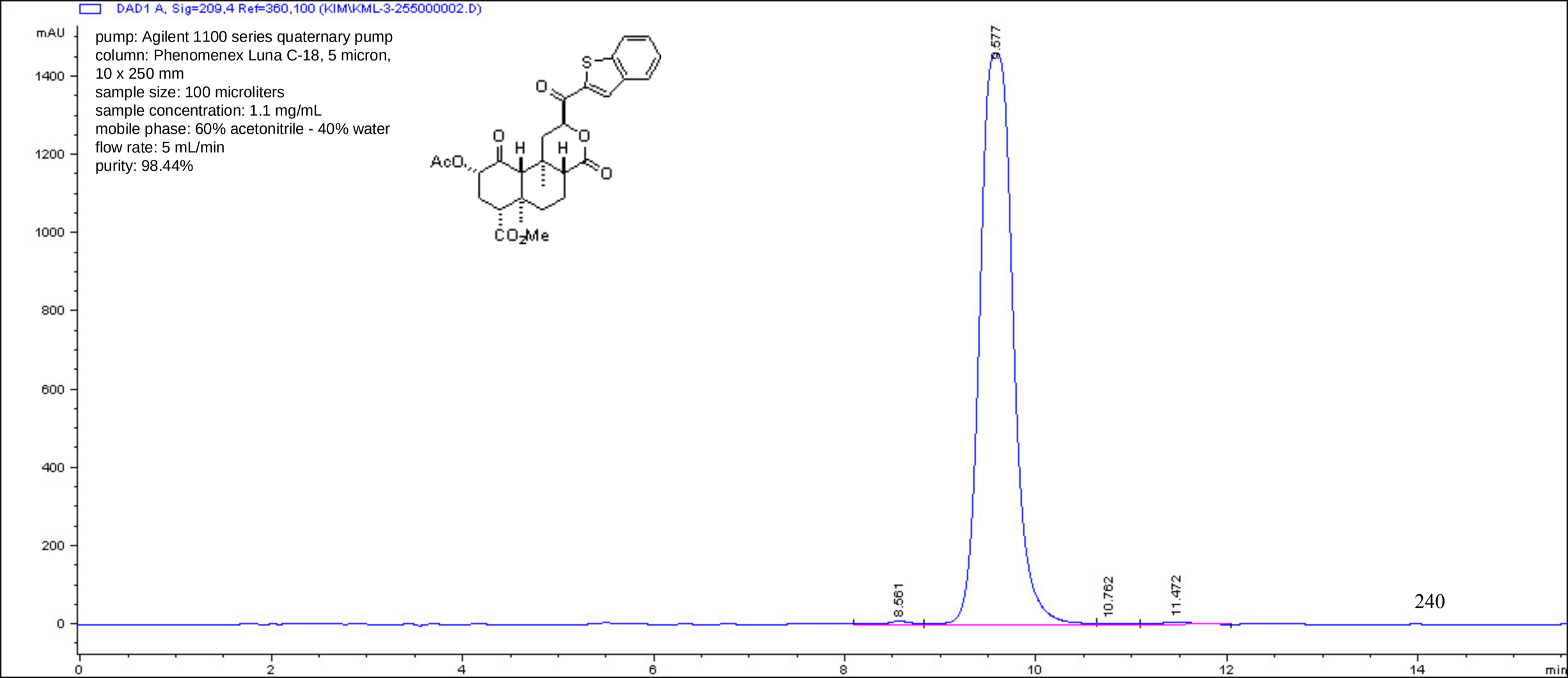
DAD1 A, Sig=209,4 Ref=360,100 (KIM\KML-3-255000002.D)
mAU
pump: Agilent 1100 series quaternary pump
column: Phenomenex Luna C-18, 5 micron,
10 x 250 mm
sample size: 100 microliters
sample concentration: 1.1 mg/mL
mobile phase: 60% acetonitrile - 40% water
flow rate: 5 mL/min
purity: 98.44%
AcO
CO2Me
9.577
8.561
10.762
11.472
240
min

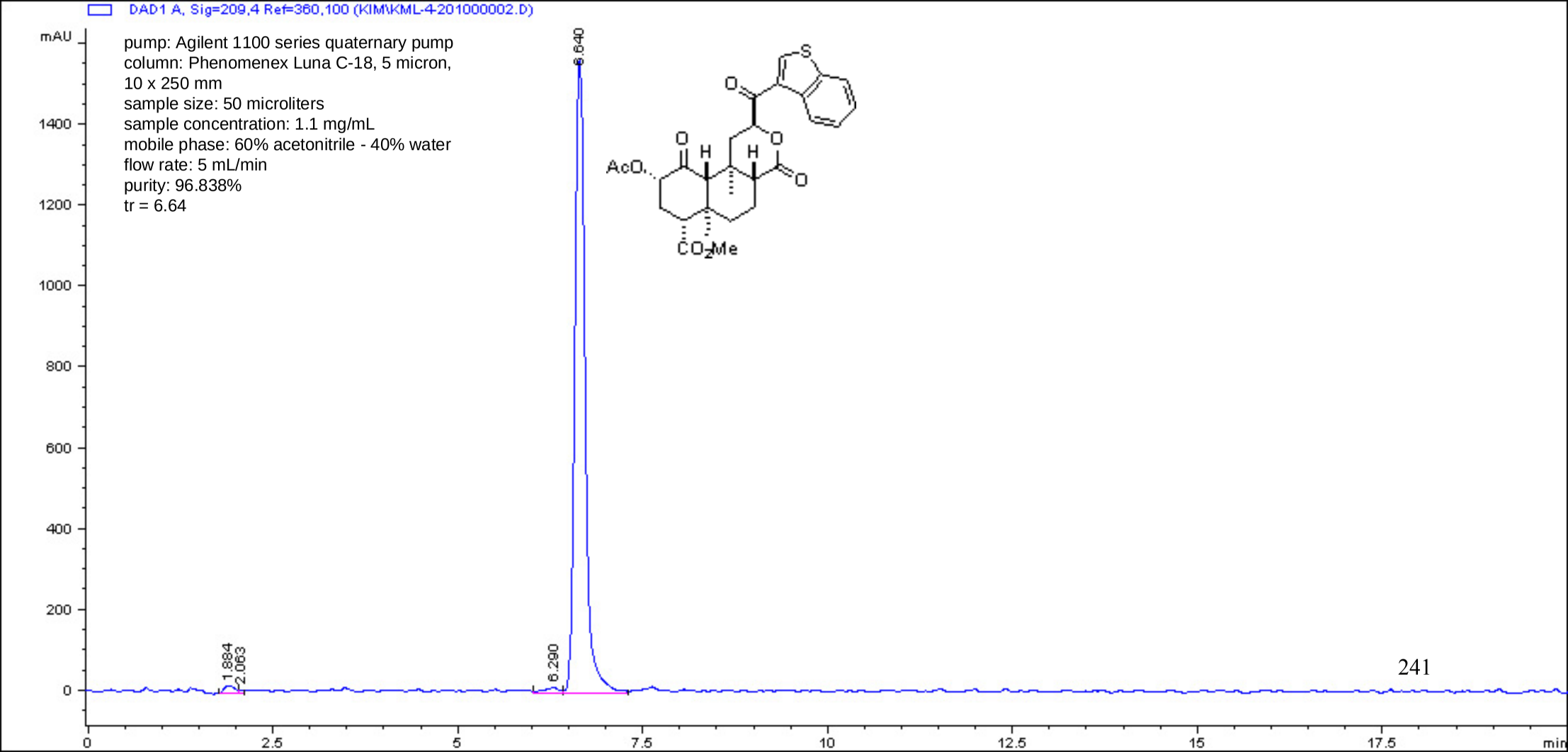
DAD1 A, Sig=209,4 Ref=360,100 (KIM\KML-4-201000002.D)
mAU
pump: Agilent 1100 series quaternary pump
column: Phenomenex Luna C-18, 5 micron,
10 x 250 mm
sample size: 50 microliters
sample concentration: 1.1 mg/mL
mobile phase: 60% acetonitrile - 40% water
flow rate: 5 mL/min
purity: 96.838%
tr = 6.64
6.640
1.884
2.063
6.290
AcO
CO2Me
1400
1200
1000
800
600
400
200
0
0
2.5
5
7.5
10
12.5
15
17.5
min

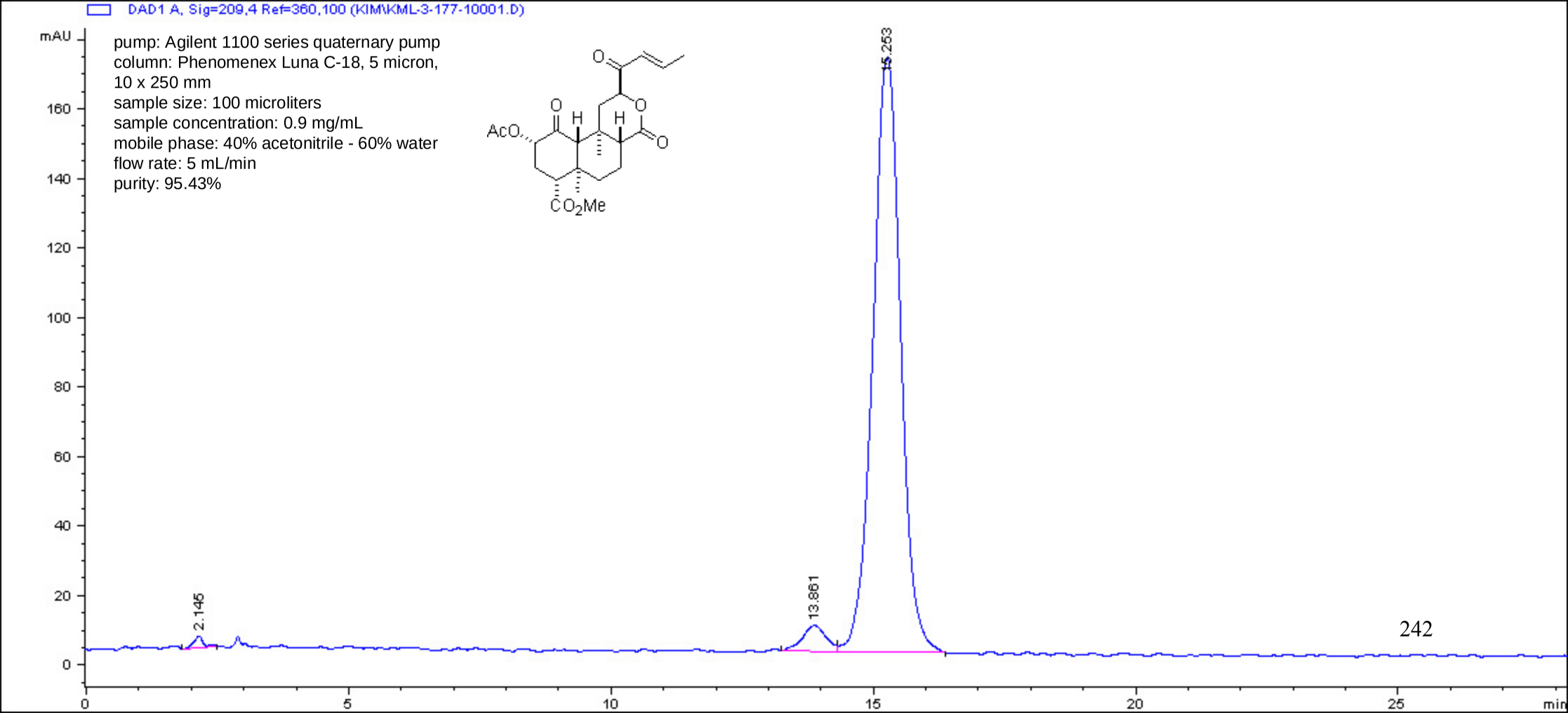
DAD1 A, Sig=209,4 Ref=360,100 (KIM\KML-3-177-10001.D)
mAU
pump: Agilent 1100 series quaternary pump
column: Phenomenex Luna C-18, 5 micron,
10 x 250 mm
sample size: 100 microliters
sample concentration: 0.9 mg/mL
mobile phase: 40% acetonitrile - 60% water
flow rate: 5 mL/min
purity: 95.43%
AcO
H
H
O
O
O
O
O
CO2Me
15.253
13.861
2.145
242
min

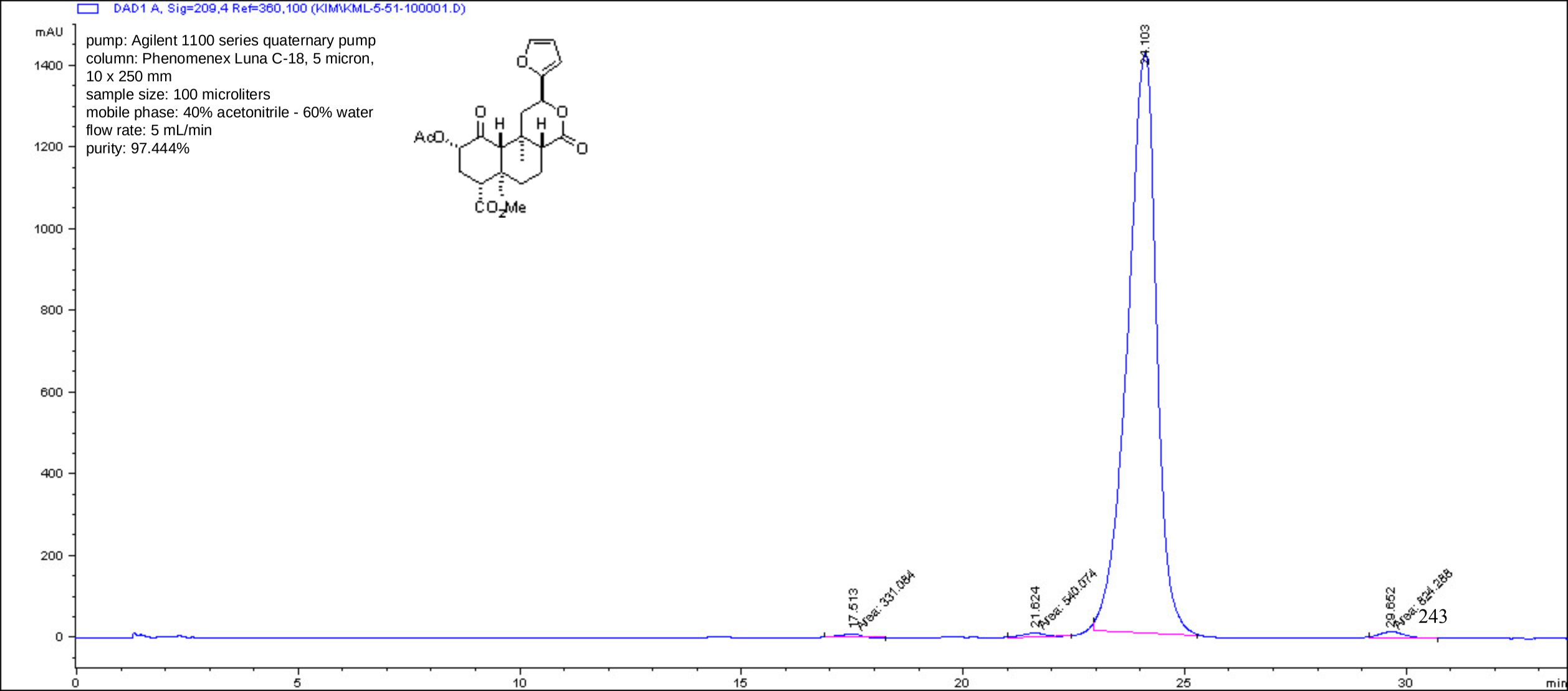
DAD1 A, Sig=209,4 Ref=360,100 (KIM\KML-5-51-100001.D)
mAU
pump: Agilent 1100 series quaternary pump
column: Phenomenex Luna C-18, 5 micron, 10 x 250 mm
sample size: 100 microliters
mobile phase: 40% acetonitrile - 60% water
flow rate: 5 mL/min
purity: 97.444%
AcO
CO2Me
17.513
Area: 331.084
21.624
Area: 540.074
24.103
29.652
Area: 824.288
min

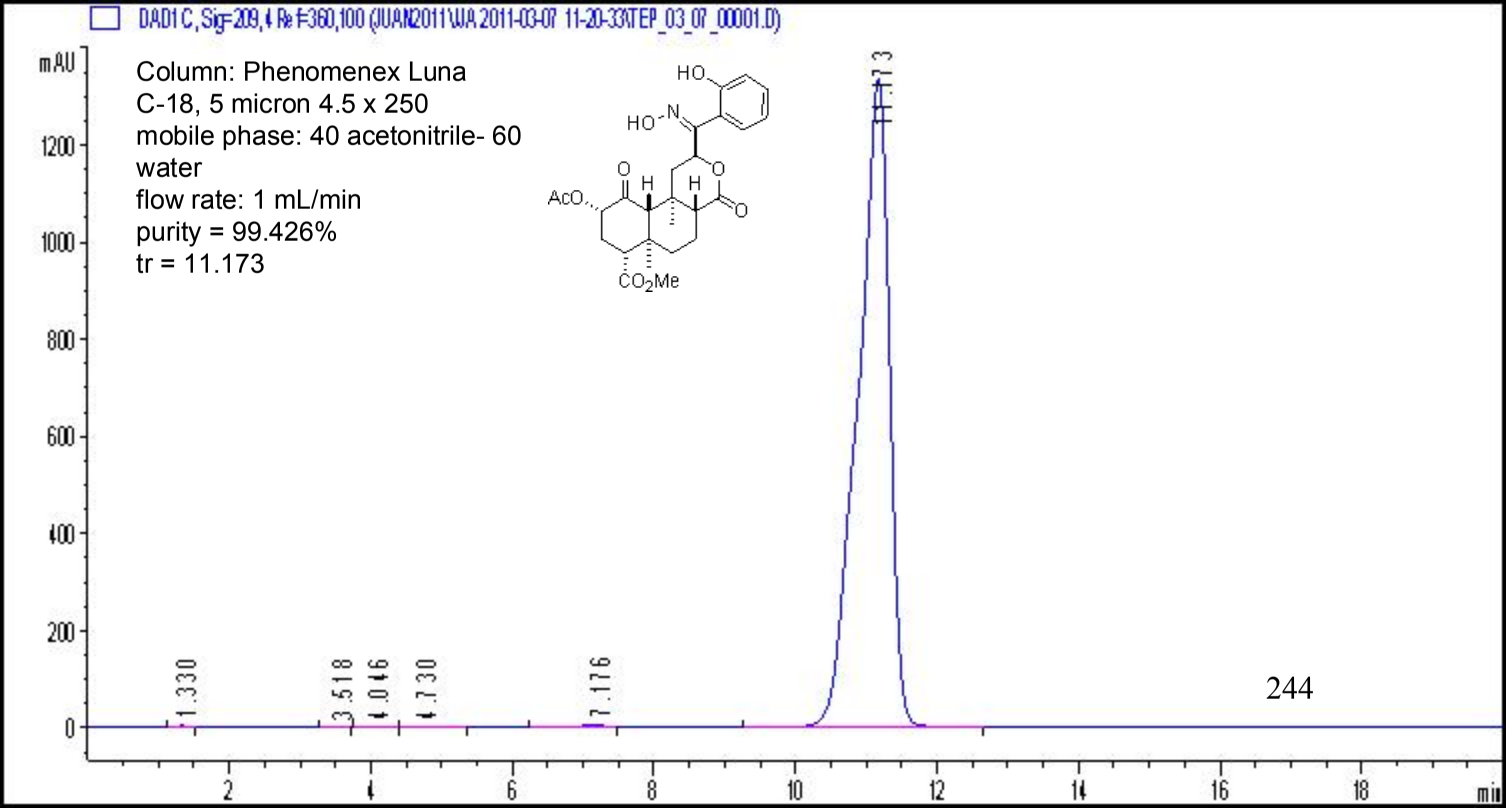
DAD1 C, Sig=209,4 Ref=360,100 (JUAN2011\JA 2011-03-07 11-20-33\TEP_03_07_00001.D)
mAU
1200
1000
800
600
400
200
0
Column: Phenomenex Luna
C-18, 5 micron 4.5 x 250
mobile phase: 40 acetonitrile- 60
water
flow rate: 1 mL/min
purity = 99.426%
tr = 11.173
HO
HO-N
AcO
O
H
H
O
O
CO2Me
11.173
1.330
3.518
4.046
4.730
7.176
2
4
6
8
10
12
14
16
18
min

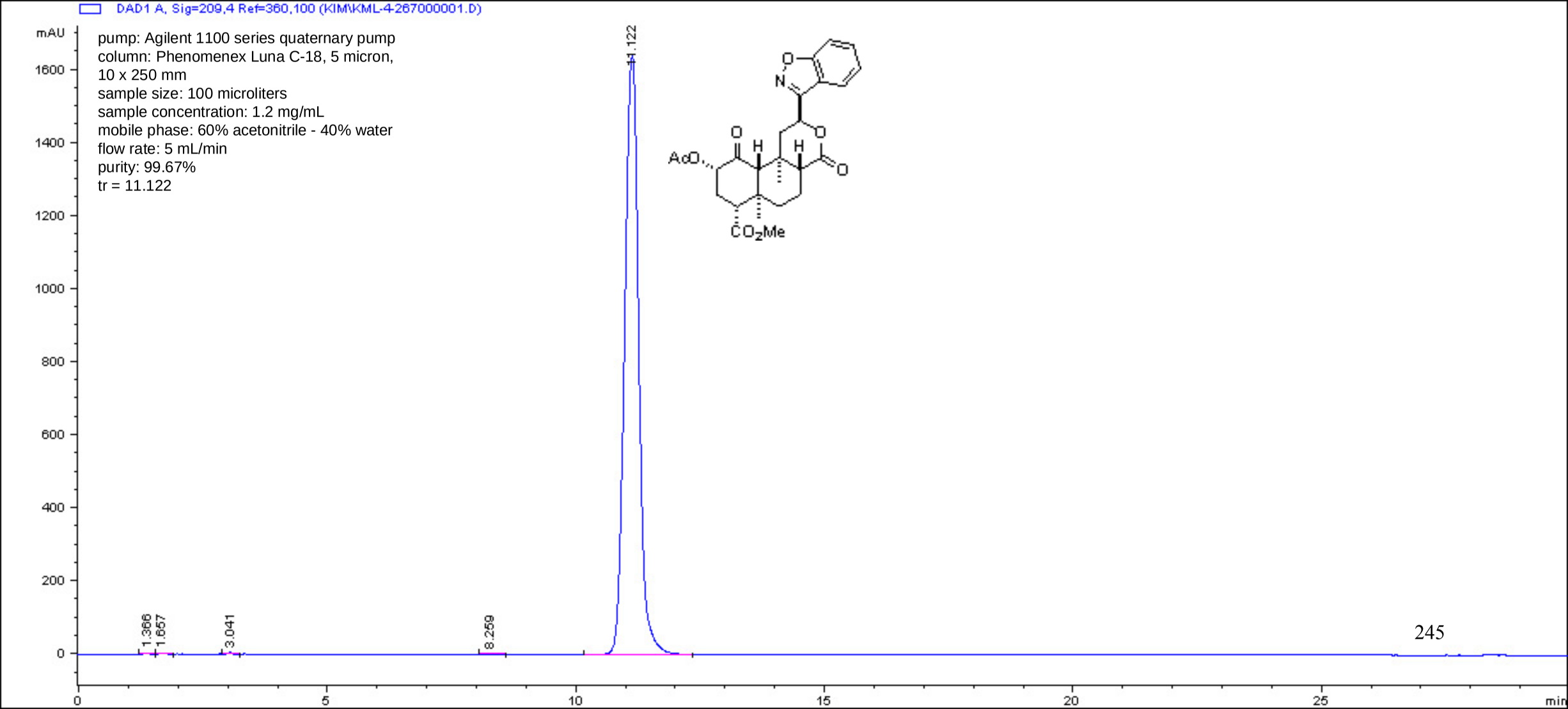
DAD1 A, Sig=209,4 Ref=360,100 (KIM\KML-4-267000001.D)
mAU
pump: Agilent 1100 series quaternary pump
column: Phenomenex Luna C-18, 5 micron,
10 x 250 mm
sample size: 100 microliters
sample concentration: 1.2 mg/mL
mobile phase: 60% acetonitrile - 40% water
flow rate: 5 mL/min
purity: 99.67%
tr = 11.122
11.122
1.366
1.657
3.041
8.259
AcO
O
H
H
O
O
O
N
O
CO2Me
1600
1400
1200
1000
800
600
400
200
0
0
5
10
15
20
25
min

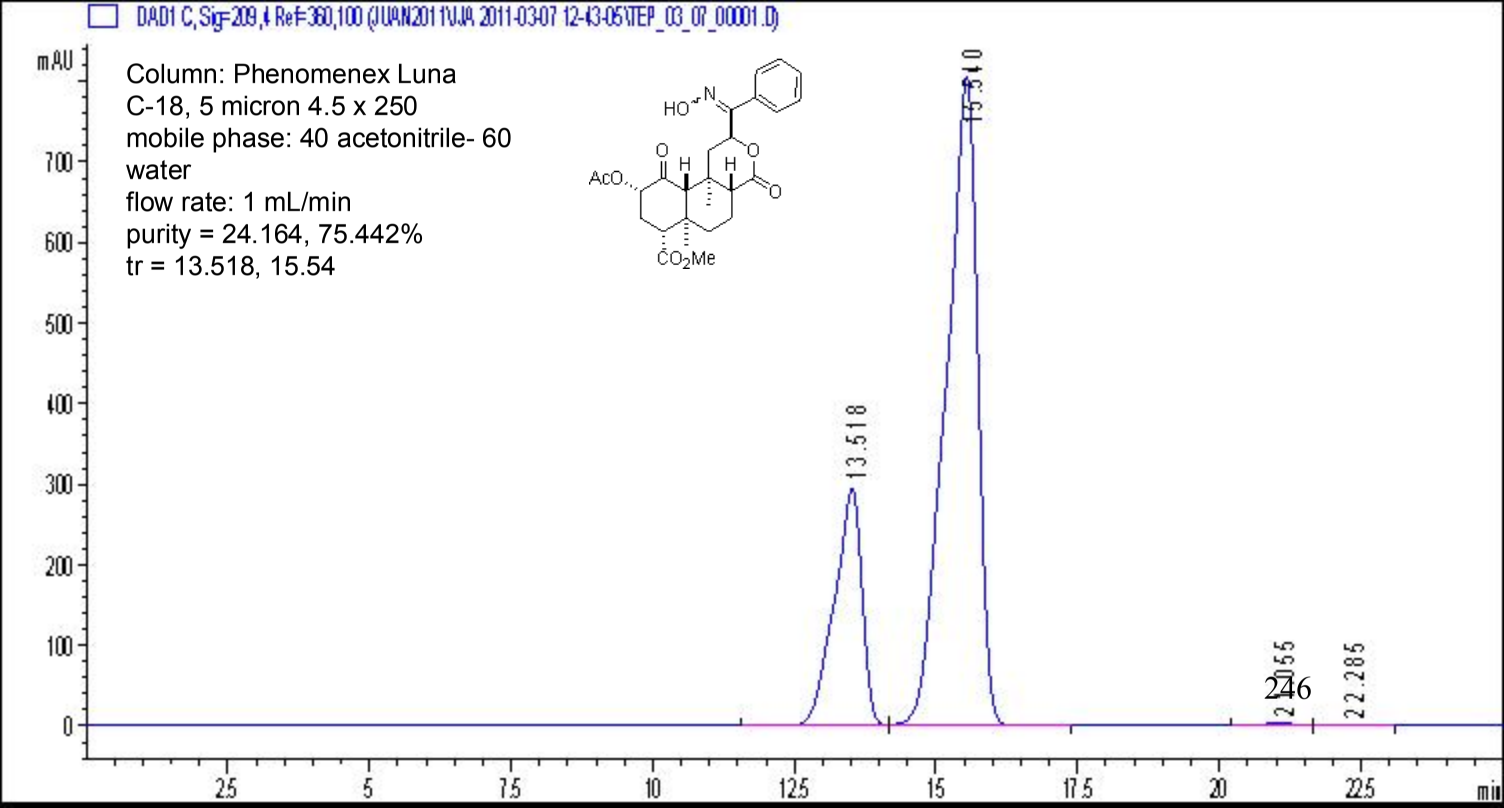
DAD1 C, Sig=209,4 Ref=360,100 (JUAN2011\JA 2011-03-07 12-43-05\TEP_03_07_00001.D)
Column: Phenomenex Luna
C-18, 5 micron 4.5 x 250
mobile phase: 40 acetonitrile- 60
water
flow rate: 1 mL/min
purity = 24.164, 75.442%
tr = 13.518, 15.54
mAU
13.518
15.540
22.055
22.285
246
min

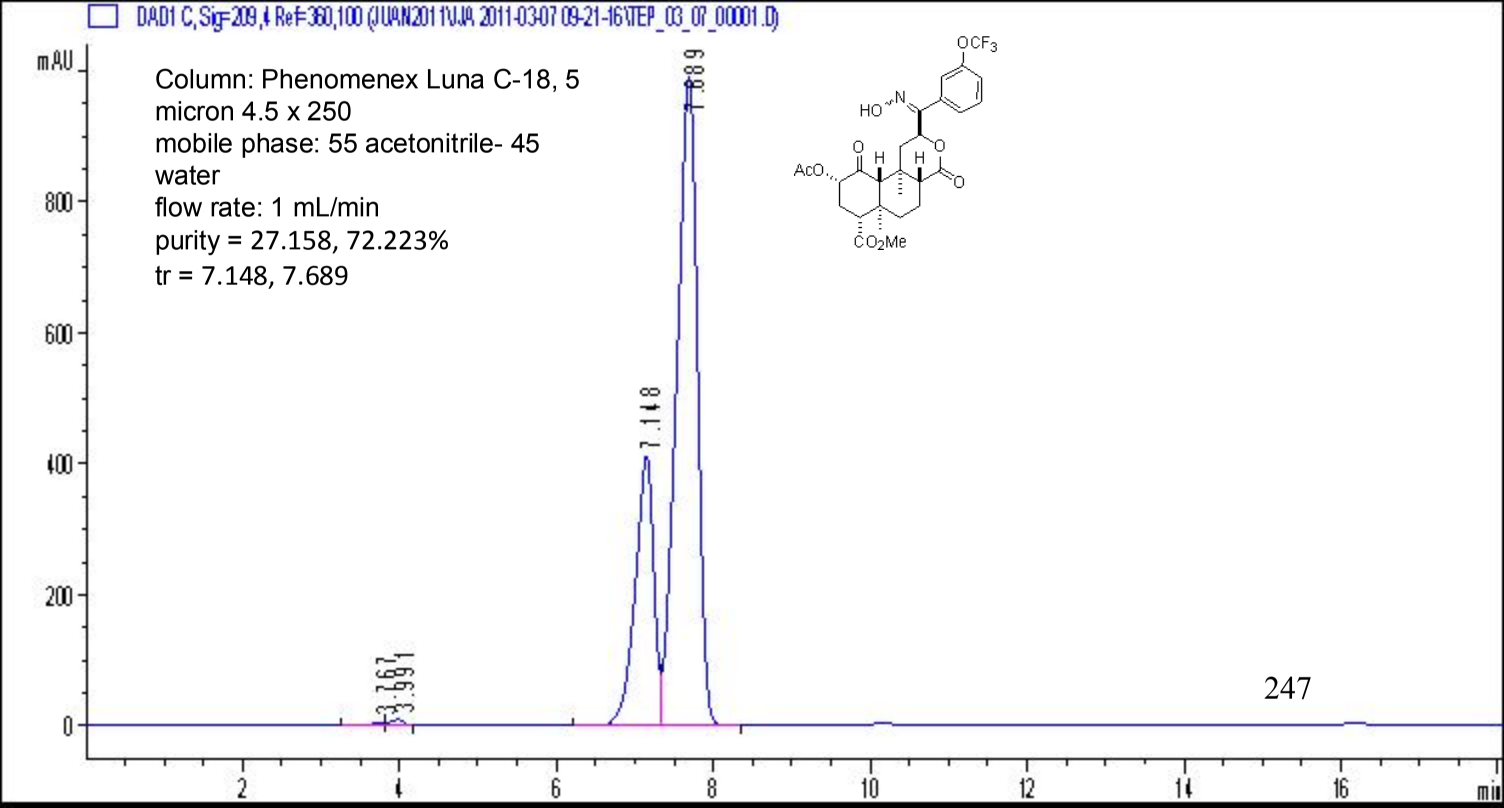
DAD1 C, Sig=209,4 Ref=360,100 (JUAN2011\JA 2011-03-07 09-21-16\TEP_03_07_00001.D)
mAU
Column: Phenomenex Luna C-18, 5 micron 4.5 x 250
mobile phase: 55 acetonitrile- 45 water
flow rate: 1 mL/min
purity = 27.158, 72.223%
tr = 7.148, 7.689
7.689
7.148
3.667
3.991
OCF3
HO
N
AcO
O
H
H
O
O
CO2Me
800
600
400
200
0
2
4
6
8
10
12
14
16
min
247

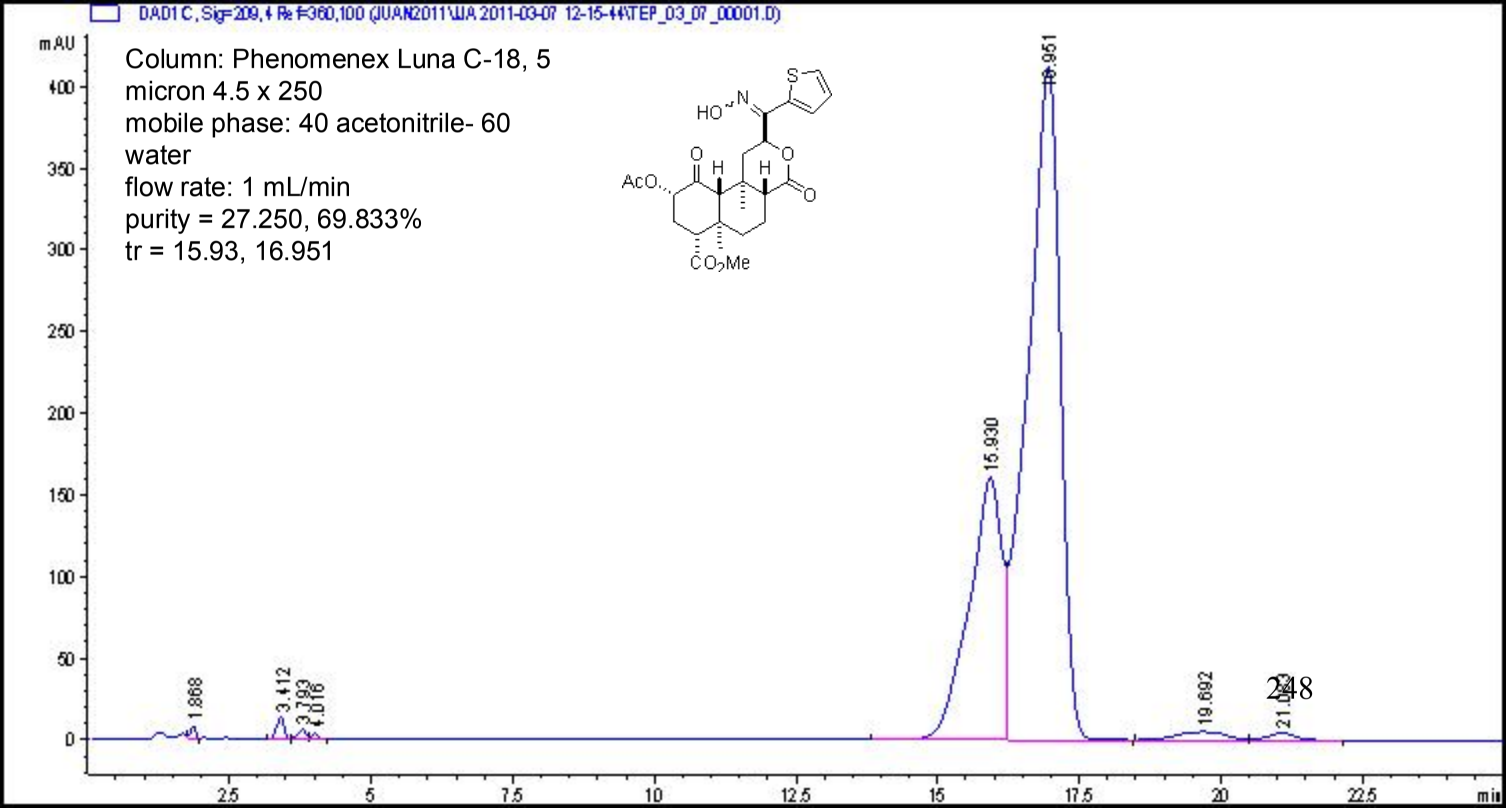
DAD1 C, Sig=209,4 Ref=360,100 (JUAN2011\JUA 2011-03-07 12-15-44\TEP_03_07_00001.D)
mAU
Column: Phenomenex Luna C-18, 5
micron 4.5 x 250
mobile phase: 40 acetonitrile- 60
water
flow rate: 1 mL/min
purity = 27.250, 69.833%
tr = 15.93, 16.951
HO
N
S
O
H
H
O
O
AcO
O
CO2Me
15.930
16.951
19.692
1.868
3.412
3.793
4.016
248
min

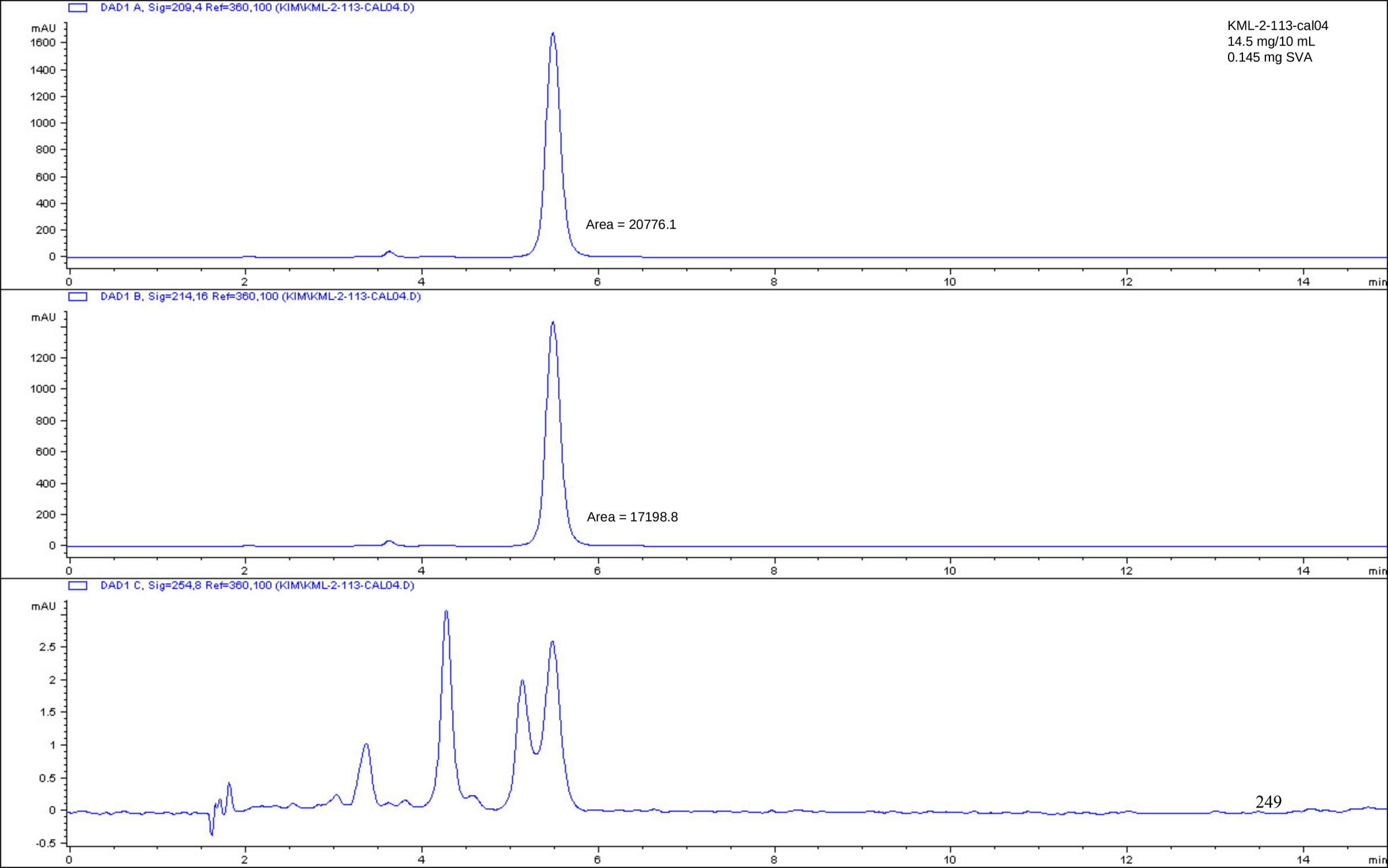
DAD1 A, Sig=209,4 Ref=360,100 (KIM\KML-2-113-CAL04.D)
KML-2-113-cal04
14.5 mg/10 mL
0.145 mg SVA
mAU
Area = 20776.1
min
DAD1 B, Sig=214,16 Ref=360,100 (KIM\KML-2-113-CAL04.D)
mAU
Area = 17198.8
min
DAD1 C, Sig=254,8 Ref=360,100 (KIM\KML-2-113-CAL04.D)
mAU
min

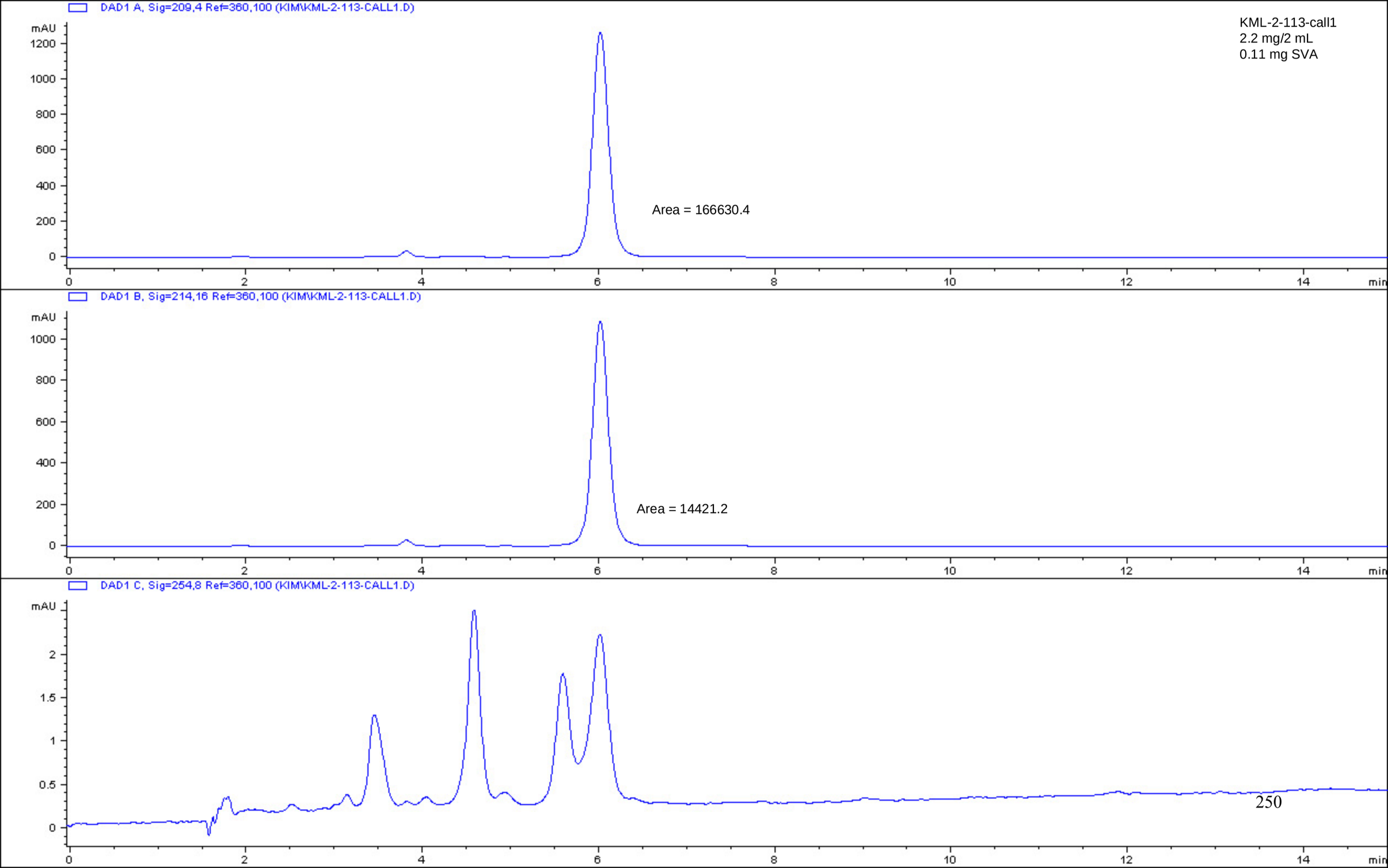
DAD1 A, Sig=209,4 Ref=360,100 (KIM\KML-2-113-CALL1.D)
KML-2-113-call1
2.2 mg/2 mL
0.11 mg SVA
mAU
Area = 166630.4
DAD1 B, Sig=214,16 Ref=360,100 (KIM\KML-2-113-CALL1.D)
Area = 14421.2
DAD1 C, Sig=254,8 Ref=360,100 (KIM\KML-2-113-CALL1.D)
min

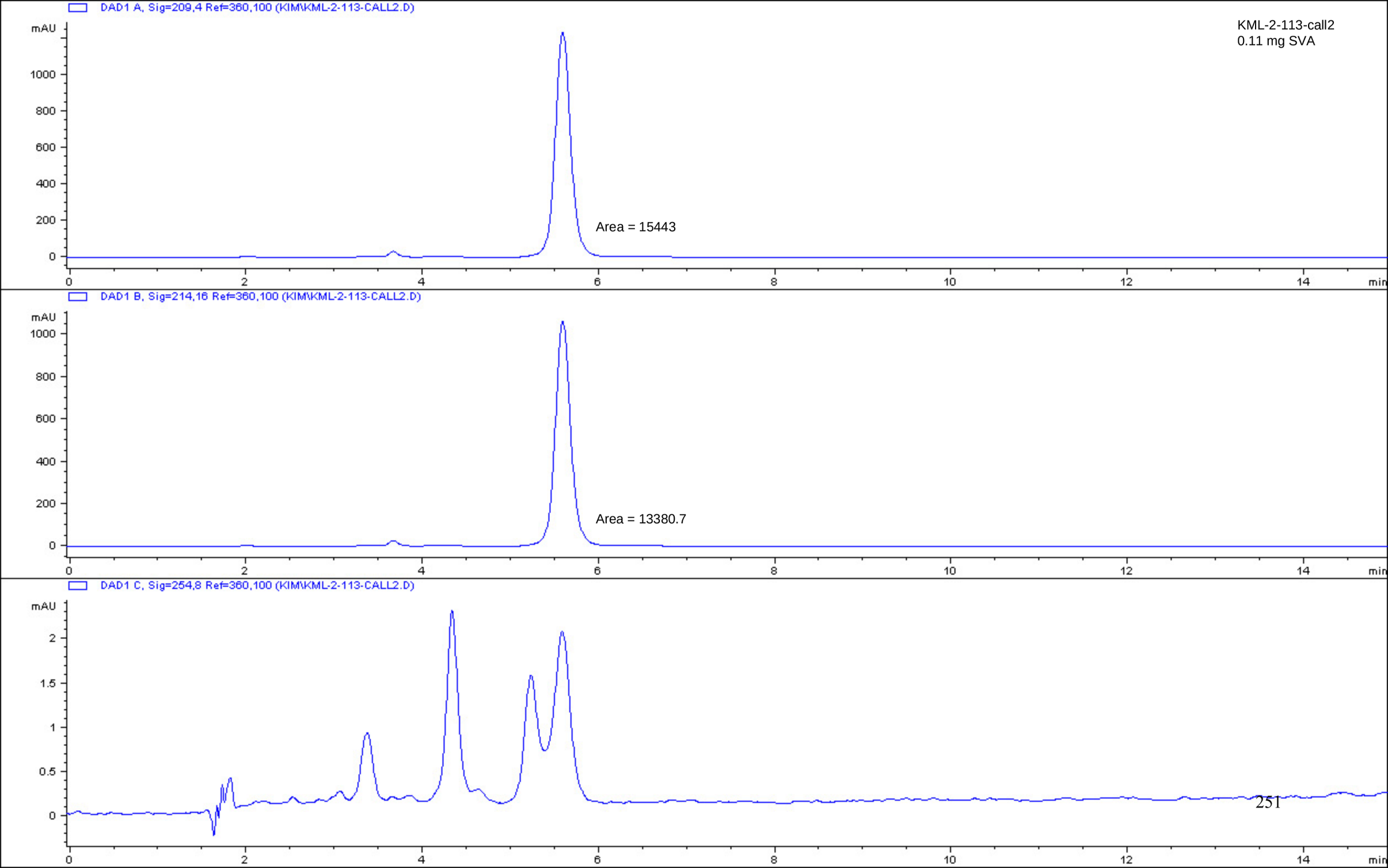
DAD1 A, Sig=209,4 Ref=360,100 (KIM\KML-2-113-CALL2.D)
KML-2-113-call2
0.11 mg SVA
mAU
Area = 15443
min
DAD1 B, Sig=214,16 Ref=360,100 (KIM\KML-2-113-CALL2.D)
mAU
Area = 13380.7
min
DAD1 C, Sig=254,8 Ref=360,100 (KIM\KML-2-113-CALL2.D)
mAU
min

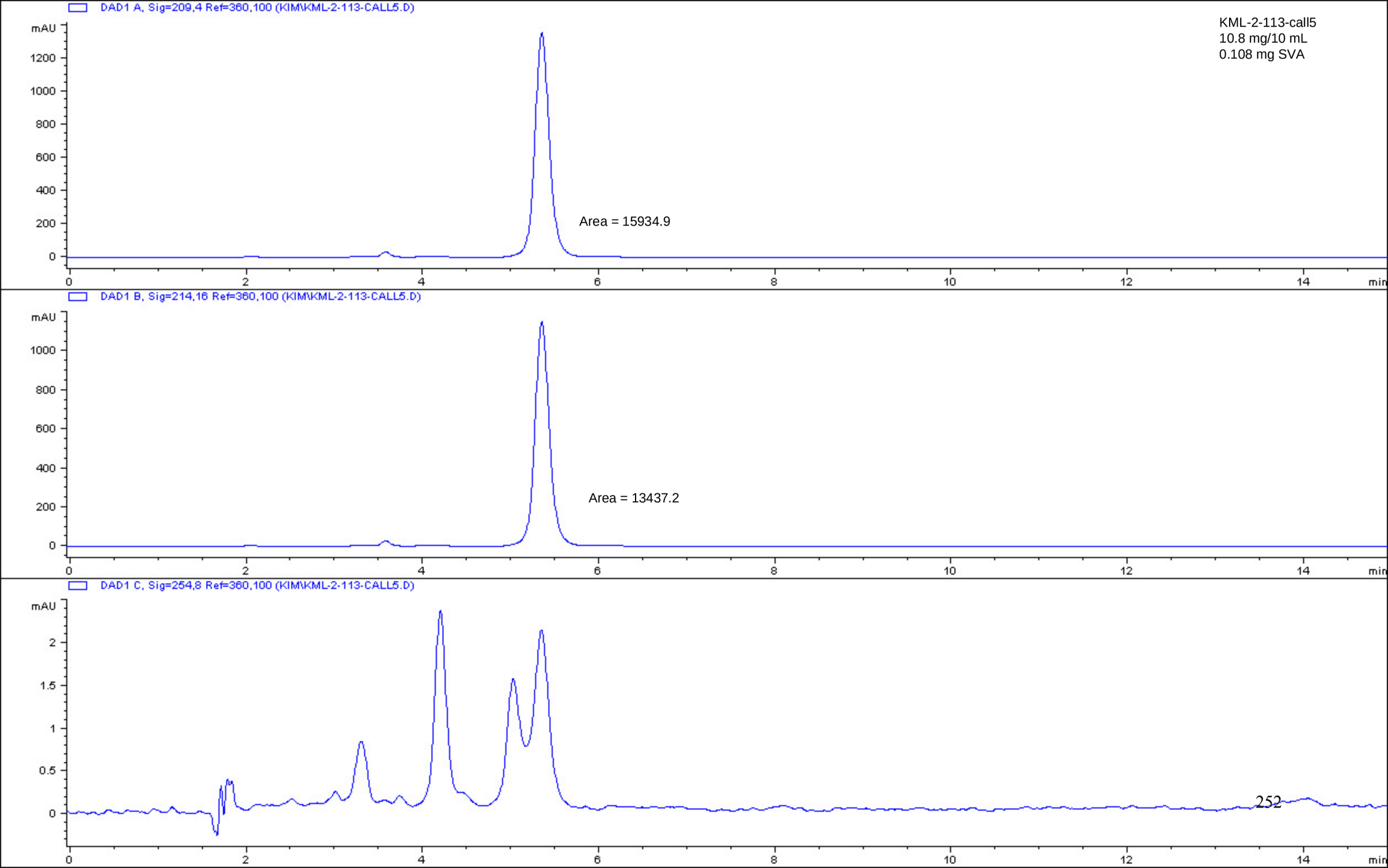
DAD1 A, Sig=209,4 Ref=360,100 (KIM\KML-2-113-CALL5.D)
KML-2-113-call5
10.8 mg/10 mL
0.108 mg SVA
mAU
Area = 15934.9
min
DAD1 B, Sig=214,16 Ref=360,100 (KIM\KML-2-113-CALL5.D)
mAU
Area = 13437.2
min
DAD1 C, Sig=254,8 Ref=360,100 (KIM\KML-2-113-CALL5.D)
mAU
min

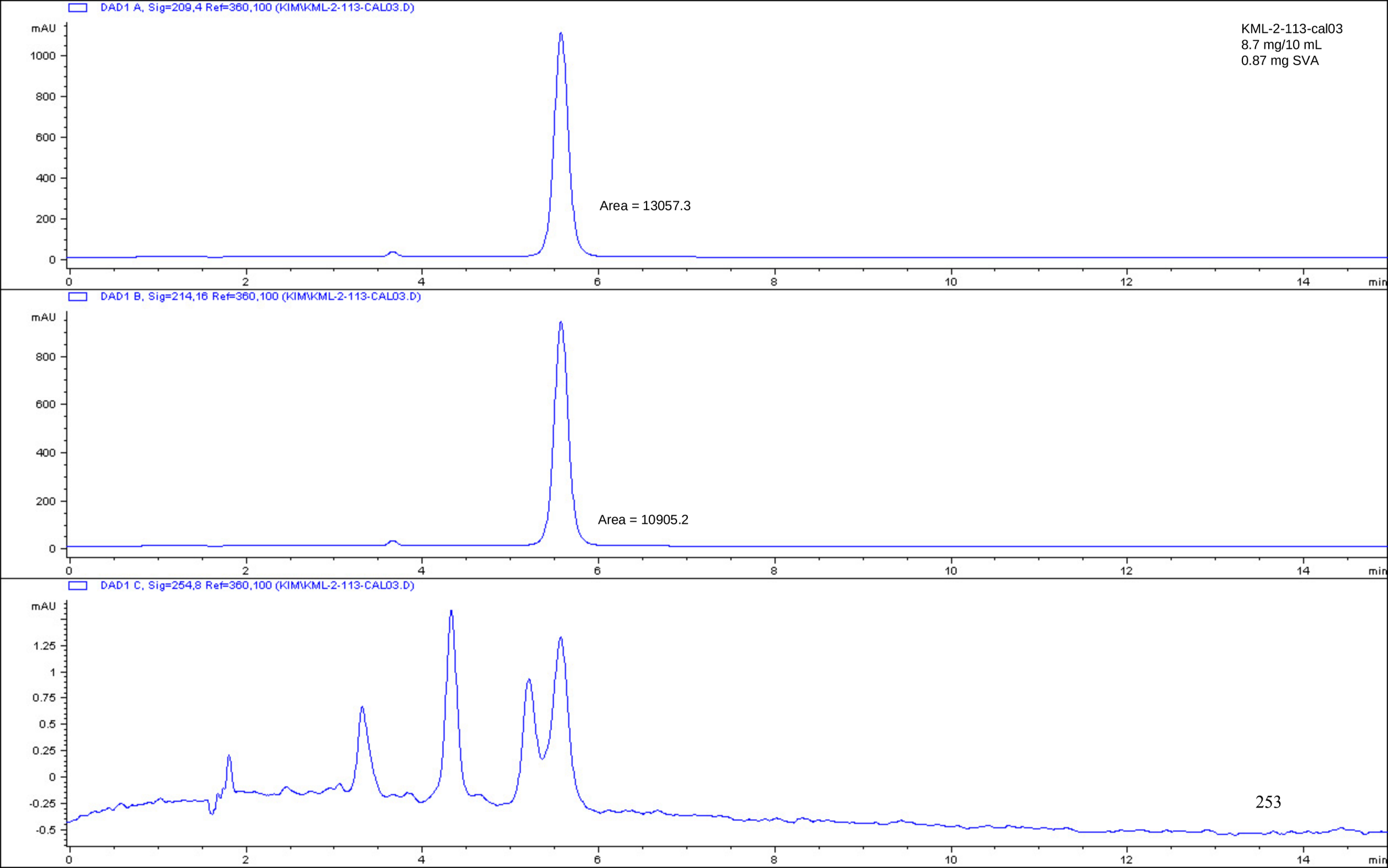
DAD1 A, Sig=209,4 Ref=360,100 (KIM\KML-2-113-CAL03.D)
mAU
1000
800
600
400
200
0
KML-2-113-cal03
8.7 mg/10 mL
0.87 mg SVA
Area = 13057.3
0
2
4
6
8
10
12
14
min
DAD1 B, Sig=214,16 Ref=360,100 (KIM\KML-2-113-CAL03.D)
mAU
800
600
400
200
0
Area = 10905.2
0
2
4
6
8
10
12
14
min
DAD1 C, Sig=254,8 Ref=360,100 (KIM\KML-2-113-CAL03.D)
mAU
1.25
1
0.75
0.5
0.25
0
-0.25
-0.5
0
2
4
6
8
10
12
14
min

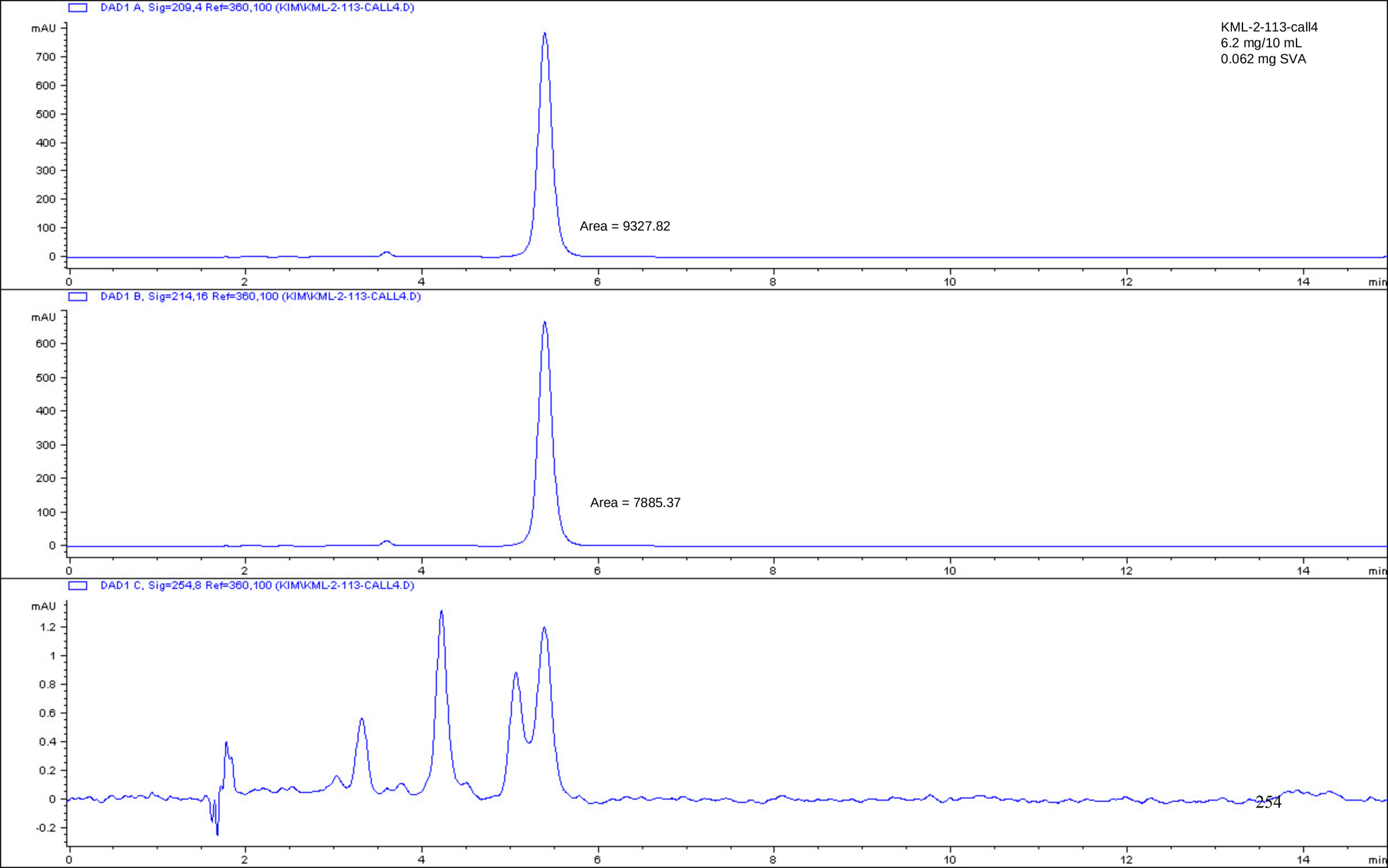
DAD1 A, Sig=209,4 Ref=360,100 (KIM\KML-2-113-CALL4.D)
mAU
KML-2-113-call4
6.2 mg/10 mL
0.062 mg SVA
Area = 9327.82
min
DAD1 B, Sig=214,16 Ref=360,100 (KIM\KML-2-113-CALL4.D)
mAU
Area = 7885.37
min
DAD1 C, Sig=254,8 Ref=360,100 (KIM\KML-2-113-CALL4.D)
mAU
min

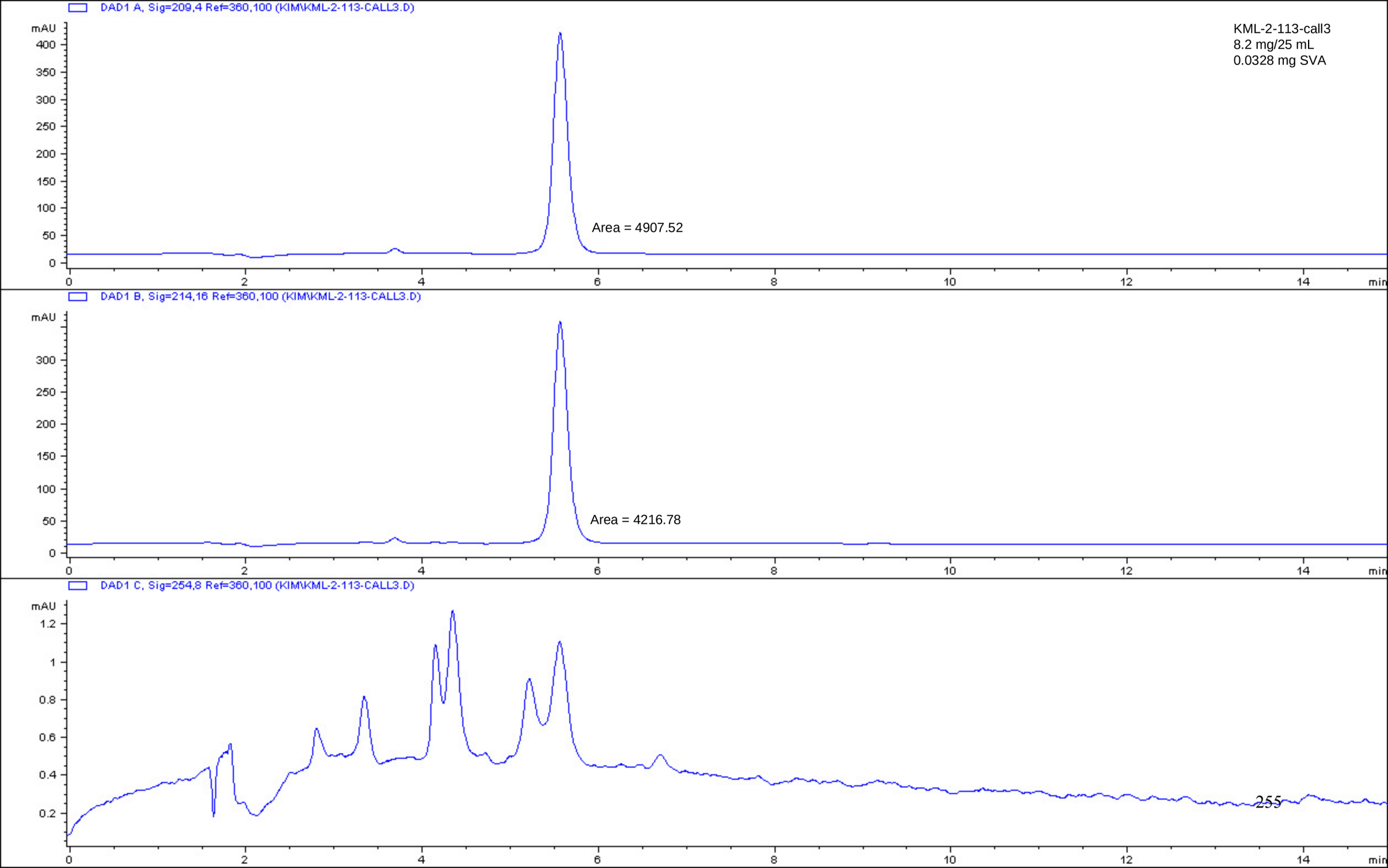
DAD1 A, Sig=209,4 Ref=360,100 (KIM\KML-2-113-CALL3.D)
KML-2-113-call3
8.2 mg/25 mL
0.0328 mg SVA
mAU
Area = 4907.52
min
DAD1 B, Sig=214,16 Ref=360,100 (KIM\KML-2-113-CALL3.D)
mAU
Area = 4216.78
min
DAD1 C, Sig=254,8 Ref=360,100 (KIM\KML-2-113-CALL3.D)
mAU
min

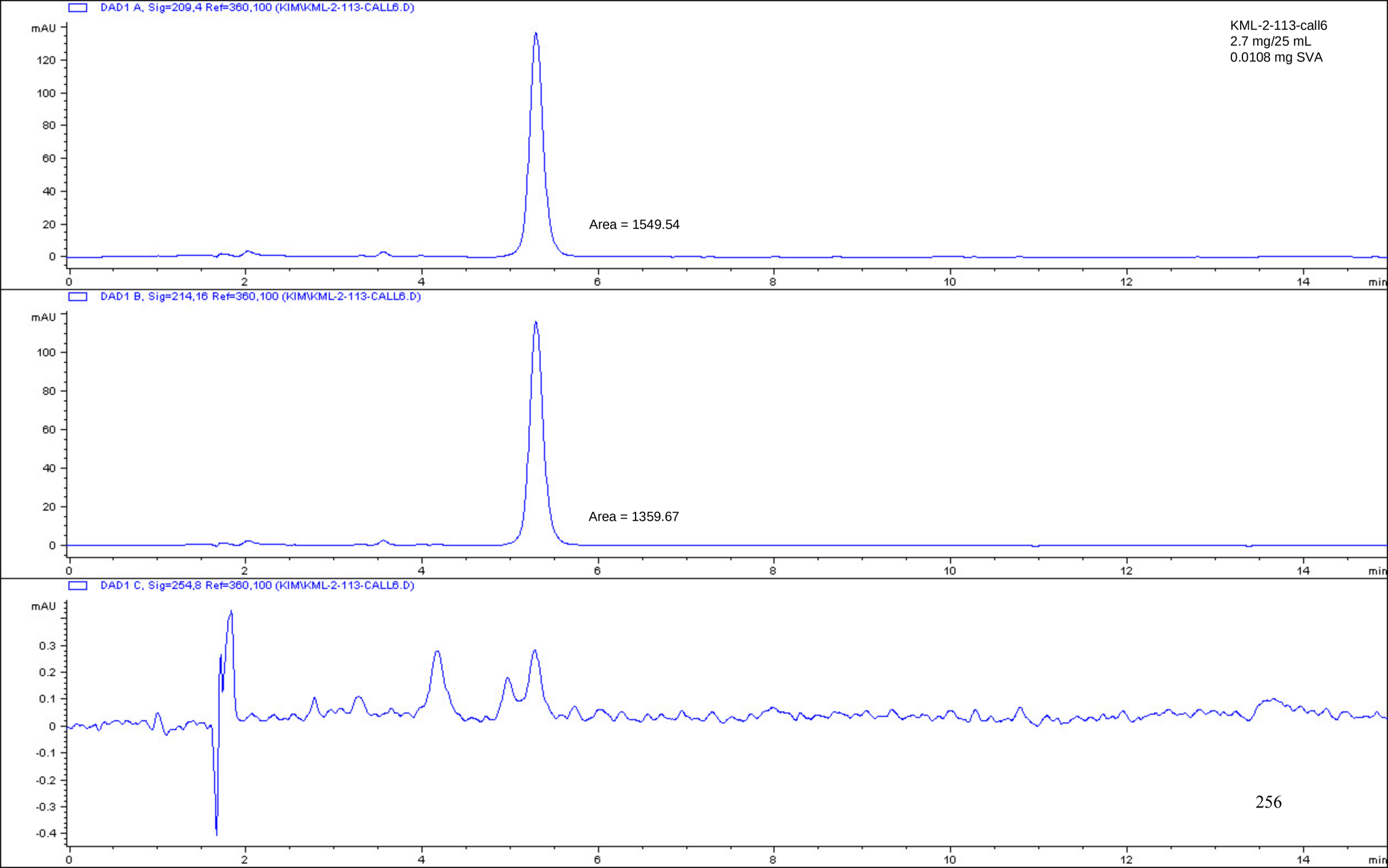
DAD1 A, Sig=209,4 Ref=360,100 (KIM\KML-2-113-CALL6.D)
KML-2-113-call6
2.7 mg/25 mL
0.0108 mg SVA
mAU
Area = 1549.54
min
DAD1 B, Sig=214,16 Ref=360,100 (KIM\KML-2-113-CALL6.D)
mAU
Area = 1359.67
min
DAD1 C, Sig=254,8 Ref=360,100 (KIM\KML-2-113-CALL6.D)
mAU
min

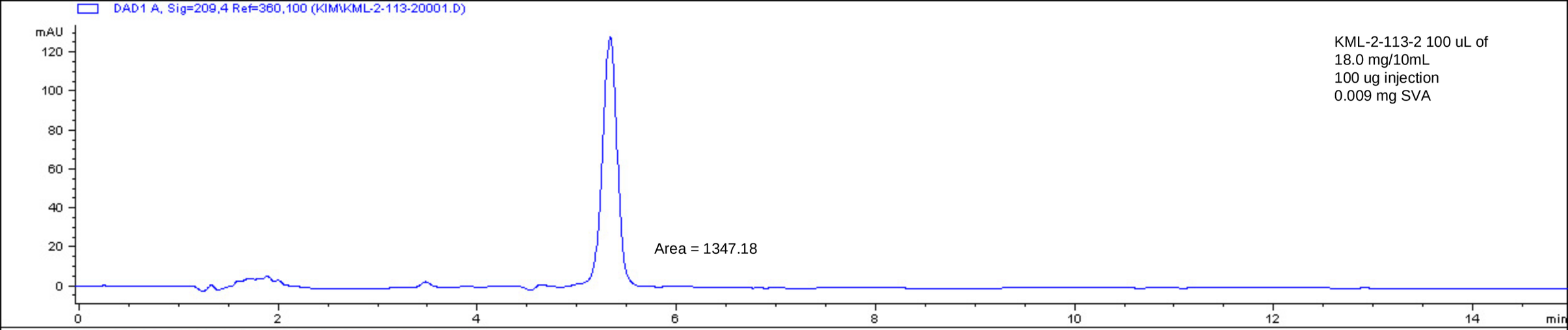
DAD1 A, Sig=209,4 Ref=360,100 (KIM\KML-2-113-20001.D)
mAU
120
100
80
60
40
20
0
KML-2-113-2 100 uL of
18.0 mg/10mL
100 ug injection
0.009 mg SVA
Area = 1347.18
0
2
4
6
8
10
12
14
min

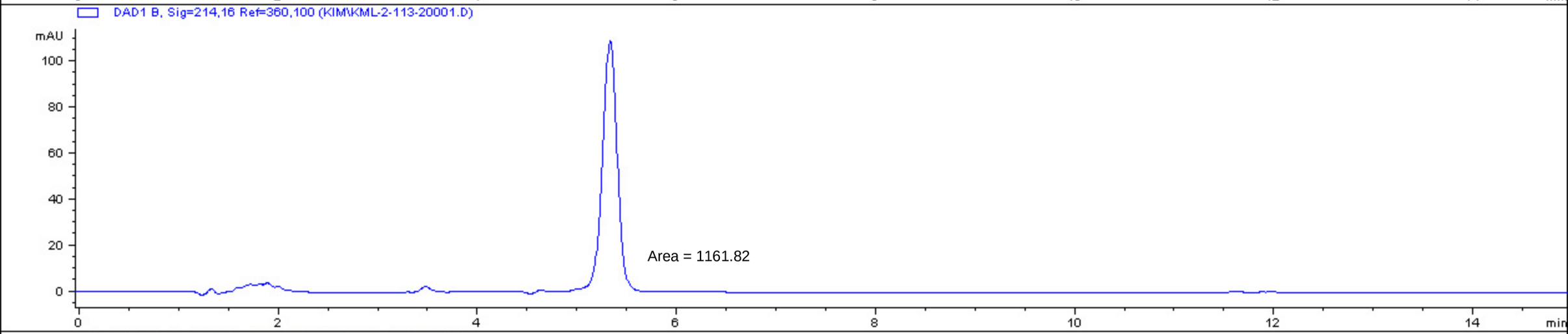
DAD1 B, Sig=214,16 Ref=360,100 (KIM\KML-2-113-20001.D)
mAU
100
80
60
40
20
0
Area = 1161.82
0
2
4
6
8
10
12
14
min

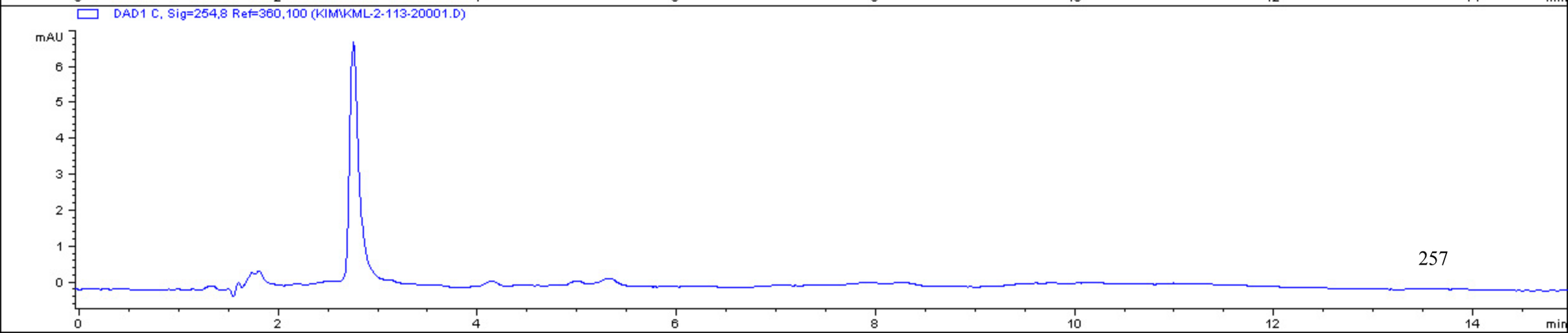
DAD1 C, Sig=254,8 Ref=360,100 (KIM\KML-2-113-20001.D)
mAU
6
5
4
3
2
1
0
0
2
4
6
8
10
12
14
min

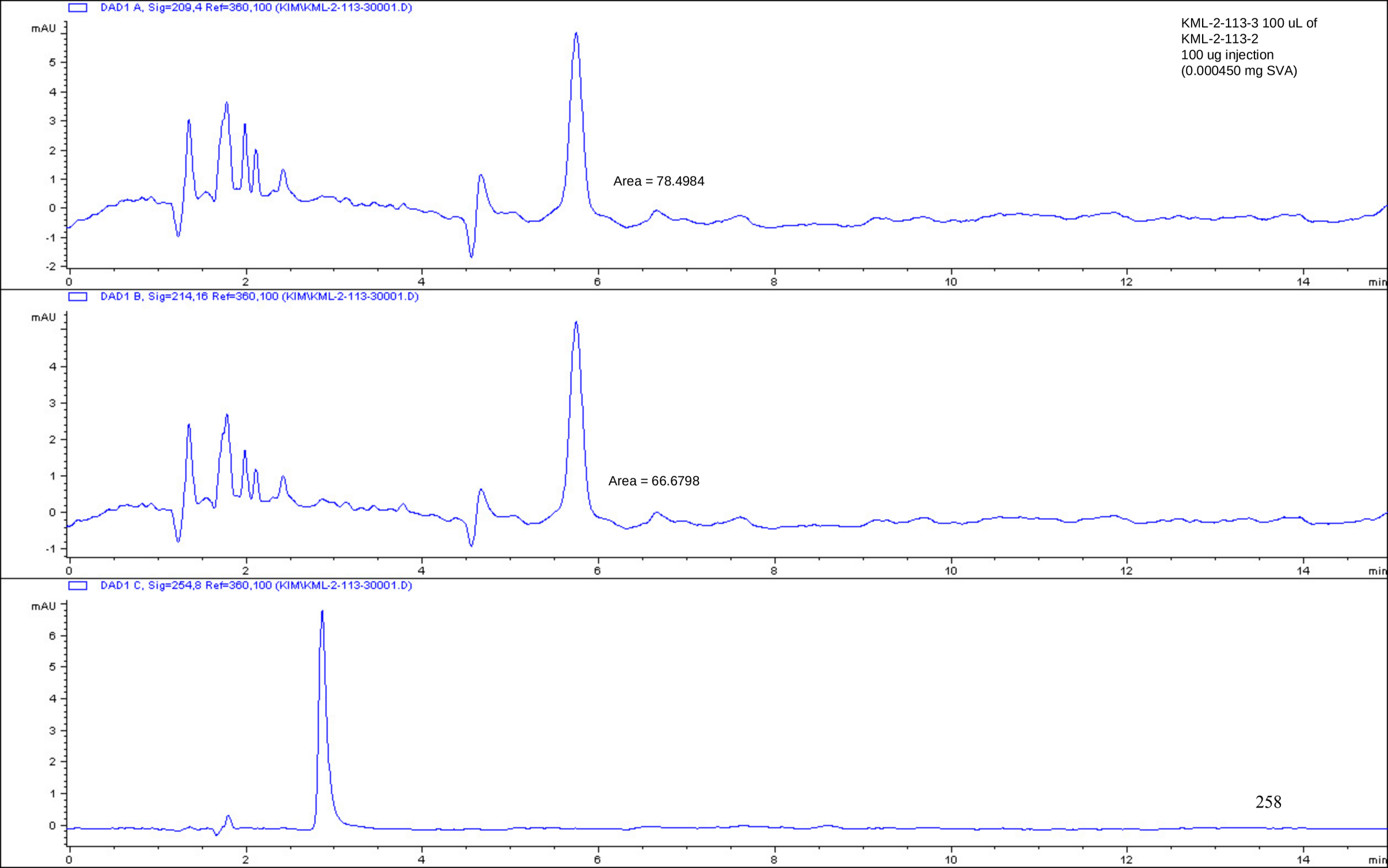
DAD1 A, Sig=209,4 Ref=360,100 (KIM\KML-2-113-30001.D)
mAU
KML-2-113-3 100 uL of
KML-2-113-2
100 ug injection
(0.000450 mg SVA)
Area = 78.4984
min
DAD1 B, Sig=214,16 Ref=360,100 (KIM\KML-2-113-30001.D)
mAU
Area = 66.6798
min
DAD1 C, Sig=254,8 Ref=360,100 (KIM\KML-2-113-30001.D)
mAU
min

KML-2-113-7A 2.5M Captisol

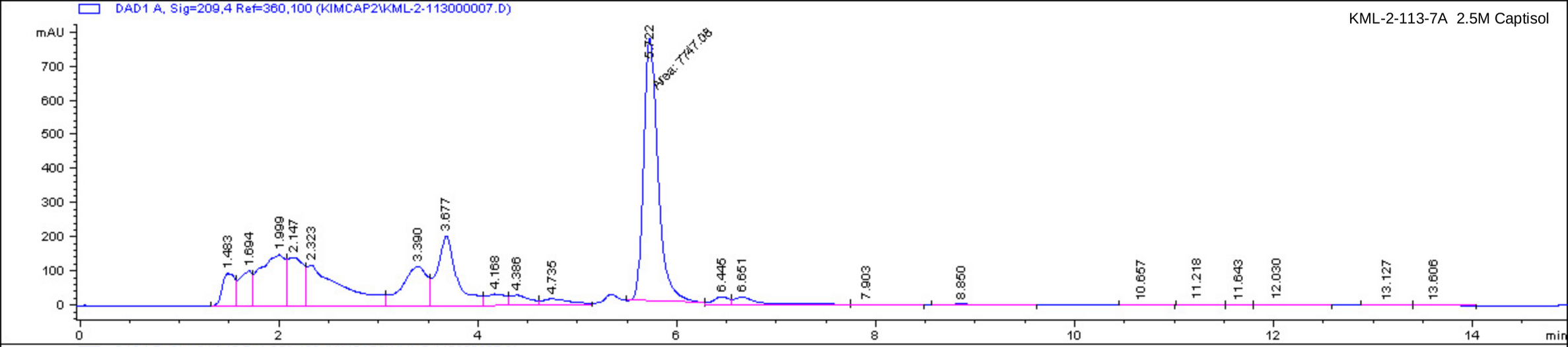

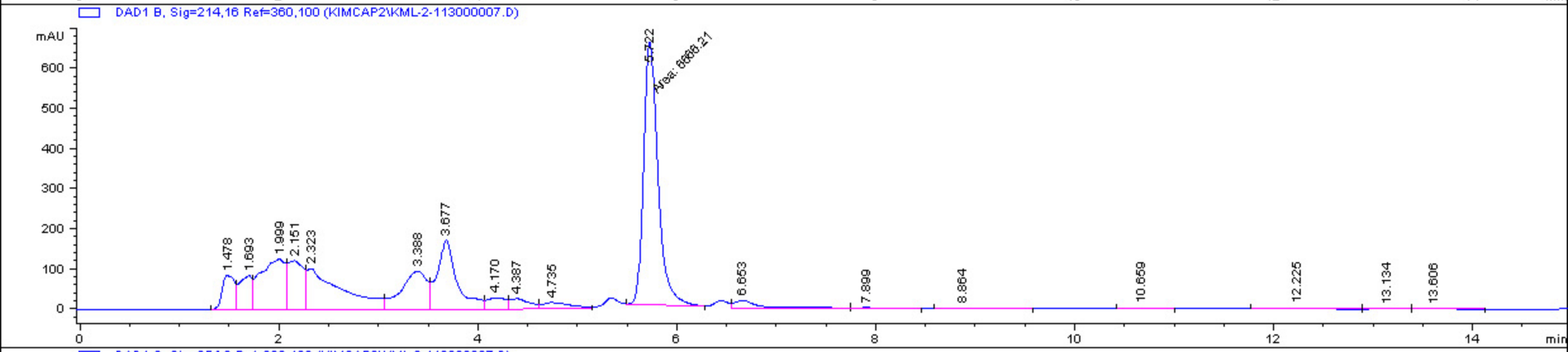

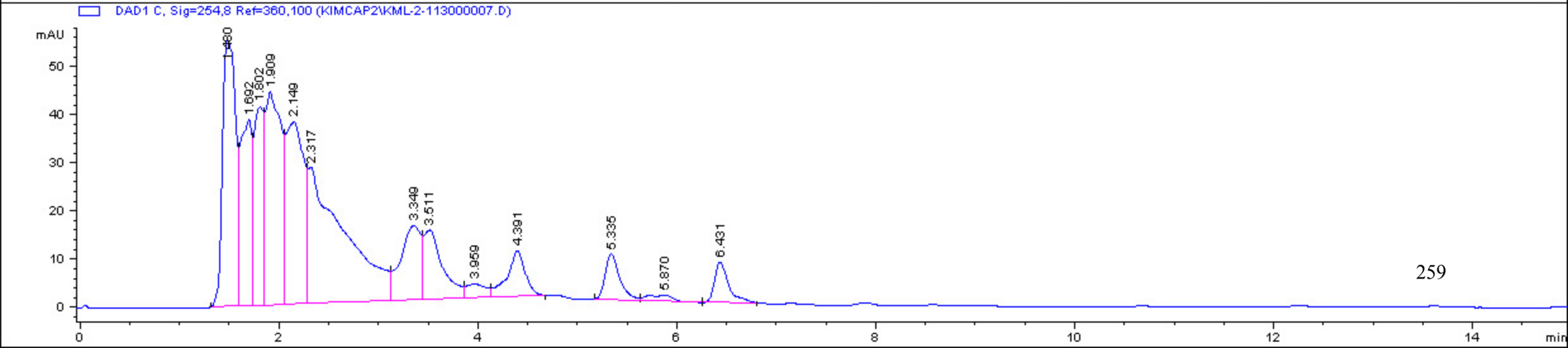

KML-2-113-7B 2.5M Captisol

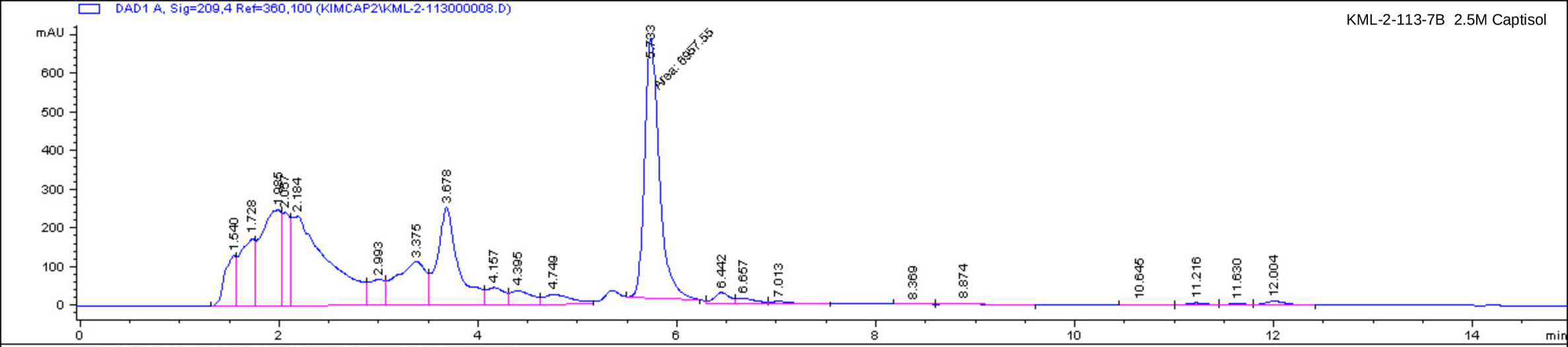

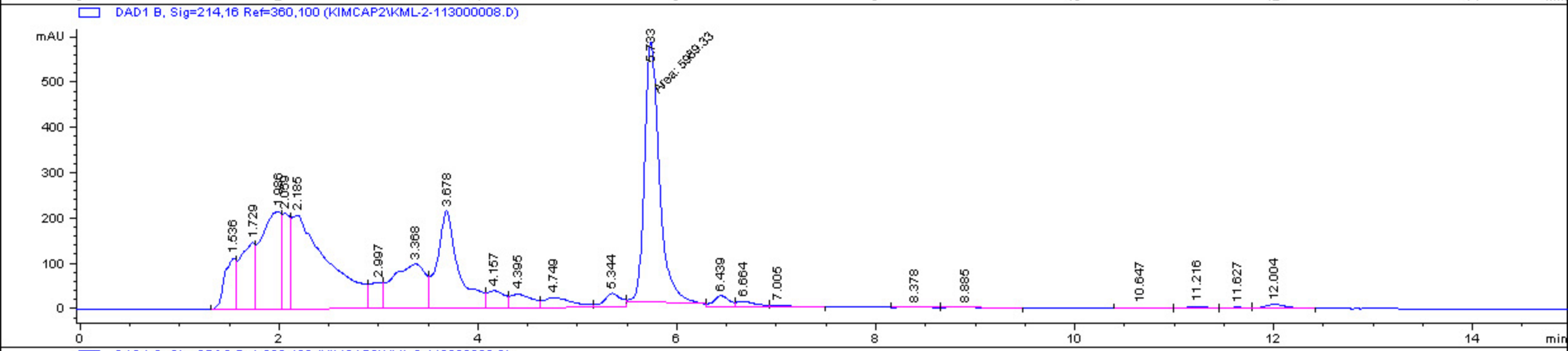

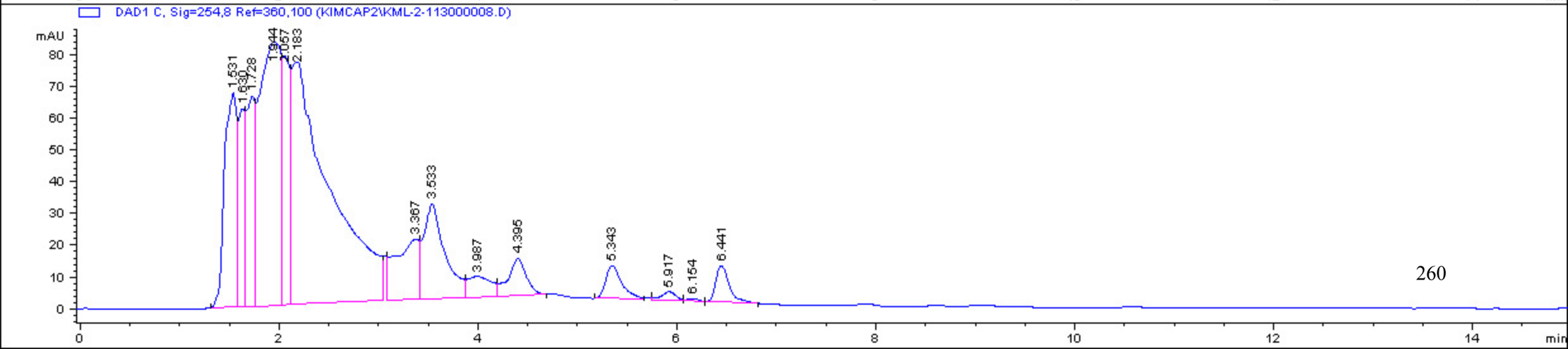

KML-2-113-7C 2.5M Captisol

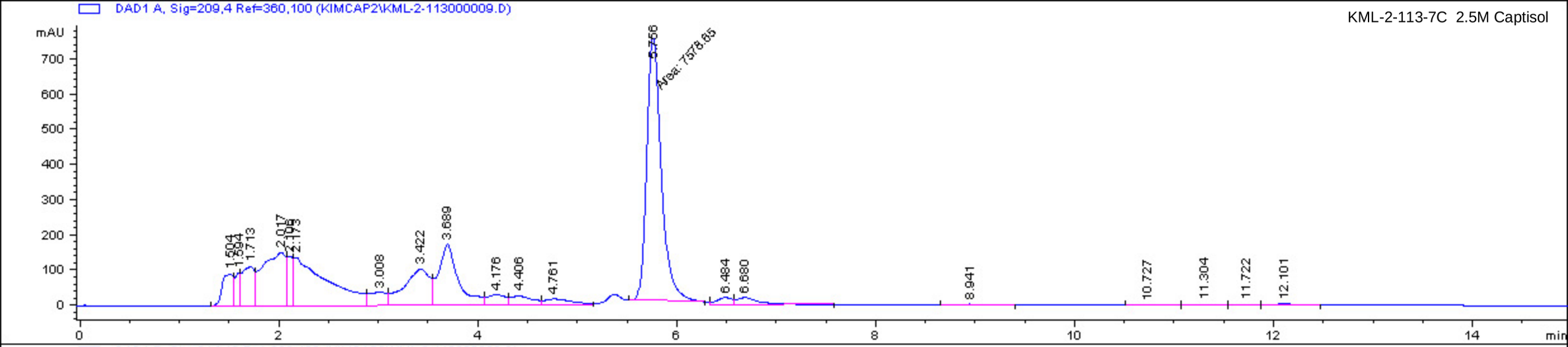

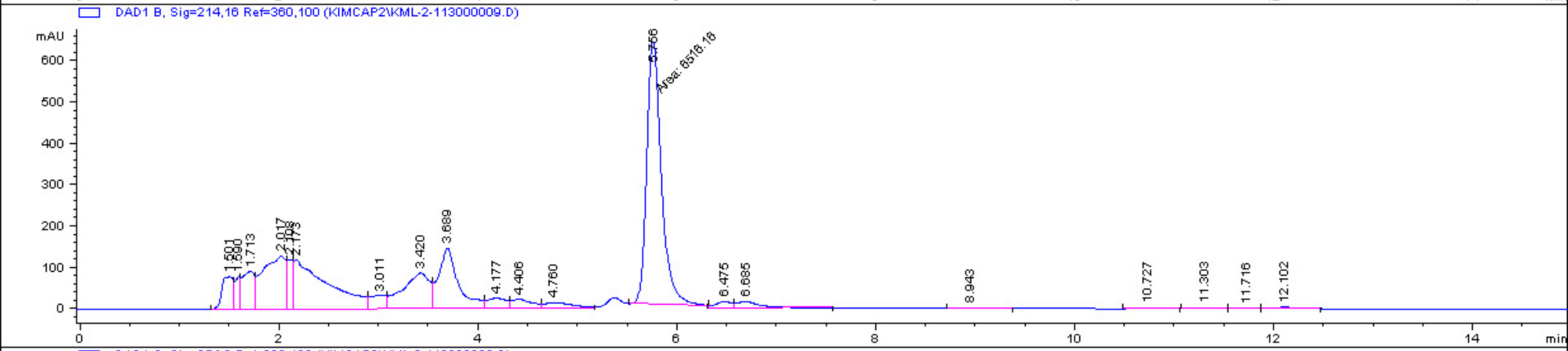

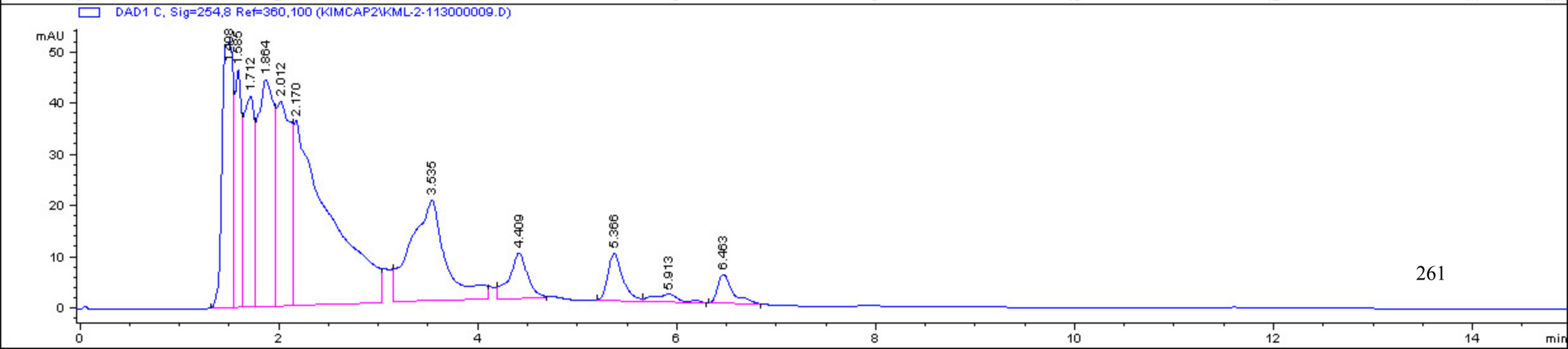

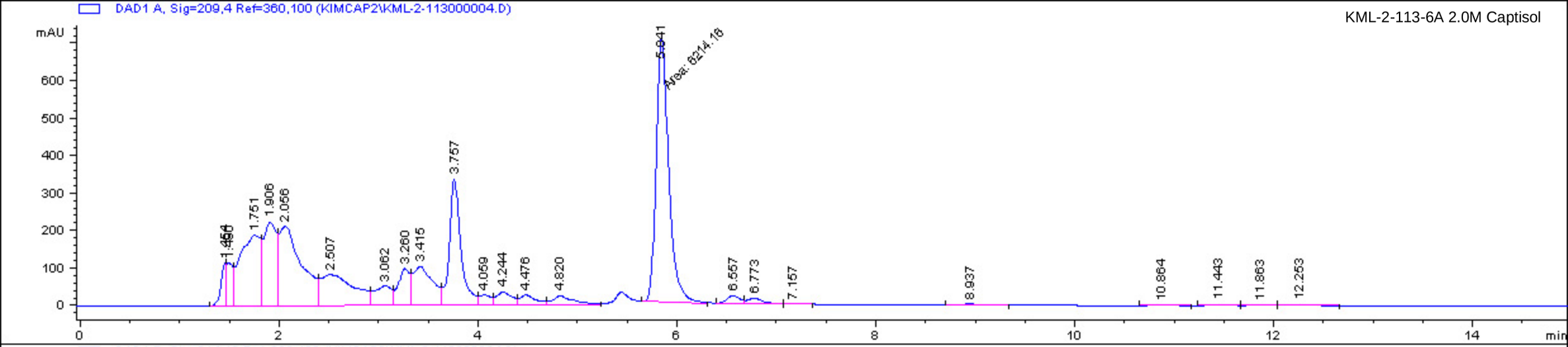
DAD1 A, Sig=209,4 Ref=360,100 (KIMCAP2\KML-2-113000004.D)
mAU
1.751
1.906
2.056
2.507
3.062
3.260
3.415
3.757
4.059
4.244
4.476
4.820
5.941
Area: 8214.18
6.557
6.773
7.157
8.937
10.864
11.443
11.863
12.253
min

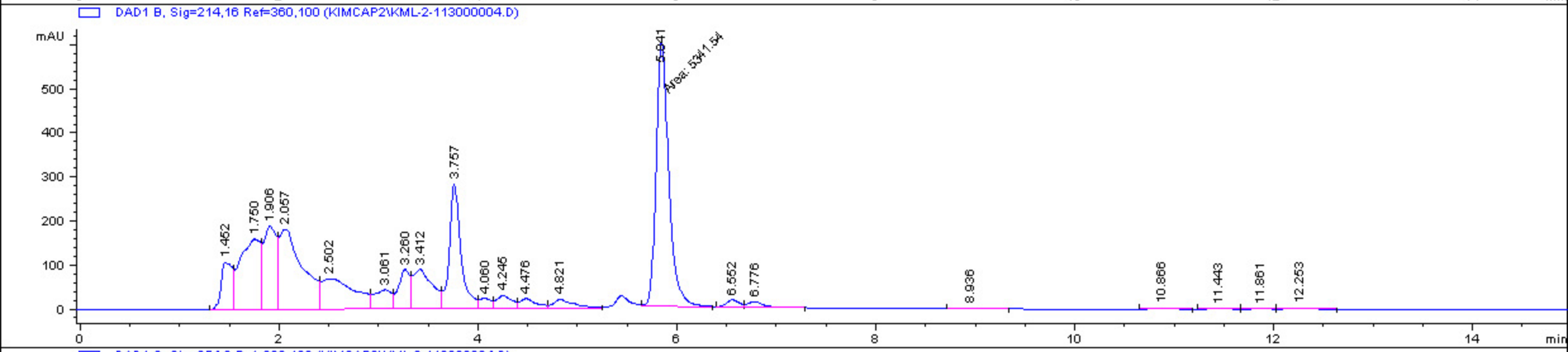
DAD1 B, Sig=214,16 Ref=360,100 (KIMCAP2\KML-2-113000004.D)
mAU
1.452
1.750
1.906
2.057
2.502
3.061
3.260
3.412
3.757
4.060
4.245
4.476
4.821
5.941
Area: 5341.54
6.552
6.776
8.936
10.866
11.443
11.861
12.253
min

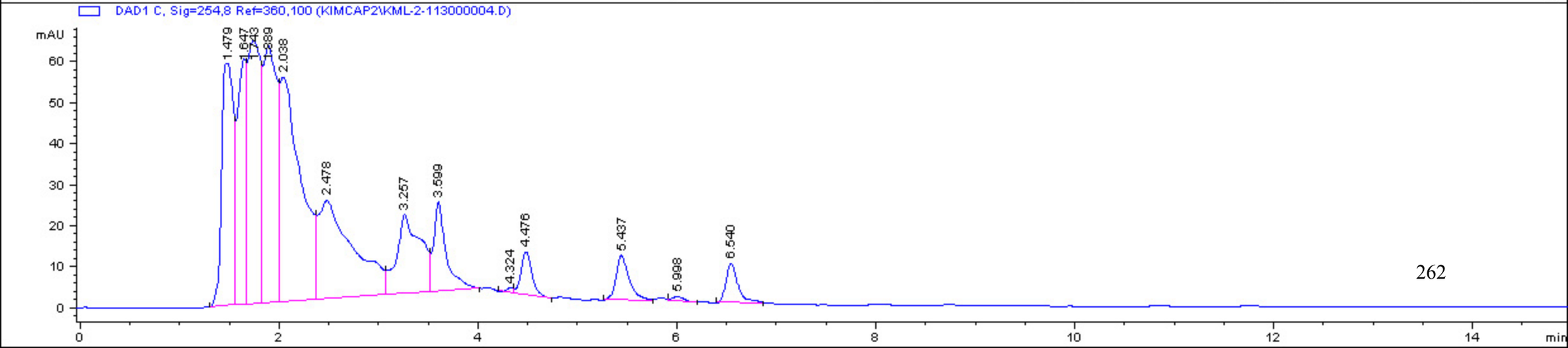
DAD1 C, Sig=254,8 Ref=360,100 (KIMCAP2\KML-2-113000004.D)
mAU
1.479
1.647
1.743
1.889
2.038
2.478
3.257
3.599
4.324
4.476
5.437
5.998
6.540
min

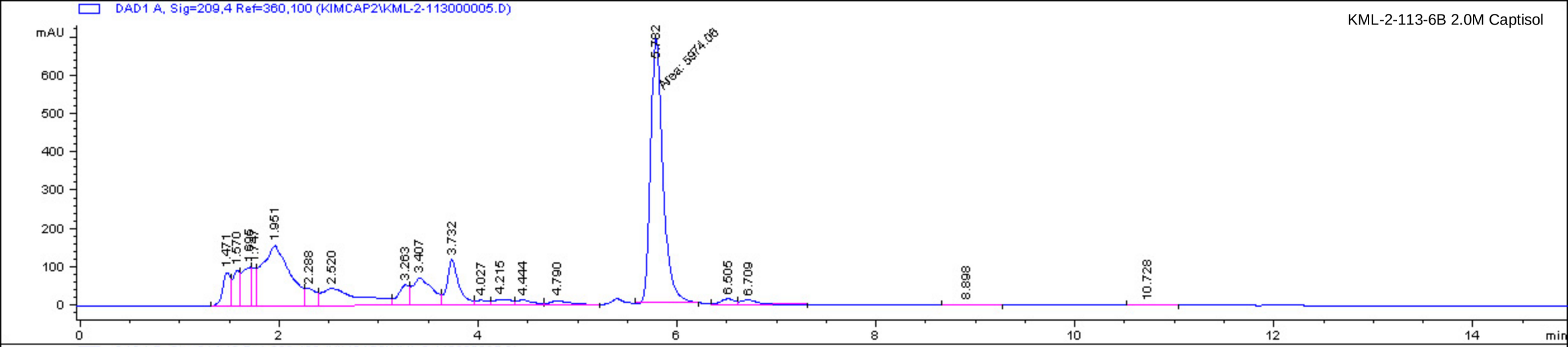
DAD1 A, Sig=209,4 Ref=360,100 (KIMCAP2\KML-2-113000005.D)
mAU
1.471
1.570
1.951
2.288
2.520
3.263
3.407
3.732
4.027
4.215
4.444
4.790
5.382
Area: 5974.08
6.505
6.709
8.898
10.728
min

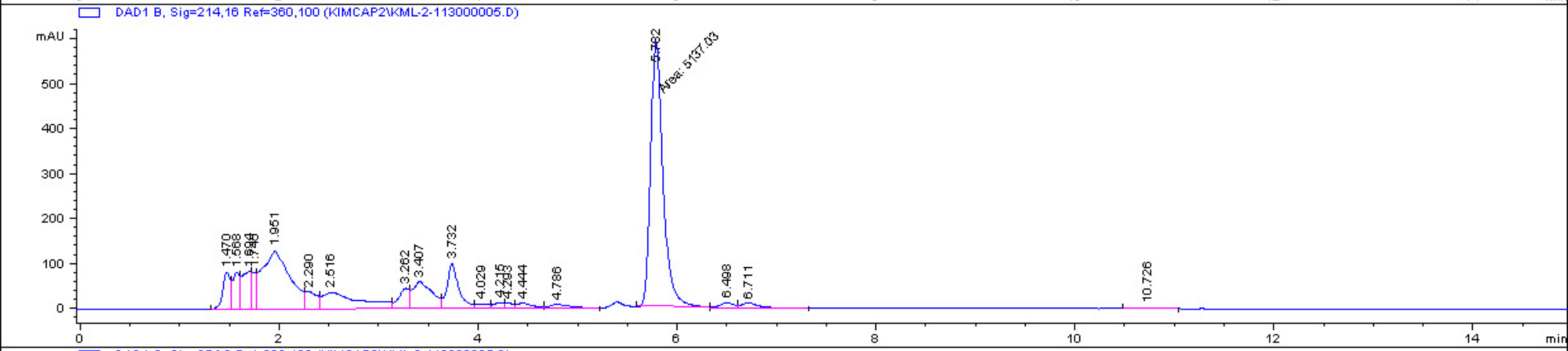
DAD1 B, Sig=214,16 Ref=360,100 (KIMCAP2\KML-2-113000005.D)
mAU
1.470
1.568
1.951
2.290
2.516
3.262
3.407
3.732
4.029
4.444
4.786
5.382
Area: 5137.03
6.498
6.711
10.726
min

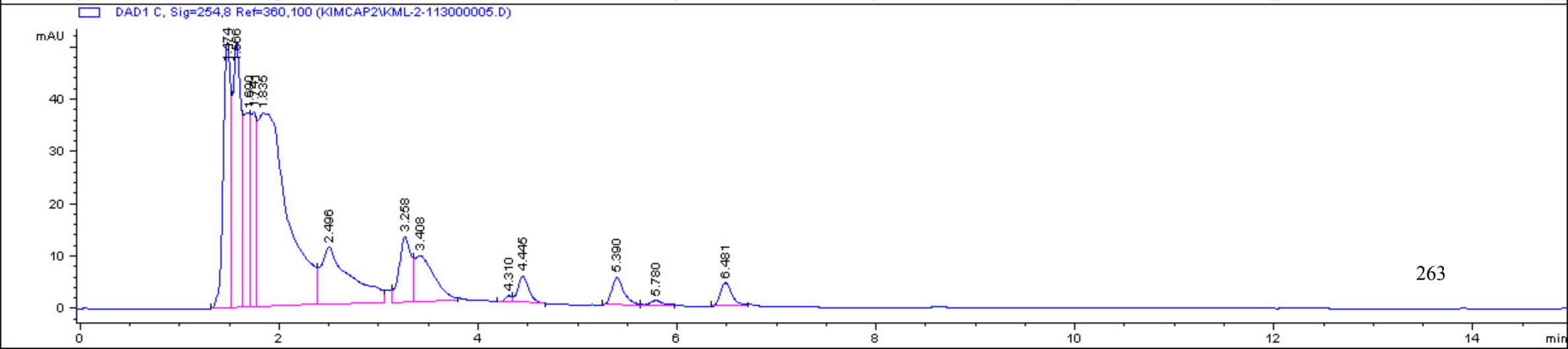
DAD1 C, Sig=254,8 Ref=360,100 (KIMCAP2\KML-2-113000005.D)
mAU
1.835
2.496
3.258
3.408
4.310
4.445
5.390
5.780
6.481
min

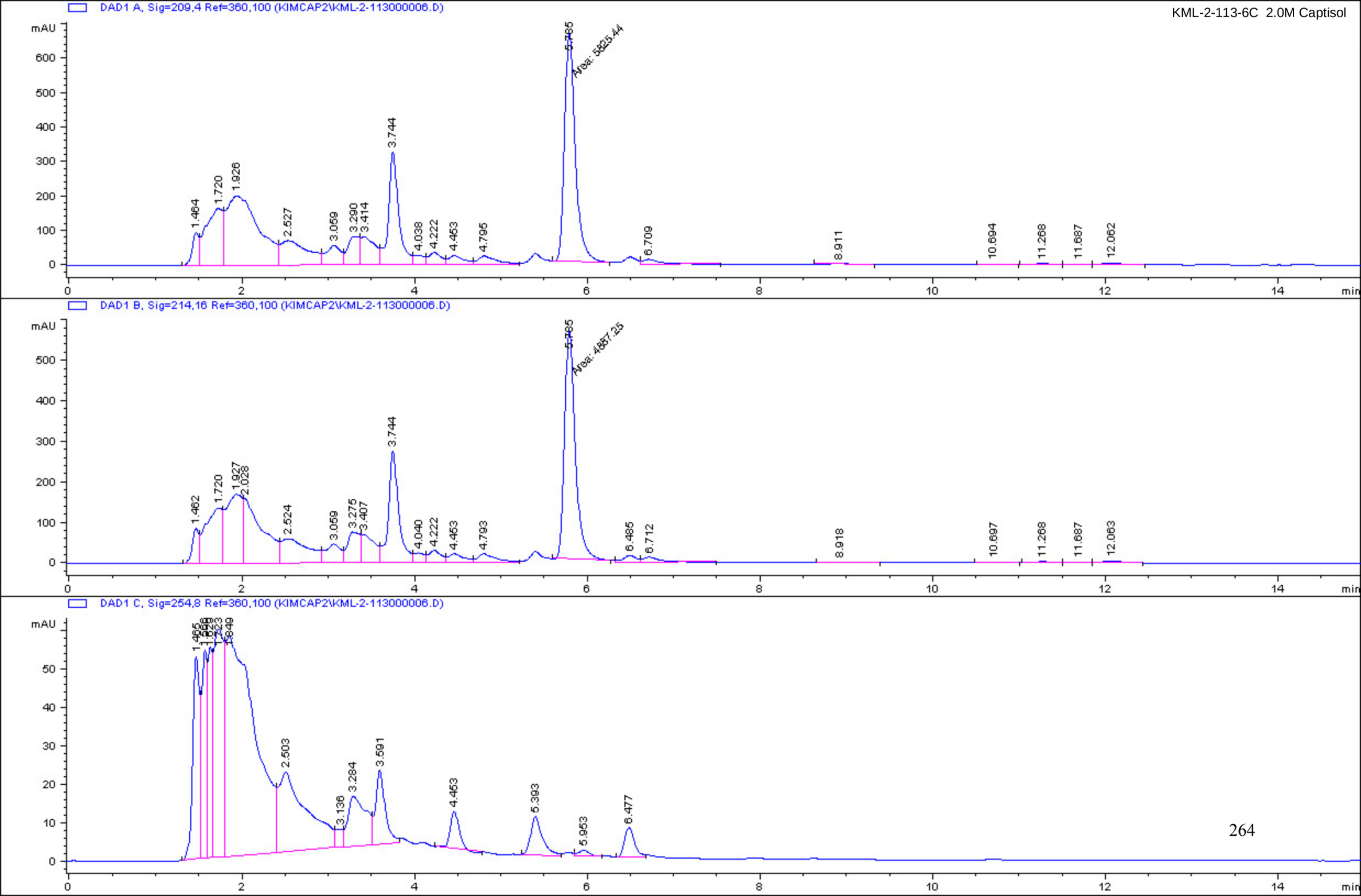
KML-2-113-6C 2.0M Captisol
DAD1 A, Sig=209,4 Ref=360,100 (KIMCAP2\KML-2-113000006.D)
mAU
1.464
1.720
1.926
2.527
3.059
3.290
3.414
3.744
4.038
4.222
4.463
4.795
5.785
Area: 5825.44
6.709
8.911
10.694
11.268
11.687
12.062
min
DAD1 B, Sig=214,16 Ref=360,100 (KIMCAP2\KML-2-113000006.D)
mAU
1.462
1.720
1.927
2.028
2.524
3.059
3.275
3.407
3.744
4.040
4.222
4.463
4.793
5.785
Area: 4887.25
6.485
6.712
8.918
10.697
11.268
11.687
12.063
min
DAD1 C, Sig=254,8 Ref=360,100 (KIMCAP2\KML-2-113000006.D)
mAU
2.503
3.136
3.284
3.591
4.463
5.393
5.963
6.477
min

KML-2-113-2A 1.5M Captisol

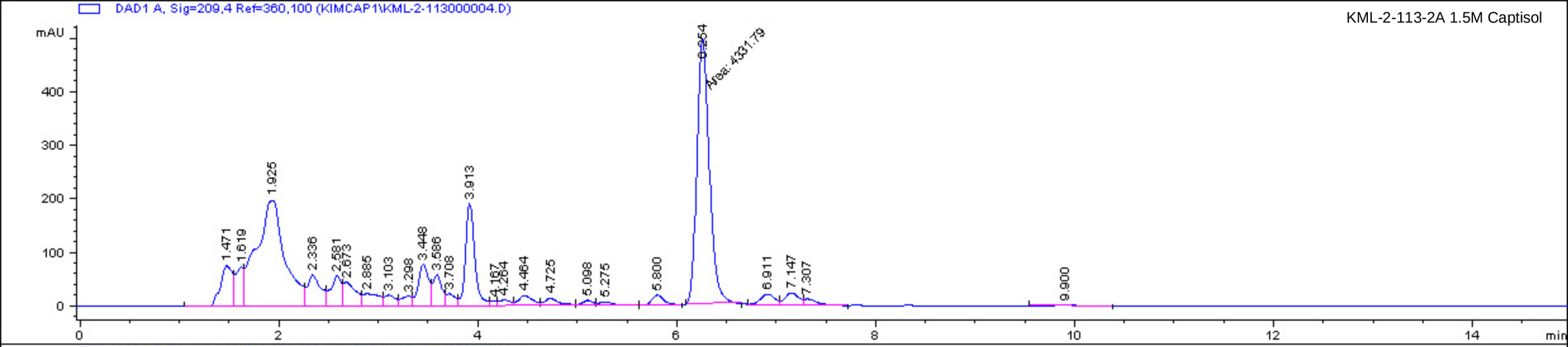

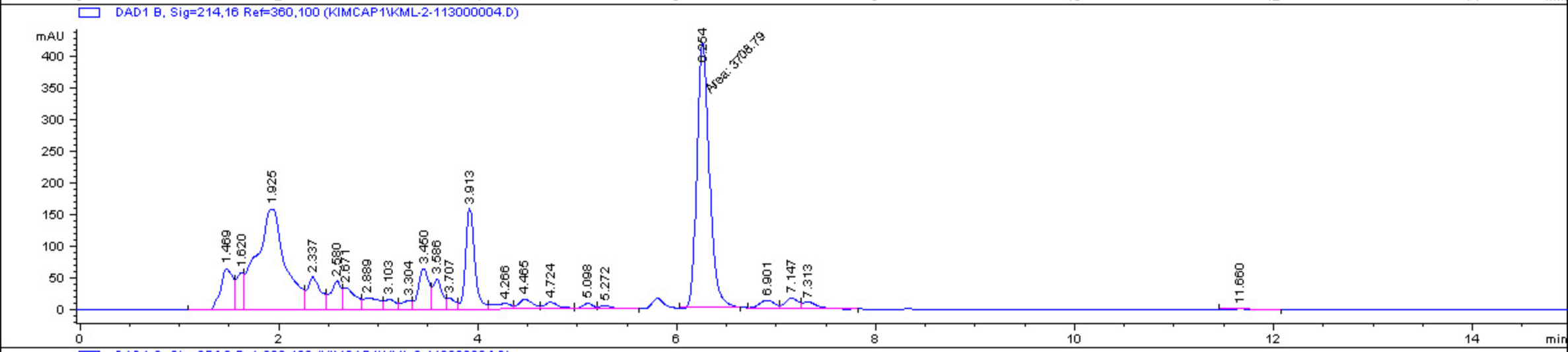

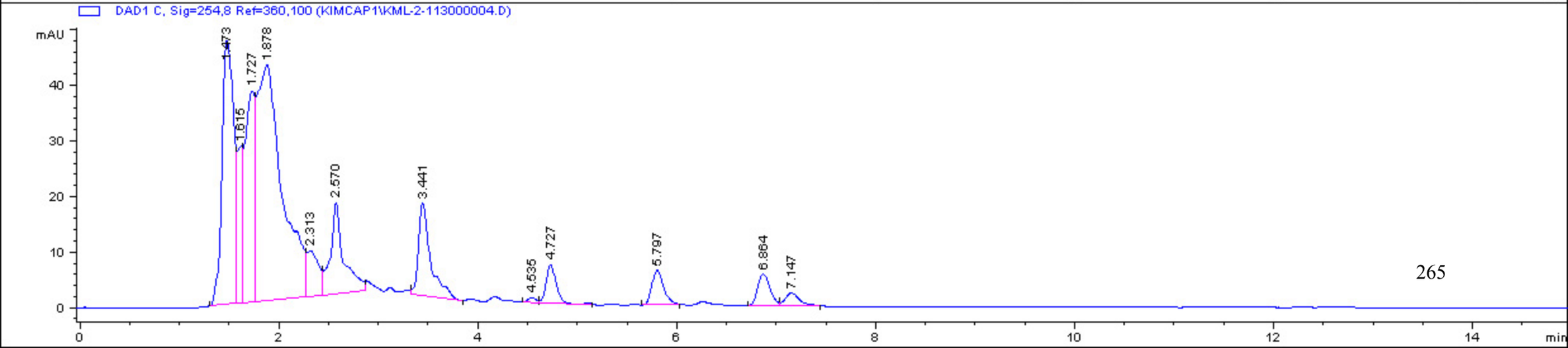

KML-2-113-2B 1.5M Captisol

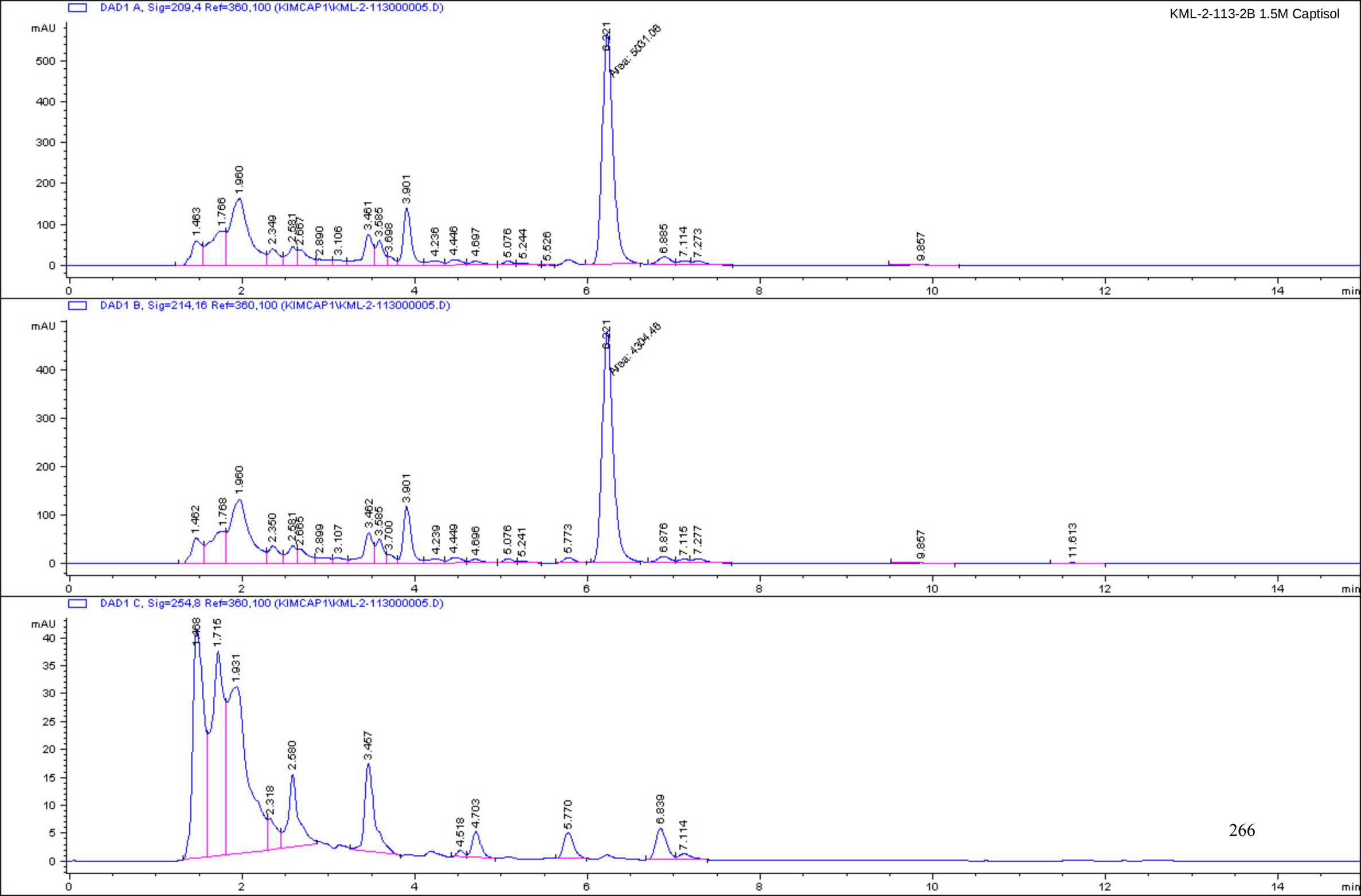

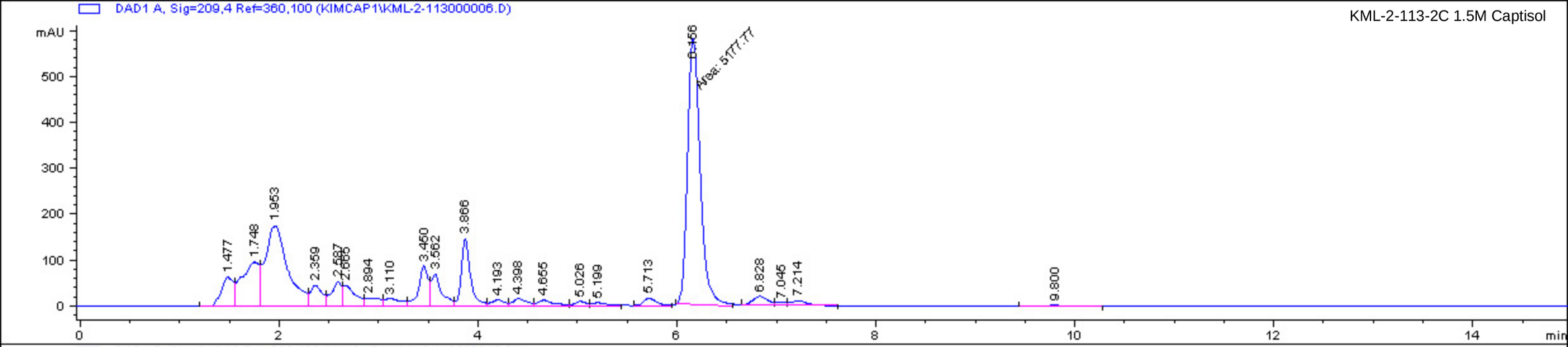
DAD1 A, Sig=209,4 Ref=360,100 (KIMCAP1\KML-2-113000006.D)
mAU
1.477
1.748
1.953
2.359
2.587
2.665
2.894
3.110
3.460
3.562
3.866
4.193
4.398
4.655
5.026
5.199
5.713
6.156
Area: 5177.77
6.828
7.045
7.214
9.800
min

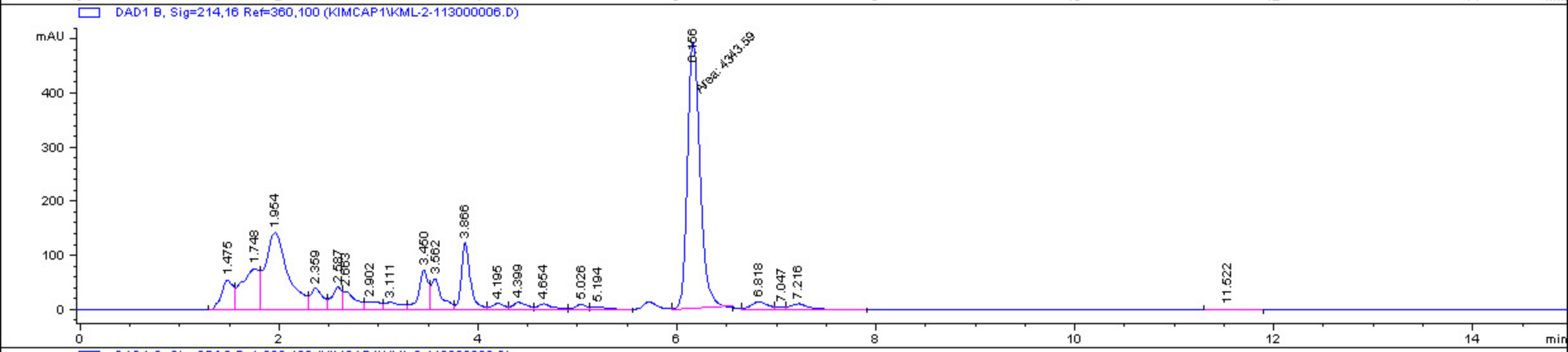
DAD1 B, Sig=214,16 Ref=360,100 (KIMCAP1\KML-2-113000006.D)
mAU
1.475
1.748
1.954
2.359
2.587
2.663
2.902
3.111
3.460
3.562
3.866
4.195
4.399
4.654
5.026
5.194
6.156
Area: 4343.59
6.818
7.047
7.216
11.522
min

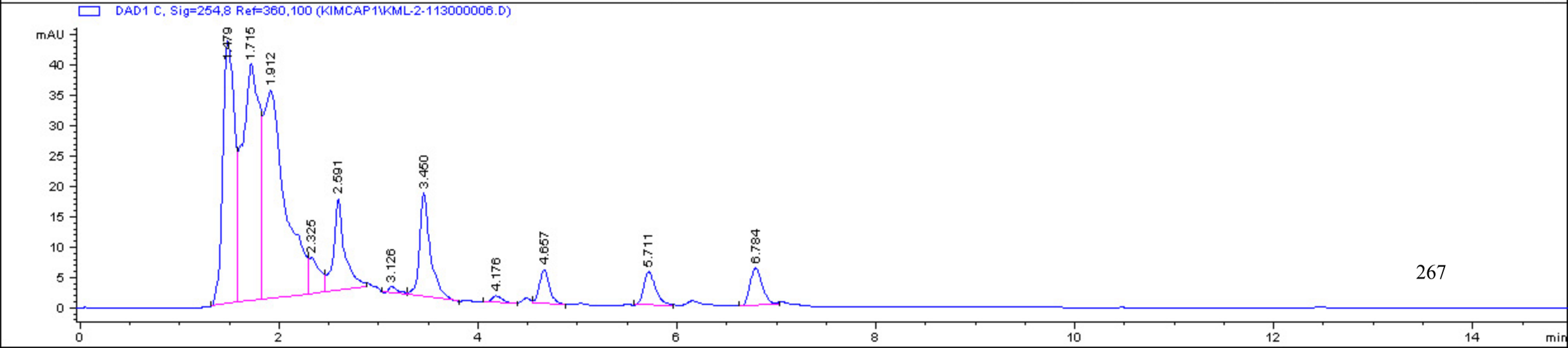
DAD1 C, Sig=254,8 Ref=360,100 (KIMCAP1\KML-2-113000006.D)
mAU
1.479
1.715
1.912
2.325
2.591
3.126
3.460
4.176
4.657
5.711
6.784
min

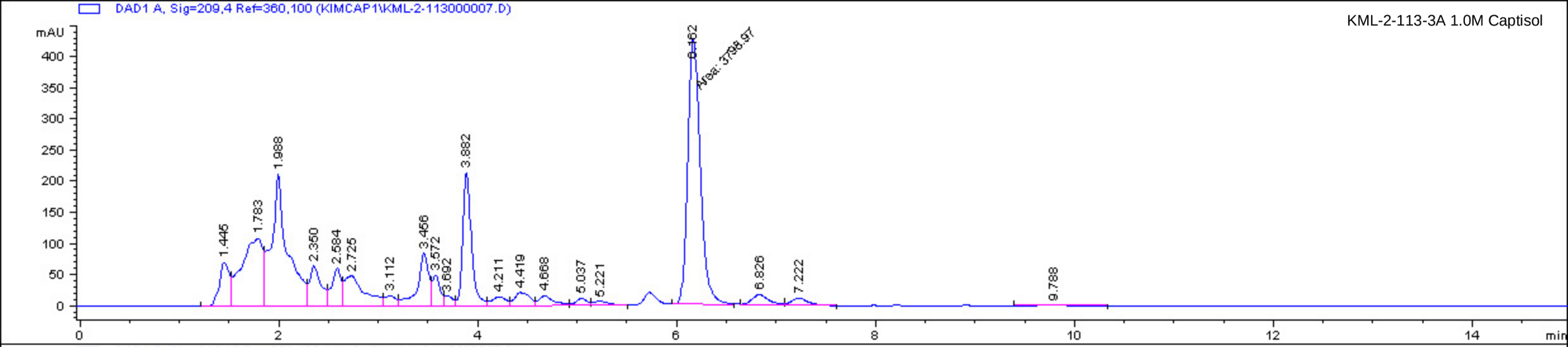
DAD1 A, Sig=209,4 Ref=360,100 (KIMCAP1\KML-2-113000007.D)
mAU
1.445
1.783
1.988
2.350
2.584
2.725
3.112
3.456
3.572
3.692
3.882
4.211
4.419
4.688
5.037
5.221
6.162
Area: 3795.97
6.826
7.222
9.788
min

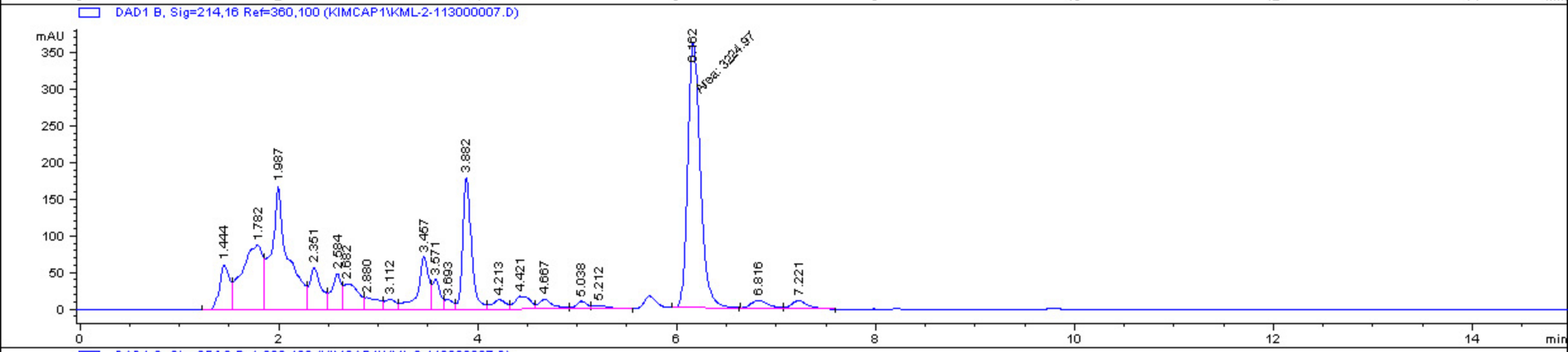
DAD1 B, Sig=214,16 Ref=360,100 (KIMCAP1\KML-2-113000007.D)
mAU
1.444
1.782
1.987
2.351
2.584
2.682
2.880
3.112
3.457
3.571
3.693
3.882
4.213
4.421
4.667
5.038
5.212
6.162
Area: 3224.97
6.816
7.221
min

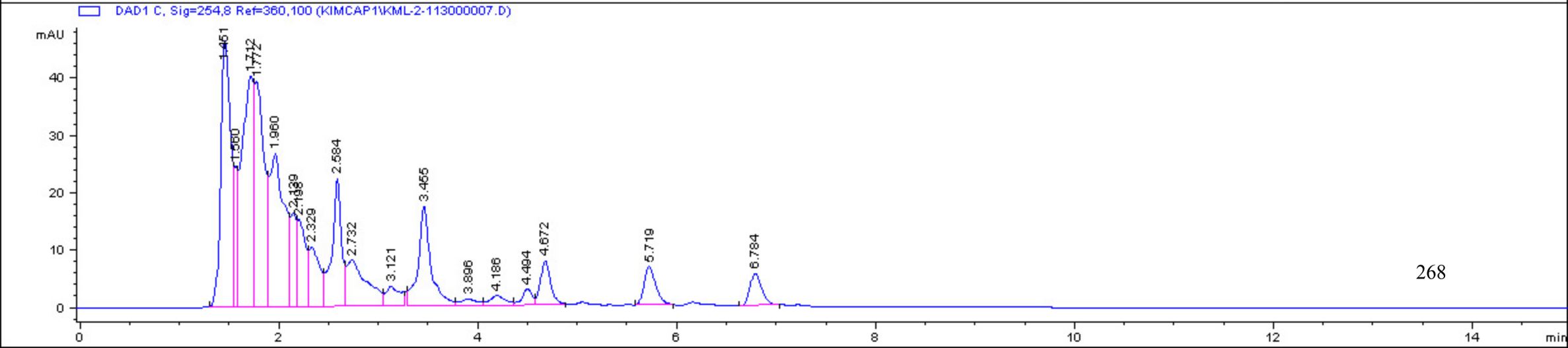
DAD1 C, Sig=254,8 Ref=360,100 (KIMCAP1\KML-2-113000007.D)
mAU
1.451
1.712
1.772
1.960
2.584
3.455
3.121
3.896
4.186
4.494
4.672
5.719
6.784
min

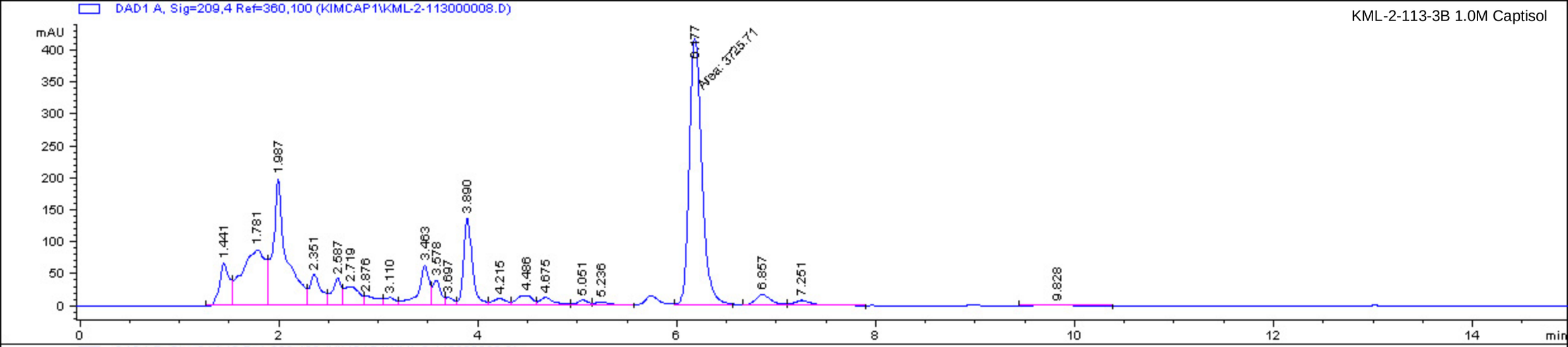
DAD1 A, Sig=209,4 Ref=360,100 (KIMCAP1\KML-2-113000008.D)
mAU
1.441
1.781
1.987
2.351
2.587
2.719
2.876
3.110
3.463
3.578
3.697
3.890
4.215
4.486
4.675
5.051
5.236
6.177
Area: 3725.71
6.857
7.251
9.828
min

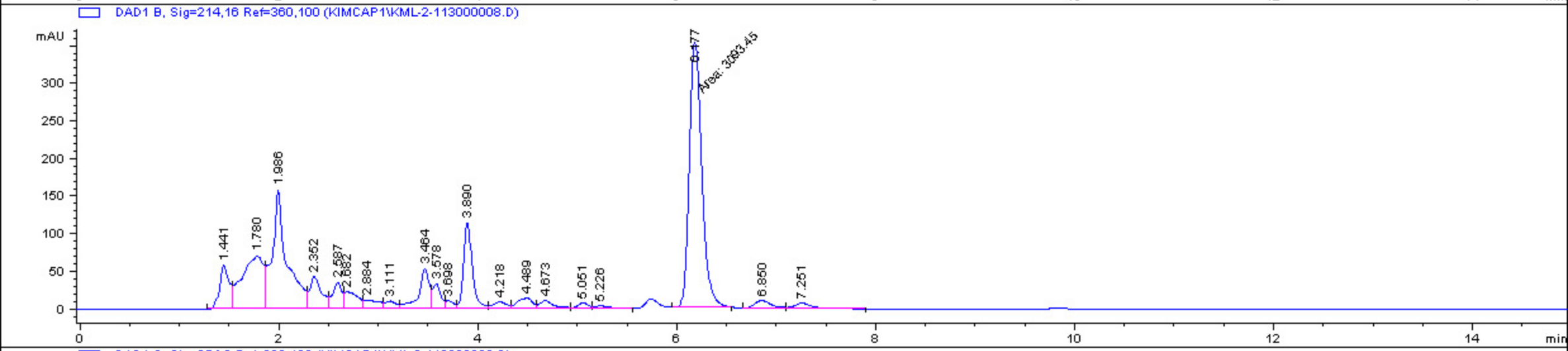
DAD1 B, Sig=214,16 Ref=360,100 (KIMCAP1\KML-2-113000008.D)
mAU
1.441
1.780
1.986
2.352
2.587
2.682
2.884
3.111
3.464
3.578
3.698
3.890
4.218
4.489
4.673
5.051
5.226
6.177
Area: 3693.45
6.850
7.251
min

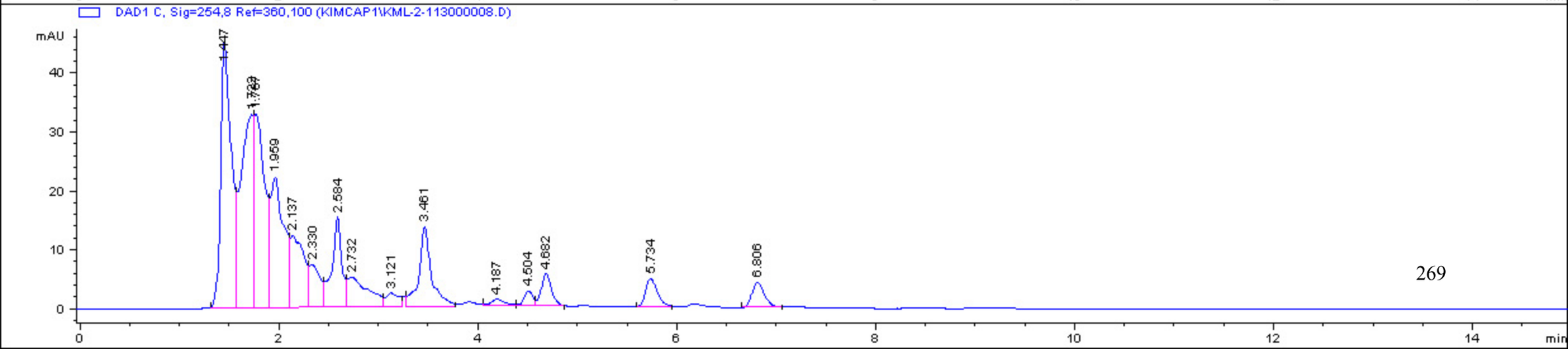
DAD1 C, Sig=254,8 Ref=360,100 (KIMCAP1\KML-2-113000008.D)
mAU
1.447
1.767
1.959
2.137
2.330
2.584
2.732
3.121
3.461
4.187
4.504
4.682
5.734
6.806
min

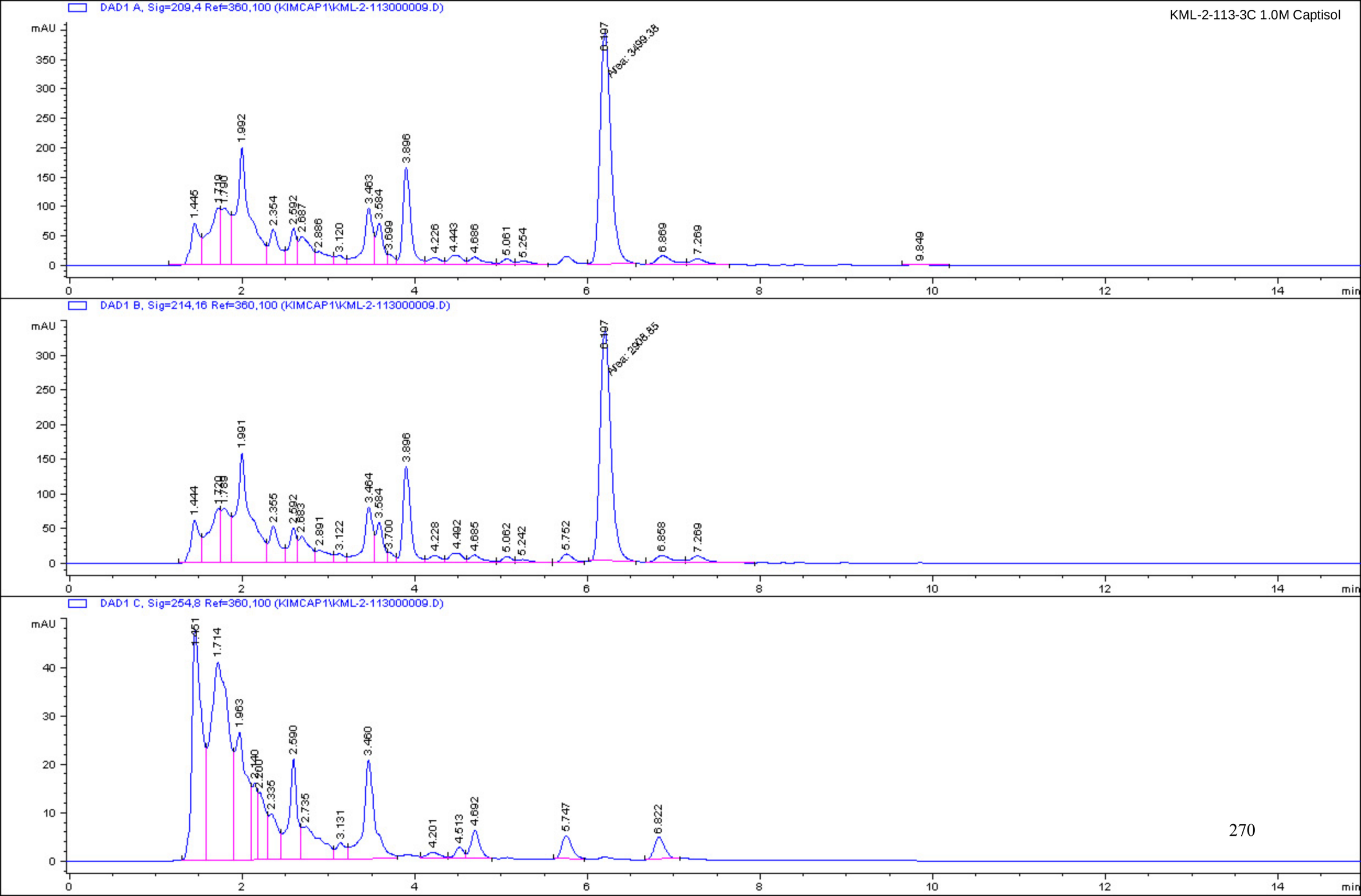
KML-2-113-3C 1.0M Captisol
DAD1 A, Sig=209,4 Ref=360,100 (KIMCAP1\KML-2-113000009.D)
mAU
1.445
1.710
1.992
2.354
2.592
2.687
2.886
3.120
3.463
3.684
3.699
3.896
4.226
4.443
4.686
5.061
5.254
6.197
Area: 3499.38
6.869
7.269
9.849
min
DAD1 B, Sig=214,16 Ref=360,100 (KIMCAP1\KML-2-113000009.D)
mAU
1.444
1.991
2.355
2.592
2.883
2.891
3.122
3.464
3.684
3.700
3.896
4.228
4.492
4.685
5.062
5.242
5.752
6.197
Area: 2908.85
6.858
7.269
min
DAD1 C, Sig=254,8 Ref=360,100 (KIMCAP1\KML-2-113000009.D)
mAU
1.451
1.714
1.963
2.590
2.735
3.131
3.460
4.201
4.513
4.692
5.747
6.822
min

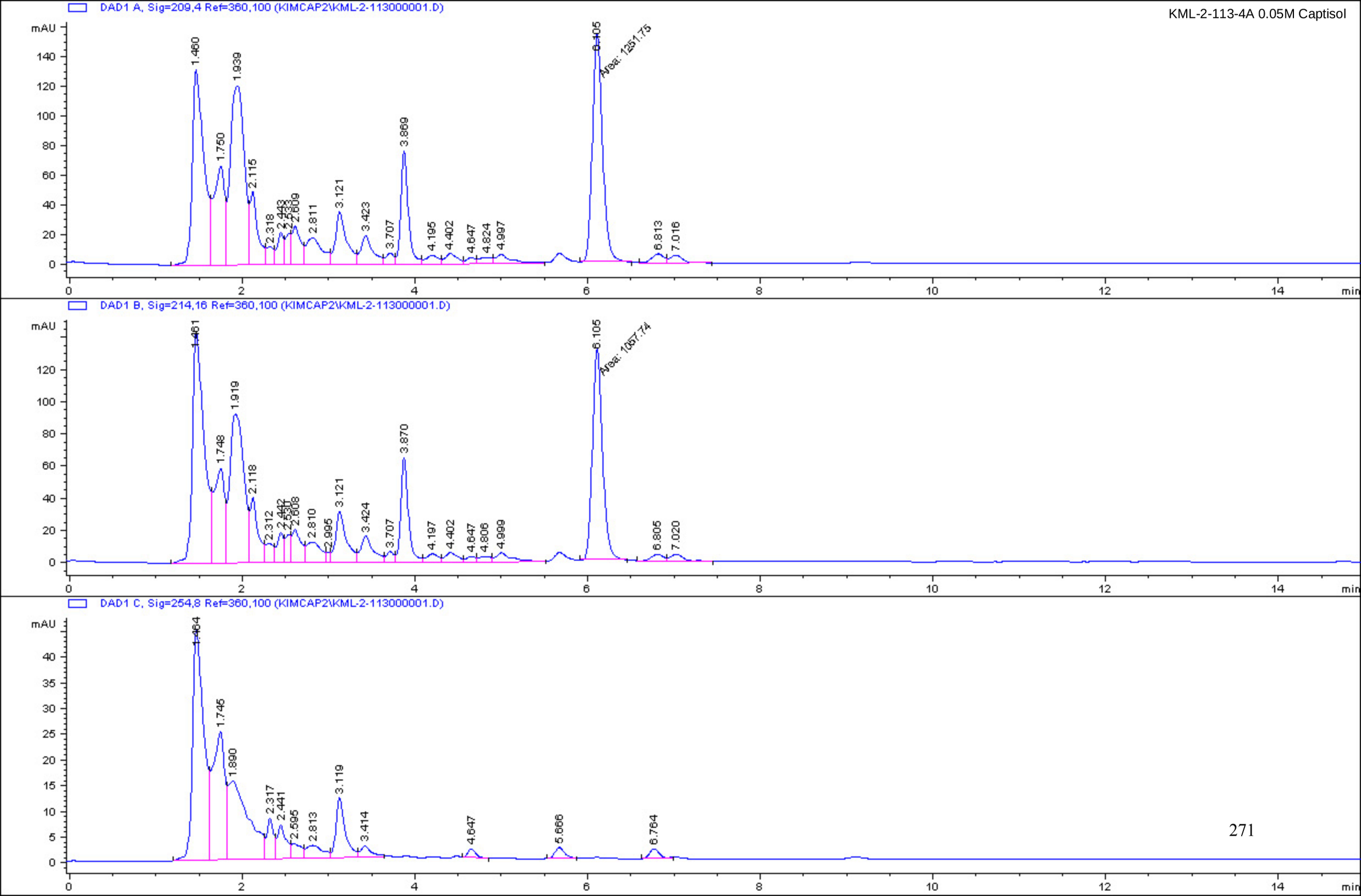
KML-2-113-4A 0.05M Captisol
DAD1 A, Sig=209,4 Ref=360,100 (KIMCAP2\KML-2-113000001.D)
mAU
1.460
1.750
1.939
2.115
2.318
2.811
3.121
3.423
3.707
3.869
4.195
4.402
4.647
4.824
4.997
6.105
Area: 1251.75
6.813
7.016
min
DAD1 B, Sig=214,16 Ref=360,100 (KIMCAP2\KML-2-113000001.D)
mAU
1.461
1.748
1.919
2.118
2.312
2.608
2.810
2.995
3.121
3.424
3.707
3.870
4.197
4.402
4.647
4.806
4.999
6.105
Area: 1057.74
6.805
7.020
min
DAD1 C, Sig=254,8 Ref=360,100 (KIMCAP2\KML-2-113000001.D)
mAU
1.464
1.745
1.890
2.317
2.441
2.595
2.813
3.119
3.414
4.647
5.666
6.764
min

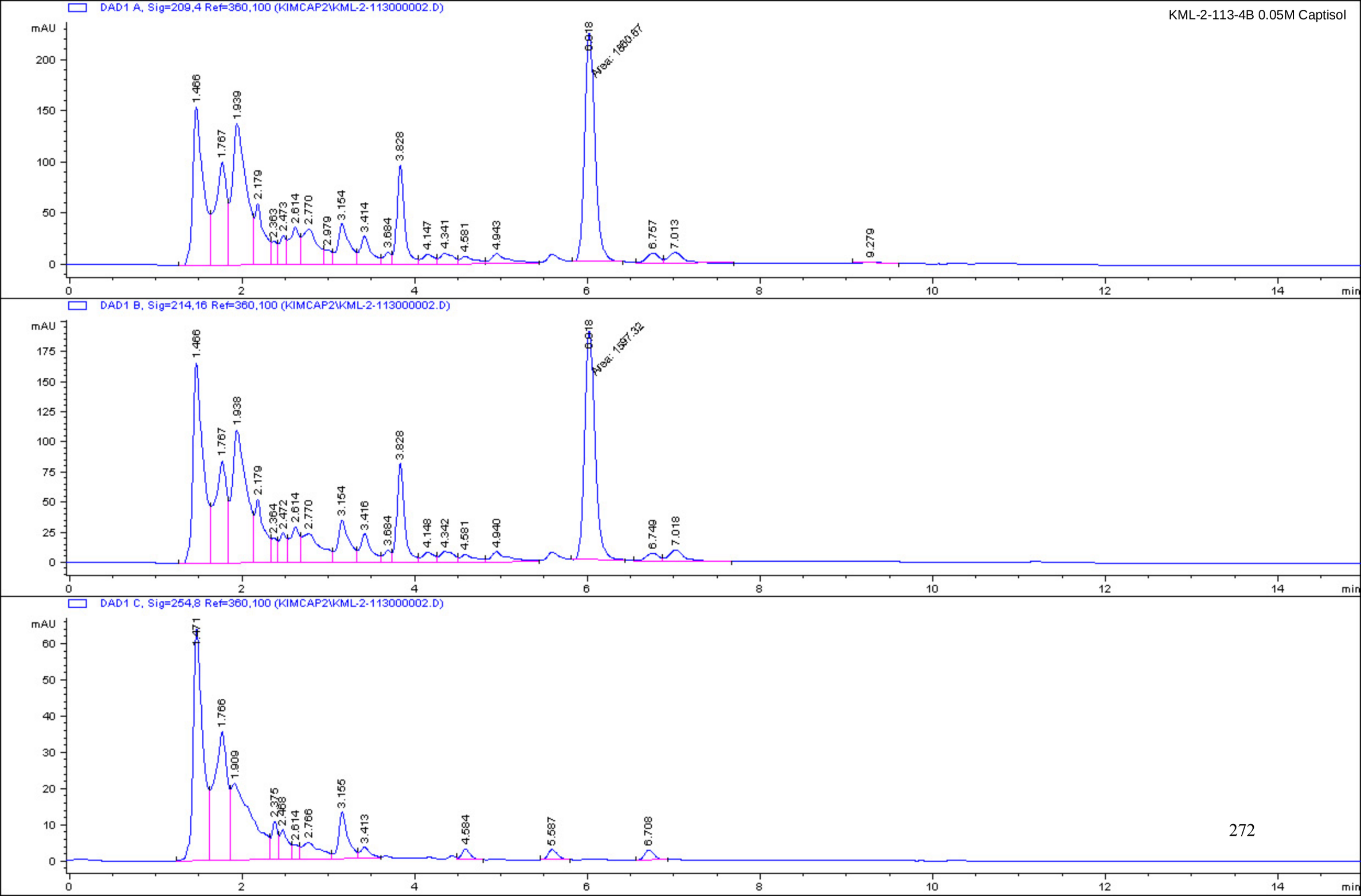
KML-2-113-4B 0.05M Captisol
DAD1 A, Sig=209,4 Ref=360,100 (KIMCAP2\KML-2-113000002.D)
mAU
1.466
1.767
1.939
2.179
2.363
2.473
2.614
2.770
2.979
3.154
3.414
3.684
3.828
4.147
4.341
4.581
4.943
6.018
Area: 1660.67
6.757
7.013
9.279
min
DAD1 B, Sig=214,16 Ref=360,100 (KIMCAP2\KML-2-113000002.D)
mAU
1.466
1.767
1.938
2.179
2.364
2.472
2.614
2.770
3.154
3.416
3.684
3.828
4.148
4.342
4.581
4.940
6.018
Area: 1597.32
6.749
7.018
min
DAD1 C, Sig=254,8 Ref=360,100 (KIMCAP2\KML-2-113000002.D)
mAU
1.471
1.766
1.909
2.375
2.468
2.614
2.766
3.155
3.413
4.584
5.587
6.708
min

KML-2-113-4C 0.05M Captisol

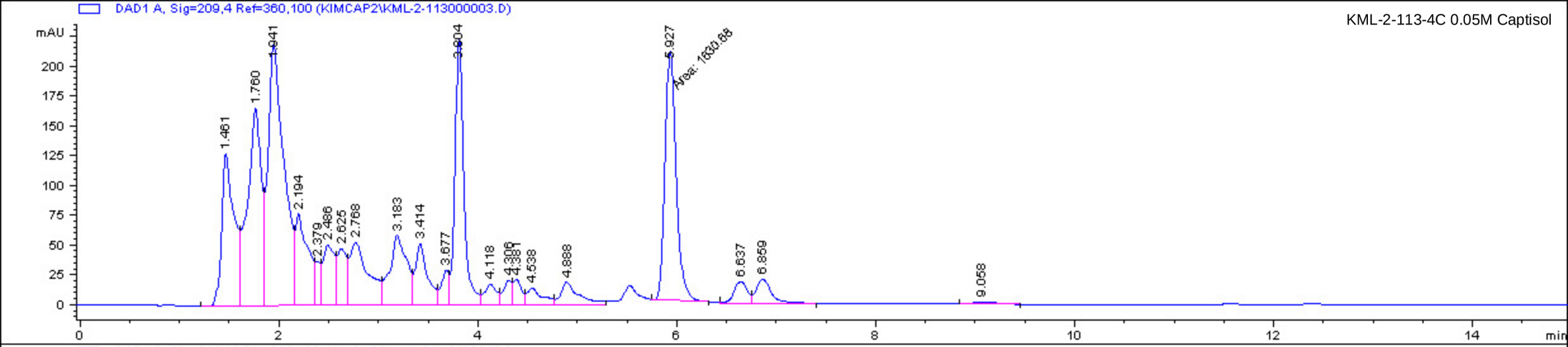

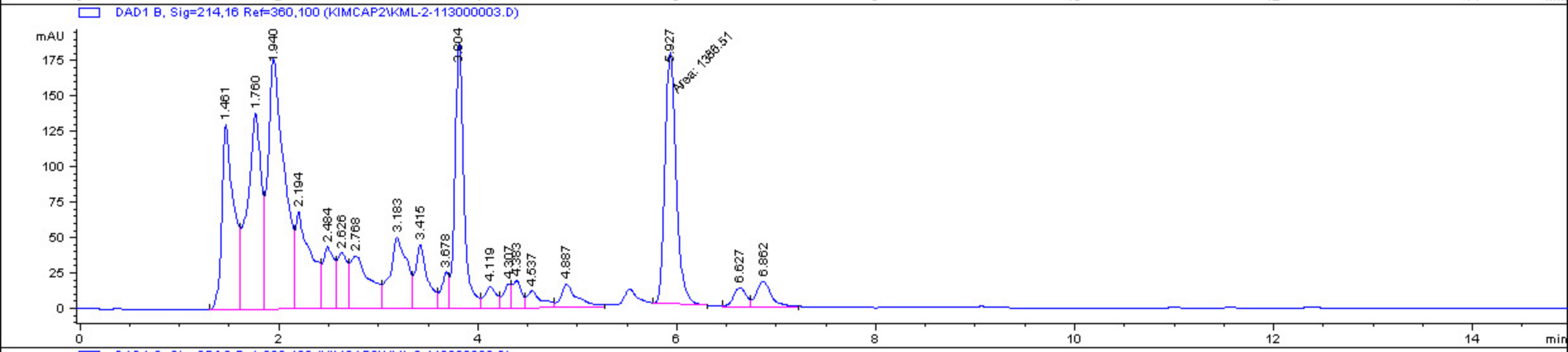

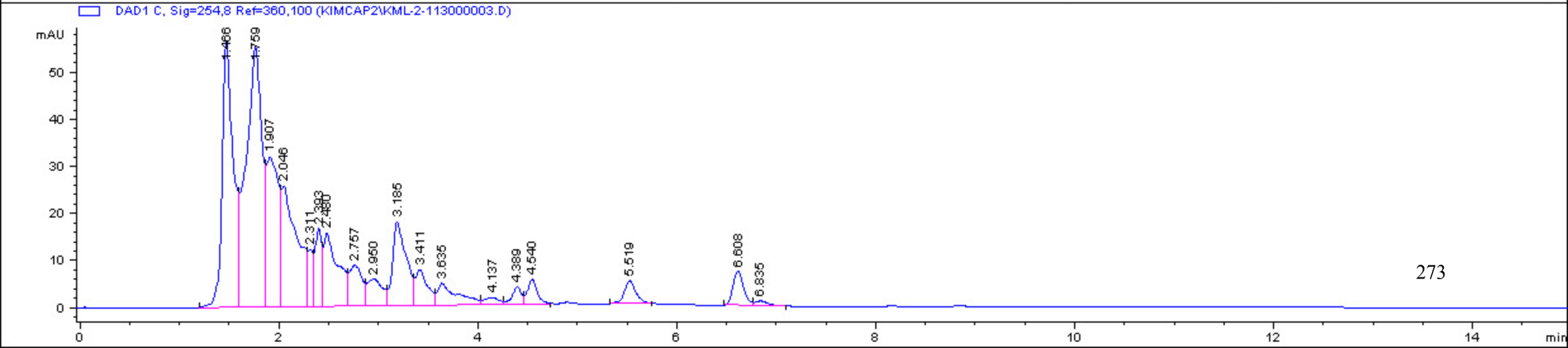

KML-2-113-5A 0.0M Captisol

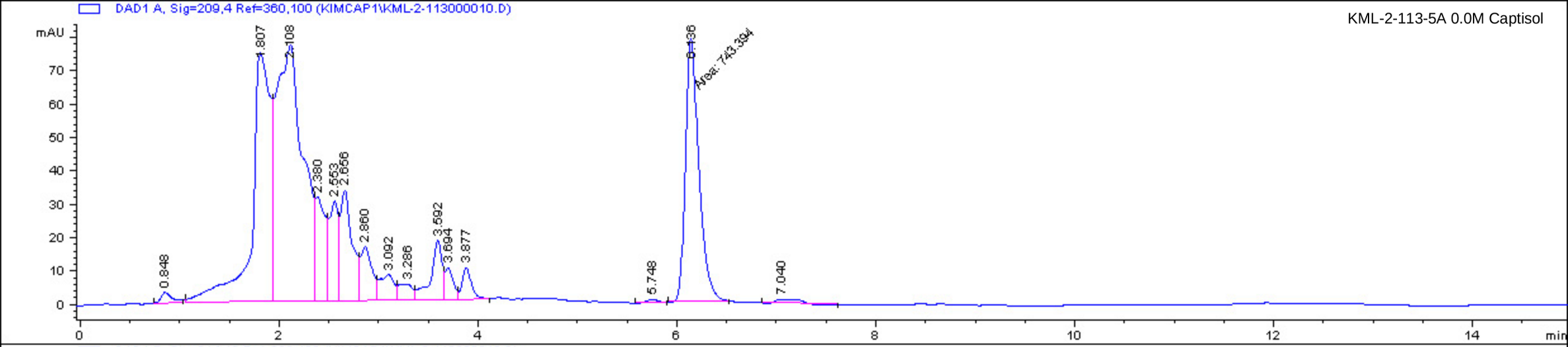

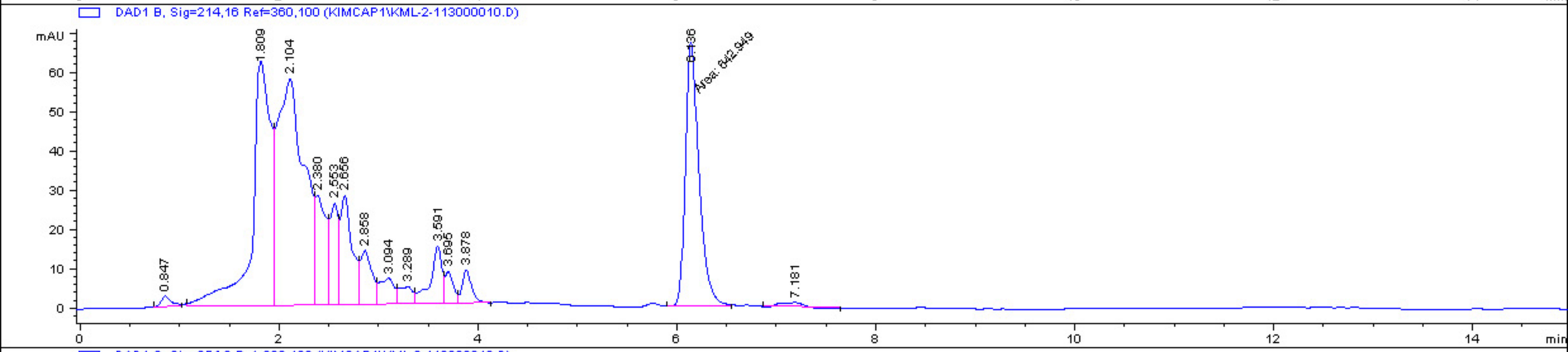

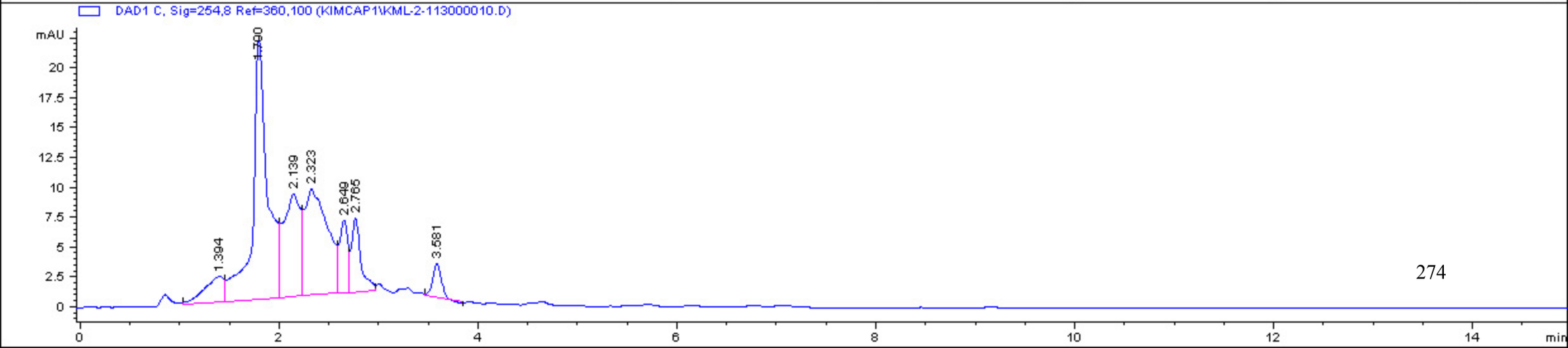

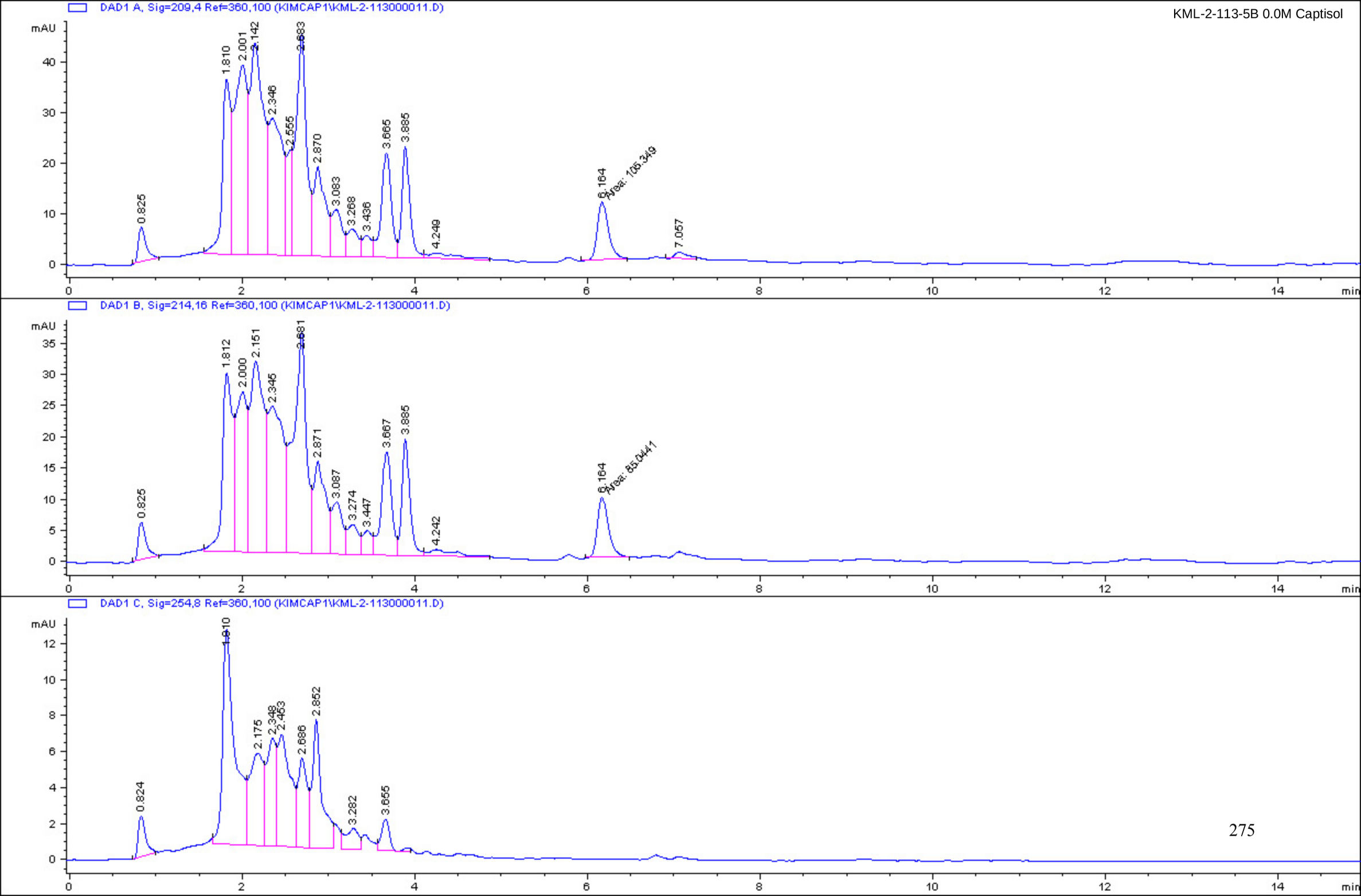
KML-2-113-5B 0.0M Captisol
DAD1 A, Sig=209,4 Ref=360,100 (KIMCAP1\KML-2-113000011.D)
mAU
1.810
2.001
2.142
2.346
2.555
2.683
2.870
3.083
3.268
3.436
3.665
3.885
4.249
0.825
6.164
Area: 105.349
7.057
min
DAD1 B, Sig=214,16 Ref=360,100 (KIMCAP1\KML-2-113000011.D)
mAU
1.812
2.000
2.151
2.345
2.681
2.871
3.087
3.274
3.447
3.667
3.885
4.242
0.825
6.164
Area: 85.0441
min
DAD1 C, Sig=254,8 Ref=360,100 (KIMCAP1\KML-2-113000011.D)
mAU
1.810
2.175
2.348
2.463
2.686
2.852
3.282
3.655
0.824
min

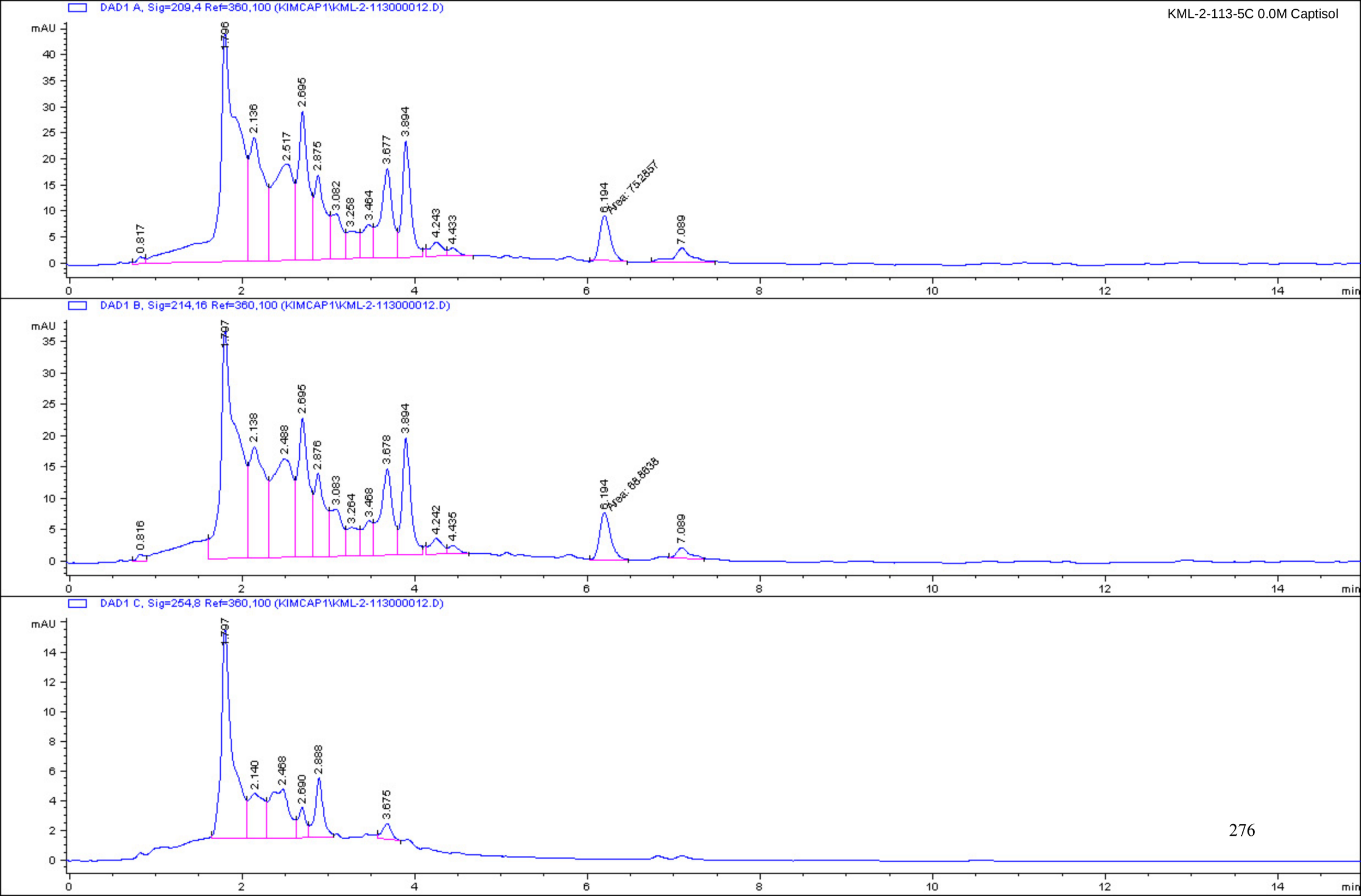
KML-2-113-5C 0.0M Captisol
DAD1 A, Sig=209,4 Ref=360,100 (KIMCAP1\KML-2-113000012.D)
mAU
0.817
1.796
2.136
2.517
2.695
2.875
3.082
3.258
3.464
3.677
3.894
4.243
4.433
6.194
Area: 75.2857
7.089
min
DAD1 B, Sig=214,16 Ref=360,100 (KIMCAP1\KML-2-113000012.D)
mAU
0.816
1.797
2.138
2.488
2.695
2.876
3.083
3.264
3.468
3.678
3.894
4.242
4.435
6.194
Area: 68.8638
7.089
min
DAD1 C, Sig=254,8 Ref=360,100 (KIMCAP1\KML-2-113000012.D)
mAU
1.797
2.140
2.468
2.690
2.888
3.675
min